PHYTOCHEMICAL INVESTIGATIONS

ON

BOSWELLIA SPECIES

Comparative Studies on the Essential Oils, Pyrolysates and Boswellic Acids

of

Boswellia carterii **Birdw.,**

Boswellia serrata **Roxb.,**

Boswellia frereana **Birdw.,**

Boswellia neglecta **S. Moore and**

Boswellia rivae **Engl.**

Dissertation for the Fulfillment of the Requirements

for the Degree of *Dr. rer. nat*.

by

Simla Basar

Istanbul

(Turkey)

Hamburg 2005

1.   Gutachter: Prof. Dr. Dr. h. c. Wittko Francke
            Institut für Organische Chemie, Universität Hamburg

2.   Gutachter: Prof. Dr. Chris Meier
            Institut für Organische Chemie, Universität Hamburg

1. Prüfer   Prof. Dr. Dr. h.c. Wittko Francke
                Institut für Organische Chemie, Universität Hamburg

2. Prüfer   Prof. Dr. Uli Hahn
                Institut für Biochemie, Universität Hamburg

3. Prüfer   Prof. Dr. Johannes Westendorf
                Institut für Toxikologie, Universitätkrankenhaus Eppendorf

Tag der Disputation: 18 März 2005

The presented work was performed from February 2000 to September 2003 at the University of Hamburg, Institute of Organic Chemistry under the supervision of Prof. Dr. Wilfried A. König.

For my parents
Sevim & Ercan Başar

Acknowledgments

First of all, I would like to express my sincere gratitude to my dear *"Doktorvater"*, Prof. Dr. Wilfried A. König[†], who deceased at 19th November 2004. Throughout this work, I appreciated his guidance, financial and scientific support, and I am very grateful for the chance he gave me to work with him and learn from him.

I thank Prof. Dr. Dr. h.c. Wittko Francke for his invaluable advise, support and efforts during the revision of the thesis.

Thanks to all professors in the Institute for Organic Chemistry and in the Department of Chemistry for giving me the possibility to study at the University of Hamburg.

Sincere thanks to Dr. Angelika Koch for her cooperation on this interesting topic. I gratefully appreciate financial and scientific support, her guidance, and her patience all the time.

Dr. Hans-Peter Hanssen's support during the correction of the thesis is gratefully acknowledged.

I like to thank the members of AK König for creating a friendly atmosphere in the working group. Especially, I would like to thank Dr. Detlev H. Hochmuth for his guidance and immediate help at any time. I very much enjoyed the team work during the organisation of ISCD-14 as well as his scientific supervision. I also thank Dr. Claudia Paul for her constructive support and help starting from the first minute that I joined AK König. I like to thank my dear friends Dr. Julia Pruns, Dr. Iris Altug, and Minoo Khedmati for the pleasant time that we had.

I like to thank my labor partner Rita Richter for the harmony she brought to the working place.

I am thankful to my colleagues in AK Francke, especially Sven Possner and Karsten Fehler for their friendship.

Invaluable help by Annegret Meiners and Manfred Preuße who measured infinite numbers of samples without any delay is gratefully acknowledged.

Ganz herzlich danke ich meinen Freunden – die eigentlich meine Familie in Deutschland sind – der Familie Kalyoncu; besonders Selda und Bahadır Kalyoncu sowie Sigrid und Baki Kalyoncu, Ilka und Baha Kalyoncu mit Devin und Linda, Sevim und Şerifali Kalyoncu; für das Gefühl, das sie mir gegeben haben, zu Hause zu sein. Liebe Selda und lieber Bahadır, ich werde eure Unterstützung, Verständnis, Herzlichkeit und Liebe, die ihr mir gezeigt habt, niemals in meinem Leben vergessen.

Besonders danke ich Zeynep Yunt für die Motivation und herzliche Liebe, die sie mir jede Minute entgegen brachte. Liebe Zeynep, ohne dein Lächeln wäre diese Zeit unerträglich gewesen!

Michael Maurer, dem ersten ehrlichen Mann in meinem Leben, danke ich herzlich für den Sonnenschein, den er mitgebracht hat, für seine liebevolle Führung und die Erfahrung, die er übertragen hat, und für das Lächeln, das er immer bei sich hat. Ich danke dir.

Contents

1 Introduction

From very early ages of history, plants and plant products have been the primary source of food, shelter and transport materials, clothing, fragrances, flavors and ingredients of medicinal substances for humankind[1].

In this context natural resins played an important role. They have been used as adhesives, as ingredients of cosmetic preparations, for their fragrance in daily rituals and in religious ceremonies, for coating materials and for their different medicinal effects, especially wound healing[2].

In ancient times Hindus, Babylonians, Assyrians, Persians, Romans, Chinese and Greeks as well as the people of old American civilisations like Incas, Mayas and Aztecs used natural resins primarily for embalming and for its incense in cultural ceremonies. Those people believed that when these materials were in contact with fire, the smoke and the fragrance they produce, would not only soothe their souls but also please their Gods. Burning of these natural resins had become an important action of their cultural life. They burned these resins during sacrification ceremonies or in their daily rituals to prevent the influence of bad spirits on their souls or to honour the dead or living people. The Egyptians used for these purposes olibanum (*Boswellia* spp.), myrrh (*Commiphora* spp.), bdellium (*Commiphora wightii*), mastic (*Pistacia lentiscus*), styrax (*Liquidamber orientalis*) as well as santal (*Santalum album*), cinnamon (*Cinnamomum aromaticum*), aloe wood (*Aloe succotrina*), cedar (*Cedrus* spp.) and juniper (*Juniperus communis*). Styrax, myrrh, colophonium (*Pinus palustris*), ceder and labdanum (*Cistus ladaniferus*) were also used for embalming.

Another extensive consumption of natural resins in the old times was their use as ingredients in cosmetic ointments. Except for the well known ones like Dragon's blood (*Daemonorops draco*), larch (*Larix decidua*) and pine turpentine (*Pinus* spp.) were also used for this purpose.

The utilisation of resins as coating material or varnish was another well known property. Surprisingly, this process was performed without diluting the resin in an organic solvent but covering the surface directly with it by fingers or by the help of a spatula. The solid resin was afterwards broken and melted with hot iron or with a torch, and the surface was polished later on. The analysis performed on the lacquer coatings of historical Egyptian graves had shown that storax (styrax oil), mastic and most probably amber were the mostly used materials for this purpose[2].

These resins were also used for their medical properties since antiquity. They served as disinfectants in operations and during the healing period of injuries. In the first pharmacopoeia written by the Greek botanist Dioscorides[2, 3] there were around 600 remedies advised, which were prepared from mixtures of natural resins and balsams as well as some herbal preparations. The antiseptic activity of resins was assumed to be known long before

since Egyptians used to burn a special mixture of them during plague and Indians had used gurjun balsam (*Dipterocarpus* spp.) against leprosy.

The dry distillation of rubber for industrial purposes in London by *Beale* and *Enderby* in the 1820's and the examination of the low boiling fraction (b.p. ca. 35 °C) for the first time by *Ure* and *Faraday* in 1825-1826 resulted in a mixture of products which were identified as C_5H_8 and C_5H_{10}. The former one was named "isoprene" by *Williams* in 1860. But it took about half a century to propose the correct structure of isoprene and elucidate the other constituent of this crude mixture as 2-methylbut-2-ene[4].

The investigation on turpentine oil in 1868 by *Hlasiwetz* and *Hinterberger*[5] resulted also in a liquid compound of the composition C_5H_8 as the vapour of the oil passed through a red-hot iron tube. Such investigations that had been done on turpentine (*Balsamum terebinthinae*), a balsam collected from the incisons on the young pine trees (*Pinaceae*) of different species, caused the term "*terpene*" to be involved in chemistry[6] since the compounds obtained during these investigations were called "*terpene*" and "*terpene derivatives*".

A little later, pharmacologist *Alexander Tschirch* (1856-1939) performed the first detailed study on natural resins. His studies involved the identification of the physical and chemical characteristics of resins, their classification into different types, and their chemical composition. Later in 1906, he published the results in his book[7]. To investigate the chemical composition of the natural resins he developed a methodology that mainly depended on the cold extraction and fractionation of the resin material with different solvents[8] (**Scheme 1.1**). Further derivatisation of these fractions such as acetylation, benzylation or esterification helped him to comment on the functionality and elemental composition of the resin constituents.

In the meantime the importance of *terpene chemistry* was increased with the proposal of the "*isoprene rule*" by *Wallach*[9] who served the natural products chemistry with more than one hundred publications in which he reported the formation of different derivatives of terpenes in crystalline form, their structure elucidations and the relationship between the basic skeletons of some monoterpenes and sesquiterpenes[10]. While he received the Nobel Prize in 1910 for his proposal of the isoprene rule, his success accelerated the development of natural product and terpenoid chemistry. The investigations of his successor, *Ruzicka*, improved this development and about a decade later he reintroduced the isoprene rule[11]. His following studies, especially on lanosterol[12], led him to formulate the "*biogenetic isoprene rule*" in 1953. As a result of these investigations and further studies, the field of *natural product chemistry* has become an intriguing and challenging area to concentrate on.

Tschirch`s Methodology

Resin material
in natural form

1) Dissolved in alcohol.
2) H_2O is added.

Pure Resin → Water soluble
and
acidic substances

Dissolved in ether.

Ether soluble
fraction → Ether insoluble
fractions

Extraction with a) $(NH_4)_2CO_3$
b) Na_2CO_3
c) KOH.

Free acids

Recrystallisation

Decantate

Resin acids

Extraction with
$Pb(Ac)_2$ in EtOH.

Acids in
amorphous
form

Resin alcohols
Essential oils
Esters

conc. KOH → Resin alcohols

Hydrodistillation → Essential oils

Esterification → Esters

Scheme 1.1. The methodology that A. Tschirch used for the analysis of natural resins.

Today plant based products, essential oils, plant extracts, natural resins and their preparations have a wide range of applications mainly in perfume and cosmetic industry, in food technology, in aroma industry and in pharmaceutical industry. This large spectrum of uses stimulated studies on natural products. The methods used in the analysis of plants that started at the end of the 19th century, only allowed investigations on crystalline constituents isolated from these extracts. Subsequent developments on vacuum distillation techniques provided the possibility to determine the volatile components of these extracts.

Along with the developments in extraction techniques, the development of chromatographic techniques primarily with planar chromatography (thin layer chromatography (TLC)) and other novel analytical methods were introduced to the benefit of scientists. Gas chromatography (GC) in the 1950's had opened a new dimension in the analysis of volatile compounds. In the meantime high performance liquid chromatography (HPLC) was introduced for the fractionation and isolation of more polar and non-volatile compounds.

The combination of gas chromatography and mass spectrometry (GC-MS) allows the rapid identification of not only volatile components but also plant extracts, by comparing their mass spectra with available libraries which build up with reference substances recorded under the same experimental parameters. The same principle has been applied in the last decade for liquid chromatography and mass spectrometry (LC-MS) for non-volatile plant constituents. Moreover, the invention of chiral stationary phases for gas chromatography, mostly based on cyclodextrins, has facilitated the identification of the enantiomeric composition of the isolated substances, especially in essential oils. Simultaneously, the advances in spectroscopic methods such as mass spectrometry (MS) and nuclear magnetic resonance (NMR) spectroscopy, have increased the speed of the identification and structure elucidation of natural products.

2 Aim of the Study

Olibanum which is an oleogum resin, exudes from incisions in the bark of *Boswellia* species. In this work chemical investigations were performed on olibanum resins obtained from different *Boswellia* species.

For at least 5000 years olibanum had been an important trade material for the civilisations located in North Africa and the Arabian Peninsula. It has been a precious commercial material even before Christian times because of the interest in this incense material of the old kings and queens like the Queen of Saba 700 B.C. With the dawn of Christianity, it was mentioned in the Bible as one of the presents which the three wise men had brought to Jesus on the night he was born, besides myrrh and gold. The wide use of this resin in religious ceremonies as incense material is still important in the Roman Catholic, Episcopal and eastern Orthodox churches that turn into an economical priority for countries like Somalia, Ethiopia, Oman, South Arabia and India in the production and import of olibanum, to western countries.

Except for its use in religious ceremonies, olibanum has been utilised as an important fixative in perfumes, soaps, creams, lotions, and detergents, with an oriental note in its scent, in the leading products of the perfume and cosmetic industry.

The interest of pharmaceutical companies created a third market for olibanum. Since ancient times it has been used in folk medicine for its antiseptic, antiarthritic and antiinflammatory effects. For this reason, in the last 20 years olibanum has gained increasing attention from scientists to better define its medical effects and identify the constituents responsible for these effects.

Therefore, in this study the primary aim was to find a rapid way to distinguish the different types of olibanum from each other and to identify the diagnostic markers for each species. This discrimination is important to improve the quality of the products obtained from olibanum, like its essential oil or the phytopharmaceuticals prepared from the resin acids. Even from an economical point of view this identification is needed for the satisfaction of the consumer. This was experienced in the 1980's in the church incense manufacturing industry. Ignorant of the quality difference between the "*Aden*" and the "*Erithrea*" types, the manufacturers chose to import the former one, because it was more available or cheaper. However, this product gives an unpleasant turpentine or rubber like smell when it is burned on charcoal,[13]. Another problem is that olibanum can be mixed with other resins which look alike to decrease the costs. For an unexperienced eye this failure is not obvious (**Fig. 2.1**) so that a rapid quality control is crucial.

Secondly, this work is intended to contribute to the studies on the acidic fraction of olibanum that has proved to have antiinflammatory activity especially against intestinal diseases like Morbus Crohn. The aim at this point was to identify the changes that come out through

different extraction methods and their influence on the composition of triterpenoic acids, "boswellic acids", of olibanum.

Fig. 2.1. **Left**: Different resins. **Right**: Different types of olibanum resins that were investigated in this study.

Besides, it was important to find out whether every type of olibanum contains these triterpenoic acids or if they are biosynthesized dependent on the species. These results can be used in the improvement and standardization of the phytopharmaceuticals prepared from olibanum, such as "*H15 Ayurmedica*" (400 mg dried *B.serrata* extract from Gufic Company/India), "*Boswellin*" (Sabinsa Corparation/Piscataway, New Jersey/USA), other olibanum preparations or in the development of more specific drugs.

Finally, it was also aimed in this study to identify the pyrolysis products of olibanum when it comes in contact with red-hot charcoal. It was supposed that hallucinogenic and carcinogenic products may be formed during this process. Moreover, it was planned to find out the fate of the biologically active triterpenoic acids and to observe the change in their activity to their former state with pharmaceutical bioassays.

Five different species of olibanum were chosen for these investigations: *Boswellia carterii*, *B. serrata*, *B. frereana*, *B. neglecta* and *B. rivae* (**Fig. 2.1**). The methods used for the fulfillment of these targets were primarily GC, GC-MS, pyrolysis-GC-MS, solid phase micro extraction (SPME), and thin layer chromatography (TLC). After isolation of the unkown compounds by chromatographic techniques, structure elucidation was attempted by 1- and 2-D NMR-spectroscopic techniques.

3 General Part

3.1 Plant Metabolites

Although plant extracts and herbal products were widely used throughout history, it was not possible to successfully isolate their active constituents prior to the 19th century. The complexity and diversity of these products and their specific pharmacological effects stimulated researchers to find explanations for the biosynthetic pathway for plant constituents starting with photosynthesis and resulting in most complex structures: Morphine, isolated from opium (*Papaver somniferum and P. setigrum*) that has powerful analgesic and narcotic effects; quinine, isolated from the bark of the *Cinchona* tree showing antimalarial activity; taxol[14], isolated from the stem bark of the western yew, *Taxus brevifolia*, having antitumor, antileukemic effects and today being used in the treatment of refractory ovarian cancer, metastatic breast and lung cancers, and Kaposi's sarcoma[15]; and salicin[16], a glycoside, first isolated from the bark of the willow tree in 1828 which led to the development of acetylsalicylic acid, the world's most widespread antiinflammatory and painkilling drug, aspirin (**Fig. 3.1**).
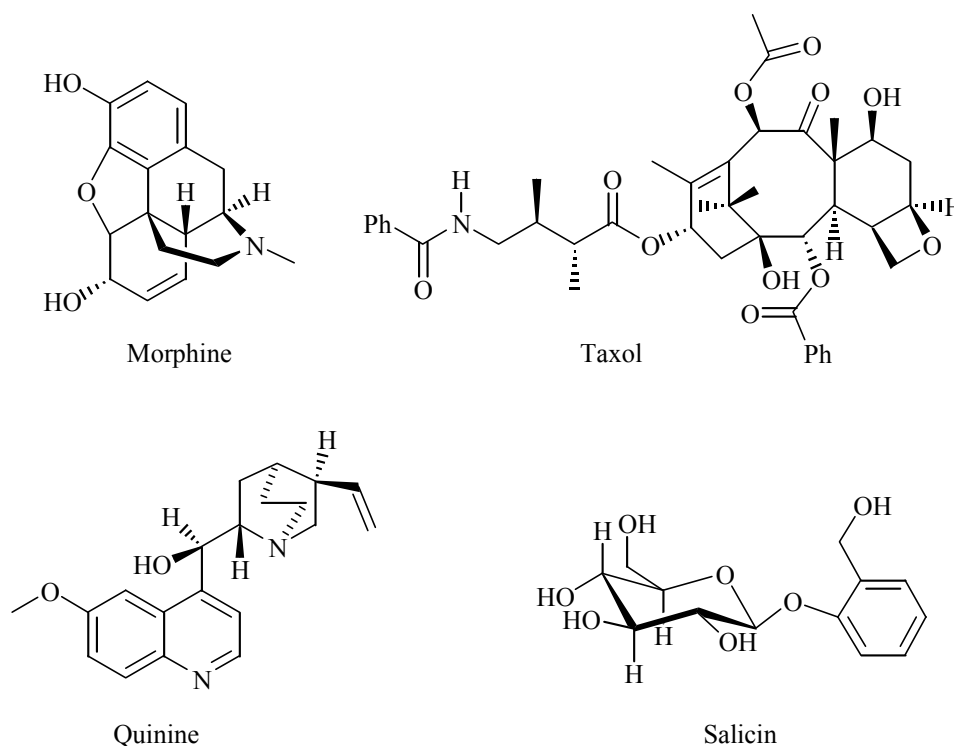
Fig. 3.1. Structures of morphine, quinine, taxol and salicin.

Within a short time the discovery of new bioactive natural compounds has increased and it has become crucial to understand the biosynthetic metabolism of plants in detail. Since these natural compunds generally do not belong to the group of compounds which are essential for the continuity of the lifecycle of a plant, it is common to distinguish between the primary and secondary metabolic pathways while studying these routes.

Primary metabolism, which actually proceeds in all living species, refers to the processes for synthesis and consumption of nucleic acids, α-amino acids, proteins, fats and carbohydrates that are essential for the survival and well-being of the organism.

In contrast, secondary metabolism, predominantly found in plants, microorganisms, fungi, marine organisms, and, to a lower extent, in animals, was proved to include processes non-essential for the continuity of the lifecycle or for growth and development. In plants, this metabolic pathway ends up with products like essential oils, resins, balsams, saponins and glycosides[17]. Secondary metabolites are produced in separate biosynthetical routes as compared to primary metabolites although primary metabolism provides some precursor molecules for the secondary metabolic pathway, such as acetylcoenzyme A which would complete its metabolic pathway with the formation of isoprenoids, the largest group of secondary natural compounds. Therefore, it is impossible to exactly distinguish between the two metabolic pathways (**Scheme 3.1**)[18].

Structures, distributions and levels of occurrence of secondary metabolites in general are valuable tools in defining evolutionary pathways and providing taxonomic markers. Quite a number of these metabolites are common in many species but some of them are characteristic to a particular family, genus or only to a single species. In fact, the specific constituents of certain species have been used for systematic determination. Groups of secondary metabolites were used as markers for chemotaxonomical classification. Such chemotaxonomy is based on the assumption that systematically related plants will show similar chemical characteristics. For such purposes, simply constructed compounds of widespread distribution are less valuable than more complex compounds formed in long reaction chains by the mediation of many enzymes and specified by many different genes[19].
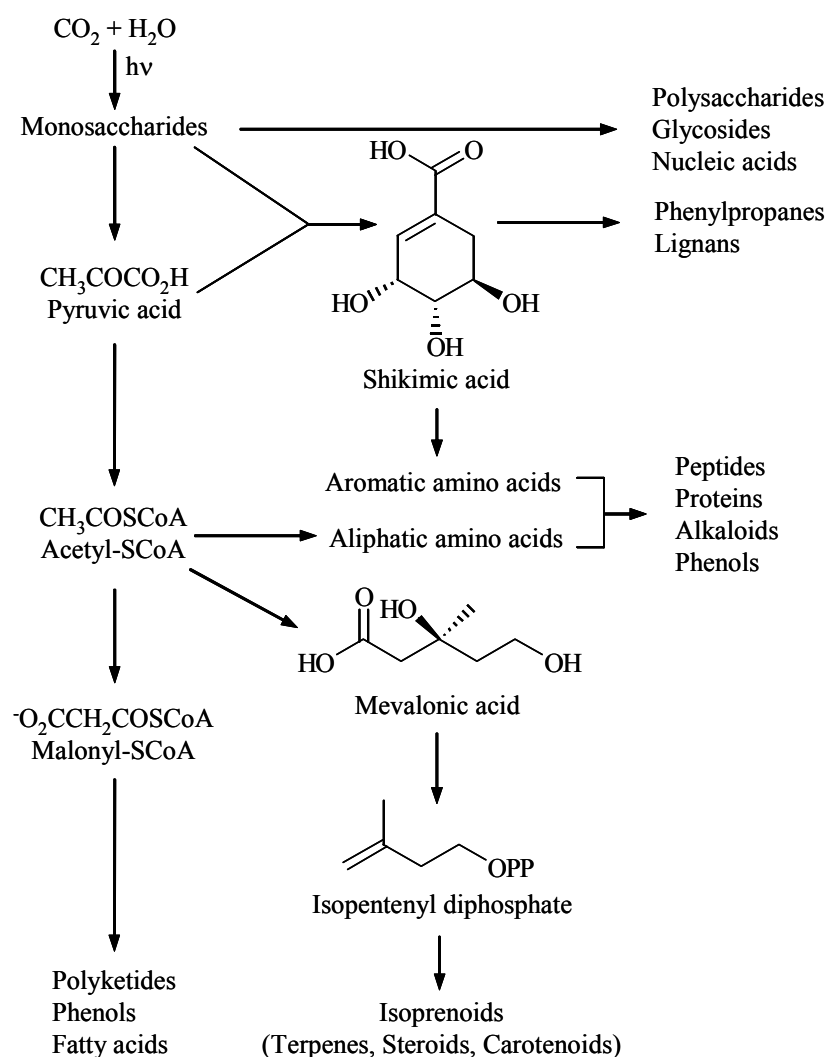
Scheme 3.1. An overview of primary metabolites and their links to secondary metabolism. PP stands for the diphosphate unit.

3.2 Isoprenoids: Terpenes, Terpenoids and Steroids

Isoprenoids are universal metabolites present in all living organisms. They include essential metabolites such as sterols, acting as membrane stabilizers in eukaryotes or as precursors for steroid hormones; the acyclic polyprenols, found in the side chain of the prenylquinones or in phytol from chlorophylls,which, via their phosphodiesters, act as sugar carriers for polysaccharide biosynthesis; the carotenoids in photosynthesizing organisms as well as a large variety of compounds with a less evident physiological role[20].

Terpenes, or terpenoids, are represented with more than 8000[6] compounds in this group of secondary metabolites comprising more than 80000[21] structures[*]. They show extraordinarily diverse structures and exhibit a large variety of physical and physiological properties. Their number increases every year with the addition of new structures, most of which have different biological effects[17].

In plants, the production of terpenoids is much more common than in animals or microorganisms. The production of large quantities of these natural products, their accumulation in cells and other storage compartments, their secretion in the plant body or emission from the plant to its surrounding is a challenging subject for biochemists, phytochemists and biologists in terms of finding out not only the biosynthetic pathway of these compounds in such specialized organisms, but also identifying their physiological properties in the association with other living organisms.

All isoprenoids, consequently terpenoids, are synthesized from one precursor "*isopentenyl diphosphate*" (IDP), which is the biological equivalent of isoprene (2-methyl-1,3-butadiene) (**Fig. 3.2**). It was formulated hypothetically as the "*isoprene rule*" first by *Otto Wallach* in 1887 that, terpenoids are the sequential combinations of isoprene (C_5) units[9]. The proposal of the "*biogenetic isoprene Rule*" in 1953 by *Leopold Ruzicka*[11,22] emphasized that this biosynthetical route has to be accomplished through a sequence of oligomerization reactions along with methylation, hydroxylation, oxidation, decarboxylation and with other cyclization and rearrangement reactions, which provide an enormous structural diversity. His hypothesis worked empirically for terpenoid biosynthesis without considering the involvement of the other possible precursors, assuming that isoprene is the only and the key precursor for this biological route.

Isoprene
2-Methyl-1,3-butadiene

Isopentenyl diphosphate
(IDP)
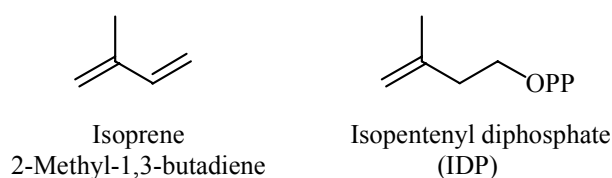
Fig. 3.2. An isoprene unit and its biological equivalent, isopentenyl diphosphate.

The classification of terpenoids depends on the number of isoprene units present in the skeleton of the product. Compounds, which are composed of one isoprene unit, are called *hemiterpenes* (C_5), in the case of dimerization of two isoprene units they are called *monoterpenes* (C_{10}). *Sesquiterpenes* (C_{15}), *diterpenes* (C_{20}), *sesterterpenes* (C_{25}), *triterpenes* (C_{30}) and *tetraterpenes* (C_{40}) follow this sequence, each having an isoprene unit more than the

---

[*] According to the data given in the Chapmann & Hall/CRC *Dictionary of Natural Products* (http://www.chemnetbase.com) this number has already reached approximately 170000 in 2003.

10

preceeding one. However, the biosynthetic routes to these terpenes do show some differences. The polymerization of an indefinite number of isoprene units results in *polyisoprenes* or *polyprenes* as in the case of natural rubber (**Scheme 3.2**)[6,23].

Steroids (C_{18-27}) belong to the group of isoprenoids as they originate from triterpenes. Labeling experiments showed that the formation of tetracyclic triterpenoids from 2,3-epoxysqualene is an introductory step in the formation of steroids[6]. The loss of carbon atoms and rearrangement reactions during their biosynthesis from triterpenes makes the isoprene units of steroids unrecognizable. Therefore, they are classified separately from terpenes[23] (**Fig. 3.3**).

Hemiterpenes
C_5
↓
Monoterpenes
C_{10}
↓
Sesquiterpenes ⟶ Triterpenes ⟶ Steroids
C_{15}   **C_{30}**   **$C_{(18-27)}$**
↓
Diterpenes ⟶ Tetraterpenes
C_{20}   (Carotenoids)
         C_{40}
↓
Sesterterpenes
C_{25}
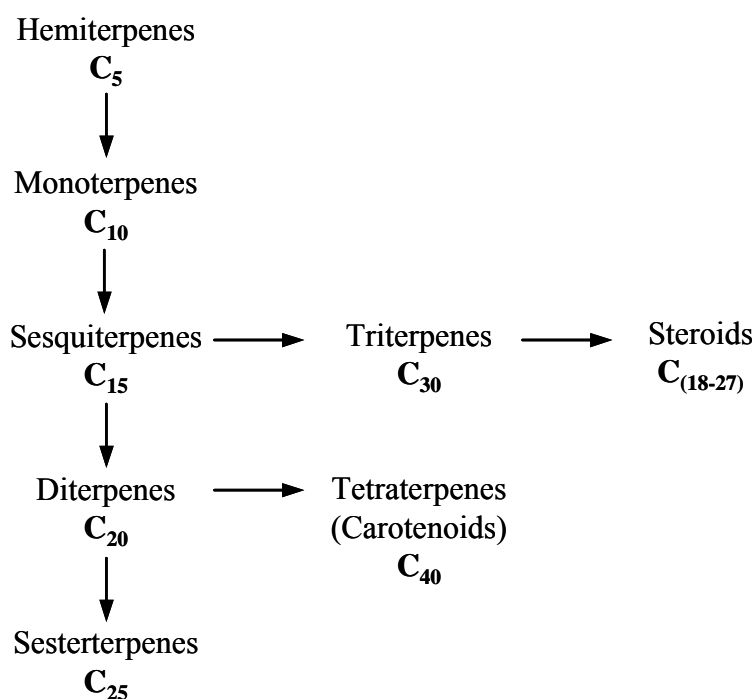
Scheme 3.2. An overview over the classification of terpenes.
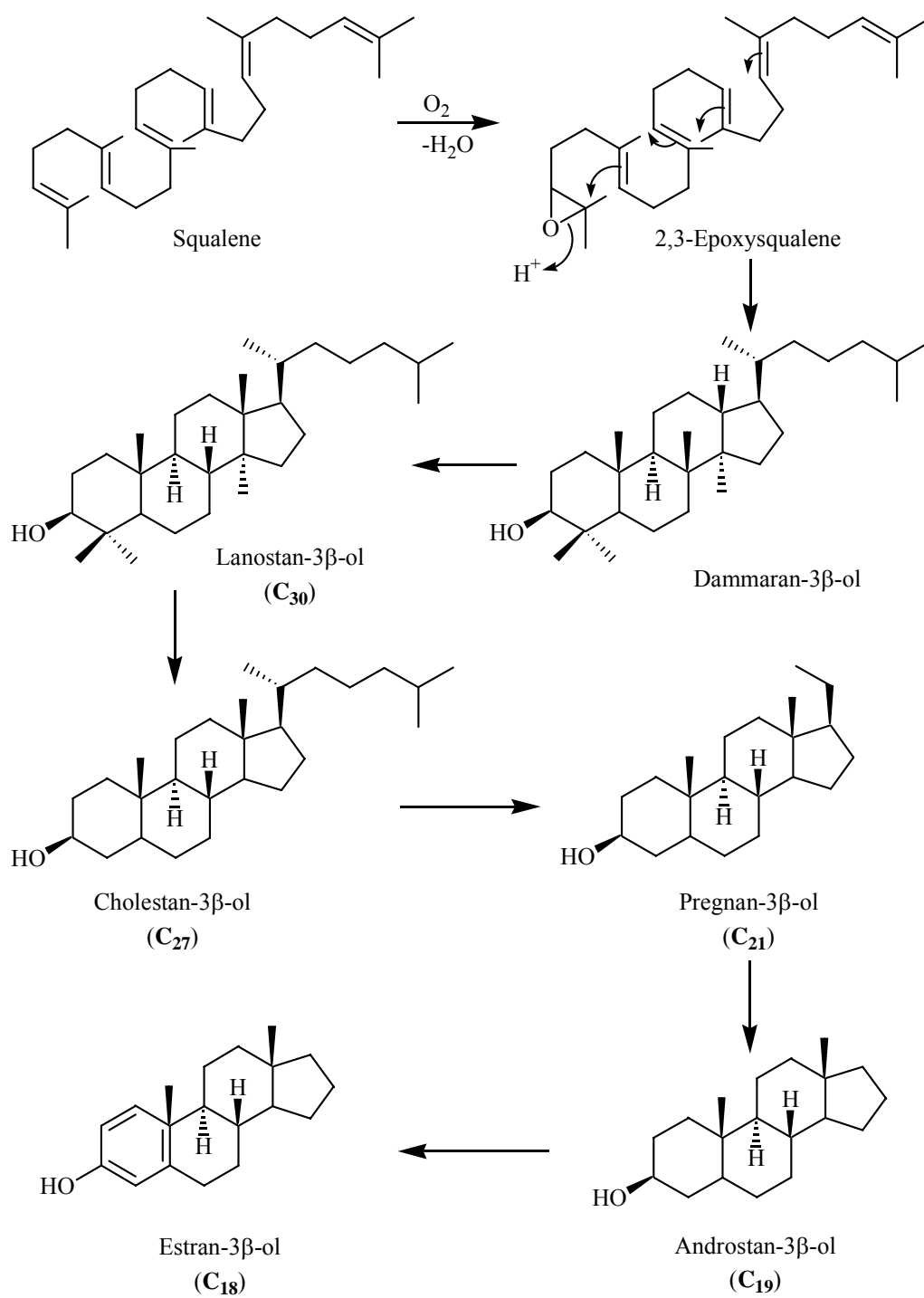
Fig. 3.3. The biosynthesis of some steroids from 2,3-epoxysqualene[6, 21].

3.2.1 Biosynthesis of Isoprenoids

Isopentenyl diphosphate (IDP) has proved to be the building block of isoprenoid biosynthesis. Until today several individual metabolic pathways were proposed for its biosynthesis. Except the classical *"acetate-mevalonate pathway"* and the recently proposed *"mevalonate-independent pathway"*-in other words *"triose-pyruvate pathway"* or *"deoxyxylulose phosphate pathway"*-there are also studies that concentrate on the incorporation of aminoacids in the isoprenoid biosynthesis especially where leucine degradation in higher plants took place through a *"mevalonic acid shunt pathway"*. However, this pathway has not been accepted completely as the former ones, because of the contradictory results on the formation of intermediates making use of free acids rather than coenzyme esters, as well as the insuffcient information on the intermediates, their regulation and their metabolic fate in plants[24].

3.2.1.1 Biosynthesis of Isopentenyl diphosphate via Acetate-Mevalonate Pathway

Since the 1950's feeding experiments with isotopically labeled precursors were performed in the field of isoprenoid biosynthesis. Mevalonic acid was first recognized as a precursor of cholesterol by *Tavormina et al.*[25] and *Cornforth et al.*[26] . Following research proved that it serves as an effective precursor of the acyclic isoprenoids squalene and rubber as well as carotenoids[27]. As a result of these studies on the incorporation of mevalonic acid into isoprenoids, the acetate-mevalonate pathway was established (**Fig. 3.4**).

The initial step in the acetate-mevalonate pathway is the reaction of two acetylcoenzyme A molecules via Claisen condensation by acetyl-coenzyme A acetyltransferase (**a**). The resultant acetoacetylcoenzyme A reacts with a third molecule of acetylcoenzyme A. This Aldol addition is catalyzed by 3-hydroxymethylglutarylsynthase (**b**) and (*S*)-3-hydroxy-3-methyl-glutaryl-coenzyme A (HMG-CoA) is formed which is reduced to (*R*)-mevalonic acid in the next step by HMG-CoA reductase[28] (**c**) with the use of ($NADPH + H^+$). The stepwise phosphorylation of mevalonic acid by mevalonate kinase (**d**) and consequently phosphomevalonate kinase (**e**) utilizing adenosine triphosphate (ATP) converts it into mevalonic acid 5-diphosphate[29]. The subsequent phosphorylation-assisted decarboxylation by mevalonate 5-diphosphate decarboxylase (**f**) yields isopentenyl diphosphate (IDP)[30].
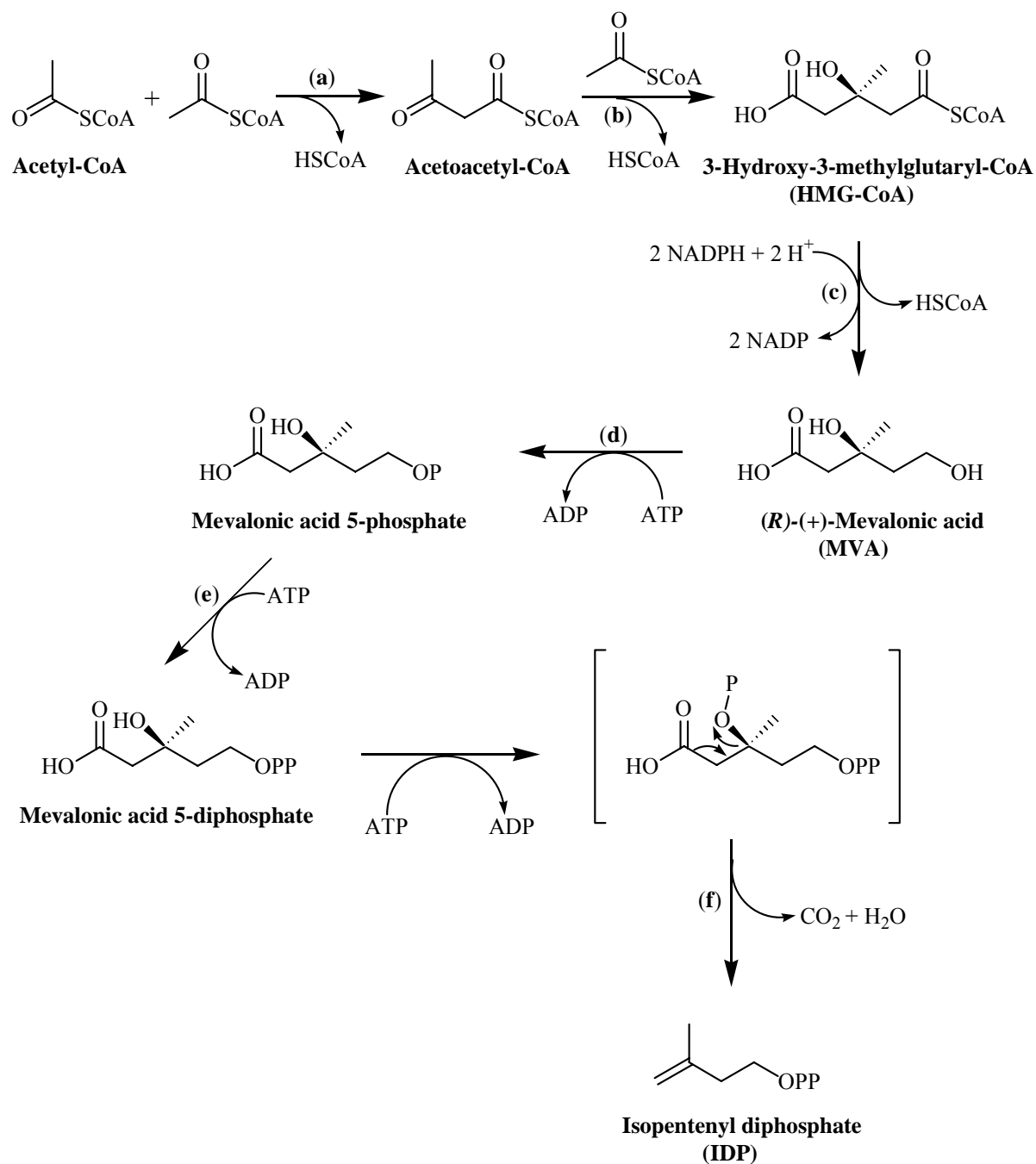
Fig. 3.4. Biosynthesis of isopentenyl diphosphate via acetate-mevalonate pathway. The enzymes involved in this pathway are: **a**: Acetyl-CoA acetyltransferase; **b**: 3-Hydroxymethylglutaryl synthase; **c**: 3-Hydroxy-3-methylglutaryl-CoA (HMG-CoA) reductase; **d**: Mevalonate kinase; **e**: Phosphomevalonate kinase; **f**: Mevalonate 5-diphosphate decarboxylase.

The acetate-mevalonate pathway has been accepted as the universal biosynthetic pathway until the end of 1980's. Nevertheless, some contradictory results have been observed.

Isotopically labeled mevalonic acid and acetate were usually not, or very poorly, incorporated into monoterpenes, diterpenes and carotenoids in higher plants although they incorporated into sterols, triterpenoids and sesquiterpenes quite efficiently[19,31]. In addition to this, it is proved that mevinolin (**Fig. 3.5**) which is an inhibitor of the HMG-CoA reductase, strongly inhibited the sterol synthesis in plants, but did not affect the production of carotenoids and chlorophyll, containing the diterpenic phytyl side-chain. These results were interpreted as the impermeability of the chloroplast membrane towards the precursor or the inhibitor[19,31]. However, the role of IDP was obviously accepted as isoprenoid precursor in chloroplasts via the mevalonate-dependent pathway although the possibility of the existence of another route could not be ruled out.
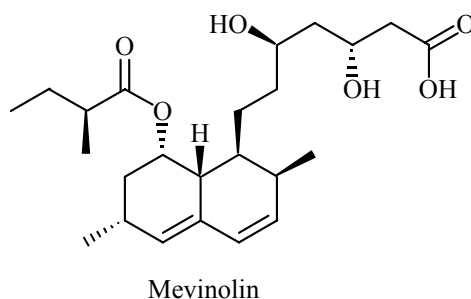
Mevinolin

Fig. 3.5. Mevinolin; HMG-CoA reductase inhibitor.

3.2.1.2 Biosynthesis of Isopentenyl diphosphate via the Deoxyxylulose Phosphate Pathway

The existence of another pathway was first proved with incorporation experiments of ^{13}C labeled D-glucose, acetate, pyruvate, and erythrose isotopomers into triterpenoids of the hopane series and the prenyl chain of ubiquinone (**Fig 3.6**) from several bacteria; *Zymomonas mobilis*, *Methylobacterium fujisawaense*, *Escherichia coli* and *Alicyclobacillus acidoterrestris*. The different labeling patterns of isoprenoids in contrast to the classical acetate-mevalonate pathway allowed the suggestion for a novel pathway for the early steps of isoprenoid biosynthesis [32,33]. Later on, the biosynthesis of the diterpenoids from two higher plants, *Gingko biloba* and *Salvia miltiorrhiza*, and the isoprenoids of the unicellular green alga *Scenedesmus obliquus* were found to be produced by this new biosynthetic route[34].

The C_5-framework of isoprene units was proposed to result initially with the transfer of a C_2-subunit derived from pyruvate to the C_3-subunit, glyceraldehyde 3-phosphate (GAP), in a thiamin dependent medium to obtain 1-deoxy-D-xylulose 5-phosphate (DXP) which is also involved in the biosynthesis of thiamin (vitamin B1) and of pyridoxol (vitamin B6). This transfer is catalyzed by DXP synthase (**a**)[35].

In the next step, DXP is converted into 2-*C*-methyl-D-erythritol 4-phosphate (MEP), the first putative intermediate with the branched isoprenic skeleton, by DXP reductoisomerase (**b**)[36]. In a cytidine 5′-triphosphate dependent reaction MEP is converted into 4-(cytidine 5′-diphospho)-2-*C*-methyl-D-erythritol by cytidine-diphospho methyl-D-erythritol synthase (**c**).

The phosphorylation of the hydroxy group at C-2 with ATP by cytidine-diphospho methyl-D-erythritol kinase (**d**) yields 2-phospho-4-(cytidine 5′-diphospho)-2-*C*-methyl-D-erythritol which will be further converted into 2-*C*-methyl-D-erythritol 2,4-cyclodiphosphate. A reductive ring opening produces 1-hydroxy-2-methyl-2-(*E*)-butenyl 4-diphosphate (HMBDP). For the last reductive reaction of HMBDP into IDP and dimethylallyl diphosphate (DMAPP), both labeling experiments[37,38] and genetic evidence[39,40] suggest two different routes, with the involvement of two different IDP isomerases[41] (**Fig. 3.7**).

Ubiquinone Q8   Aminobacteriohopanetriol
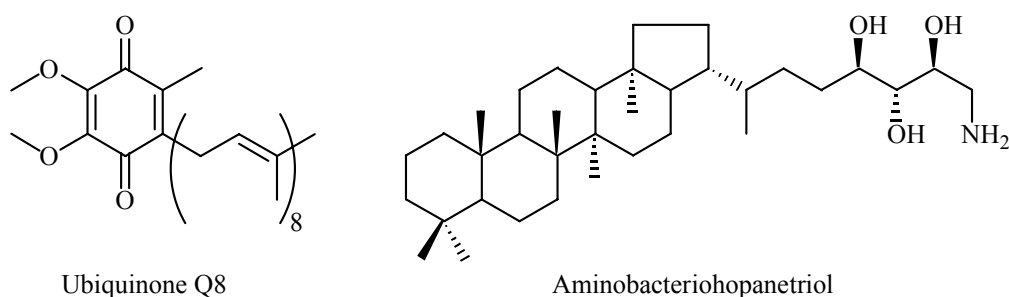
Fig. 3.6.   Structures of ubiquinone and hopane derivatives. Ubiquinone Q8 from *E. coli* and aminobacterio-hopanetriol.
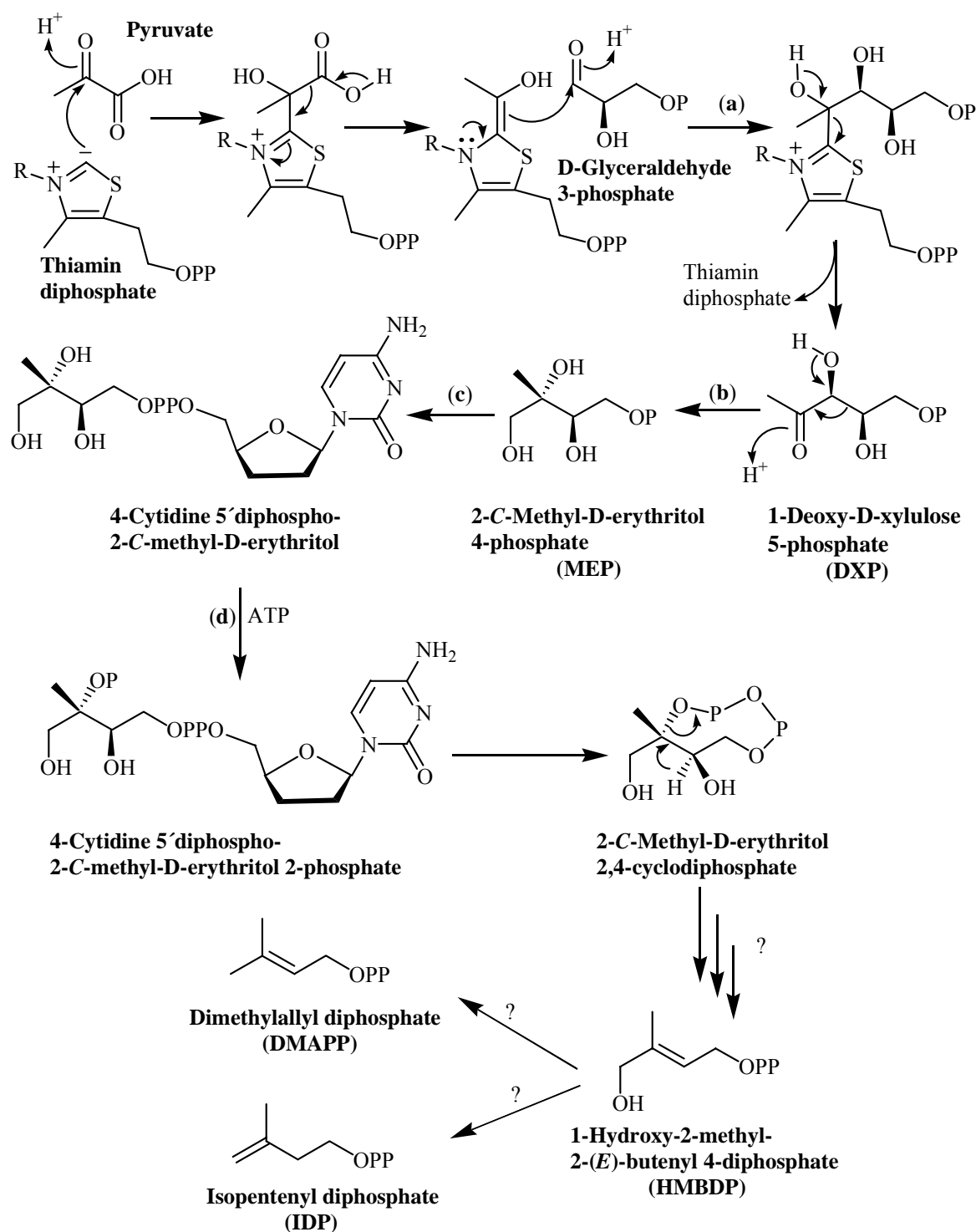
Fig. 3.7. Isopentenyl diphosphate biosynthesis through the deoxyxylulose phosphate pathway. The enzymes involved are: **a**: 1-Deoxyxylulose 5-phosphate synthase; **b**: 1-Deoxyxylulose 5-phosphate reductoisomerase; **c**: 4-Diphosphocytidyl-2-*C*-methyl-D-erythritol synthase; **d**: 4-Diphosphocytidyl-2-*C*-methyl-D-erythritol kinase.

Labeling experiments using D-glucose have been carried out to determine the differences between the mevalonate pathway and deoxyxylulose pathway in the biosynthesis of isopentenyl diphosphate and the origin of the C_2 and C_3 subunits, which are pyruvate and D-glyceraldehyde 3-phosphate (GAP) in the latter route, respectively. It is recognized that with most bacteria the glucose catabolism is proceeding via the *Entner-Doudoroff pathway* as it is observed with *Zymomonas mobilis*, a facultative anaerobic and fermentative bacterium[33,42]. However, a second route, the *Embden-Meyerhof-Parnas pathway*, takes also place in higher plants such as *Ginkgo biloba* and in some bacteria as *Escherichia coli*[33], since D-glucose is metabolized.

In the case of the *Entner-Doudoroff pathway*, D-glucose is converted to 2-keto-3-desoxy-6-phosphogluconate, followed by a cleavage into pyruvate and glyceraldehyde 3-phosphate (GAP). GAP is further converted into pyruvate that would yield acetylcoenzyme A upon oxidative decarboxylation (**Fig. 3.8**).
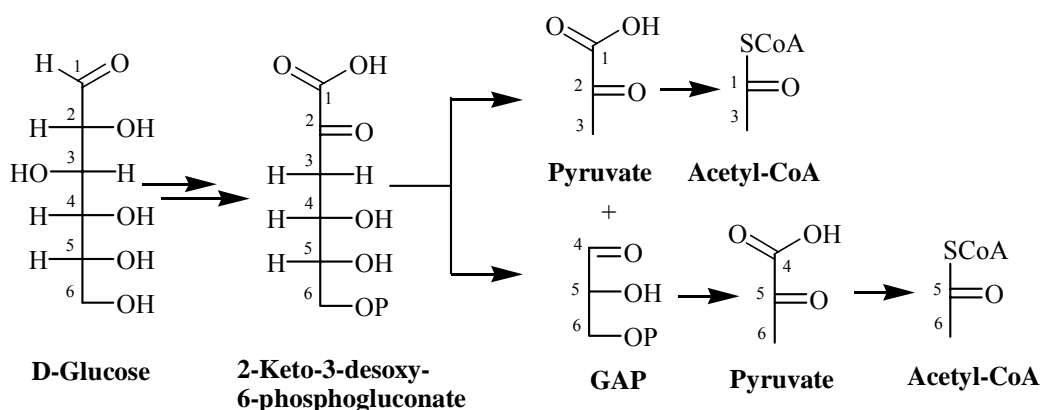
Fig. 3.8. Glucose catabolism via the Entner-Doudoroff pathway.

On the other hand, in the *Embden-Meyerhof-Parnas pathway*, D-glucose is first isomerised to D-fructose. Subsequent phosphorylation produces D-fructose-1,6-biphosphate, which is later cleaved into dihydroxyacetone phosphate and GAP. Dihydroxyacetone phosphate is interconverted to GAP via the triosephosphate isomerase. The terminal step, as in the Entner-Doudoroff pathway, is the conversion of GAP into pyruvate and subsequently to acetylcoenzyme A[43] (**Fig. 3.9**).

The two different catabolic pathways of D-glucose and the two possible biosynthetic routes result in four different labeling patterns of the synthesized isopentenyldiphosphate molecules where most carbons have dual characters, depending on the initially labeled D-glucose isotopomers (**Fig. 3.10**).
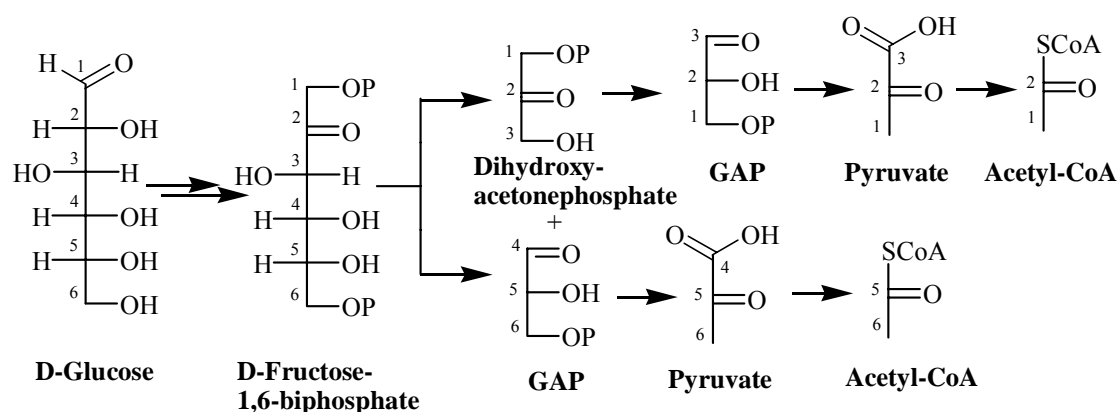
Fig. 3.9. Glucose catabolism via the Embden-Meyerhof-Parnas pathway.

With the use of these labeling patterns it is possible to determine which catabolic and biosynthetic pathways are preferred by the organism. Recent studies indicated that in nature both biosynthetic pathways can occur simultaneously in the organism. The choice of the biosynthetic pathway is variable for different organisms[41]. For example in bacteria, with different species, both mevalonate and deoxyxylulose pathways are observed. There is still no correspondence found with the type of the bacterium and the biosynthetic pathway that it utilizes.
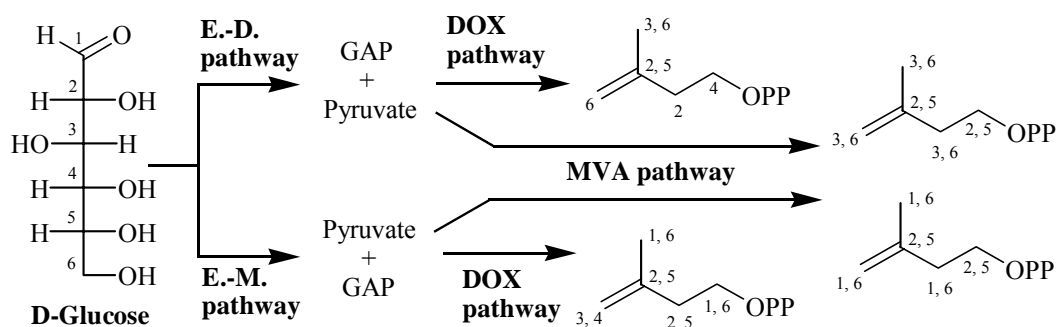
Fig. 3.10. The labeling patterns of isopentenyl diphosphate produced from labeled D-glucose.

Higher plants also utilize both metabolic pathways in terpenoid biosynthesis but they organize the production of different types of terpenes in various subcellular compartments[44]. The biosynthesis of monoterpenes, diterpenes, and carotenoids takes place in the plastids via the deoxyxylulose phosphate pathway; as in the case of ginkgolides, diterpenoic constituents of *Ginkgo biloba*, or of taxane diterpenes from *Taxus* [43]; in contrast to the biosynthesis of sesquiterpenes, triterpenes, polyterpenes, steroids and ubiquinones which are produced in the cytosol and in the endoplasmatic reticulum via the acetate-mevalonate pathway.

Plastoquinones are also biosynthesized by the deoxyxylulose pathway but in mitochondria. In other words, the deoxyxylulose pathway is bound to the plastidic compartment whereas the classical acetate-mevalonate pathway proceeds in the cytoplasmatic region[45,46,47]. Nevertheless, this compartmentation is no handicap for the organism since the exchange of some terpene precursors between the two compartments is possible. Recent studies reported that the synthesis of chamomile sesquiterpenes as well as the synthesis of the mono- and sesquiterpenoic volatiles emitted by lima beans (*Phaseolus lunatus*) and isoprenoid synthesis in *Arabidopsis thaliana* even in the presence of inhibitor molecules such as lovastatin and fosmidomycin, which is an antimalarial drug that inhibits the enzyme 1-deoxy-D-xylulose-5-phosphate reductoisomerase[48], produced evidences for this crosstalk[49] (**Fig. 3.11**).
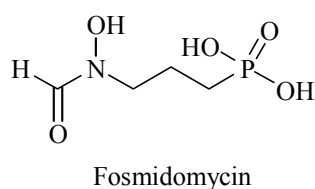
Fosmidomycin

Fig. 3.11. Fosmidomycin, antimalarial drug.

3.2.1.3 Biosynthesis of Isoprenoids from Isopentenyl diphosphate

After the biosynthesis of isopentenyl diphosphate (IDP), the next step in the biosynthesis of isoprenoids is its isomerisation into dimethylallyl diphosphate (DMAPP).

The isomerisation of IDP into DMAPP is postulated as a 1,3-allylic rearrangement reaction via a two-base cationic mechanism. This interconversion is catalysed by isopentenyl diphosphate isomerase (IDP isomerase) (**Fig. 3.12**)[30].
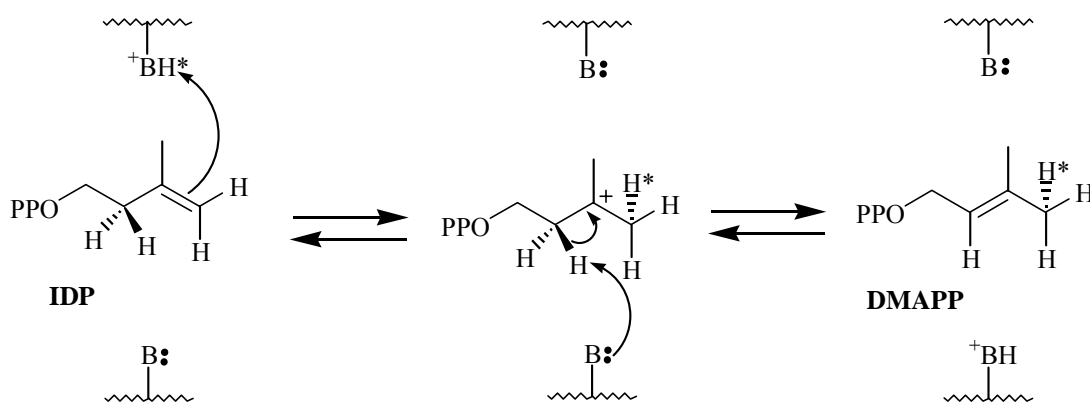
Fig. 3.12. Isomerisation of IDP into DMAPP.

The isomerisation of IDP to DMAPP is followed by the condensation of IDP and DMAPP or other prenyl diphosphates to give higher homologues which are the precursors of all isoprenoids[33]. The reaction sequence is catalyzed by prenyltransferases.

It is assumed that the first step in this sequence is the formation of the allylic cation which will condense with a second molecule of IDP to allow the formation of geranyl diphosphate or the monoterpenes in general. The condensation occurs in a "*head-to-tail*" fashion where the nucleophilic site of IDP is named "head" and the electrophilic site "tail". Analogous condensation reactions may proceed either by addition of IDP in each step or the condensation of the synthesized prenyl diphosphates in "*tail-to-tail*" fashion, to biosynthesize the precursor molecules of other terpene classes; i.e, the addition of an IDP to geranyl diphosphate yields farnesyl diphosphate, which will form geranylgeranyl diphosphate after the addition of another IDP molecule. The latter two diphosphates are the starting substances in the biosynthesis of sesquiterpenes and diterpenes, respectively. The condensation of two farnesyl diphosphate molecules produces squalene for further biosynthesis of triterpenes. Similarly, the condensation of two geranylgeranyl diphosphates ends up with the formation of 16-*trans*-phytoene the precursor of the biosynthesis of tetraterpenes, the carotenoids (**Fig. 3.13**)[6, 33].
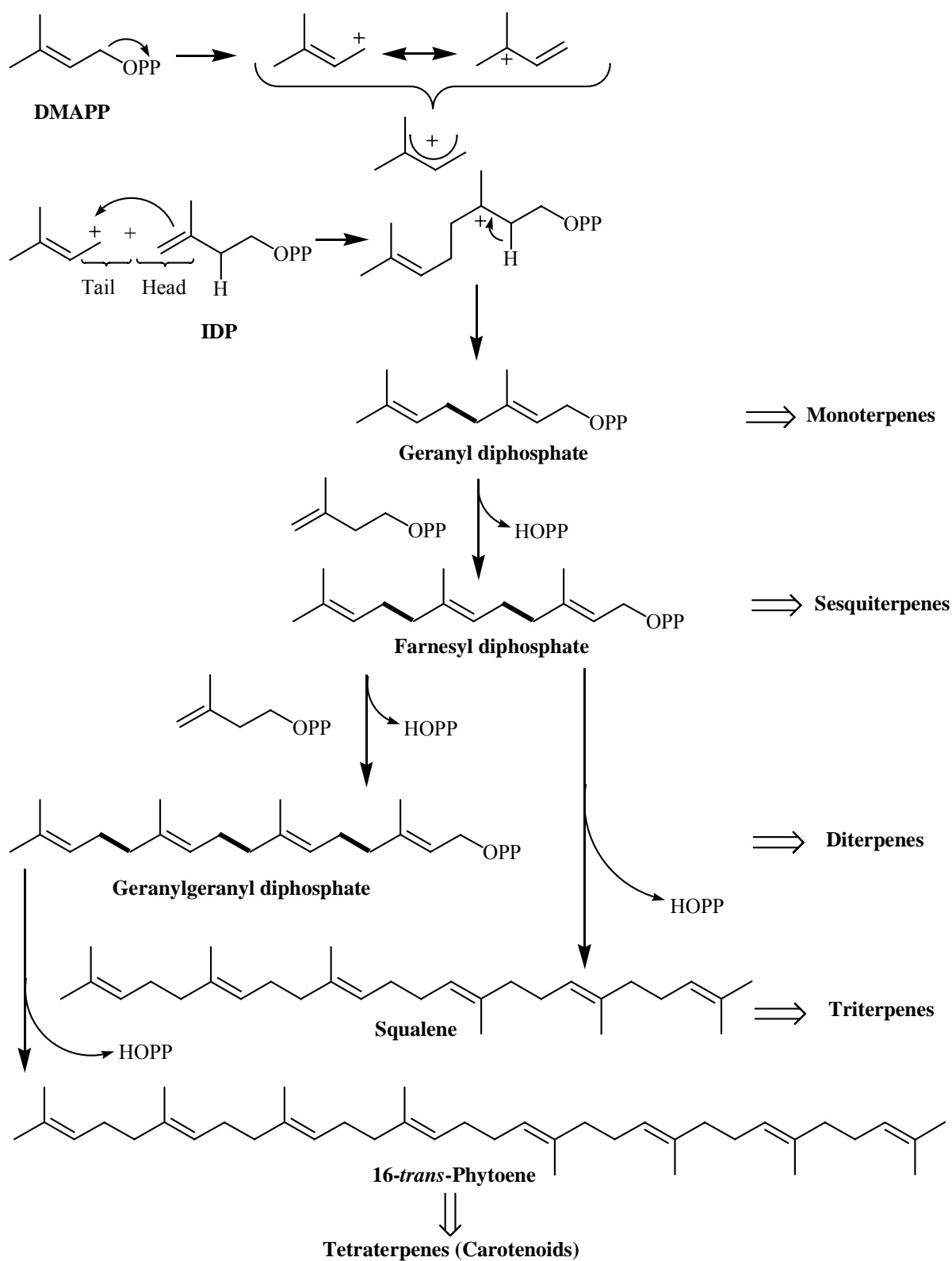
Fig. 3.13. Schematic expression of the biosynthesis of different terpene classes.

3.2.1.4 Biological Significance of Terpenoids and Other Secondary Metabolites

The need to explain the *raison d'être* of the enormously rich structural variations of the secondary metabolites that are encountered rather in plants than in animals, brought up some arguments claiming that they can not be simply "waste products" of primary metabolism accumulated in the plant cell because of the absence of an efficient excretory system in these organisms. Beginning with the latter half of the last century, reasons for their existence have been confirmed in many studies in the field of chemical ecology[50].

The immobile living style of plants has forced them to develop a self-defense system against herbivores, insects or microorganisms, as well as an intraspecific communication system and exchange of information with other living organisms that would support their production and the continuity of their race. Secondary metabolites as terpenoids, flavonoids, alkaloids and many other compounds are responsible for data transfer between different kinds of living organisms.

For example, a group of these metabolites called phytoalexines, in which isoflavonoids, sesquiterpenes, furanoterpenes, polyacetylenes and dihydrophenanthrenes can be encountered, exhibit antimicrobial activities and act in the plant body against phytopathogenic microorganisms such as fungi and viruses. The production of these compounds in the cell is induced as a response to infections in the plant, to stress situations like drought, cold, severe exposure to UV-light or to herbivorous attack[51].

In this context, terpenoids are very valuable sources for plants because of their toxic and deterrent properties which are useful in defense systems and because of their volatility which renders them ideal signals in communication systems.

Terpenoids, from volatile monoterpenoids to nonvolatile triterpenoids, may be broadly deterrent against herbivory on plants. Not only individual compounds but also mixtures of related structures often contribute to produce antifeedent and toxic effects. The pine bark beetle, *Dendroctonus brevicomis* avoids feeding on pine trees which are high in limonene content, although α- and β-pinene, myrcene and 3-carene do not disturb its feeding. Most sesquiterpene lactones and some diterpenes appear to have repellent effects towards insect herbivores. The triterpenoid azadirachtin is a well known natural insecticidal agent. Slugs and snails are also known to feed on a wide variety of plant species. But two sesquiterpenes, petasin and furanopetasin which occur in *Petasites hybridus* repel snails feeding on this plant (**Fig. 3.14**)[50].

Azadirachtin

Petasin   Furanopetasin
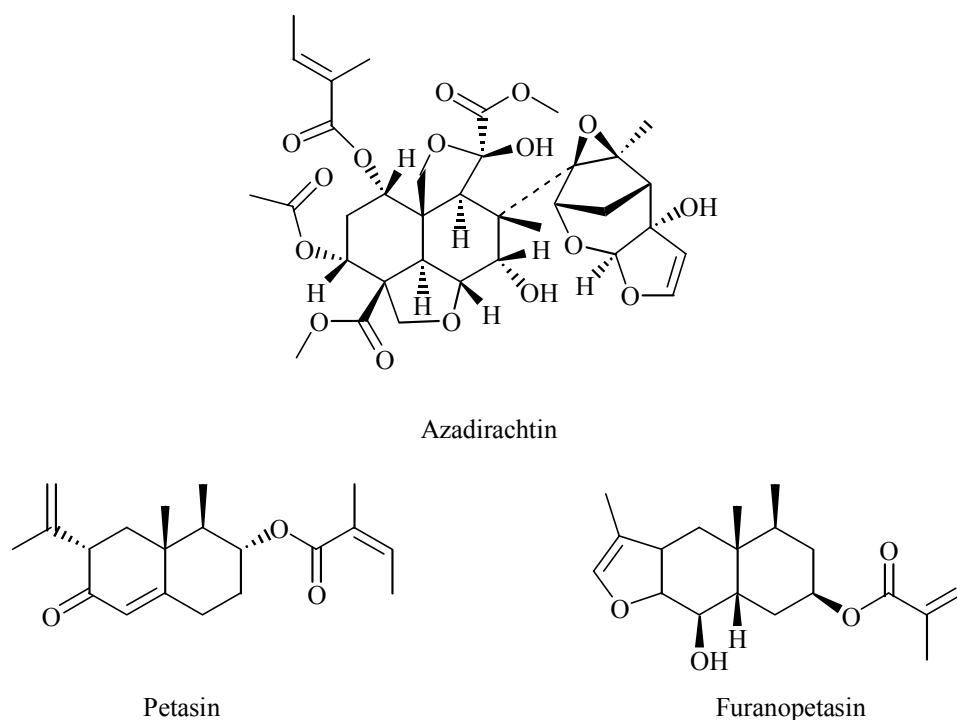
Fig. 3.14. Structures of azadirachtin, petasin and furanopetasin.

It should be noted that the volatile isoprenoids also control insect behaviour and development. The volatile semiochemicals which generally cover isoprenoids in the range C_5-C_{20}[52], are used by insects for signalling over some distance.

The various biological effects of secondary metabolites, which are recognized through traditional medicine, affect the drug discovery and development nowadays. Many sesquiterpenes showing a variety of pharmacological effects, like cytotoxic, antibiotic, antifungal, antiviral, even sedative effects[53], as well as many biologically active diterpenes[54] and triterpenes[55], are utilized or modified as precursors of active substances to discover new antimalarial, antiviral, anticancer, and many other drugs.

3.3   Essential Oils

Essential oils are defined as mixtures of volatile compounds excreted by glandular hairs or deposited in the plant body in cell organelles, idioblasts (oil cells or bodies), schizogenous or lysigenous cavities or ducts[56]. The essential oils occur in various parts of the plant, sometimes in all organs and sometimes in certain tissues only. They are the end products of secondary metabolism, and most of their components are terpenoids, generally monoterpenes and sesquiterpenes, as well as some diterpenes and aromatic compounds, such as phenylpropane

derivatives. Hydrodistillation is the most frequently used technique to isolate these lipophilic mixtures.

In addition to their ecological significance in nature, essential oils are important raw materials for perfume, cosmetic, food and pharmaceutical industries. Some of them have a long history as phytopharmaceuticals, especially in Egypt and in India, since 1600 B.C.[57]. They have proved to possess antimicrobial, spasmolytic, antiseptic, diuretic, sedative, antiphlogistic and many other activities[58, 59].

3.4 Natural Resins

Besides the essential oils, considerably larger amounts of non-volatile substances are produced in the plant cells as a result of their metabolic routes. They are generally known as "*resins*" and their solutions in essential oils as "*balsams*". Nevertheless, it is difficult to classify the different types and find a common identification for resins.

Since resins and essential oils are mostly composed of terpenoids they would be classified by plant physiologists as secretions, as the end-products of plant metabolism which are collected in secretory depots and become immobile although research results proved that they may undergo chemical rearrangements[2].

A. Tschirch was the first scientist who tried to classify them. He thought that common features among resins were not their properties but their origin. He also indicated that resins represent plant excretes, that is substances, which should be eliminated from the plant at the end of the metabolic pathways, in contrast to secretions actually serving the plant metabolism.

He divided resins into two groups: "*physiological*" for the usual metabolic end products and "*pathological*" where the production of these substances was observed first when the plant was wounded. Although the chemical route for resin formation was not very clear, for their accumulation in the plant body he assumed that cellulose in many cases played an important role. He called "*lysigenous resin formation*" when the cell walls in the plants were dissolved and instead of a cell a cavity was formed which was then filled with resin.

A second type of formation was the development of the resin in the cell and its diffusion through the cell wall. The plants which had this kind of cell formation had usually bigger intercellular gaps where the resin was collected. These gaps were usually small at the beginning but grew with time either equally in all directions or only in one direction which was mostly parallel to the stem to form the "*resin channels*". This kind of formation of resin channels through restructuring of the cell gaps and accumulation of the resin in these gaps was called "*schizogenous resin formation*".

At the end of his survey about the resins from different plant families, *Tschirch* concluded that mostly these two types of resin formation occur together as "*schizo-lysigenous*" in which

first the schizogenous formation occurred then the cell wall disappeared with a chemical regeneration, and the resin channels were enlarged[7, 8]. His terminology in resin chemistry is still in use although some of his hypothesis was proved to be incorrect[2] such as the disappearance of the cell walls. They only became unrecognizable because of the enlarged excrete channels.

Such channels are typically observed in many plant families; *Pinaceae*, *Anacardiaceae*, *Hypericaceae*, *Guttiferae*, *Dipterocarpaceae*, *Burseraceae*. These channels are surrounded with epithel, thin walled and very tight placed cells, like the excrete pockets. This kind of cellular organization has a double function for the plant; first it isolates excrete in a separate space and secondly it closes the excrete passage hermetically from the intercellular system of the body. These resin channels are generally connected to each other through horizontal gaps to the interior. By this way, the plant succeeds to impede secretions to flow outside.

It is possible to make different classifications for the resins, for example, according to their appereance or their chemical composition. In many cases three classes of resin types were recognized: "*balsam*", viscous but fluent plant products; "*resin*", when this fluent product becomes solid after a short time; "*gumresin*", contains the resin constituents together with the plant gum[8].

Chemical classification of resins is based on their constituents. It is common to classify them into three groups: "*terpenresins*", "*benzresins*" and "*gumresins*".

Terpenresins contain mainly diterpenoic and triterpenoic acids or triterpenoic alcohols. Colophonium, dammar, mastics belong to this class of resins.

On the other hand, *benzresins* are composed of mostly phenylpropane derivatives. Besides cinnamic acid and coniferylalcohol they contain lignanes, xanthone and highly condensed coumarines. In most cases they are found in their esterified forms. Peru balsam and guajak resin can be considered as examples of this class.

Gumresins flow as a yellow or white latex from the incisions of the plant and hardens there into amorphous, tear shaped products with an aromatic scent. They are composed of 30-60 % resin, 5-10 % essential oil, which is soluble in organic solvents, and the rest is made up of polysaccharides, which are soluble in water. The darkening of the color is a result of autoxidation, polymerization and enzymatic reactions. The most well-known examples are myrrh and olibanum[60].

Still, the significance of the resin for a plant is not precisely known. But in contrast to *Tschirch* who believed that they do only serve for the healing of wounded parts in the plant organism since some of them exhibit no obvious physiological activities, they, nevertheless, have been used in folk medicine since very old times, as antiinflammatory and antiseptic materials or to cover wounds like the plasters of today. In daily rituals and religious ceremonies, resins have been burned for their aromatic scents. Olibanum and myrrh are the oldest scents mentioned in history since 5000 B.C.[61]. Today the utilisation of resins is still

common in pharmaceutical, perfume and cosmetic, aroma, laquer and varnish industries in addition to their cultural and folkloric uses.

4   Methods Used for The Analysis of Plant Extracts

Plants metabolise a wide range of constituents that have diverse properties. Several methods have been developed to extract these constituents out of plants as analysis material. Hydrodistillation, Soxhlett extraction, super critical fluid CO_2 extraction, simple solvent extraction, solid phase micro extraction (SPME) are some of the techniques used for this purpose in natural products chemistry.

The analytical identification of a plant extract requieres an investigations by GC-MS, and recently developed LC-MS, where analytical data of the constituents of the essential oil or the plant extract are compared with those compiled in databases constructed under the same experimental parameters, which known compounds are verified during this procedure, the unidentified mass spectra are considered to be new substances most of the time and their isolation proceed through different chromatographic methods.

The isolation of a substance follows a general procedure in which the fractionation of the whole extract by column chromatography (CC) on different stationary phases such as silica gel, sephadex, etc. that helps to group the substances according to their polarity or molecular size, respectively. This is usually the first step that is followed by the optimization of the separation technique for the target molecule by other chromatographic means: Thin layer chromatography (TLC), high performance liquid chromatography (HPLC), gas chromatography (GC). The optimization of the separation process; the search for the suitable mobile phase, adsorbent, flow rate or temperature; is reached in analytical scale and the seperation of the target molecule is performed in preparative scale. The last step in the isolation procedure is the end-purification of the molecule which will be followed by its preparation for structure elucidation.

The identification of a molecule is proceed through the interpretation of the data obtained from spectroscopic analysis. The chromophores existing on the molecule is detected by UV/Vis spectroscopy (UV) where the functional groups that it possess are identified by Infrared and Raman spectroscopy (IR). The molecule mass is detected by a mass spectrometric (MS) analysis.

The structure elucidation of the molecule is achieved by the interpretation of a combination of different 1- and 2-D NMR measurements. The most used techniques in structure elucidation are ^{1}H-NMR, ^{13}C-BB-NMR, DEPT, PENDANT, HMQC, ^{1}H-^{1}H COSY, HMBC and NOESY spectra.

From ^{1}H-NMR spectrum one can determine the chemical shift values of the proton signals, information about the chemical environment of the protons as well as the number of neighbouring protons from the splitting of the multiplets. The integration of the area under the signals provides information about the relative number of protons in the molecule.

^{13}C-BB-NMR produce information about the chemical shifts of the carbon signals in the molecule.

DEPT spectrum (distortionless enhancement by polarisation transfer) provides the classification of the carbon signals as methyl, methylene or methine groups. However, DEPT does not permit the detection of the quaternary carbon nuclei. This problem is annihilated by the introduction of a new NMR pulse sequence. PENDANT (polarization enhancement nurtured during attached nucleus testing) permits to observe the resonances from ^{13}C in all chemical environments, including quaternary carbon nuclei.

With the help of HMQC spectrum (heteronuclear multiple quantum correlation) the correlation of ^{1}H- and ^{13}C-NMR spectra is possible. It provides the identification of $^1J_{CH}$ connectivities and thereby applies only to those C atoms which are linked to H and not to quaternary C atoms.

^{1}H-^{1}H COSY experiment yields NMR spectrum in which ^{1}H chemical shifts along both frequency axes are correlated with each other. As a result not only the proximity of protons but also some long range couplings (like W coupling) are detected.

In HMBC spectrum (heteronuclear multiple bond correlation) the C*H* relationships through both two and three bonds ($^2J_{CH}$ and $^3J_{CH}$ connectivities) are indicated.

All these 2-D NMR experiments provide information about the basic skeleton of a molecule. The relative structure of a molecule is determined by the interpretation of its NOESY spectrum. Changes in signal intensities caused by spin decoupling are reffered to as the Nuclear Overhauser Effect (NOE). NOE difference spectroscopy has proved to be a useful method for studying the spatial proximity of protons in a molecule[62,63,64,65].

The determination and specification of absolute configuration is an essential part in the characterization of a molecule. According to *Cross* and *Klyne* (1976), configuration of a molecule is identified as the arrangement of the atoms in space of a molecule of defined constitution without regarding arrangements that differ only as after rotation about one or more single bonds[66].

Stereoisomers are the compounds whose molecules have the same connectivity but differ in the arrangement of their atoms in space. They are studied under two categories, *enantiomers* including the stereoisomers that are mirror images of each other and *diastereomers* which do not show this property.

Enantiomers occur only with those compounds whose molecules are *chiral*. A chiral molecule is defined as one that is not superposable on its mirror image. Existence of *stereocenters* in a molecule establishes this geometrical difference between its enantiomers. A stereocenter is defined as an atom bearing groups of such nature that an interchange of any two groups will produce a stereoisomer[67]. Nevertheless, chirality does not influence the physical properties of these enantiomeric substances. Enantiomers have the same melting and boiling points,

refractive indexes, show the same solubility in common solvents and other than some exceptions have the same spectroscopic properties. However, through their behaviour toward the plane polarized light they can be recognized. The different enantiomers of a molecule can rotate the plane of polarization in equal amounts but in opposite directions as the beam of plane polarized light passes through this enantiomer. Therefore they are called as optically active compounds.

It is not earlier than the latter half of the 19th century that the optical activity, chirality and molecular assymmetry became intriguing topics after the inventions of *Pasteur*. Subsequently, chirality is recognized as a phenomenon that dominates the living world.

Enantiomers exist for many organic and anorganic substances and practically in all molecules which are decisive for the emergence, development and maintenance of living organisms. Chiral centers are common in the building blocks of proteins, carbohydrates and nucleic acids.

The biochemical processes proceeding in the organism are therefore mostly stereoselective in which the matching of the spatial arrangements of reactants and key molecules play an important role.

The high stereoselectivity of biomolecules in the body is also reflected to the compounds involved to this system externally. The concept of chirality is seriously considered in drug design after a tragedy is experienced in past years.

Thalidomide, a racemate of a glutamic acid derivative, was developed in 1963 to alleviate the symptoms of morning sickness of pregnant women. However, the (*S*)-(-)-enantiomer found in this racemic mixture exerted embroyotoxic and teratogenic effects whereas the (*R*)-(+)-enantiomer had no such effects under the same experimental conditions.

Another example emphasizing the importance of using pure enantiomers in drug design is 3,4-dihydroxyphenylalanine (DOPA). The L-enantiomer is recognized as an effective medicine in the treatment of Parkinson's disease. On the other hand, the D-enantiomer is found to have toxic effects (**Fig. 4.1**)[68, 69].

(*R*)-(+)-Thalidomide   L-DOPA
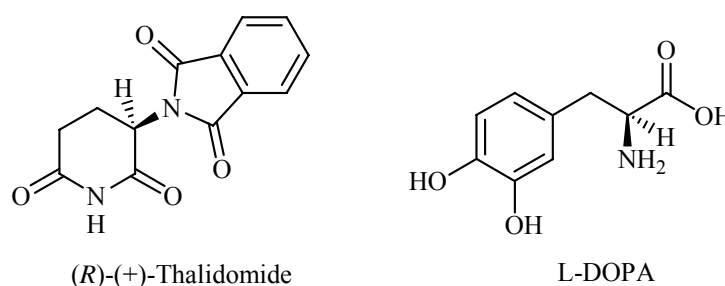
Fig. 4.1. Structures of (*R*)-(+)-thalidomide and L-DOPA.

The detection of enantiomers separately and identification of their absolute configurations are not only important for pharmaceutical studies, but also for flavour and fragrance substances containing different olfactometric properties, as well as other organic substances such as pesticides, pheromones having diverse biological effects with their enantiomers.

One method, used for the analysis of such naturally occurring enantiomers is gas chromatography. However, their detection is only possible with chiral stationary phases. The introduction of modified cyclodextrine phases is considered to be the most progressive step in this area.

Cyclodextrines (CD) are α-(1→4)-connected glucose oligomers with 6, 7, 8 glucose units that correspond to α-, β- and γ-CD. They can be prepared by enzymatic degradation of starch with cyclodextrin-glucanosyltransferase (CGTase) from *Bacillus macerans* or *Bacillus megaterium*. Their torus-shaped geometry establish the intramolecular hydrogen bonding of 2- and 3-hydroxy groups at the wider opening releaving the hydrophilic character of the outer surface. However, it is the hydrophobic character of the inner cavity which favours the selective inclusion complexes of flavour and fragrance compounds, pharmaceuticals and other bioactive molecules (**Fig. 4.2**)[70].
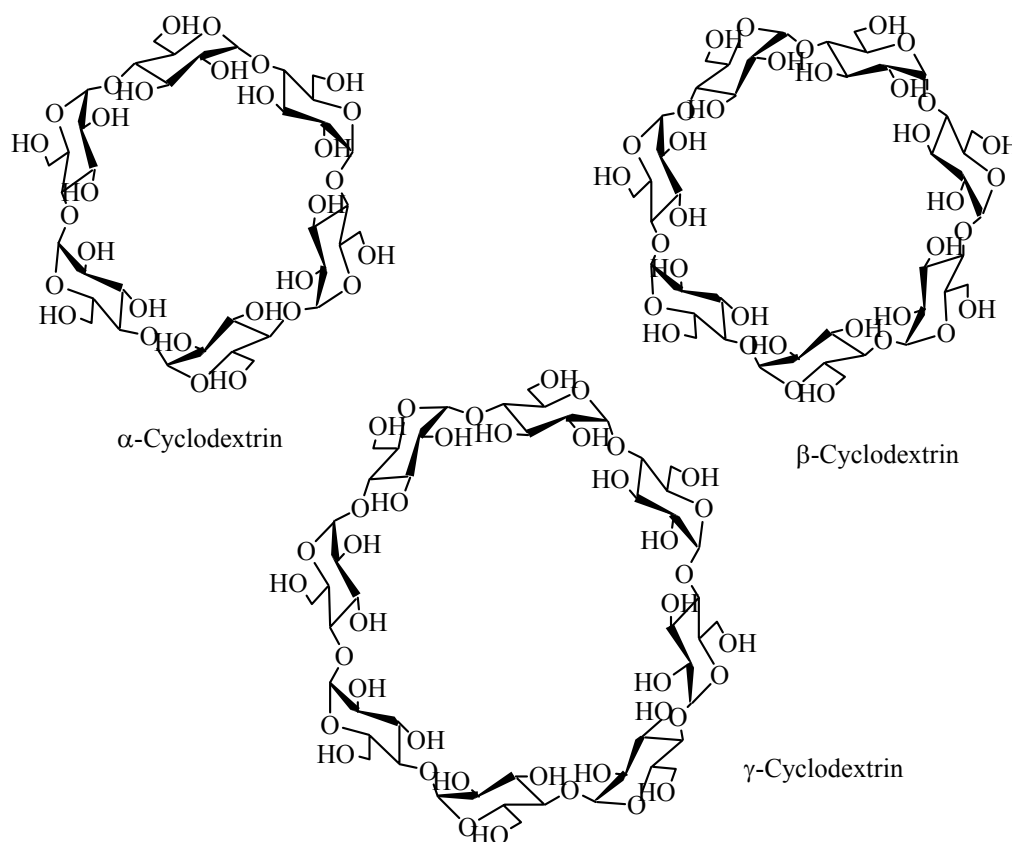
Fig. 4.2. Structures of α-, β- and γ-cyclodextrin.

The first gas chromatographic enantiomer separation is reported by *Koscielski*, *Sybilska* and *Jurczak* in 1983 involving CDs as chiral additives to formamide as a stationary phase in short packed columns. The recognition of the nonavailability of unmodified CDs with capillary columns *per-O*-methylated CDs are used by *Szejtli et al*. However, these CDs have rather high melting points which are unfavourable for gas-liquid chromatography. *Schurig* und *Nowotny* tried to lower the melting point of the stationary phase by using a solution of *per-O*-methylated β-CD dissolved in a considerably polar polysiloxane (OV 1701).

On the other hand, *König*, *Wenz* and *Lutz* introduced modified CD phases with longer alkyl- or acylchains. Most of the *per-O*-pentylated and selectively 3-*O*-acylated-2,6-di-*O*-pentylated α-, β- and γ-CDs were found to be liquid at room temperature, highly stable, soluble in non-polar solvents and with high enantioselectivity towards many chiral compounds.

Subsequent modifications on CDs resulted in new chiral phases[71] like

Hexakis(2,3,6-tri-*O*-pentyl)-α-cyclodextrin (Lipodex A[®])

Hexakis(3-*O*-butyryl-2,6-di-*O*-pentyl)-α-cyclodextrin (Lipodex B[®])

Heptakis(2,3,6-tri-*O*-pentyl)-β-cyclodextrin (Lipodex C[®])

Heptakis(3-*O*-acetyl-2,6-di-*O*-pentyl)-β-cyclodextrin (Lipodex D[®])

Octakis(3-*O*-butyryl-2,6-di-*O*-pentyl)-γ-cyclodextrin (Lipodex E[®])

Octakis(2,3,6-tri-*O*-pentyl)-γ-cyclodextrin

Octakis(2,3-di-*O*-pentyl)-γ-cyclodextrin

Octakis(6-*O*-methyl-2,3-di-*O*-pentyl)-γ-cyclodextrin

Octakis(6-*O*-acyl-2,3-di-*O*-pentyl)-γ-cyclodextrin

Heptakis(6-*O*-*tert*-butyldimethylsilyl-2,3-di-*O*-methyl)-β-cyclodextrin (6T-2,3-me-β-CD)

Heptakis(2,6-di-*O*-methyl-3-*O*-pentyl)-β-cyclodextrin (2,6-me-3-pe-β-CD)

Octakis(2,6-di-*O*-methyl-3-*O*-pentyl)-γ-cyclodextrin (2,6-me-3-pe-γ-CD).

To increase their selectivity, different substitutions or mixtures of different kinds of cyclodextrin phases is still researched[72].

In the light of these results enantiomer separations were achieved in preparative scale using modified CDs as stationary chiral phases[73]. With this isolation possibility of enantiomers a high number of reference substances were supplied especially in terpene chemistry[74], which

were used subsequently in the determination of absolute configuration studies of new compounds[75, 76] or for the purity control of essential oils[77].

The absolute configuration investigations can be applied by enantioselective GC with modified CDs. However, the method is not applicable if no reference substance exists with known absolute configuration. Nonetheless, the unknown molecule can still produce a derivative with known absolute configuration by stereoselective reactions.

5   Chemical Investigations on *Boswellia* Species

5.1   Botanical Aspect of *Boswellia*

The botanical origin of *Boswellia* species has been characterized as [78]:

Division: *Spermatophyta*

Subdivision: *Angiospermae*

Tribe: *Rosopsida*

Subtribe: *Rosidae s. lat.*

Overclass: *Rutanae*

Class: *Anacardiales*

Family: *Burseraceae*

Genus: *Boswellia*

The family of *Burseraceae* is represented in the plant kingdom with 17 genera and 600 species, widespread in all tropical regions. The species are often a predominant component of the vegetation in dry, lowland areas. Some species of the two most important genera of this family, *Commiphora* and *Boswellia*, produce resins that are of considerable commercial value as raw materials of balm, myrrh and frankincense[79].

Boswellia species are trees or shrubs with an outer bark often peeling in parchment like flakes, inner bark greenish, with watery aromatic resin, wood with milky latex. The leaves are imparipinnate, mostly congested at the end of the branches. Flowers are bisexual in panicles or racemes. *Boswellia* trees are found at areas from the sea level up to 1000 meters, usually in rocky slopes and gullies, often on limestone boulders, more rarely on vertical rock-faces, growing to a height of 3 up to 12 meters[80].

Olibanum; gum olibanum, incense or frankincense, (in German Weihrauch, Gummiresina, Kirchenharz); are the common names given to the oleo-gum resin that exudes from incisions in the bark of trees of *Boswellia* (*Burseraceae*)[81]. There are about 25 species known belonging to this genus that are widespread in India, Arabia and the northeastern coast of Africa. Since ancient times, three of these species have been considered as the "true Frankincense" producing trees[82].

The first species grows in South Arabia. *Boswellia sacra* Flueck. is known by the Arabians as "maghrayt d'sheehaz" and the resin it produces as "lubãn dhakar".

The second one grows in Somalia, known as *Boswellia carterii* Birdw., and in native language it is called "moxor". Recently, *Boswellia bhau-dajiana* Birdw. has been identified as identical to *B. carterii*. Generally, the resins that both species produce are called "lobãn dakar" or more commonly as "beeyo" quality.

The third important olibanum is from another Somalian species, *Boswellia frereana* Birdw. or natively as "jagcaar". The resin produced by this species is called "lobãn majdi" or commonly "maydi". It is the most expensive brand of olibanum on the market.

Boswellia papyrifera Hochst. (*B. papyrifera* Rich.) produces another olibanum quality which is known as "boido" in Somalia, Ethiopia, especially in Eritrea, in Sudan and in the other east African countries. *Boswellia neglecta* S. Moore (*B. hildebrandtii* Engl., *B. multifoliolata* Engl.) in Kenia and Ethiopia, *Boswellia rivae* Engl. (*B. boranensis* Engl) in Ethiopia, *Boswellia odorata* Hutch. and *Boswellia dalzielli* Hutch in tropical regions of Africa produce resins similar to olibanum[82].

Another resin producing species with a similar fragrance to frankincense is known as "Indian olibanum" or in botanical terms as *Boswellia serrata* Roxb. (syn.: *B. thurifera* Roxb., *B. thurifera* Colebr., *B. serrata* Stachh., *B. glabra* Roxb., *Canarium balsamiferum* Willd.). *B. serrata* , "salpha tree", is found in the middle and northern parts of East India producing olibanum resin with various qualities which are commonly known as "salai guggul".

The *Boswellia* tree contains resin channels on the bark. When the bark is incised, a white emulsion exudes and dries into globular, pear or club shaped light yellow to dark brown tears[83].

The resin is generally harvested all through the sommer and autumn after the tree has been wounded in March or April[81]. It is supposed that a *Boswellia* tree can produce this exudate in good quality only for three subsequent years. After this period, the quality of the collected resin decreases considerably. Therefore, even in the ancient records, it has been recommended that the tree should be left to rest for some years after this harvesting period[82].

5.2   The Chemical History of Olibanum

Although the oil of olibanum had occupied the shelves of the 16th century pharmacies as "*oleum thuris*", the first investigation on its chemical composition was performed in 1788 by *Johann Ernst Baer* at the University of Erlangen[#]. Following his work, the first elementary

---

[#] J. E. Baer, Dissertation for PhD in Chemistry, University of Erlangen, Germany, **1788**.

Experimenta chemica cum Gummi-Resinis nonnullis instituta

analysis was carried out by *F.W. Johnston* in 1839. The constituents of the essential oil were first investigated by *J. Stenhouse* in 1840, and he identified depending on the origin of the resin fourteen monoterpenoic constituents including pinene, dipentene, phellandrene and cadinene[84]. In 1898, *A. Tschirch* and *O. Halbey* published for the first time that olibanum had an acidic constituent, boswellic acid, with a molecular formula of $C_{32}H_{52}O_4$ but they could not suggest a structure at that time[85].

At the beginning of the 1930's, the olibanum resin was investigated in more detail. The study of *A. Winterstein* and *G. Stein* in 1932[86] drew the attention to the resin acids, the pentacyclic triterpenoic α- and β-amyrin like skeletons with different functional groups, which were attempted to be isolated and identified with the analytical methods possible for that time[87, 88]. Nevertheless, by the 1960's several of these acids such as α- and β-boswellic acids, 11α-hydroxy-β-boswellic acid and 3-*O*-acetyl-11-hydroxy-β-boswellic acid were identified by various derivatisation methods (**Fig. 5.1**).

R_1 = OH, R_2, R_3 = H β-Boswellic acid
R_1 = OH, R_2 = OH, R_3 = H 11-Hydroxy-β-boswellic acid
R_1 = Ac, R_2 = OH, R_3 = H 3-*O*-Acetyl-11-hydroxy-β-boswellic acid
R_1 = Ac, R_2, R_3 = H 3-*O*-Acetyl-β-boswellic acid
R_1 = OH, R_2, R_3 = O 11-Keto-β-boswellic acid
R_1 = Ac, R_2, R_3 = O 3-*O*-Acetyl-11-keto-β-boswellic acid

R = OH, 3-Hydroxy-8,9,24,25-tetradehydrotirucallic acid
R = Ac, 3-*O*-Acetyl-8,9,24,25-tetradehydrotirucallic acid
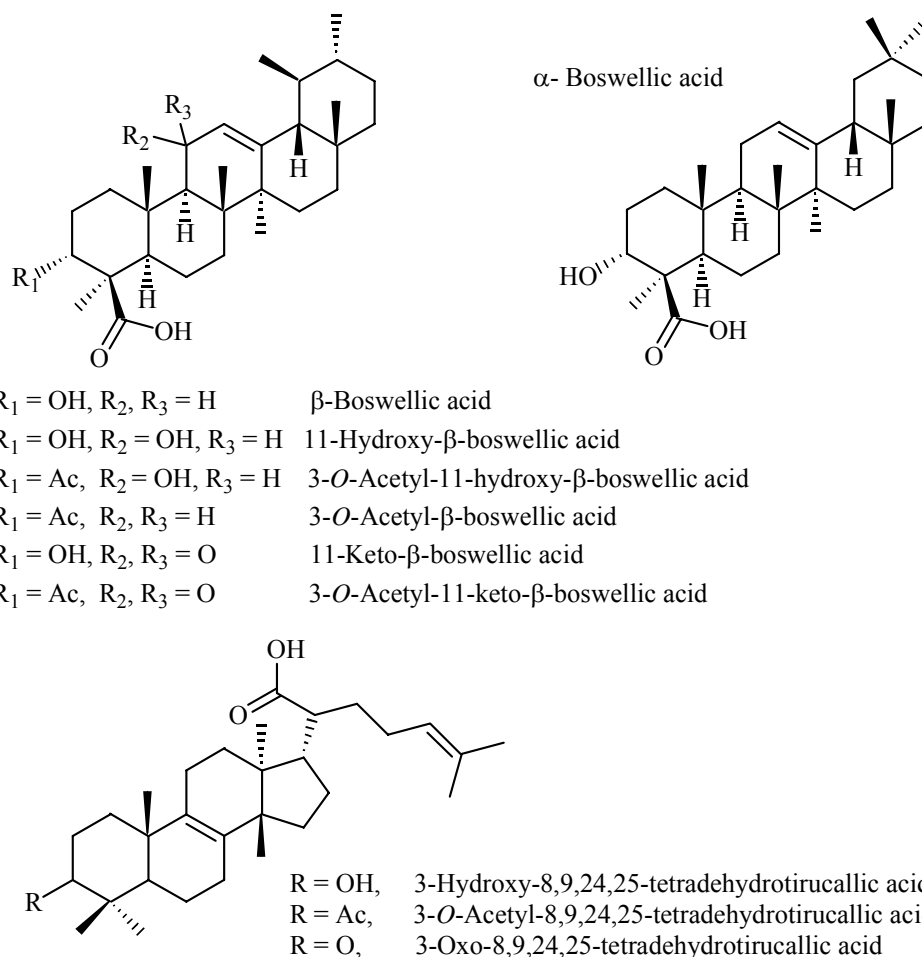R = O, 3-Oxo-8,9,24,25-tetradehydrotirucallic acid

Fig. 5.1. Some of the triterpenoic acids that were identified from olibanum.

In 1967, *G. Snatzke* and *L. Vértesy* published the structures of acetyl-11-keto-β-boswellic acid[89] as well as *epi*-α- and *epi*-β-amyrin and their acetates, α- and β-amyrenone and viridiflorol from the neutral fraction of olibanum, adding that it is composed of 5-9 % essential oil, 15-16 % resin acids, 25-30 % of material insoluble in ether containing the polysaccharides and 45-55 % ether soluble compounds.

In 1978 *R.S. Pardhy* and *S.C. Bhattacharya* identified tirucallic acids as well as β-boswellic acid, acetyl-β-boswellic acid, 11-keto-β-boswellic acid, acetyl-11-keto-β-boswellic acid from *B. serrata* Roxb.[90,91] (**Fig. 5.1**) and a diterpenoic cembrene derived alcohol, "serratol"[92]. Studies on the isolation and identification of the boswellic acids with modern analytical techniques and on their pharmacological effects are still going on. Therefore these topics will be further discussed in the following parts of this work.

The first important and comparative study on the essential oil of olibanum of different origins was performed by *H. Obermann* from Dragoco (Holzminden, Germany) in 1977[93]. He investigated two different commercial brands of olibanum, "*Eritrea*" and "*Aden*" by GC-MS, which corresponded to *B. carterii* and *B. serrata* resins, respectively. As a result of this investigation it was reported that not only the fragrance of these two qualities but also the composition of the constituents in the oils were different.

The "*Eritrea*" oil was reported to have octylacetate as the major constituent (52 %) as well as α-pinene, camphene, p-methoxytoluol, hexyl acetate, limonene, 1,8-cineole, octanol, linalool, bornyl acetate, cembrene A, incensole, incensyl acetate and an unknown diterpenoic constituent. In contrast, "*Aden*" oil was found to contain α-pinene as the major constituent (43 %), camphene, β-pinene, sabinene, o-cymol, limonene, 1,8-cineole, p-cymol, campholenaldehyde, verbenone, octyl acetate and cembrenol, a diterpene alcohol with cembrene skeleton which was identified later by the same group, which was expected not be different than "serratol" described before (**Fig. 5.2, Fig. 5.48**).

In 1985 a detailed review was published by *P. Maupetit* on the "*Aden*" brand of olibanum[94]. He reported 47 new constituents identified in the resinoid and in the oil of olibanum in addition to 169 formerly identified substances including the pyrolysis products. Recent studies by *Verghese* on *B. serrata* oil and by *A.M. Humprey et al.*[95] comparing *B. carterii* oil with cumin, ginger, rosemary oil, were reinvestigations of known facts. These studies pointed to the difficulties in the identification of the origin of olibanum resin as well as in the determination of standard olibanum oil. A complete list of major constituents of olibanum resin hitherto described are given in Figure 5.2, 5.3 and 5.4.
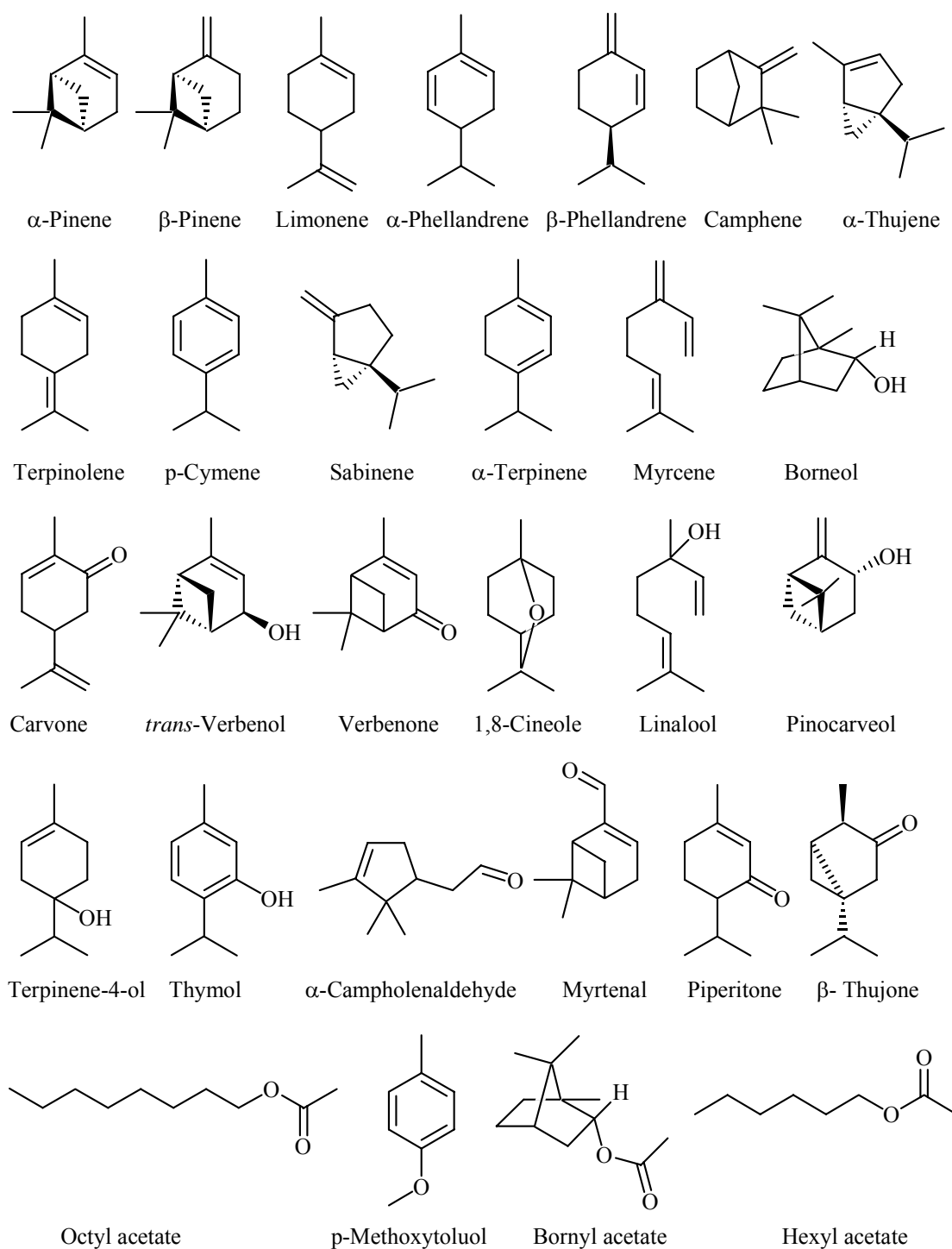
Fig. 5.2. Some of the monoterpenoic constituents identified in olibanum resin.

β-Elemene   δ-Elemene   α-Cubebene   α-Ylangene   α-Copaene

β-Bourbonene   α-Gurjunene   α-Guaiene   Aromadendrene   Viridifolorol

E-β-Caryophyllene   α-Humulene   cis-α-Bergamotene   α-Muurolene   γ-Muurolene

β-Cadinene   δ-Cadinene   γ-Cadinene   T-Cadinol
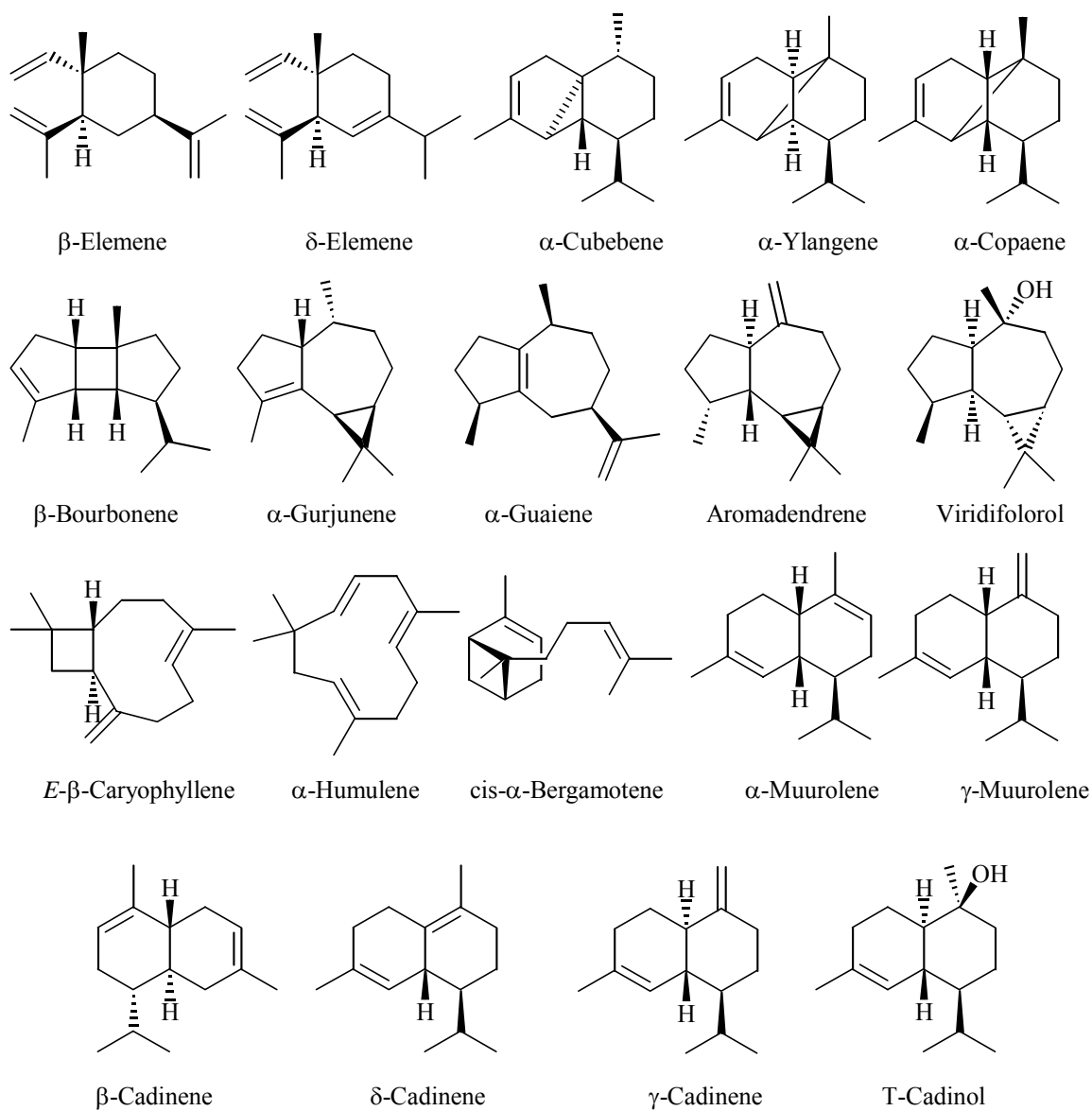
Fig. 5.3. Some of the sesquiterpenoic constituents identified in olibanum resin.

Cembrene   Isocembrene   Cembrene A

Cembrenol   Incensole   Isoincensoleoxide
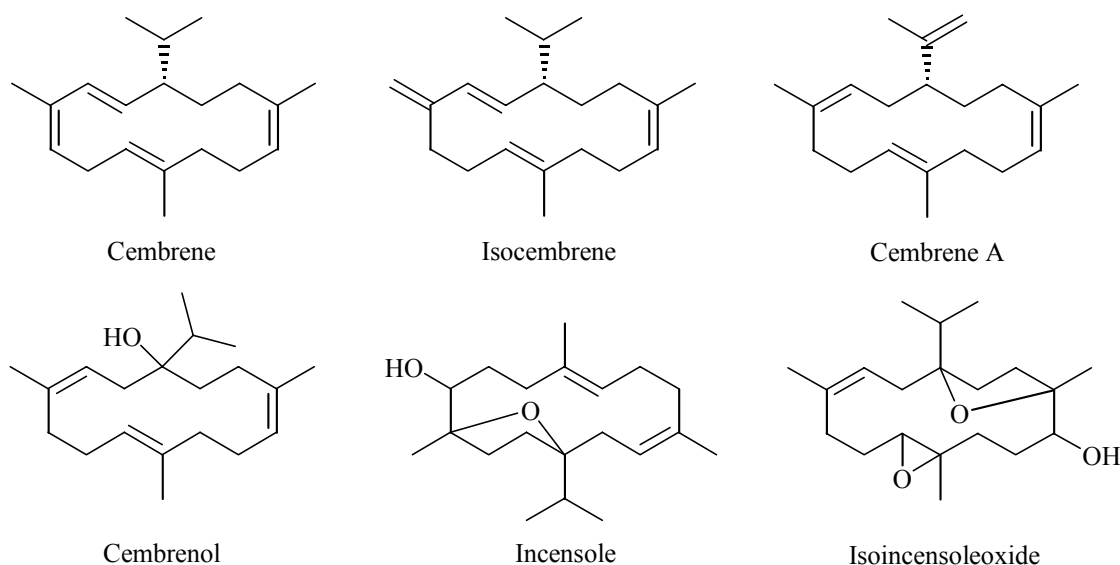
Fig. 5.4. Some diterpenoic constituents identified in olibanum resin.

5.3 Investigated Material

In this work *Boswellia carterii* Birdw., *B. serrata* Roxb., *B. frereana* Birdw., *B. neglecta* S. Moore and *B. rivae* Engl. were investigated. These resin samples were selected from a number of variable qualities obtained from different wholesalers in Germany or provided as authentic samples. The total list of the studied samples is compiled in the experimental part of this work. Only five of them were subjected to the whole work. *B. carterii* was an authentic sample from Ethiopia certified for its authenticity from the Agricultural Department of the Ethiopian government; *B. serrata* as well as *B. frereana* were obatined from Willy Benecke GmbH (Hamburg, Germany). *B. neglecta* and *B. rivae* were obtained as authentic samples from Ethiopia as "*Borena*" and "*Ogaden*" type, respectively.

5.4 Essential oil of Olibanum

The essential oil of olibanum was prepared by hydrodistillation and collected in *n*-hexane. The oil was investigated by GC and GC-MS. The evaluation of the results of GC-MS measurements was accomplished by comparing mass spectra and retention indices with published data and a spectral library established under identical experimental conditions[96,97]. To detect the possibility of artifact formation during hydrodistillation, plant extracts were prepared in different organic solvents (*n*-hexane, dichloromethane, diethylether, etc.), alternatively. Using chromatographic techniques, such as column chromatography (CC), preparative GC or TLC, the unknown components were isolated. Structure elucidation was carried out on the basis of MS, 1- and 2-D NMR techniques.

5.4.1   Essential Oil of *Boswellia carterii* Birdw.

The essential oil of *Boswellia carterii* has been one of the most intensively studied oil of olibanum. The resin was characterised as the "Eritrea" type, and the major constituent of its oil was found to be octyl acetate predominating the oil by approximately 60%. The presence of cembrene type diterpenoid constituents was also reported[93, 98, 99, 100, 101].

The hydrodistillate of *B. carterii* was a pale yellow oil. Its major constituents were identified as (+)-α-thujene (1.7%), (-)-α-pinene (10.9%), camphene (1.0%), sabinene (0.7%), β-pinene (0.7%), myrcene (0.5%), hexylacetate (0.3%), p-cymene (1.4%), *Z*-β-ocimene (0.4%), *E*-β-ocimene (1.7%), (-)-limonene (1.5%), 1,8-cineole (1.2%), 1-octanol (11.9%), (-)-linalool (2.1%), α-pinene epoxide (0.5%), *trans*-verbenol (0.4%), terpinene-4-ol (0.4%), octylacetate (39.3%), (-)-bornylacetate (2.2%), geranylacetate (0.4%), *E*-nerolidol (0.2%), cembrene A (2.1%), cembrene C (0.1%), verticilla-4(20),7,11-triene (**1**) (6.0%), incensole (1.0%) and incensole acetate (**2**) (2.3%) (**Fig. 5.5**, **Fig. 5.6**). Verticilla-4(20),7,11-triene (**1**) was isolated and identified for the first time in this study[102].
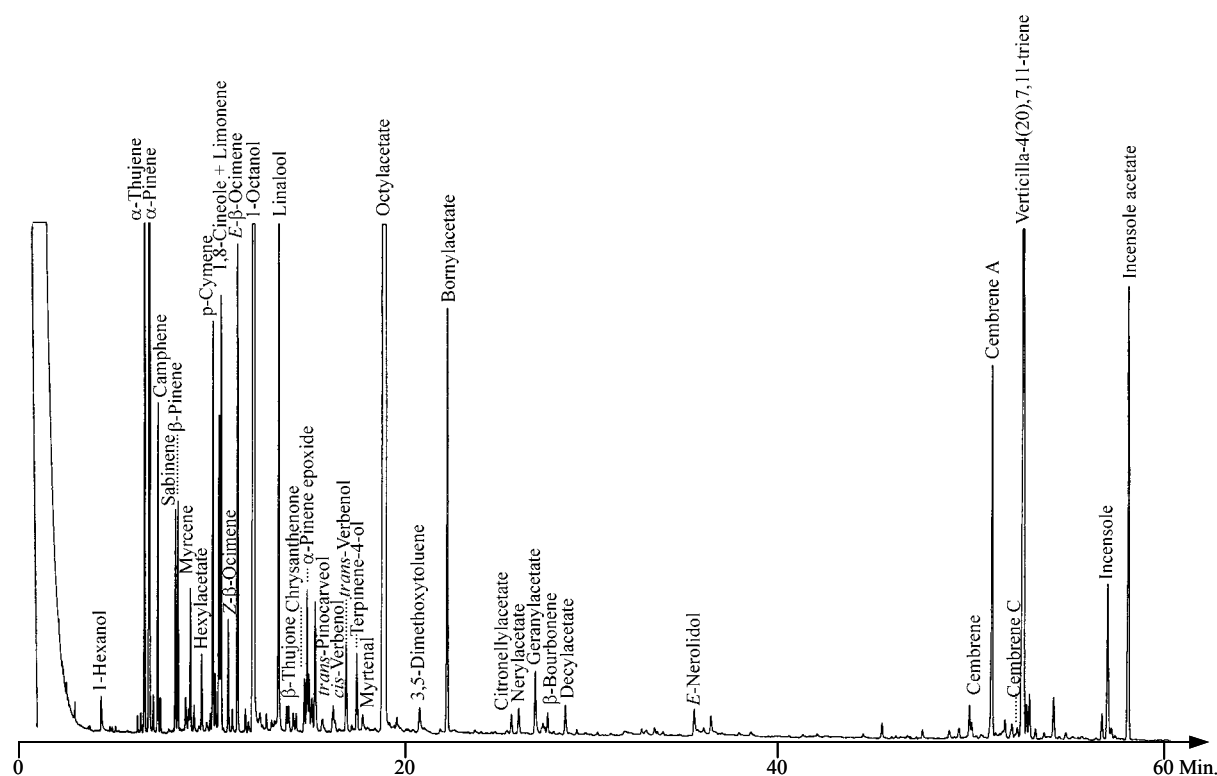
Fig. 5.5.   Gas chromatogram of the essential oil of *Boswellia carterii* (25 m fused silica capillary column with CPSil 5CB, 50 °C, 3 °C/min, 230 °C, injector at 200 °C, detector at 250 °C, carrier gas 0.5 bars H_2).

42

α-Thujene α-Pinene Camphene Sabinene β-Pinene Myrcene p-Cymene 1,8-Cineole

Limonene Z-β-Ocimene E-β-Ocimene Linalool β-Thujone Terpinene-4-ol 3,5-Dimethoxytoluene

Chrysanthenone α-Pinene epoxide trans-Pinocarveol cis- Verbenol trans-Verbenol Myrtenal

1-Hexanol

Hexyl acetate

1-Octanol

Neryl acetate Geranyl acetate E-Nerolidol

Octyl acetate

Decyl acetate Bornyl acetate β-Bourbonene Citronellyl acetate

Cembrene   Cembrene A   Cembrene C

Verticilla-4(20),7,11-triene   Incensole   Incensyl acetate
(1)   (2)

Fig. 5.6. The constituents of the essential oil of *Boswellia carterii*.

The *n*-hexane extract of *B. carterii* was also found to contain the diterpenoid constituents as well as octylacetate but lower amounts of the monoterpenoid constituents. However, in contrast to previous reports incensole oxide[103] and isoincensole oxide[104, 105, 106] were not observed in any of the *B. carterii* samples investigated in this study.

The MS and NMR data of cembrene A[107, 108], incensole[109] were found to be in accordance with data given in the literature. Only the presence of cembrene C[107] was verified by the comparison of MS with literature data. For the first time, NMR data of incensyl acetate are presented in the following sections.

5.4.1.1   Isolation and Identification of Verticilla-4(20),7,11-triene (*1*)

Verticilla-4(20),7,11-triene (**1**) was isolated from the essential oil of *B. carterii* after the oil was separated into its non-polar and polar parts on silica gel by column chromatography with *n*-hexane and diethylether, respectively. The diterpenoid constituent, **1**, was found in the hexane fraction. The same separation was also achieved with Sephadex LH-20 with dichloromethane. Further purification of the compound was carried out by preparative GC using a SE-30 column.

The pure compound produced a molecular ion signal at *m/z* = 272 in its mass spectrum that corresponded to an elemental composition of $C_{20}H_{32}$ (**Fig. 5.7**).
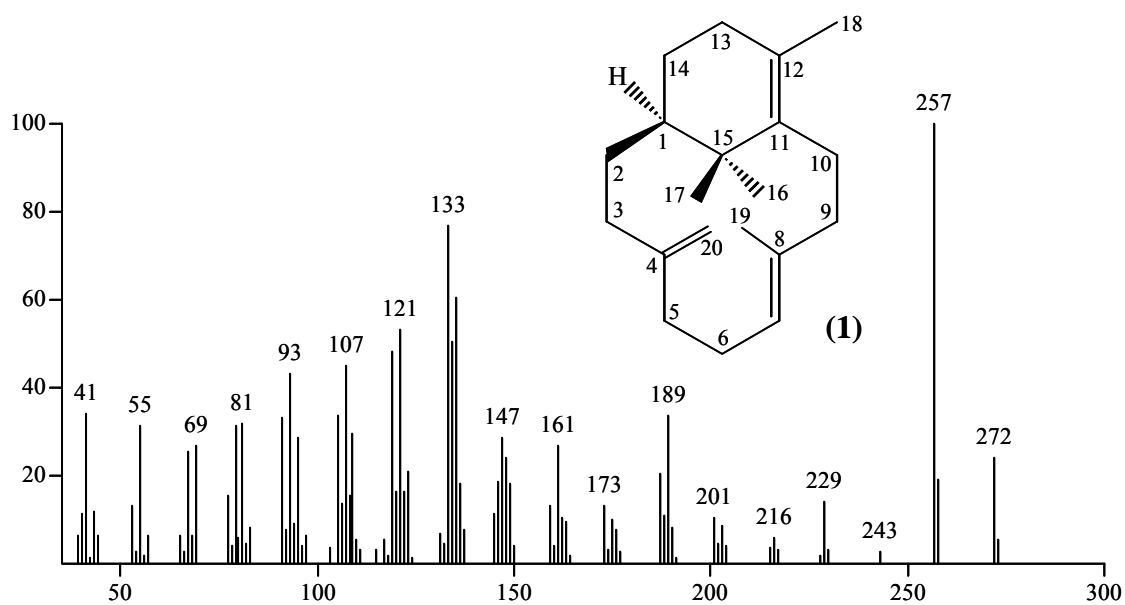
Fig. 5.7. Mass spectrum of verticilla-4(20),7,11-triene (**1**).

The fragmentation pattern of **1** first indicated an allyl cleavage of a methyl group in the molecule with the fragment ion signal at *m/z* = 257 representing the base peak in its MS. A *Retro-Diels-Alder* (RDA) reaction was observed in the cyclohexene ring of the molecule followed by further fragmentation.
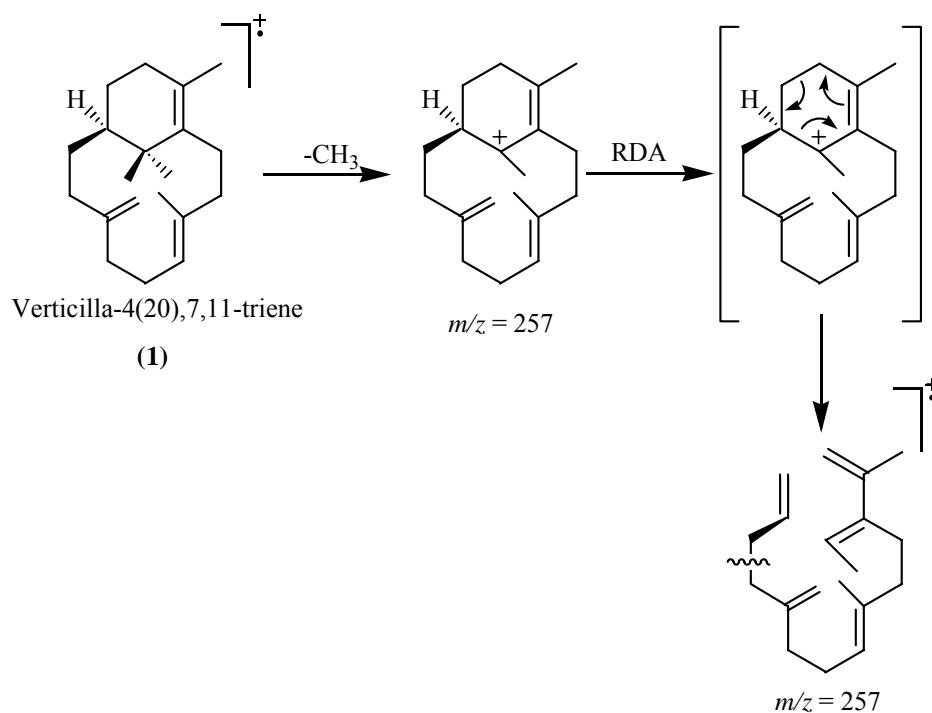
Fig. 5.8. Possible fragmentation of **1**.

45

The ^{1}H-NMR spectrum of **1** showed four singlets at δ 0.95, 1.02, 1.54, 1.60 for two geminal and two allylic methyl groups, respectively. Three olefinic protons were observed at δ 5.18 (dd, J = 3.9, 10 Hz) 4.83 and 4.80. Two multiplets at δ 2.45 (td, J = 4.4, 12.6 Hz) and δ 2.81 (ddd, J = 3.9, 10.1, 15.7 Hz) were also detected, each corresponding to one proton (**Fig 5.9**).
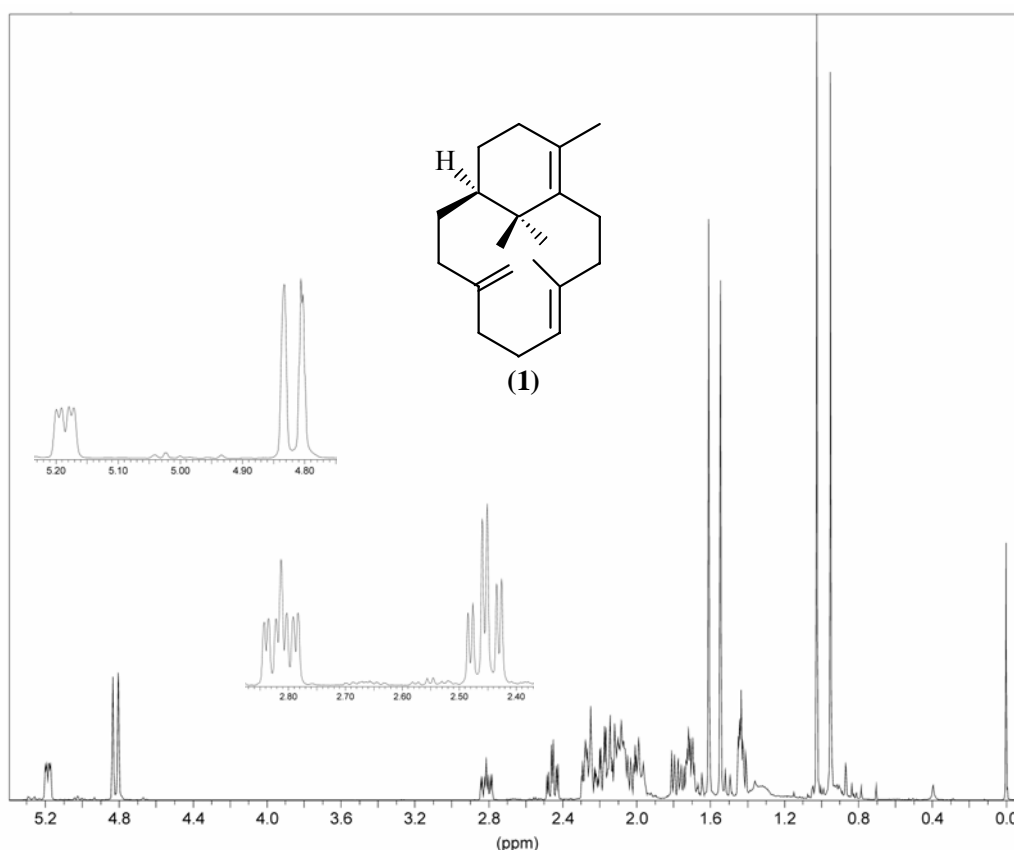
Fig. 5.9. ^{1}H-NMR spectrum of verticilla-4(20),7,11-triene (**1**).

The ^{13}C-NMR and DEPT spectra showed signals corresponding to four primary carbons at δ 16.79, 21.01, 26.86, 33.38; nine secondary carbons at δ 25.84, 26.11, 29.94, 30.71, 31.96, 32.97, 36.56, 39.57, 108.94; two tertiary carbons at δ 44.09, 130.0 and four quaternary carbons at δ 37.58, 133.47, 136.80, 153.34 (**Fig 5.10**). Five of these carbon signals at low field, δ 108.94, 130.0, 133.47, 136.80, 153.34, indicated three double bond systems in the molecule. The signal of the sixth carbon was deduced from ^{13}C-NMR measurements in CDCl$_3$ and from HMBC correlations to appear at δ 128.03.

The correlations between ^{1}H- and ^{13}C-NMR resonance were derived from the ^{1}H-^{13}C COSY (HMQC) spectrum. The connectivity of carbon atoms was deduced from ^{1}H-^{1}H COSY and HMBC spectra.
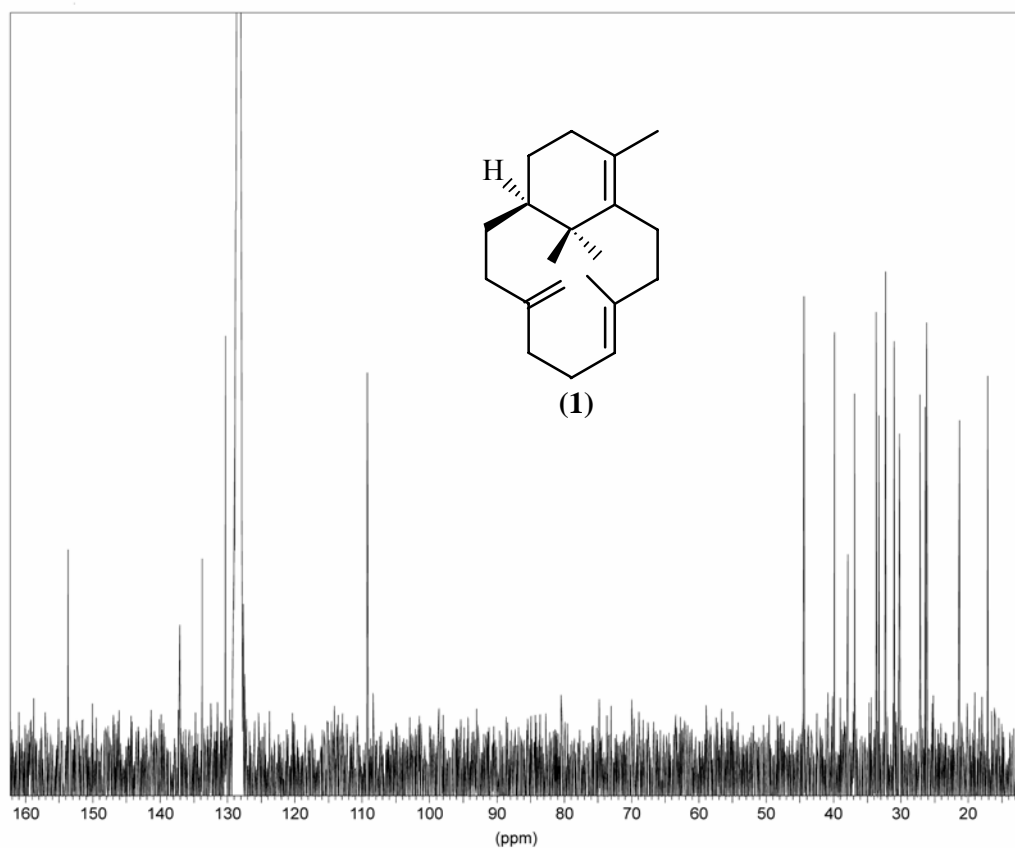
Fig. 5.10. ^{13}C-NMR spectrum of verticilla-4(20),7,11-triene (**1**).

An exocyclic double bond was detected in the HMQC spectrum from correlations of the protons at δ 4.80, 4.83 to the carbon at δ 108.94. The other olefinic proton at δ 5.18 was found to be connected to the carbon at δ 130.00. Methyl group signals at δ 0.95, 1.02, 1.54, 1.60 were found to correlate to carbons at δ 26.86, 33.38, 16.79, 21.01, in the ^{13}C-NMR-spectrum, respectively. The protons at δ 2.45 and 2.81 were found to correlate to the carbons at δ 39.57 and 32.97. Their low field shift was related to their proximity to the double bond systems. In addition, the tertiary carbon at δ 44.09 was correlated to the multiplet at δ 1.40-1.44, which was also regarded as an important connection point for the molecule (**Table 5.1, Fig. 5.11**).
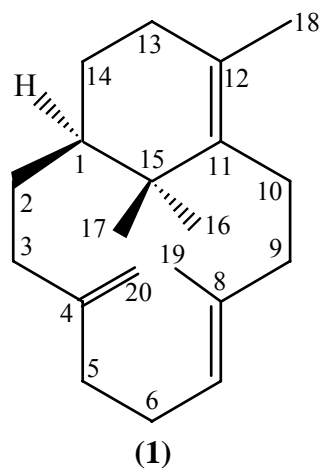
Fig. 5.11. Numbered structure of **1**.

Table 5.1. HMQC correlations of **1**.

No.	^{13}C (ppm)	^{1}H (ppm)	No.	^{13}C (ppm)	^{1}H (ppm)
1	44.09	(1.40-1.44)	**11**	136.80	
2	31.96	(1.68-1.73), (2.04-2.12)	**12**	128.03	
3	32.97	(2.04-2.12), 2.81	**13**	30.71	(1.74-1.80), (2.04-2.12)
4	153.34		**14**	25.84	(2.12-2.15), (2.22-2.29)
5	36.56	(2.04-2.12), (2.22-2.29)	**15**	37.58	
6	29.94	(2.04-2.12), (2.15-2.18)	**16**	33.38	1.02
7	130.0	5.18	**17**	26.86	0.95
8	133.47		**18**	21.01	1.60
9	39.57	(1.96-2.03), (2.45	**19**	16.79	1.54
10	26.11	(1.40-1.44), (2.18-2.23)	**20**	108.94	4.80, 4.83

The HMBC spectrum indicated C*H*-relationships through two and three bond ($^{2}J_{CH}$ and $^{3}J_{CH}$) connectivities. Together with observed couplings in the ^{1}H-^{1}H COSY spectrum the correlations of HMBC resulted in small subunits of the molecule which were connected to each other.

In this case the first fragment was deduced from the coupling of two geminal methyl groups with an aliphatic quaternary carbon (δ 37.58, C-15; 1.02, 33.38, CH$_3$-16; 0.95, 26.86, CH$_3$-17). This quaternary carbon was further connected to a double bond system (δ 136.80, C-11, 128.03, C-12), which was again coupled to a methyl group (δ 1.60, 21.01, CH$_3$-18). On the other side, C-15 was also coupled to a tertiary carbon (δ 1.40-1.44, 44.09, C-1). A second fragment was deduced as an exocyclic double bond system (δ 153.34, C-4, 4.80, 4.83, 108.94, C-20). The third fragment was also interpretated as a double bond system (δ 5.18, 130.0, C-7, 133.47, C-8). The proximity of C-2 and C-3 (δ 31.96, 32.97), C-5 and C-6 (δ 36.56, 29.94), C-13 and C-14 (δ 30.71, 25.84) was deduced from the correlations in the ^{1}H-^{1}H COSY spectrum (**Fig. 5.12**).
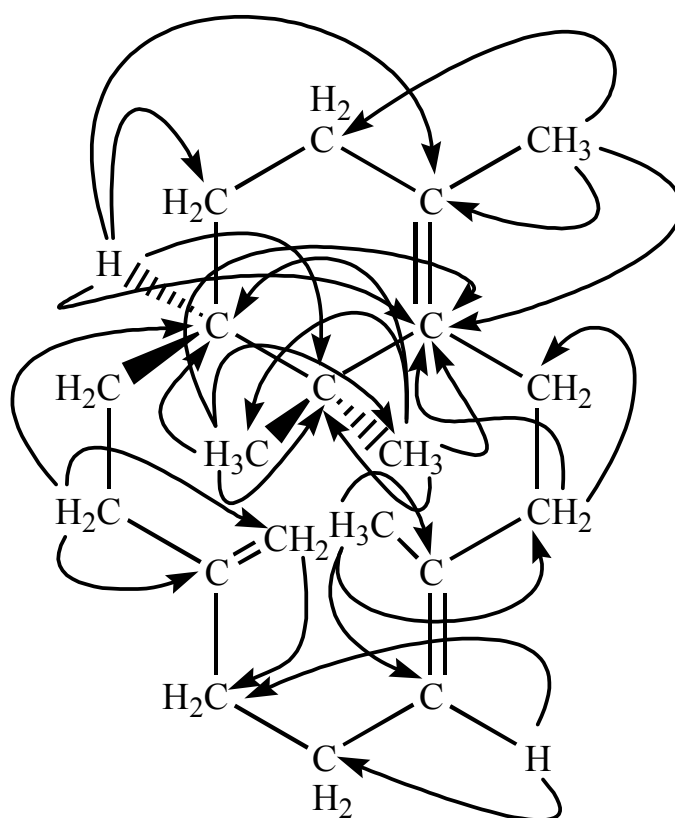
Fig. 5.12. HMBC correlations of **1**.

The relative configuration of the molecule was derived from its NOESY spectrum. The interactions between H-3β (δ 2.81) and CH_3-17 (δ 0.95, 26.86), CH_3-17 and CH_3-19 (δ 1.54, 16.79) CH_3-17 and H-2β (d 1.68-1.73), CH_3-17 and H-10β (d 1.40-1.44) indicated that these protons are in β positions to the ring system. This was confirmed by the interactions between H-3β and H-20 (δ 4.80), H-2β and H-20 (δ 4.80), CH_3-19 and H-9β (δ 1.96-2.03).

The correlations between H-1 and CH_3-16 (δ 1.02, 33.38) indicated that it was located below the ring system. The interactions between H-5α (δ 2.22-2.29) and H-9α (δ 2.45), H-9α and H-7 (δ 5.18), H-5α and H-20 (δ 4.83) showed the correlations below the ring system. Finally the coupling of CH_3-18 to H-10α and H-9α indicated that CH_3-18 was intending to absorb below the ring system (**Fig 5.13**).
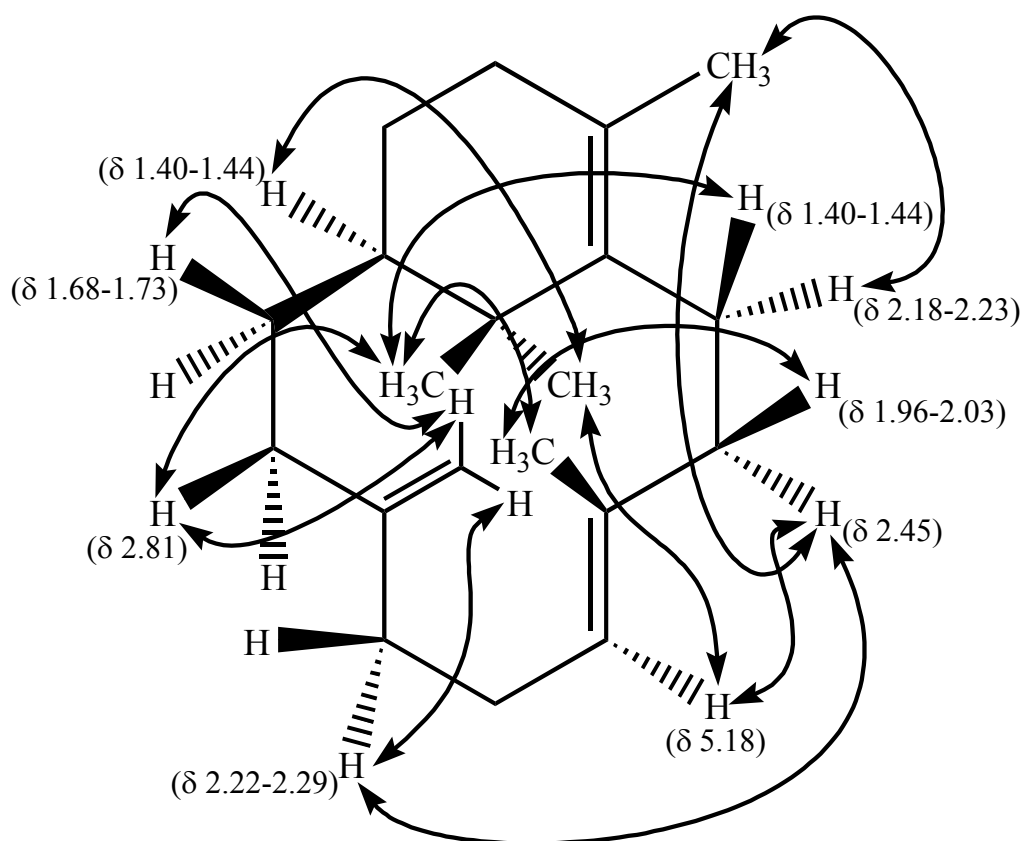
Fig. 5.13. NOESY correlations of **1**.

Only a few members of verticillane type diterpenes are known. The isolation of verticillol[110], a corresponding tertiary alcohol to **1**, was first reported from *Sciadopitys verticillata* (*Taxodiaceae*). Moreover, a hydrocarbon, *ent*-verticillene, along with four hydroxylated derivatives[111] was identified as a constituent of the Japanese liverwort *Jackiella javanica* (*Hepaticae*) (**Fig. 5.13**). The absolute configuration of verticillol has been determined[112] and although it could not be proved, **1** and verticillol were expected to have the same absolute configuration. The verticillane diterpenes can be considered as the putative biogenetic precursors of the taxane group of diterpenes (e.g. taxol) some of which show anti-leukemic activities. It is also assumed that verticillanes origin from geranylgeranyl diphosphate and are derived from cembrene derivatives by an 11,15-cyclisation[113, 114, 115, 116, 117] (**Fig. 5.14**).
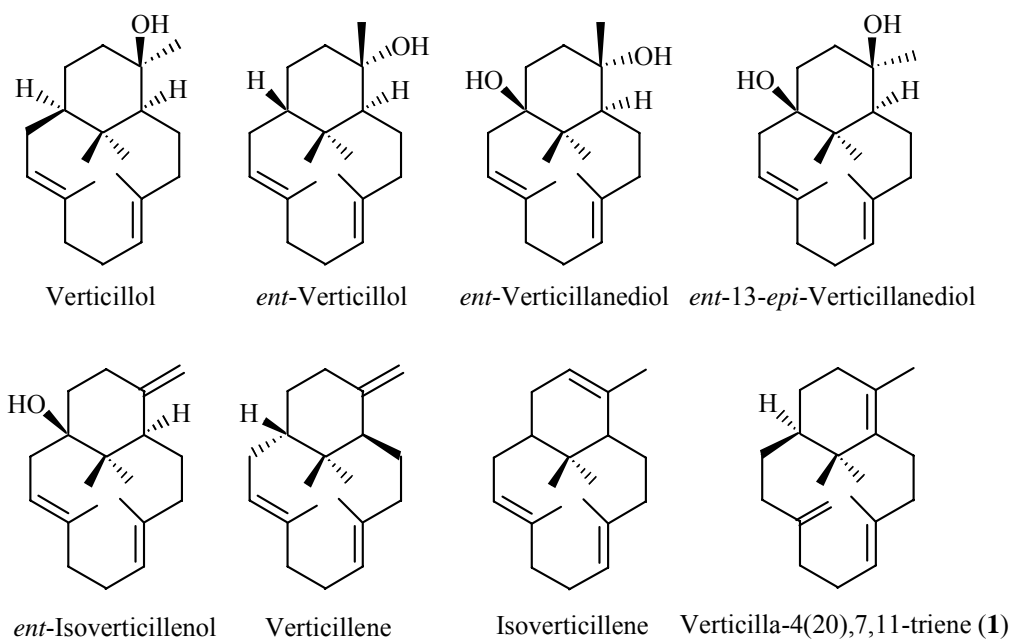
Fig. 5.13. Known verticillane type diterpenoids.
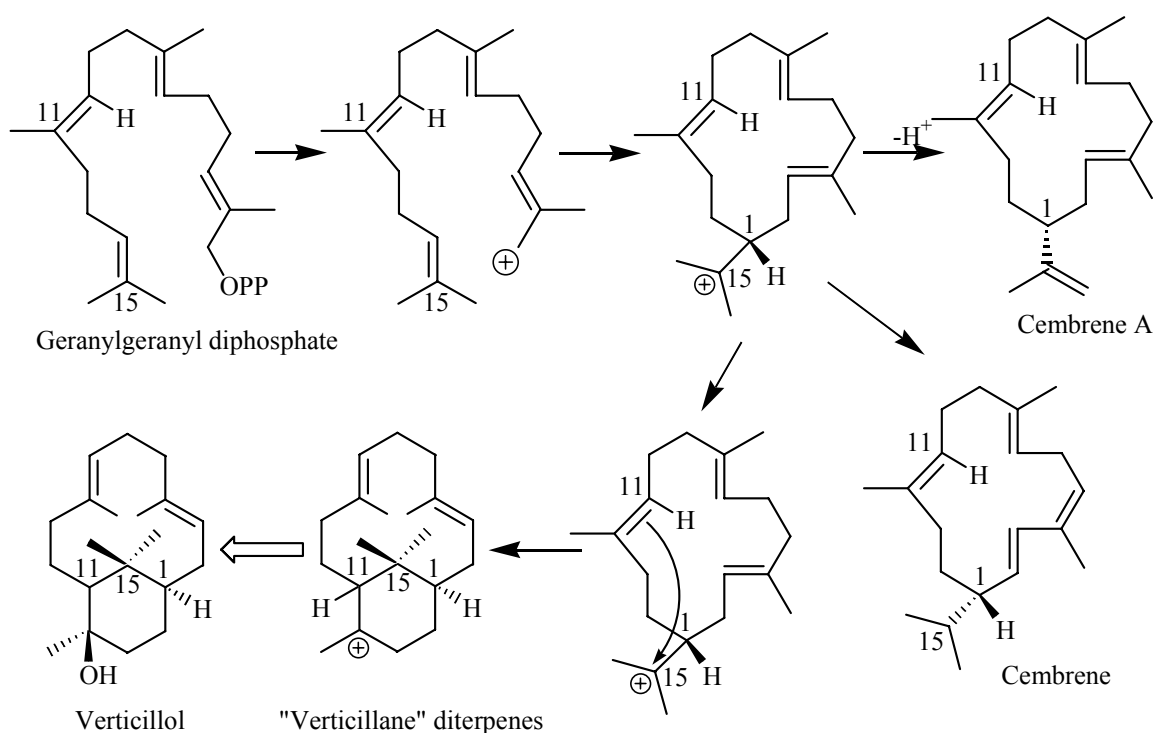
Fig. 5.14. The biogenetic formation of verticillane type diterpenes via the cembrene skeleton. Note that numbering of the skeletons is different in acyclic precursor and bicyclic verticillol.

5.4.1.2 Isolation and Identification of Incensyl acetate (2)

Incensyl acetate was first mentioned by *Obermann*[93]. He indicated that the identification was achieved by GC-MS analysis. However, no spectral data for this compound were reported.

In the course of the present study, incensyl acetate (**2**) was isolated from the hydrodistillate of *B. carterii* essential oil on silica gel by preparative TLC. The hydrodistillate was developed on TLC plates with *n*-hexane: diethylether (7:3). The detection with anisaldehyde after heating at 105 °C furnished a dark yellow spot at $R_\mathrm{f} = 0.65$ (**Fig. 5.15**). Isolation of the corresponding compound was followed by structure elucidation using MS, as well as 1- and 2-D NMR.
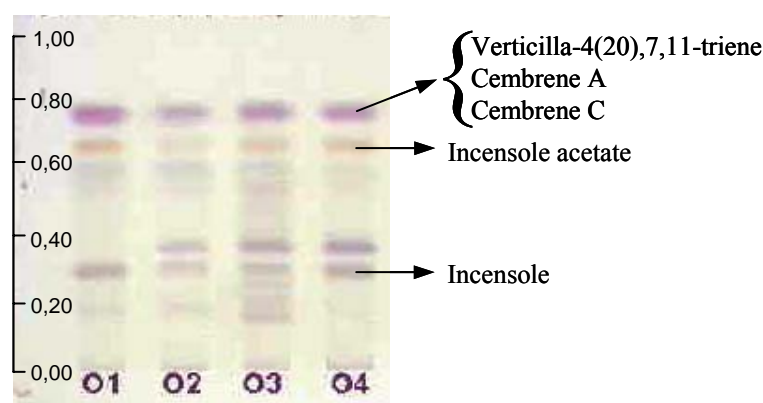
Fig. 5.15. The TLC separation of the essential oils of some *B. carterii* samples[#]. (LiChrospher RP-18 (Merck) plate, mobile phase: *n*-hexane: diethylether (7:3), development distance: 7 cm., detection with anisaldehyde spray solution and heating at 105°C).

The mass spectrum of **2** indicated a molecular ion signal at $m/z = 348$ and an elemental composition of $C_{22}H_{36}O_3$ (**Fig. 5.16**).

High resolution MS indicated that $m/z = 305$ corresponded to a fragment with an elemental composition of $C_{19}H_{29}O_3$ whereas $m/z = 288$ was equal to $C_{20}H_{32}O$, $m/z = 245$ equal to $C_{17}H_{25}O$ and $m/z = 219$ to $C_{15}H_{23}O$.

The fragment ion signal $m/z = 305$ was observed as a result of the cleavage of the isopropyl group from the molecule ion. The loss of an acetic acid group from the molecule ion resulted in the fragment ion signal $m/z = 288$. This was followed by the loss of an isopropyl group producing a signal $m/z = 245$. This signal could also be formed by the loss of an acetic acid group from the fragment ion $m/z = 305$.

[#] The list of the investigated olibanum samples is given in the experimental part.
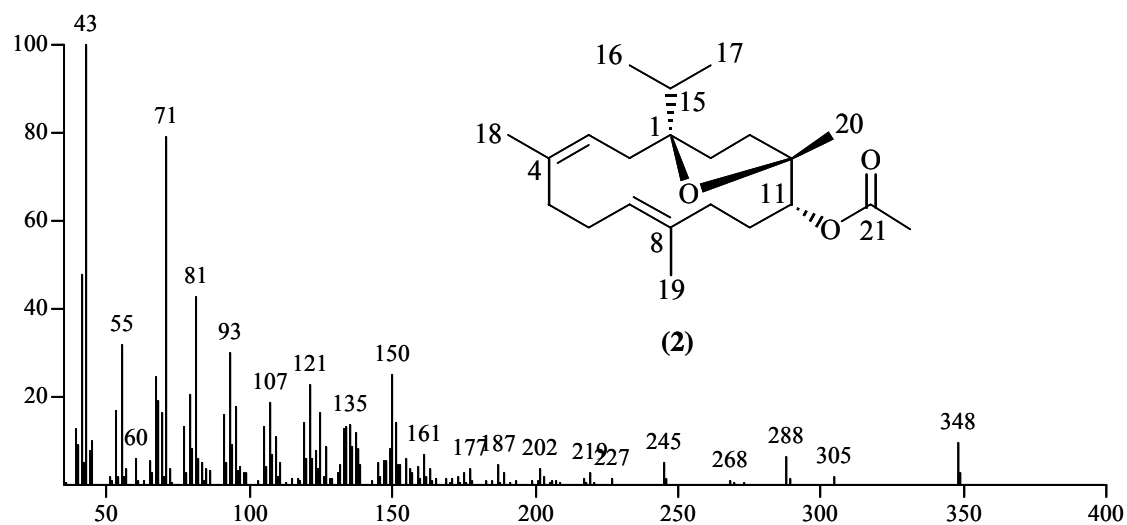
Fig. 5.16. The mass spectrum of incensyl acetate (**2**).
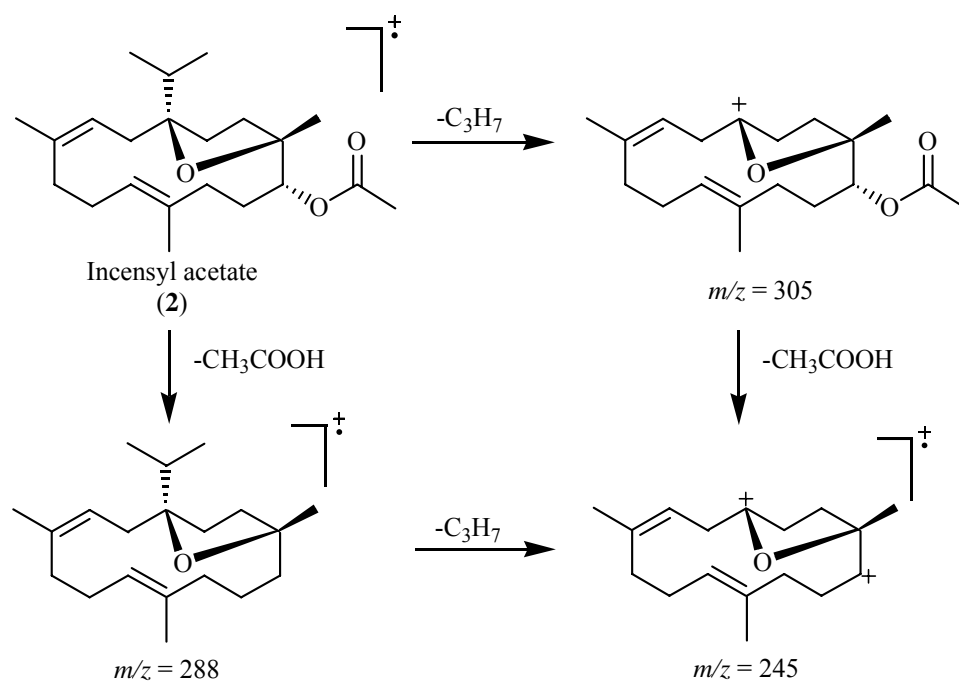
Fig. 5.17. Possible fragmentation of incensyl acetate (**2**).

The ^{1}H-NMR spectrum of **2** showed two methyl groups as doublets at δ 0.88 (d, J = 6.9 Hz) and 0.93 (d, J = 6.9 Hz) and four methyl groups as singlets at δ 1.18, 1.61, 1.66, 1.71. Three

olefinic protons were detected at δ 5.13 (d, J = 10.1 Hz) as a doublet and two multiplets at δ 5.40 (dd, J = 12, 6.1 Hz) and 5.47 (**Fig 5.18**).
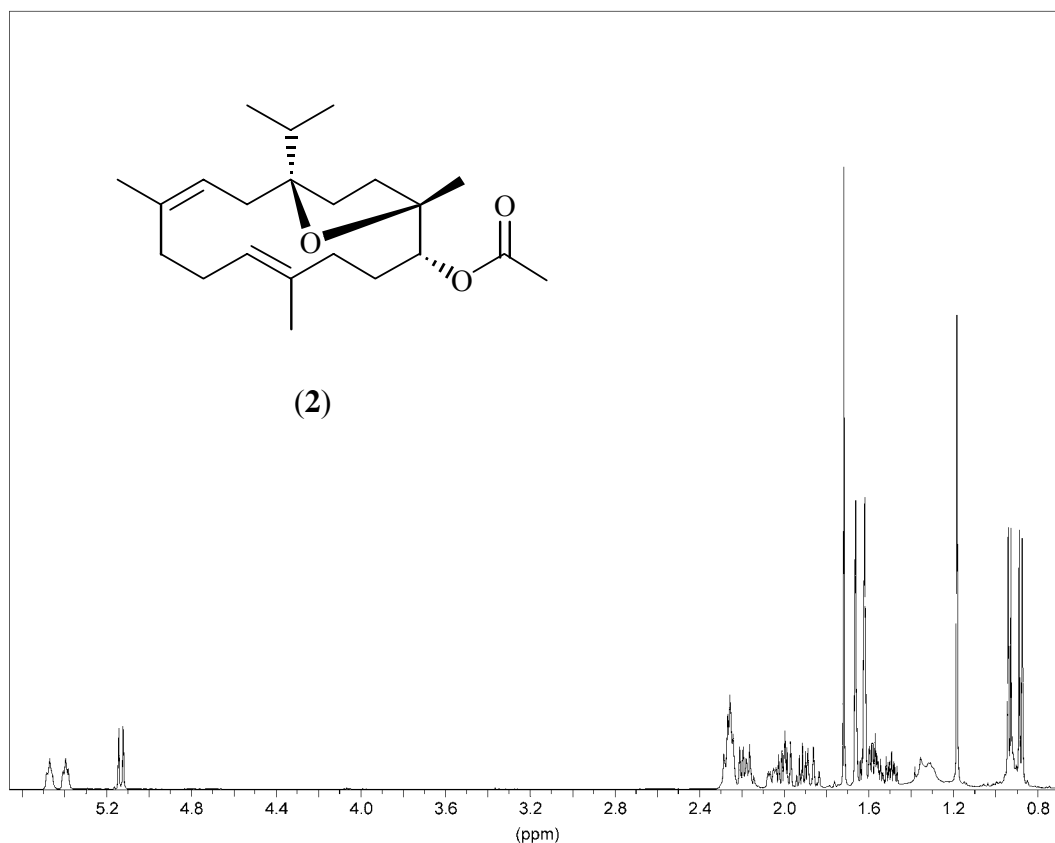
Fig. 5.18. ^{1}H-NMR spectrum of **2**.

The ^{13}C-PENDANT spectrum of **2** indicated six primary carbons at δ 16.24, 17.81 18.10, 18.23, 20.84, 22.37, seven secondary carbons at δ 25.31, 28.29, 30.85, 32.34, 33.91, 35.88, 38.94, four tertiary carbons at δ 35.46, 76.45, 121.51, 126.01, five quaternary carbons at δ 83.49, 89.41, 133.29, 135.31, 170.34 (**Fig. 5.19**). The signal at δ 170.34 indicated a carboxyl group whereas the four low field carbon signals at δ 121.51, 126.01, 133.29, 135.31 proved the presence of two double bonds in the molecule. The aliphatic carbons at δ 76.45, 83.49, 89.41 which were influenced by the electron withdrawing effect of oxygen atoms showed a shift to low field.
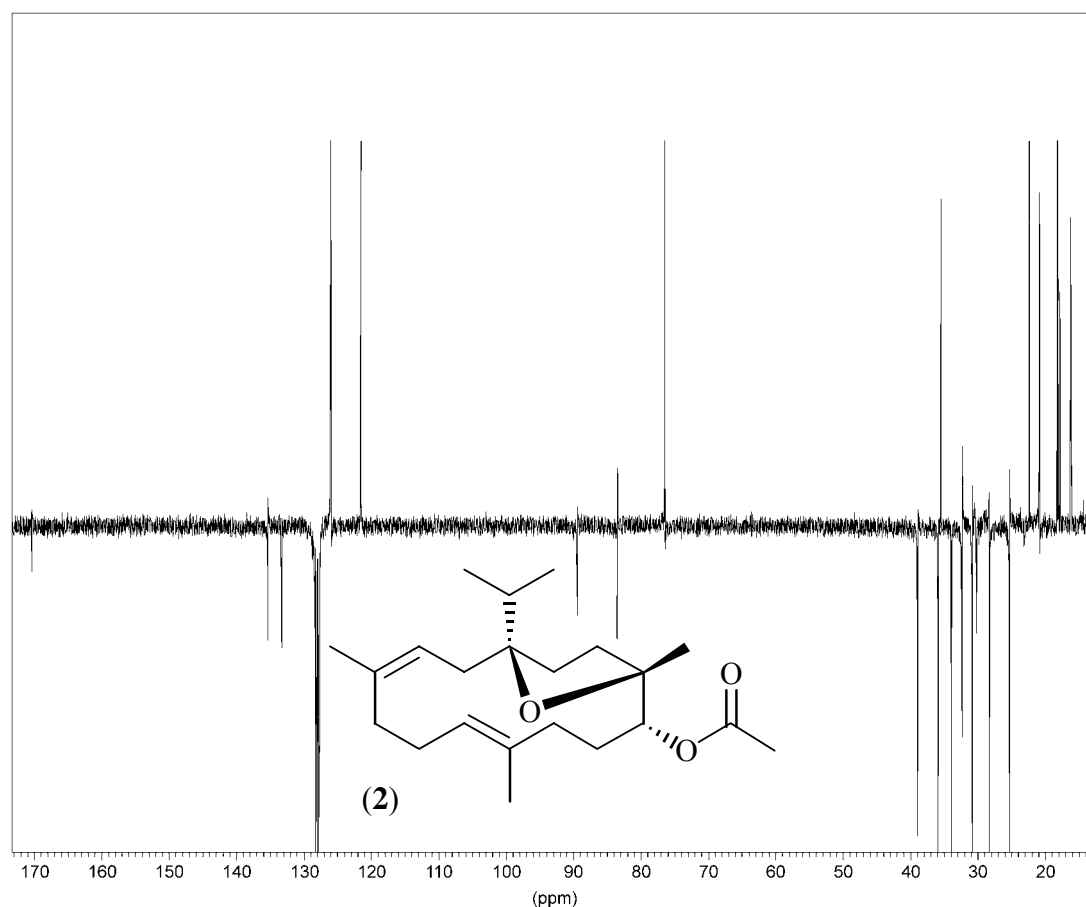
Fig. 5.19. ^{13}C-PENDANT spectrum of **2**.

The correlations in the HMQC spectrum indicated that the olefinic protons at δ 5.40 and 5.47 were coupled to the carbon signals at δ 121.51 and 126.01, respectively. The third olefinic proton at δ 5.13 was found to couple with an aliphatic carbon at δ 76.45 which indicated that it was close to an electron withdrawing group. Methyl groups were also identified by the correlation of the proton signals at δ 0.88, 0.93, 1.18, 1.61, 1.66, 1.71 to the carbon signals at δ 18.23, 18.10, 22.37, 16.24, 17.81, 20.84, respectively (**Table 5.2, Fig. 5.20**).

Table 5.2. HMQC correlations of **2**.

No.	^{13}C (ppm)	^{1}H (ppm)	No.	^{13}C (ppm)	^{1}H (ppm)
1	89.41		12	83.49	
2	32.34	(2.14-2.28, 2H)	13	35.88	(1.46-1.53), (1.96-2.02)
3	121.51	(5.40)	14	30.85	(1.53-1.59, 2H)
4	135.31		15	35.46	(1.88-1.94)
5	38.94	(2.14-2.20), (2.14-2.28)	16	18.23	(0.88)
6	25.31	(2.24-2.26, 2H)	17	18.10	(0.93)
7	126.01	(5.47)	18	16.24	(1.61)
8	133.29		19	17.81	(1.66)
9	33.91	(1.83-1.89), (2.01-2.07)	20	22.37	(1.18)
10	28.29	(1.53-1.59), (1.96-2.01)	21	170.34	
11	76.45	(5.13)	22	20.84	(1.71)

(2)
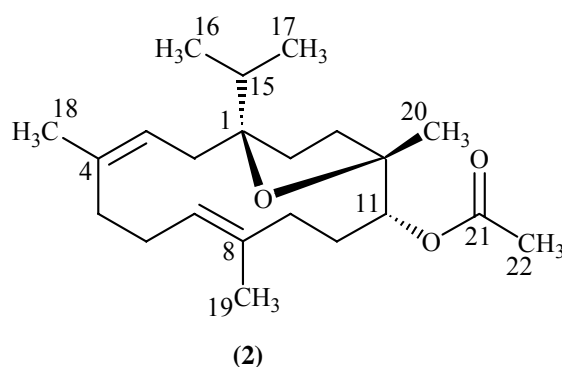
Fig. 5.20. Numbered structure of **2**.

The HMBC spectrum of **2** provided data to establish some fragments of the molecule. The final connections of these fragments were deduced from the ^{1}H-^{1}H COSY spectrum.

The first fragment was identified as a double bond through the coupling of CH$_3$-18 (δ 1.61, 16.24) to two olefinic carbons at δ 135.31, 121.51 and further to a methylene carbon at δ 38.94. The proton at δ 121.51 was also coupled to this secondary carbon.

The second double bond system was deduced from the coupling of CH$_3$-19 (δ 1.66; 17.81) to the olefinic carbon signals at δ 126.01 and 133.29. The two doublets for two methyl groups CH$_3$-16 (δ 0.88, 18.23) and CH$_3$-17 (δ 0.93, 18.10) indicated that both should be adjacent to a single hydrogen atom. This was confirmed by the couplings between these methyl groups to the tertiary carbon C-15 (δ 1.91, 35.46). Both methyl groups and H-15 were further coupled to the quaternary C-1 (δ 89.4).

Another fragment was established by the coupling of the methyl group CH_3-22 (δ 1.71, 20.84) to the carboxyl carbon C-21 (δ 170.34). H-11 (δ 5.13) was also coupled with C-21 that confirmed the low field shift of this proton. It was observed that C-11 (δ 76.45) showed another coupling to CH_3-20 (δ 1.18, 22.37) that was further coupled to a quaternary (δ 83.49) and a secondary carbon (δ 35.88) atom. The strong shift of the two aliphatic carbons to lower field at δ 83.49 and 89.40 can be explained by an ether bridge.

The protons of C-2 (δ 32.34, 2.14-2.20, (1H), 2.24-2.28, (1H)) were coupled to the carbons at δ 89.4 and 121.51 that belong to two different fragments. A methylene chain was derived from the correlations in the ^{1}H-^{1}H COSY spectrum of the two adjacent secondary carbons at δ 28.29 and 33.91. The coupling of H-11 (δ 5.13) was also detected to both of these carbons. In addition to this, CH_3-19 (δ 1.66, 17.81) was also found to couple to the carbon at δ 33.91 so that the connection of this methylene bridge between two main fragments was completed.

Finally, CH_3-18 (δ 1.61, 16.24) was found to couple to C-5 (δ 38.94). C-4 (δ 25.31) was detected as an adjacent carbon to C-5 from the correlations in the ^{1}H-^{1}H COSY spectrum. It was further coupled to the olefinic proton H-7 (δ 5.47) (**Fig. 5.21**).
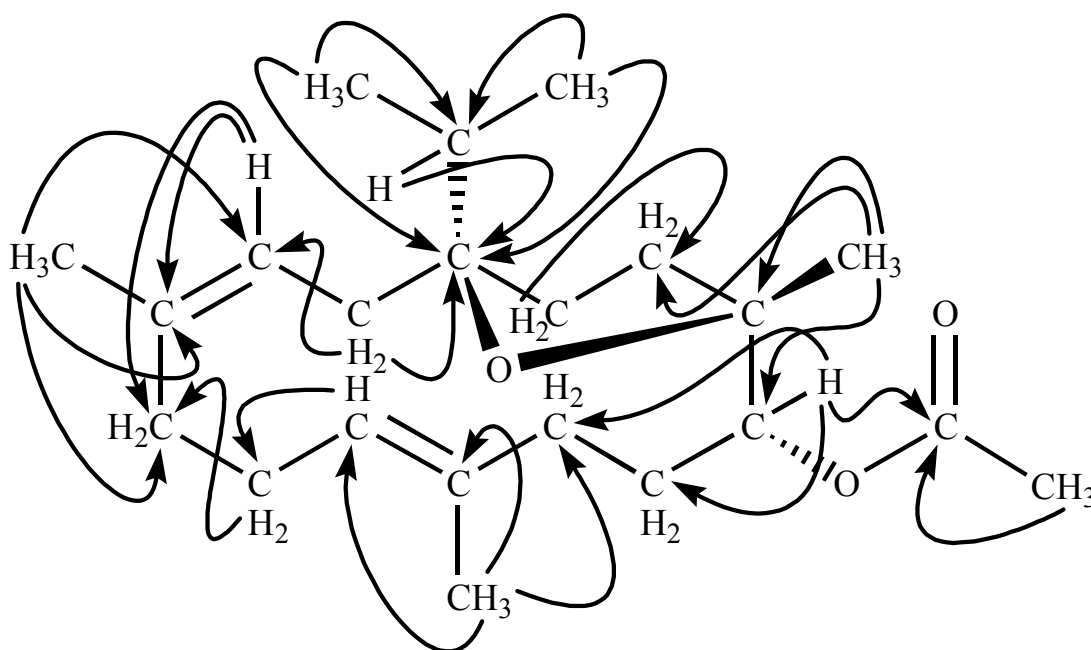
Fig. 5.21. HMBC correlations of incensyl acetate (**2**).

The relative configuration of the molecule was assigned from its NOESY spectrum. The couplings between H-11 (δ 5.13) and H-3 (δ 5.40), H-11 and H-7 (δ 5.47) indicated that although H-11 was found in α position it was coplanar with the olefinic protons H-3 and H-7. This also confirmed that the acetyl group was β to the ring system. The ether bridge was found to be out of the plane of the molecule. The correlations detected between CH_3-18 (δ

1.61, 16.24) and CH$_3$-16 (δ 0.88, 18.23), CH$_3$-18 and CH$_3$-17 (δ 0.93, 18.10), CH$_3$-20 (δ 1.18, 22.37) and CH$_3$-22 (δ 1.71, 20.84), H-3 and CH$_3$-18, H-3 and CH$_3$-19 (δ 1.66, 17.81), H-7 and CH$_3$-19, H-11 and CH$_3$-20, H-3 and H-7 was found to be coplanar to the molecule (**Fig 5.22a**).
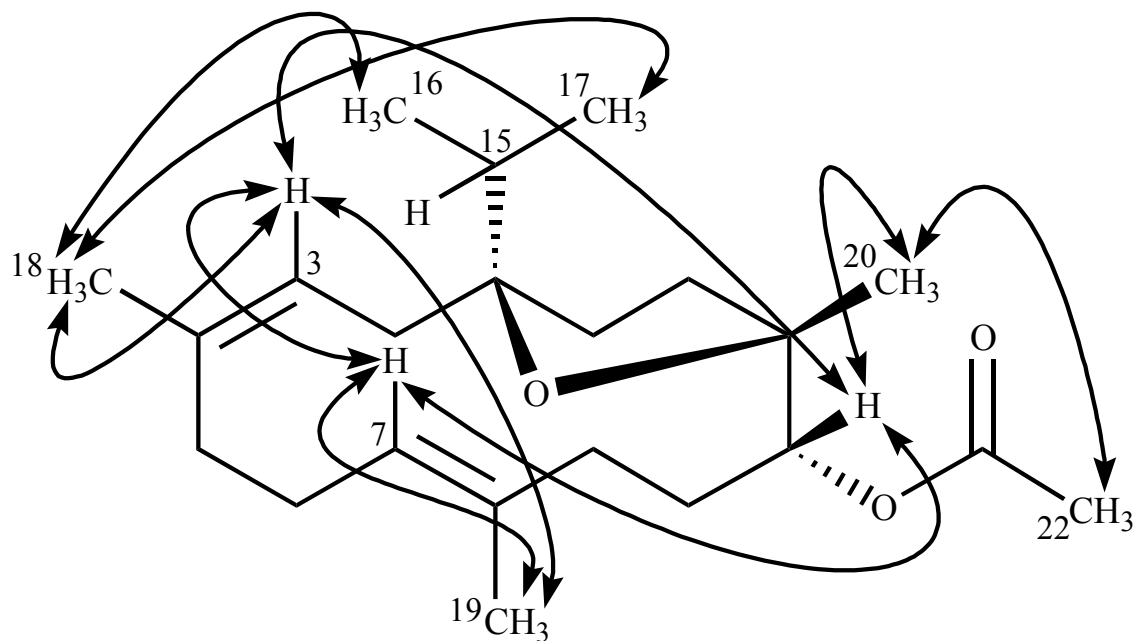
Fig. 5.22a. NOESY correlations of incensyl acetate (**2**).
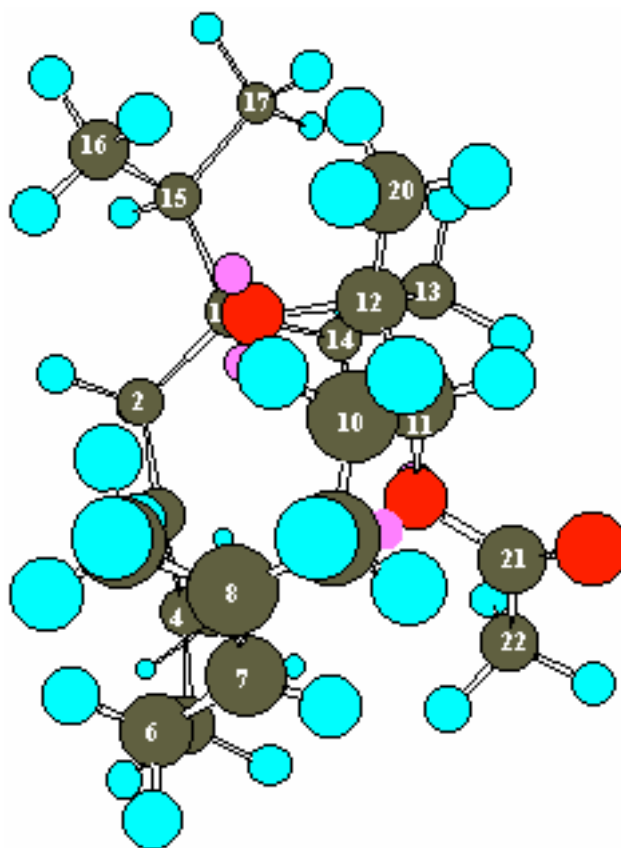
Fig. 5.22b. 3D model of incensyl acetate (**2**).

5.4.2 Essential Oil of *Boswellia serrata* Roxb.

The essential oil of *Boswellia serrata* has also been well studied. It has been known as "*Indian olibanum*" or "*Aden*" type. The major component of the oil was reported to be α-pinene, representing approximately 45% of the oil[93].

The hydrodistillate of *B. serrata* is a colorless oil. The GC and GC-MS investigations indicated that the oil consists of α-thujene (12%), α-pinene (8%), sabinene (2.2%), β-pinene (0.7%), myrcene (38%), α-phellandrene (1%), p-cymene (1%), limonene (1.9%), linalool (0.9%), perillene (0.5%), methylchavicol (11.6%), methyleugenol (2.1%), germacrene D (2.0%), kessane (0.9%), cembrene A (0.5%) and cembrenol (**6**) (1.9%) as the major constituents. In addition to these, a monoterpene 5,5-dimethyl-1-vinylbicyclo-[2.1.1]hexane (**3**) (2%) and two diterpenoic components, m-camphorene (**4**) (0.7%) and p-camphorene (**5**) (0.3%) were isolated and identified from the essential oil of *B. serrata* for the first time (**Fig. 5.23**, **Fig 5.24**).
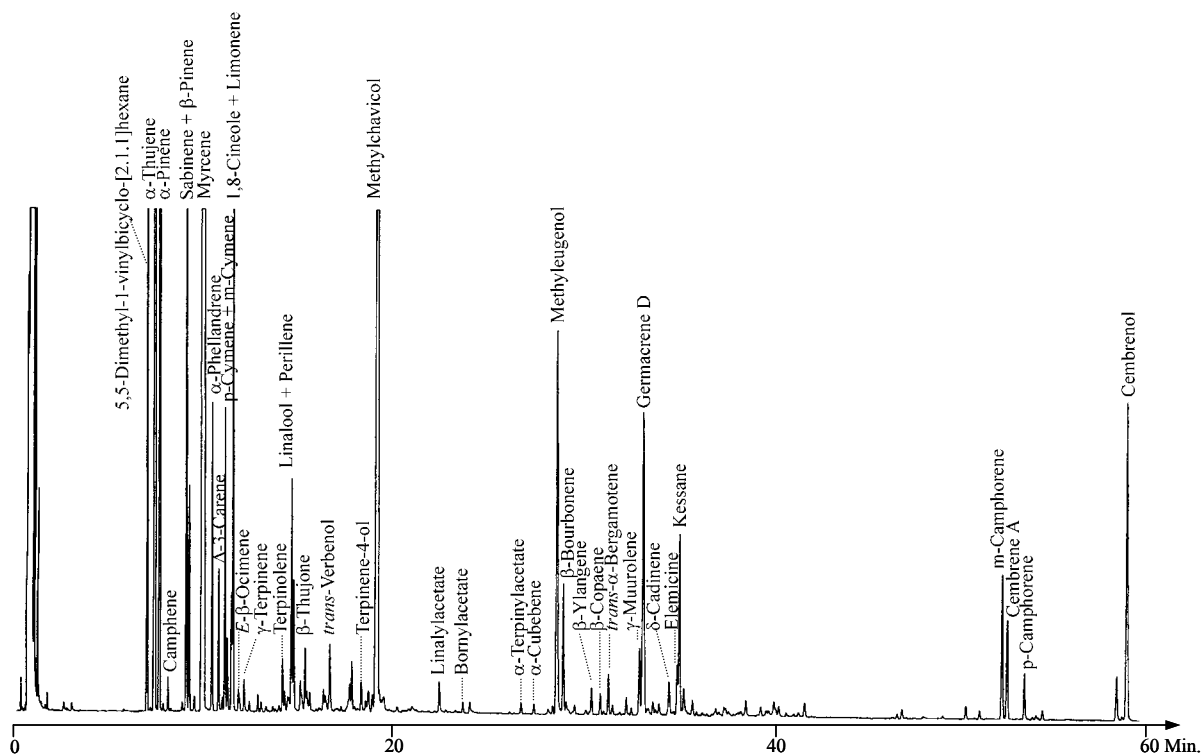
Fig. 5.23. Gas chromatogram of the essential oil of *Boswellia serrata* (25 m fused silica capillary column with CPSil 5CB, 50°C, 3 °C/min up to 230 °C, injector at 200 °C, detector at 250 °C, carrier gas 0.5 bars H$_2$).

5,5-Dimethyl-1-
vinylbicyclo-
[2.1.1]hexane (**3**)   α-Thujene   α-Pinene   Camphene   Sabinene   β-pinene   Myrcene

α-Phellandrene   Δ-3-Carene   m-Cymene   p-Cymene   1,8-Cineole   Limonene   *E*-β-Ocimene

γ-Terpinene   Terpinolene   Linalool   Perillene   β-Thujone   *trans*-Verbenol   Terpinene-4-ol

Methylchavicol

Methyleugenol   Linalyl acetate   Bornyl acetate   α-Terpinyl acetate   α-Cubebene

Elemicine   β-Bourbonene   β-Ylangene   β-Copaene

γ-Muurolene   Germacrene D   δ-Cadinene   *trans*-α-Bergamotene

Kessane   m-Camphorene (**4**)   p-Camphorene (**5**)

Cembrene A   Cembrenol (**6**)

Fig. 5.24. The constituents of the essential oil of *Boswellia serrata*.

5.4.2.1   Isolation and Identification of 5,5-Dimethyl-1-vinylbicyclo-[2.1.1]hexane (*3*)

The hydrodistillate of *Boswellia serrata* was separated into its nonpolar and polar fractions by CC on silica gel with *n*-pentane and ethylacetate, respectively. The nonpolar part of the oil was further fractioned by preparative GC on SE-30 column. A further separation by preparative GC on a thick film capillary DB-1(Hewlett Packard) column was performed to obtain **3** as pure substance (**Fig. 5.25**). The structure of the compound was elucidated by the interpretation of its mass-, 1- and 2-D NMR spectra.
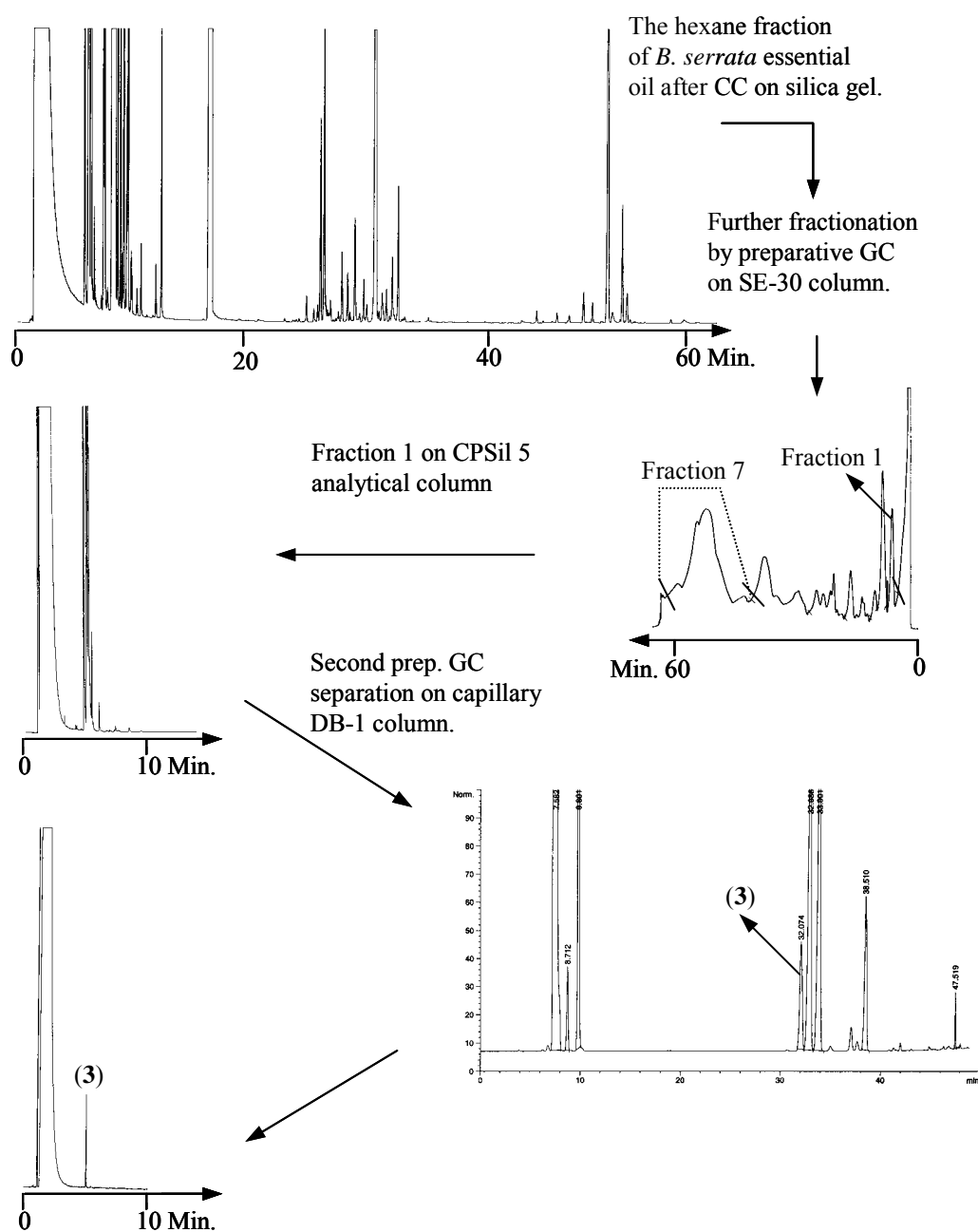
Fig. 5.25. Schematic expression of the isolation steps of compound **3**. **Left side**: 25 m fused silica capillary column with CPSil 5CB, 50 °C, 3 °C/min up to 230 °C. **Right side, above**: 2 m packed SE-30 column, 75 °C, 2 °C/min up to 200 °C, **below**: 30 m capillary DB-1 column, 50 °C, 1.5°C/min up to 110 °C, 10 °C/min up to 200°C.

The pure compound produced a molecular ion signal at *m/z* = 136 in its mass spectrum that corresponded to an elemental composition of $C_{10}H_{16}$ (**Fig. 5.26**).
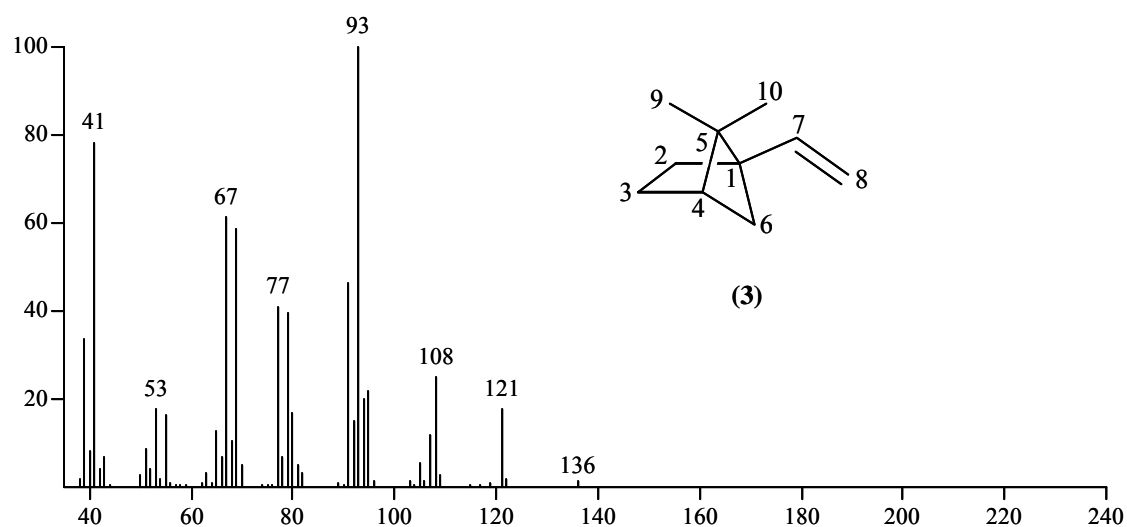
Fig. 5.26. Mass spectrum of 5,5-dimethyl-1-vinylbicyclo-[2.1.1]hexane (**3**).
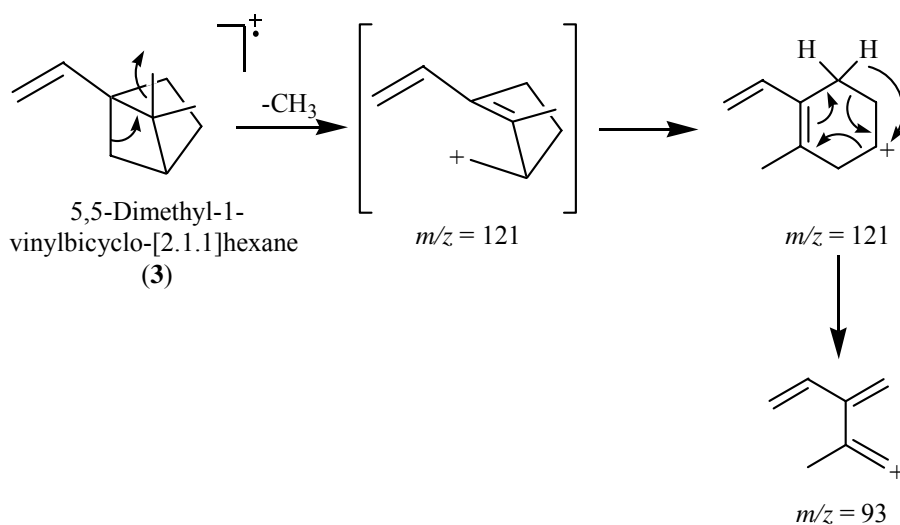
Fig. 5.27. Possible fragmentation pattern of **3**.

The ^{1}H-NMR spectrum showed two singlets at δ 0.69 and 1.08 for two geminal methyl groups, a doublet at δ 0.89 (d, J = 7.25 Hz) for a single aliphatic proton and three olefinic protons at δ 5.02 (dd, J_{trans} = 15.7, J_{gem} = 2.2 Hz), 5.08 (dd, J_{cis}= 11.3, J_{gem} = 2.2) and 5.88 (dd, J_{trans} = 17, J_{cis} = 10.7 Hz) (**Fig. 5.28**).
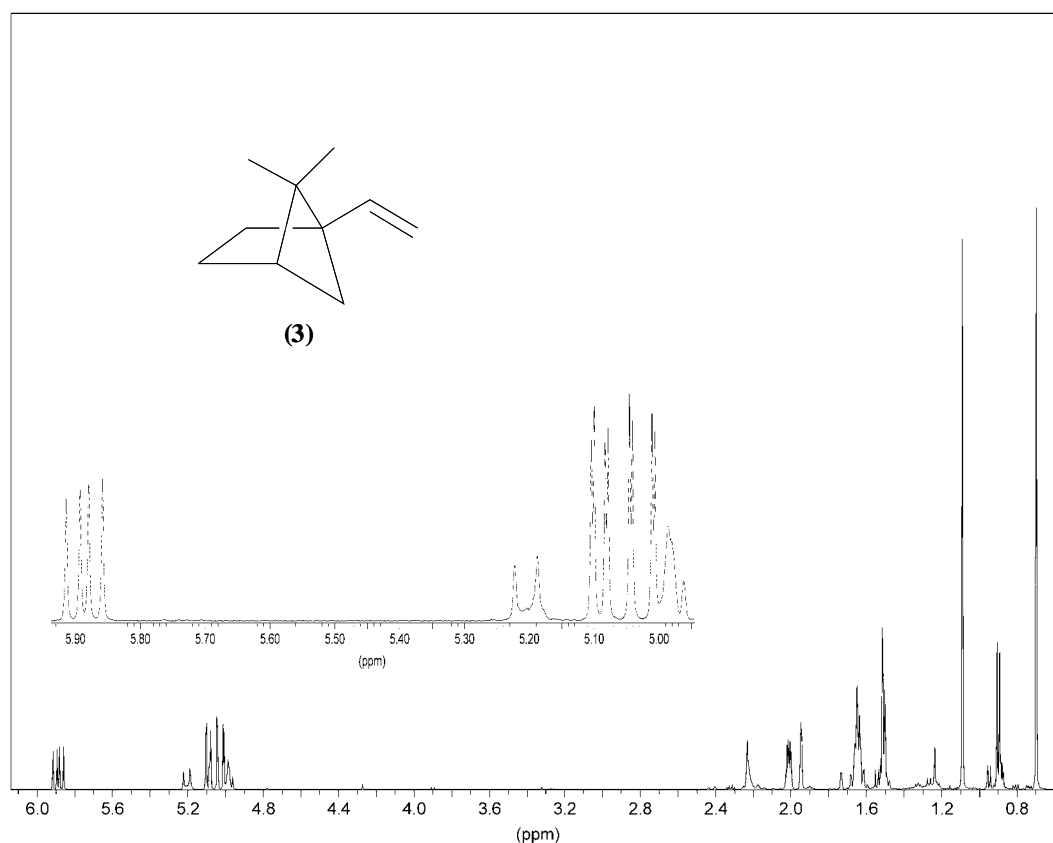
Fig. 5.28. ^{1}H-NMR spectrum of **3**.

The ^{13}C-NMR and PENDANT spectra indicated eight carbon signals, two primary carbons at δ 19.83, 19.39, four secondary carbons at δ 26.55, 30.43, 39.12, 115.15, two tertiary carbons at δ 44.44 and 137.91. Two more quaternary carbons were identified from the HMBC spectrum at δ 56.2 and 47.0 (**Fig. 5.29**). The carbon signals shifted to the low field at δ 115.15 and 137.91 indicated a double bond in the molecule.

The interpretation of the HMQC spectrum showed that C-8 (δ 115.15) correlated to the protons at δ 5.02 and 5.08 and C-7 was coupled with the third olefinic proton at δ 5.8. The broad singlet at δ 1.94 was found to correlate to the tertiary carbon C-4 (δ 44.44). The methyl groups were derived as CH$_3$-9 (δ 19.83, 1.08) and CH$_3$-10 (δ 19.39, 0.69).

The connectivity of the fragments was determined mainly from the HMBC spectrum. A double bond system was the first fragment formed from C-7 (δ 137.91) and C-8 (δ 115.15). The second fragment was established by the couplings of two geminal methyl groups to two quaternary C-1 (δ 56.2), C-5 (δ 47.0) and one tertiary carbon C-4 (δ 44.44). The coupling of olefinic protons, H-8 to C-1 confirmed the connection of these two fragments to each other. The positioning of the three secondary carbons, C-2 (δ 26.55), C-3 (δ 30.43) and C-6 (δ

39.12) were deduced from the correlations observed in the ^{1}H-^{1}H COSY spectrum (**Table 5.3**, **Fig. 5.30**).
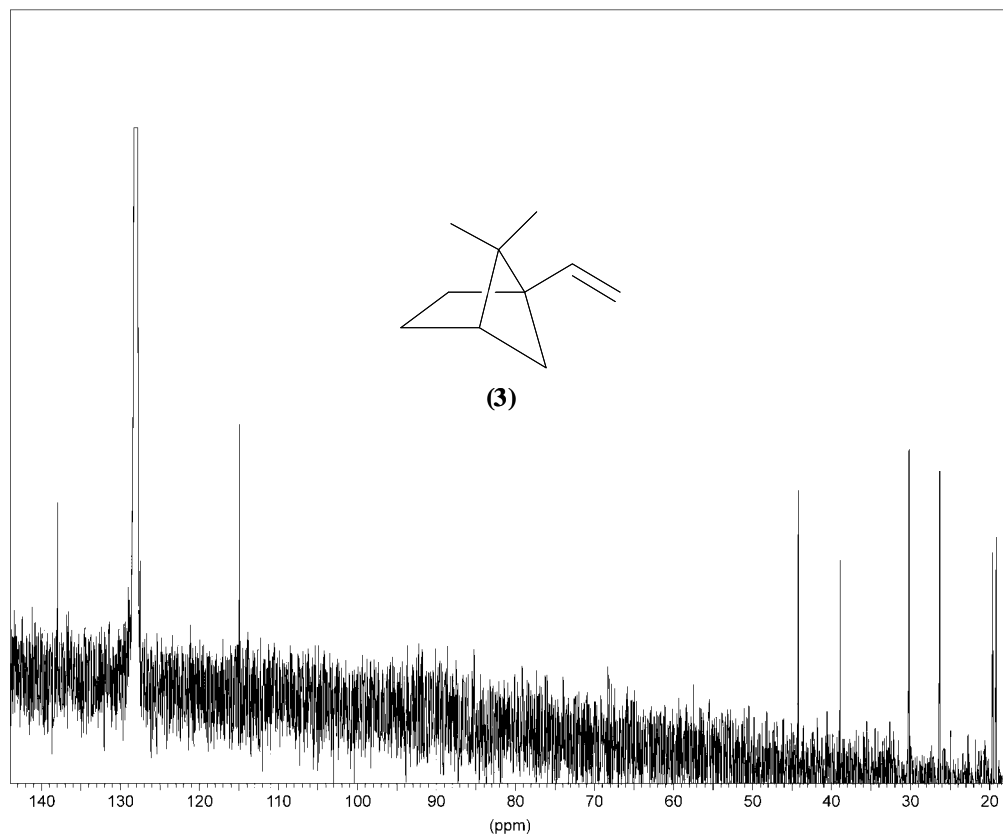
Fig. 5.29. ^{13}C-NMR spectrum of **3**.

Table 5.3. HMQC correlations of **3**.

No.	^{13}C (ppm)	^{1}H (ppm)	No.	^{13}C (ppm)	^{1}H (ppm)
1	56.20		6	39.12	0.89, 2.0
2	26.55	(1.49-1.54), (1.61-1.68)	7	137.91	5.88
3	30.43	(1.49-1.54), (1.61-1.68)	8	115.15	5.08, 5.02
4	44.44	1.94	9	19.30	0.69
5	47.00		10	19.80	1.08
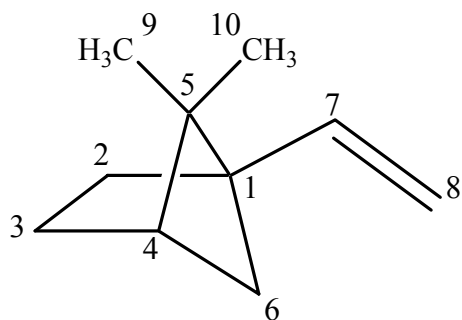
Fig. 5.30. Numbered structure of **3**.

This compound had already been isolated from *Mentha cardiaca* as a natural product [118] but it was identified for the first time in *Boswellia* species.

5.4.2.2 Isolation of m-Camphorene (*4*) and p-Camphorene (*5*)

The non-polar part of the essential oil of *B. serrata* was fractionated by preparative GC on SE-30 column (**Fig. 5.25**). Fraction 7 was found to contain the two diterpenoic compounds and cembrene A (**Fig. 5.31**). The separation of these compounds was optimised on a modified cyclodextrin stationary phase (6T-2,3-methyl-β-CD) with a different order of elution. Pure compounds of m-camphorene (**4**) and p-camphorene (**5**) were obtained by performing the same separation on preparative scale.
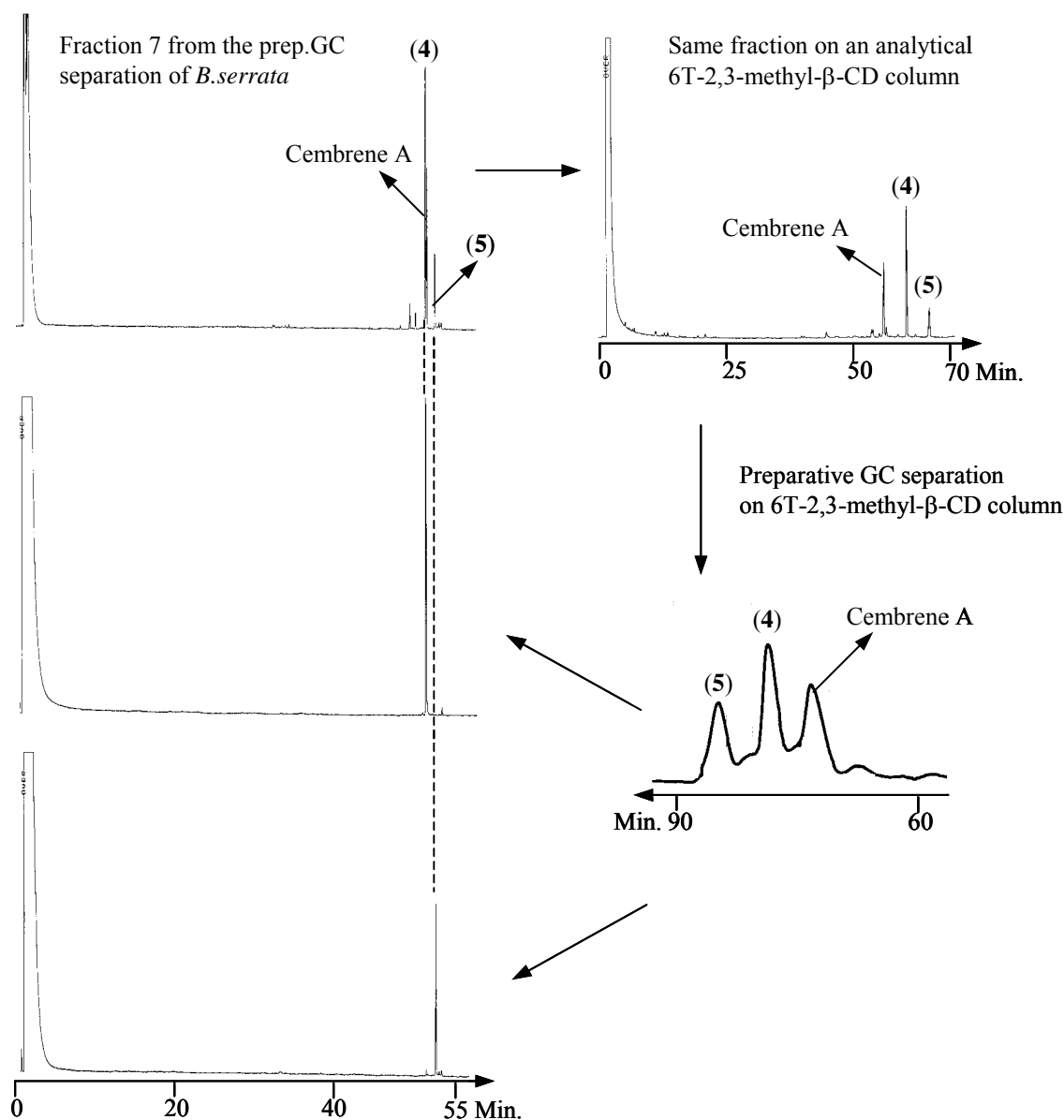
Fig. 5.31. Schematic expression of the isolation steps of m-camphorene (**4**) and p-camphorene (**5**). **Left side**: 25 m fused silica capillary column with CPSil 5CB, 50 °C, 3 °C/min up to 230 °C. **Right side, above**: 25 m capillary column with 6T-2,3-methyl-β-CD, 130 °C for 20 min, 1 °C/min up to 180 °C, **below**: 2 m packed column with 6T-2,3-methyl-β-CD, 130 °C for 20 min, 1 °C/min up to 150 °C, 0.5 °C/min. up to 170 °C.

5.4.2.2 Identification of m-Camphorene (4)

The pure compound produced a molecular ion signal at *m/z* = 272 in its mass spectrum that corresponded to an elemental composition of $C_{20}H_{32}$ (**Fig 5.32**).

Fig. 5.32. Mass spectrum of m-camphorene (**4**).

The fragmentation pattern of m-camphorene (**4**) showed primarily allyl cleavages or RDA reaction followed by allyl cleavages which explains the base peak at *m/z* = 69 (**Fig. 5.33**).
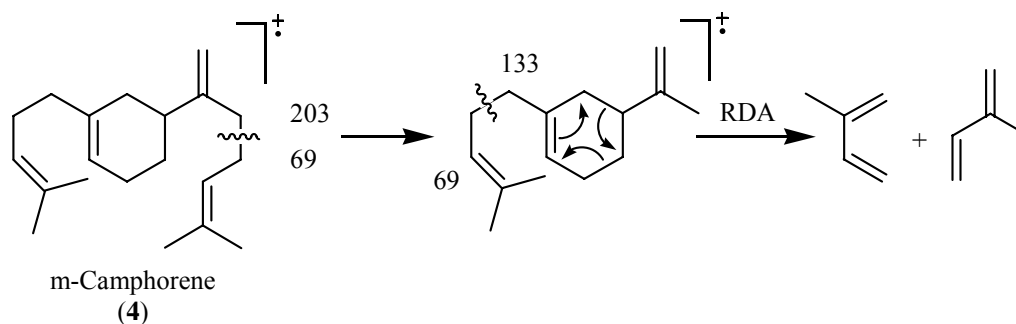
Fig. 5.33. Possible fragmentation of **4**.

The ^{1}H-NMR spectrum of **4** indicated four methyl groups two of which overlap at δ 1.68 and showed a singlet whereas the others absorbed at δ 1.61 and 1.60 as two singlets. Five olefinic hydrogens were recognized in the spectrum at δ 4.75, 4.76, 5.39 and at δ 5.10 (dd, *J* = 6.9, 6.6 Hz, 1H) and 5.12 (dd, *J* = 6.3, 6.3 Hz, 1H). The latter two appeared as overlapping doublets for two hydrogens (**Fig. 5.34**).
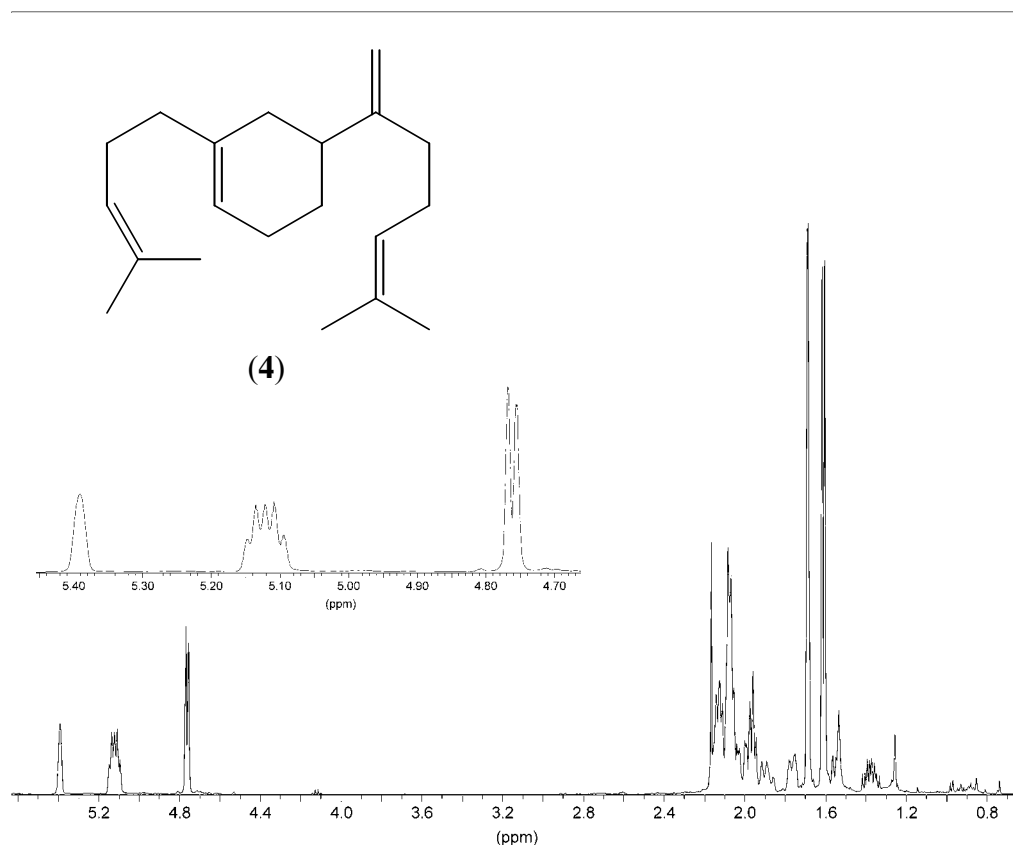
Fig. 5.34. ^{1}H-NMR spectrum of **4**.

The ^{13}C-NMR and PENDANT spectra of **4** showed three primary carbons at δ 17.70, 17.72, 25.70, eight secondary carbons at δ 25.87, 26.54, 26.87, 28.01, 34.62, 34.87, 37.87, 107.16, four tertiary carbons at δ 40.41, 120.29, 124.34, 124.43 and four quaternary carbons at δ 131.35, 131.51, 137.51, 154.45, a total of 19 signals. The integration of the carbon signals showed that two carbon signals were overlapping at δ 25.70. Additionally the low field carbon signals at δ 107.16, 120.29, 124.34, 124.43, 131.35, 131.51, 137.51, 154.45 indicated four double bonds in the molecule (**Fig. 5.35**).

The HMQC spectrum of **4** indicated that the olefinic protons at δ 4.75 and 4.76 were correlating to a single carbon at δ 107.16. The other olefinic protons at δ 5.10, 5.12, 5.39 were found to couple to three tertiary carbons at δ 124.43, 124.34, 120.29, respectively. The two methyl singlets at δ 1.61, 1.60 were found to correlate with carbons at δ 17.70, 17.72, respectively. The methyl signals at δ 1.684 and 1.689 were overlapping with each other and showed a broad singlet. Both were correlated with the carbon signal at δ 25.70 which was already identified for two carbon atoms (**Table 5.4, Fig. 5.36**).
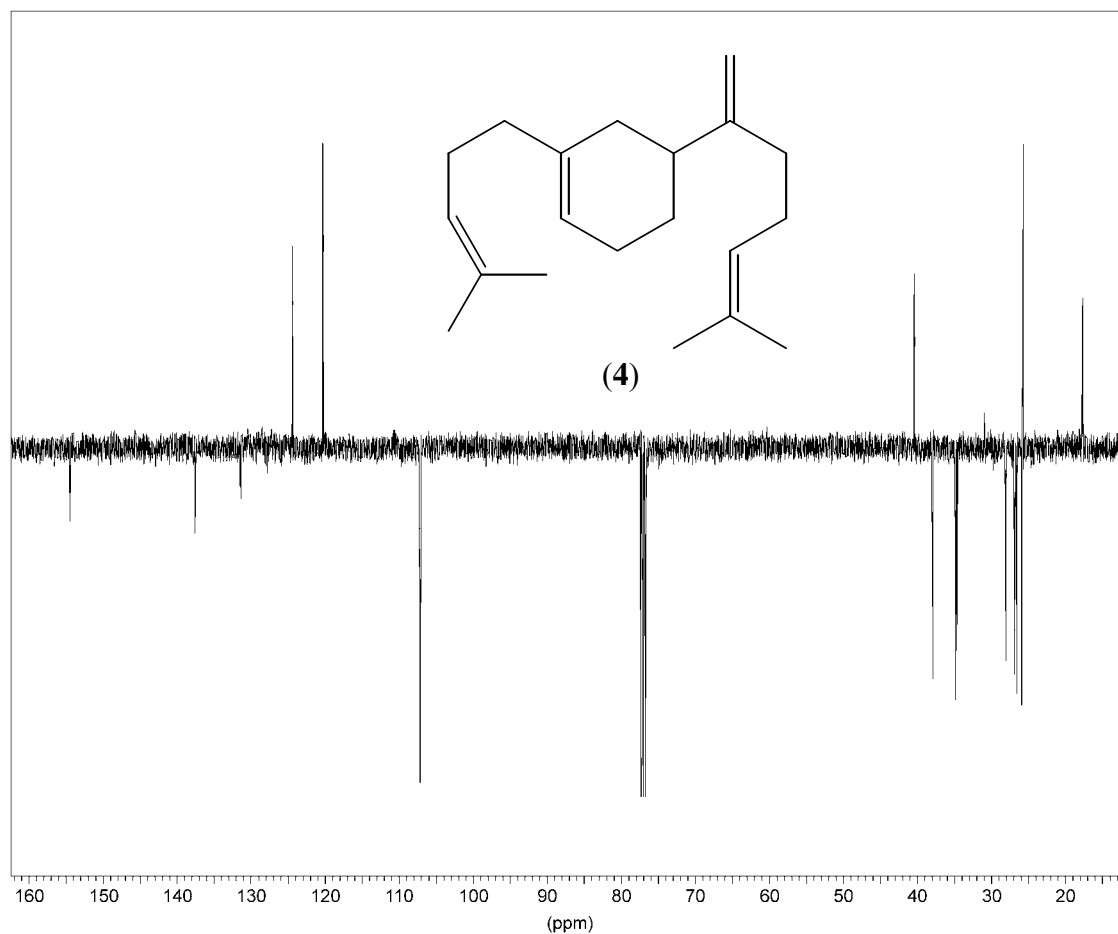
Fig. 5.35. ¹³C-NMR (PENDANT) spectrum of **4**.

Table 5.4. HMQC correlations of **4**.

No.	¹³C (ppm)	¹H (ppm)	No.	¹³C (ppm)	¹H (ppm)
1	137.51		11	25.70	1.684
2	120.29	5.39	12	17.72	1.60
3	26.54	(2.06-2.08), 2H	13	154.45	
4	34.62	(1.85-1.91), (1.99)	14	34.87	(2.02-2.05), (2.06-2.08)
5	40.41	(2.11-2.15)	15	26.87	(2.11-2.15), 2H
6	28.01	(1.33-1.41), (1.75-1.77)	16	124.34	5.12
7	37.87	(1.94-1.97), 2H	17	131.51	
8	25.87	(2.06-2.08), 2H	18	107.16	4.75, 4.76
9	124.43	5.10	19	25.70	1.689
10	131.35		20	17.70	1.61
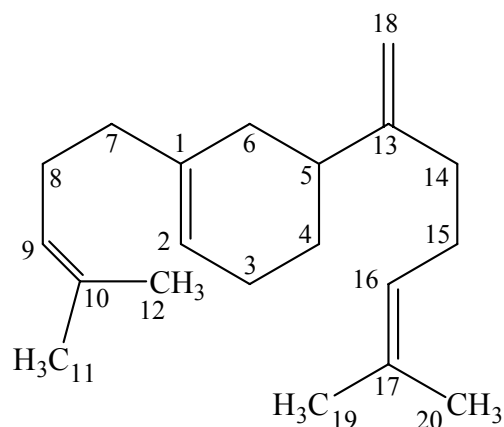
Fig. 5.36. Numbered structure of **4**.

The connectivity of the carbons of compound **4** was derived from HMBC and ^{1}H-^{1}H-COSY spectra. First the double bonds in the molecule were determined. The coupling of H-9 (δ 5.10) to C-10 (δ 131.35) and the couplings of the methyl groups CH$_3$-11 (δ 1.684, 25.70) and CH$_3$-12 (δ 1.60, 17.72) to C-10 and C-9 (δ 124.43) were assigned to the first double bond system.

The second fragment was derived from the coupling of H-2 (δ 5.39), which correlated with C-2 (δ 120.29), to the quaternary carbon C-1 (δ 137.51).

The couplings of the C-18 protons (δ 4.75, 4.76) to a quaternary carbon C-13 (δ 154.45) indicated the third double bond.

The last fragment was deduced from the couplings of H-16 (δ 5.12) to C-17 (δ 131.51) as well as from the couplings of the methyl groups CH$_3$-19 (δ 1.689, 25.70) and CH$_3$-20 (δ 1.61, 17.70) to C-16 (δ 124.34).

The connectivity of the secondary carbons C-3 (δ 26.54) and C-4 (δ 34.62), C-7 (δ 37.87) and C-8 (δ 25.87), C-14 (δ 34.87) and C-15 (δ 26.87) were deduced from ^{1}H-^{1}H COSY spectrum through the correlations of the protons. Finally, the connectivity of these methylene bridges to the double bond fragments were derived from the HMBC spectrum (**Fig. 5.37**).
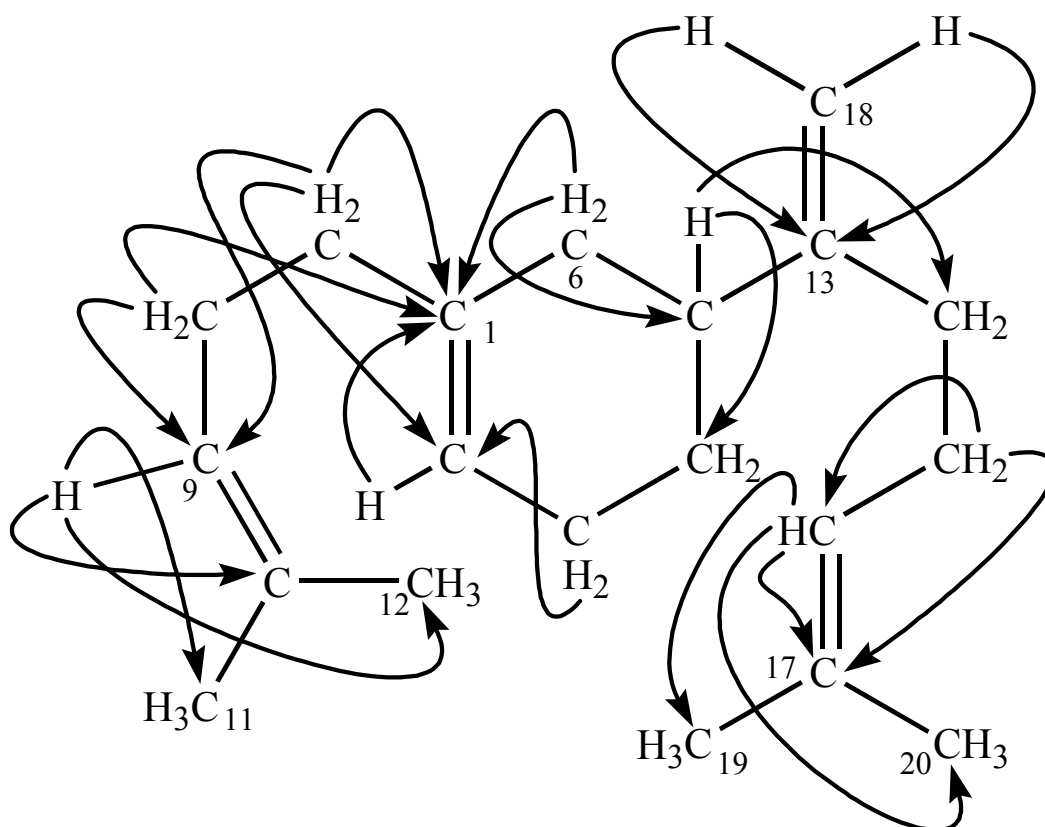
Fig. 5.37. HMBC correlations of m-camphorene (**4**).

The 3-D model of **4** provided to detect its NOESY correlations easily (**Fig. 5.38**). The exocyclic double bond was found to be orthogonal to the plane of the molecule. This caused H-18 (δ 4.76) to correlate with the protons absorbing in β position. For this reason the correlations of H-18 (δ 4.76) to H-4β (δ 1.85-1.91), H-3β (δ 2.06-2.08), H-6β (δ 1.75-1.77), and to H-5 (δ 2.11-2.15) were observed in the NOESY spectrum. On the other hand H-18 (δ 4.75) was found to correlate to H-14α (δ 2.06-2.08) and H-15α (δ 2.11-2.15). The coupling of H-4β to H-14β (δ 2.02-2.05) confirmed these correlations. H-9 (δ 5.10) was observed to correlate to CH_3-11 (δ 1.68, 25.70) as well as H-7β (δ 1.94-1.97) that was further coupled to H-2 (δ 5.39). CH_3-12 (δ 1.60, 17.72) was found to correlate to H-8α (δ 2.06-2.08) and H-3β (δ 2.06-2.08) which was further coupled to H-6α (δ 1.33-1.41). On the other side chain of the molecule the correlations of H-16 (δ 5.12) to CH_3-19 (δ 1.68, 25.70), CH_3-20 (δ 1.61, 17.70) to H-15 (δ 2.11-2.15) were observed (**Fig 5.39**).
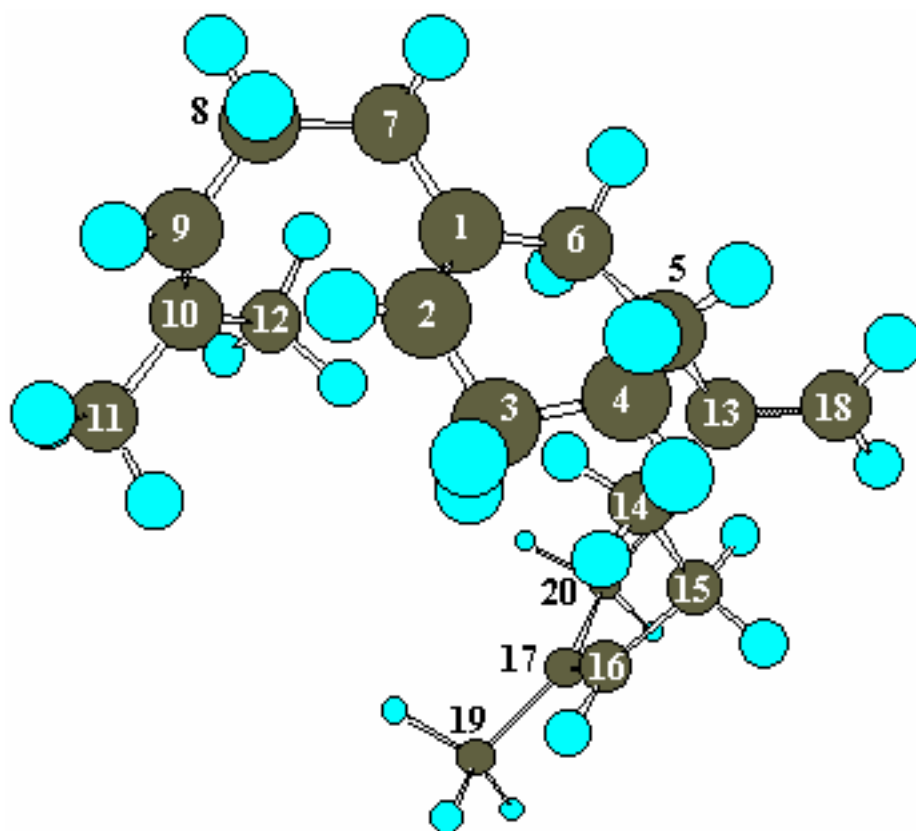
Fig. 5.38. 3-D model of m-camphorene (**4**).
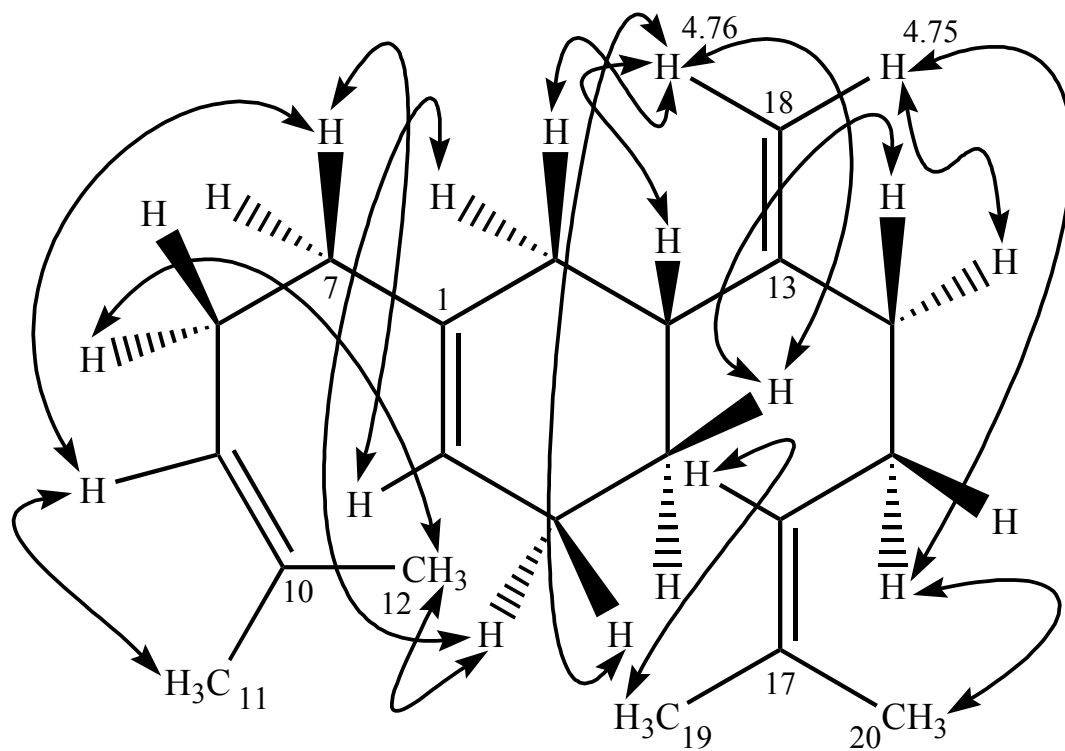
Fig. 5.39. NOESY correlations of **4.**

5.4.2.3 Identification of p-Camphorene (5)

The pure compund produced a very similar mass spectrum as m-camphorene (**4**) with a molecular ion signal at $m/z = 272$ that corresponded to an elemental composition of $C_{20}H_{32}$ (**Fig. 5.40**).
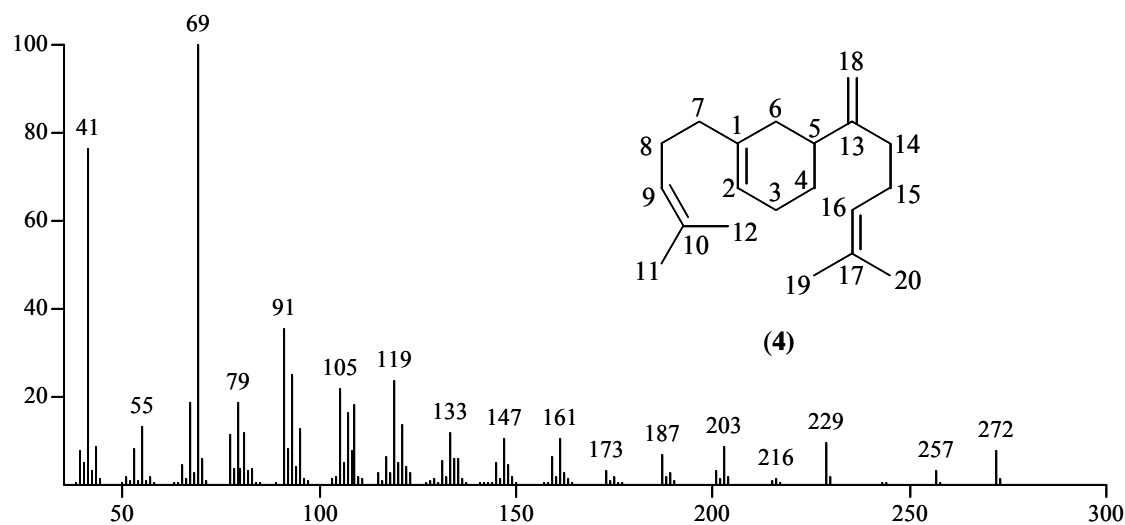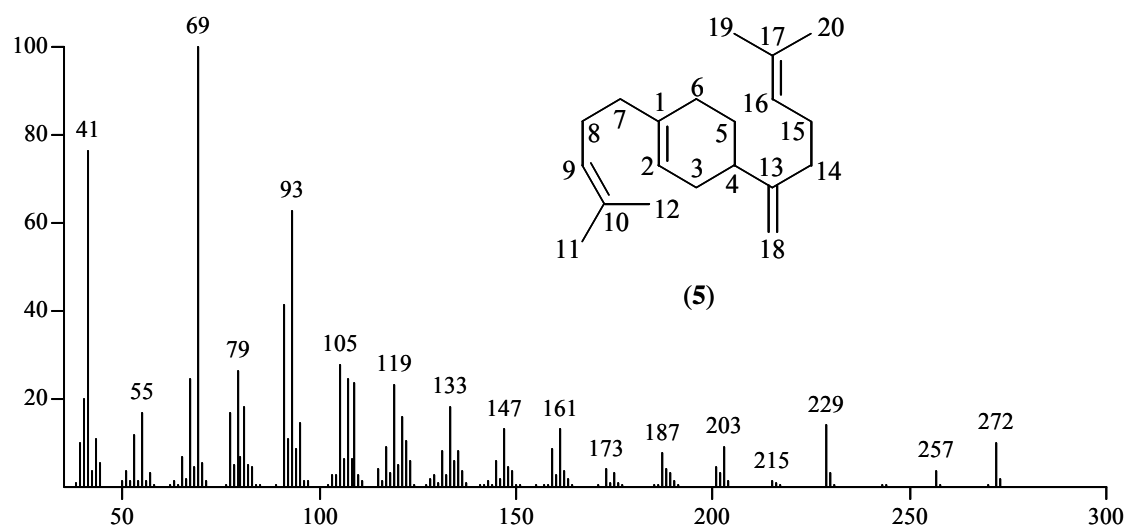

Fig. 5.40. Mass spectrum of p-camphorene (**5**).

The fragmentation of **5** was similar to m-camphorene (**4**). Allyl cleavages of the side chains and RDA reaction were the mainly observed splitting reactions of the molecule in its mass spectra (**Fig. 5.41**).
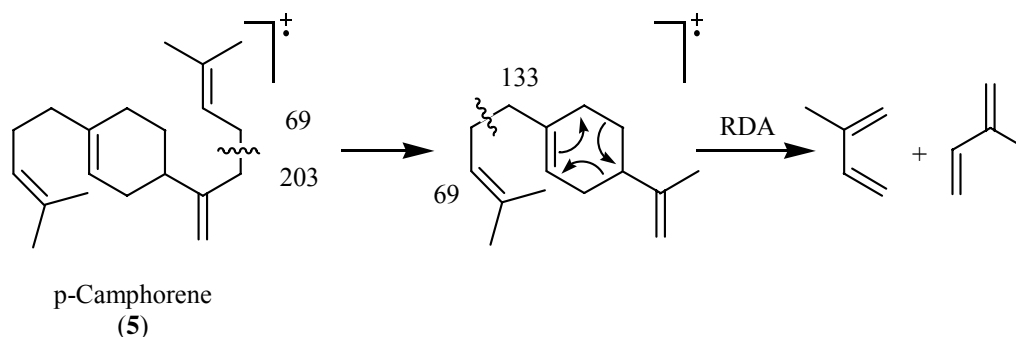
Fig. 5.41. Possible fragmentation of p-camphorene (**5**).

Similar to m-camphorene (**4**), the ^{1}H-NMR spectrum of p-camphorene (**5**) also showed four methyl group signals two of which overlap at δ 1.68 as a broad singlet whereas the others absorbed at δ 1.61 and 1.60 as two singlets. Five olefinic hydrogens were deduced from the spectrum at δ 4.74, 4.76, 5.41 as three singlets each were representing a proton and at δ 5.10 and 5.12 as two overlapping multiplets for two protons (**Fig. 5.42**).
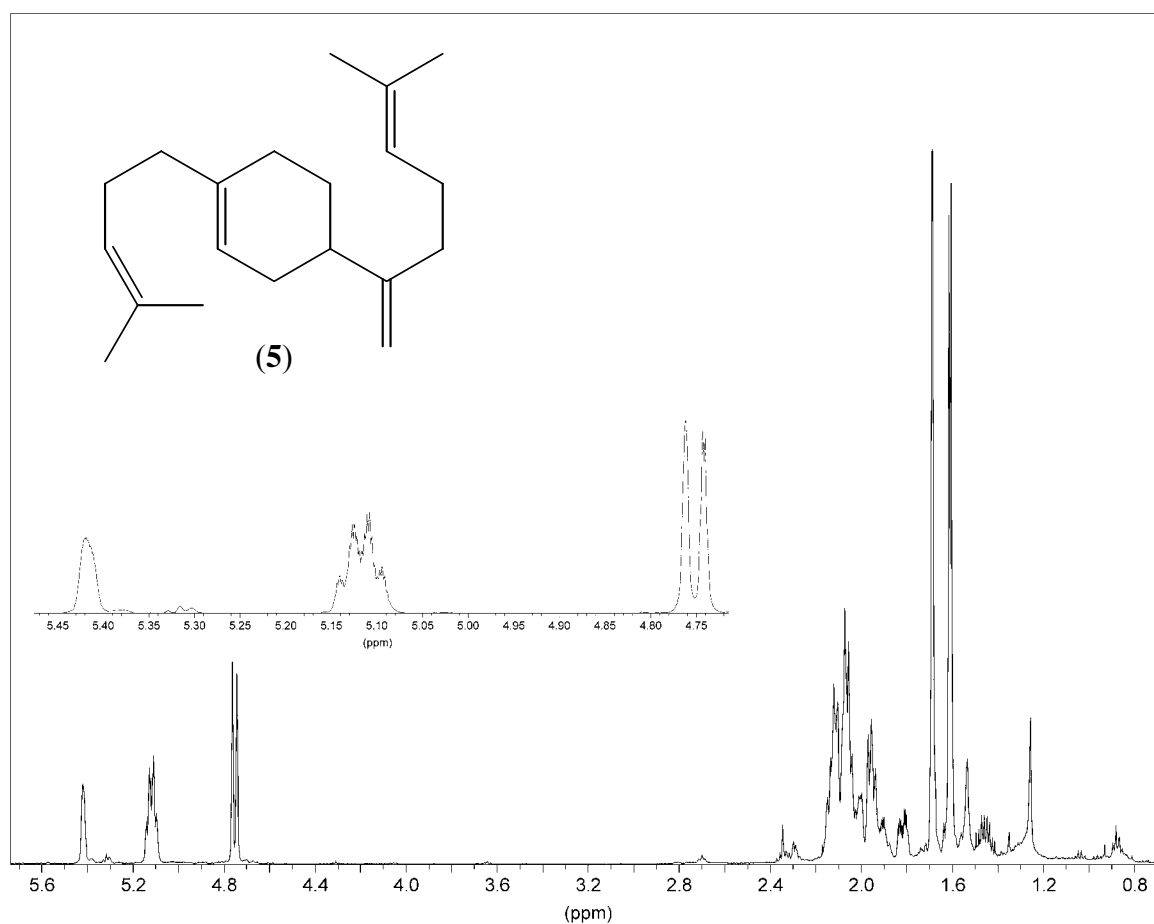
Fig. 5.42. ^{1}H-NMR spectrum of **5**.

The ^{13}C-NMR and PENDANT spectra of **5** showed three primary carbons at δ 17.70, 17.72, 25.69, eight secondary carbons at δ 26.53, 26.86, 28.37, 29.09, 31.44, 34.89, 37.61, 107.09, four tertiary carbons at δ 40.00, 120.40, 124.35, 124.43 and four quaternary carbons at δ 131.35, 131.50, 137.43, 154.34, a total of 19 signals. The integration of the carbon signals indicated that two carbon signals were overlapping at δ 25.69. Eight carbon signals found at

76

low field of the spectrum between δ 107–154, indicated four double bonds in the molecule (**Fig. 5.43**).
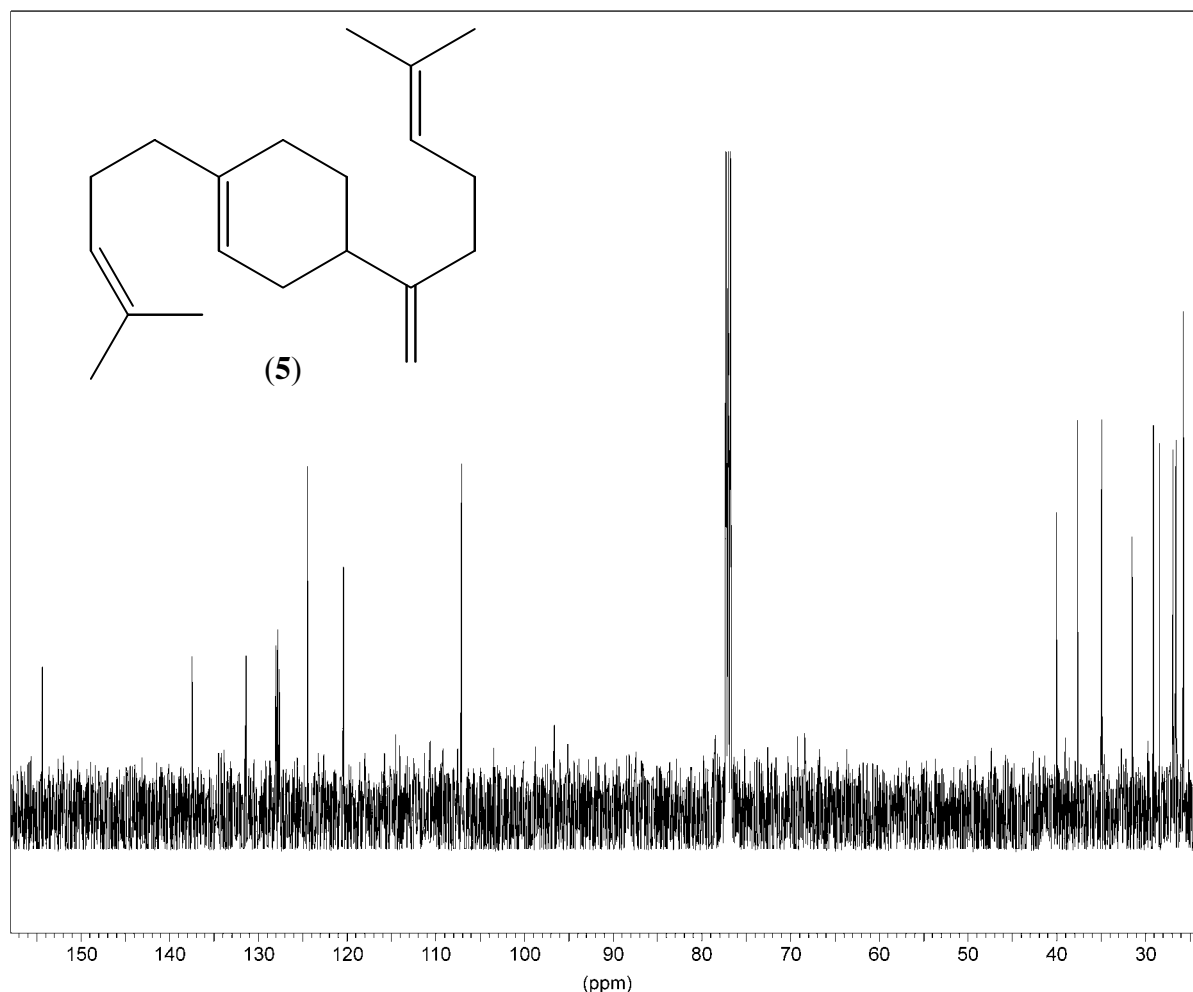
Fig. 5.43. ^{13}C-NMR spectrum of **5**.

The HMQC spectrum of **5** indicated that the carbon at δ 107.09 correlated with both hydrogens at δ 4.74 and 4.76. The other olefinic protons at δ 5.10, 5.12 and 5.41 were found to couple to three tertiary carbons at δ 124.43, 124.35 and 120.40, respectively. The two singlets appeared for two metyhl group protons at δ 1.61 and 1.60 were found to correlate to the carbon signals at δ 17.70 and 17.72, respectively. Two overlapping methyl signals at δ 1.68 were found to be correlated to the carbon signal at δ 25.69. The chemical shifts of carbons and hydrogens in compound **5** were found to be very close to compound **4** and the connectivity of these signals showed that they were constitutional isomers (**Table 5.5**, **Fig. 5.44**).

Table 5.5. HMQC correlations of **5**.

No.	^{13}C (ppm)	^{1}H (ppm)	No.	^{13}C (ppm)	^{1}H (ppm)
1	137.43		11	25.69	1.68
2	120.40	5.41	12	17.70	1.61
3	31.44	(1.87-1.94), (2.10-2-14)	13	154.34	
4	40.00	(2.10-2.14)	14	34.89	(2.04-2.07), 2H
5	28.37	(1.41-1.49), (1.79-1.84)	15	26.86	(2.10-2.14), 2H
6	29.09	(2.00-2.02), (2.04-2.07)	16	124.35	5.12
7	37.61	(1.93-1.96), 2H	17	131.35	
8	26.53	(2.04-2.07), 2H	18	107.09	4.74, 4.76
9	124.43	5.10	19	25.69	1.68
10	131.50		20	17.72	1.60
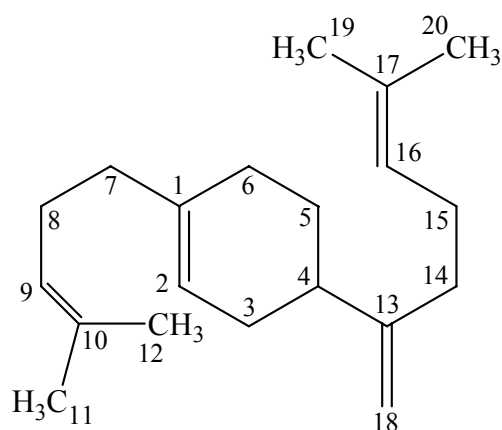
Fig. 5.44. Numbered structure of p-camphorene (**5**).

Four double bond systems were derived from the couplings detected in the HMBC spectrum of **5**. The correlations of H-9 (δ 5.10) to C-10 (δ 131.50) and the couplings of the methyl groups CH$_3$-11 (δ 1.68, 25.69) and CH$_3$-12 (δ 1.61, 17.70) to C-10 and C-9 (δ 124.43) were established as the first fragment.

The second fragment was deduced from the couplings between H-2 (δ 5.41) with the quaternary C-1 (δ 137.43).

The couplings of the C-18 hydrogens (δ 107.09, 4.74, 4.76) to another quaternary carbon C-13 (δ 154.34) indicated the third double bond.

The last fragment detected from the correlations of H-16 (δ 5.12) to C-17 (δ 131.35) and from the couplings of the methyl groups CH$_3$-19 (δ 1.68, 25.69) and CH$_3$-20 (δ 1.60, 17.72) to C-16 (δ 124.35).

The connectivity of the secondary carbons C-5 (δ 28.37) and C-6 (δ 29.09), C-7 (δ 37.61) and C-8 (δ 26.53), C-14 (δ 34.89) and C-15 (δ 26.86) were derived from the correlations detected in the ^{1}H-^{1}H COSY spectrum.

Finally, in **5,** the change in the position of the tertiary carbon to C-4 (δ 40.00) instead of C-5 in compound **4** and its coupling with H-2 (δ 5.41) resulted in para configuration of the two side chains in the molecule (**Fig. 5.45**).
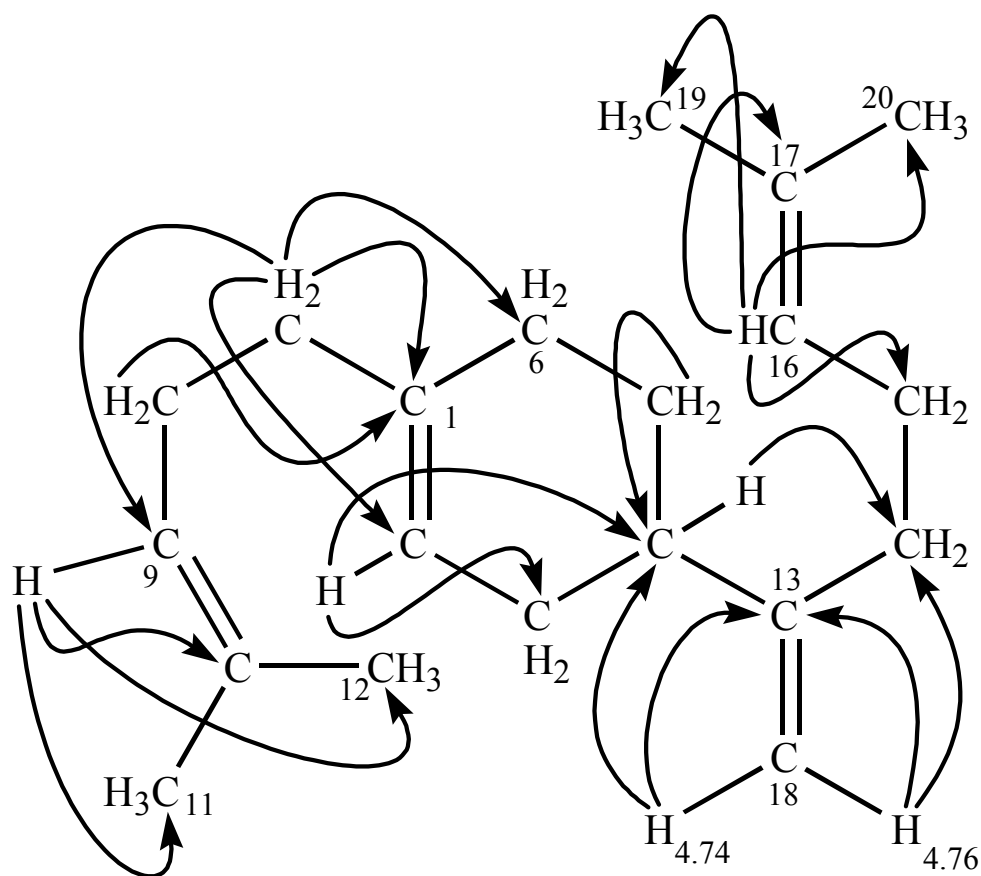
Fig. 5.45. HMBC correlations of p-camphorene (**5**).

Contrarily to m-camphorene (**4**) the 3-D model of **5** indicated that the H-18 protons were coplanar with the plane of the molecule (**Fig. 5.46**). The NOESY correlations of **5** showed correlations of H-18 (δ 4.74) to H-5α (δ 1.41-1.49), H-7α (δ 1.93-1.96), H-6α (δ 2.00-2.02). The other H-18 proton (δ 4.76) was found to be correlated to H-15α (δ 2.04-2.07), H-14α (δ 2.10-2.14) and H-5α. H-5α was further correlated to H-3α (δ 2.10-2.14). H-10 (δ 5.10) was found in relation to CH$_3$-11 (δ 1.68, 25.69) which was further coupled to H-7α (δ 1.93-1.96).

On the other hand H-2 (δ 5.41) was found to be coupling to H-7β (δ 1.93-196). The other side chain of the molecule showed correlations of H-16 (δ 5.12) to CH$_3$-19 (δ 1.68, 25.69) and CH$_3$-20 (δ 1.60, 17.72) to H-15 (**Fig. 5.47**).
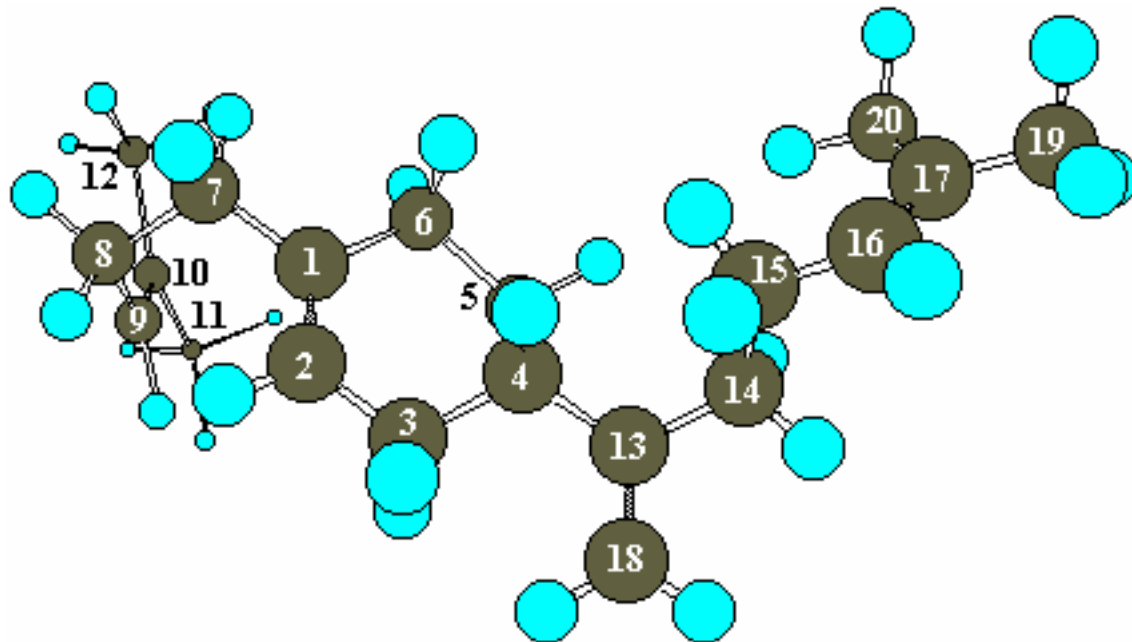
Fig. 5.46. 3-D model of p-camphorene (**5**).

Fig. 5.47. NOESY correlations of p-camphorene (**5**).

Both m-camphorene (**4**) and p-camphorene (**5**) were identified before as constituents of hop oil[119, 120]. Nevertheless, they were isolated and identified for the first time in *Boswellia*.

The presence of a cembrene alcohol, serratol or cembrenol, from *B. serrata* was reported in earlier studies[92, 121]. However, both compounds were reported with different structures (**Fig. 5.48**). The 1- and 2-NMR studies performed in this study was consistent with the cembrenol (**6**) structure.

Serratol   Cembrenol
                    (**6**)

Fig. 5.48. Two cembrene alcohols reported from *B. serrata*.

These diterpenoic constituents, m-camphorene (**4**), p-camphorene (**5**) as well as cembrenol (**6**) in *Boswellia serrata* essential oil turned out to be diagnostic markers for this species.

5.4.3 Essential Oil of *Boswellia frereana* Birdw.

The essential oil of *Boswellia frereana* was studied together with *B. carterii* for comparative reasons in earlier work[99, 100] since they originate from the same region in Africa. However, it was recognized that *B. frereana* has a very different monoterpenoic composition as the other olibanum resins. p-Cymene was reported to be the most abundant component in the oil[122].

The hydrodistillate of *B. frereana* determined in this work was light yellow in color. The investigation of the essential oil by GC (**Fig. 5.49, Fig. 5.50**) and GC-MS indicated that the oil was predominantly composed of α-thujene (8.1%), α-pinene (38%), p-cymene (11%), limonene (2.4%), sabinene (2.6%), *trans*-verbenol (4.2%) and bornylacetate (2.8%). As diterpenoic constituents, isomers of α-phellandrene dimers were observed. They were recognized as the diagnostic markers of *B. frereana*. The major isomer (**7**) (1.8%) was isolated and identified.

Fig. 5.49. Gas chromatogram of the essential oil of *Boswellia frereana* (25 m fused silica capillary column with CPSil 5CB, 50 °C, 3 °C/min up to 230 °C, injector at 200 °C, detector at 250 °C, carrier gas 0.5 bars H_2).
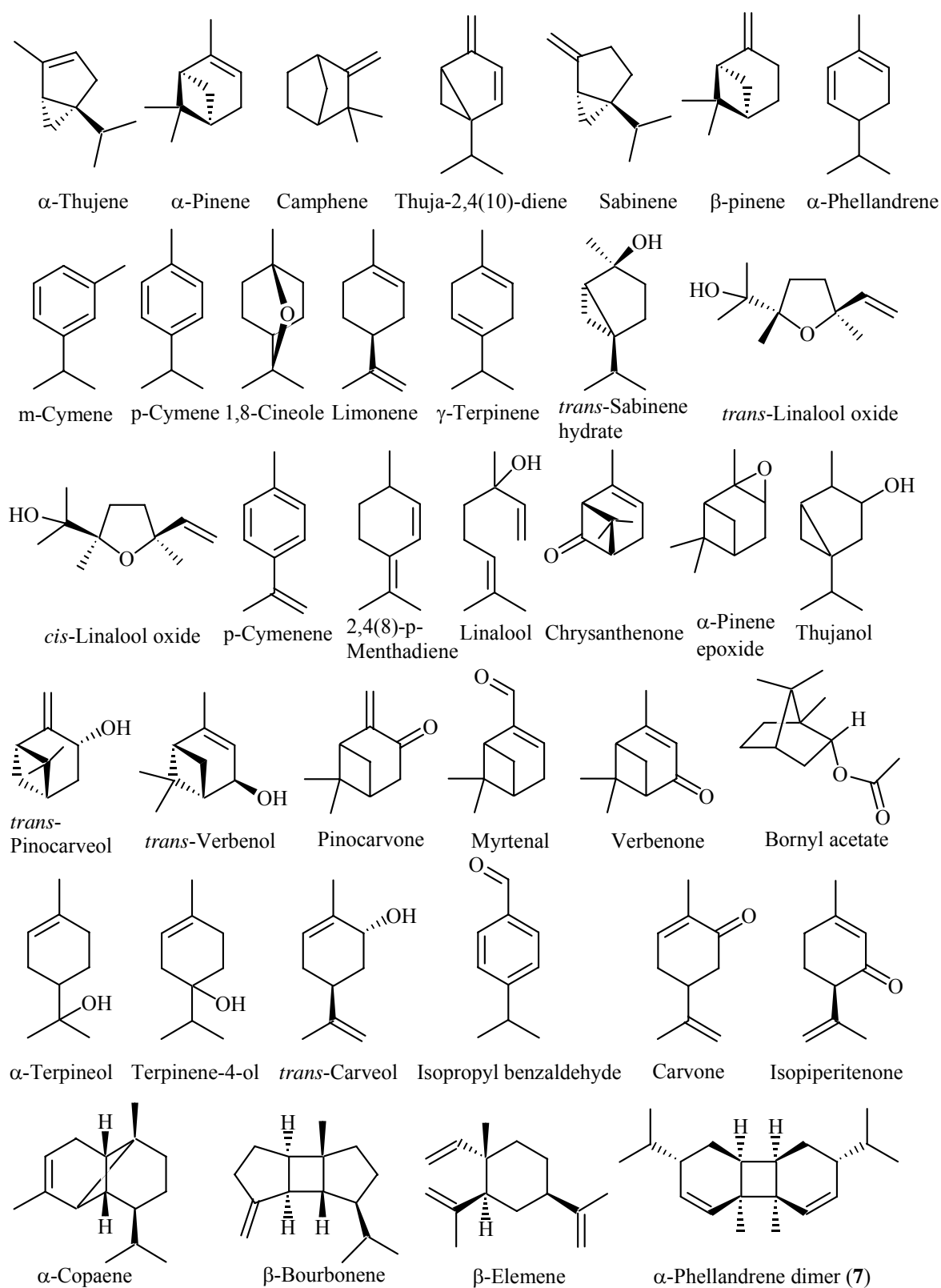
Fig. 5.50. Constituents of the essential oil of *Boswellia frereana.*

5.4.3.1 Dimer of α-phellandrene (7)

The essential oil of *B. frereana* was separated into its non-polar and polar fractions by CC on silica gel with *n*-hexane and diethylether, respectively. The diterpenoic components were recognized in the non-polar fraction. The major peak of these diterpenoic constituents was purified by preparative GC on a SE-30 column.

The mass spectrum of **7** produced a molecular ion signal *m/z* = 272 that corresponded to an elemental composition of $C_{20}H_{32}$ (**Fig. 5.51**).
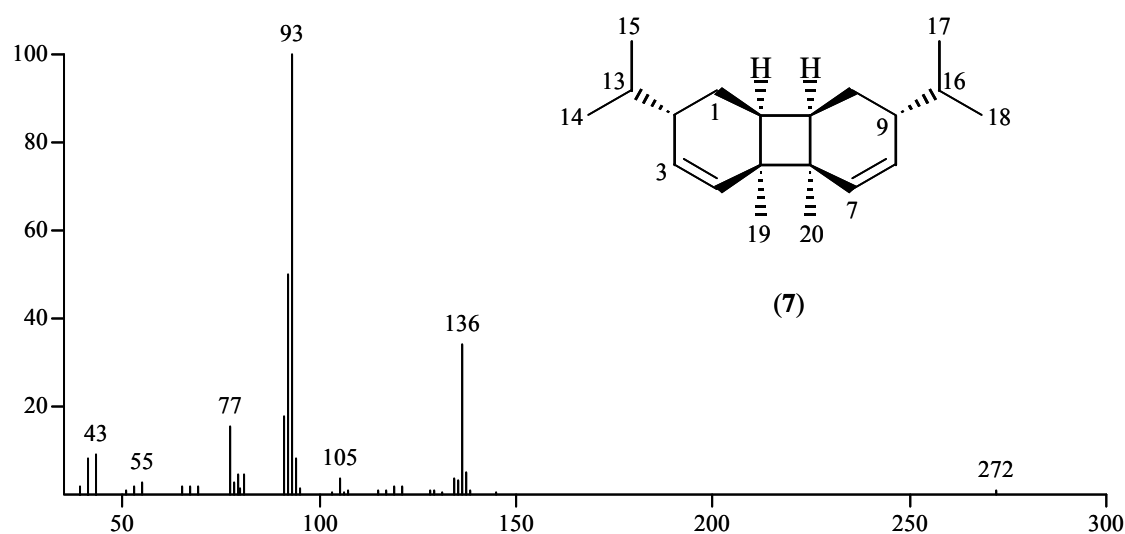
Fig. 5.51. The mass spectrum of α-phellandrene dimer (**7**).

In the fragmentation pattern of the dimer of α-phellandrene (**7**), the splitting of the dimer into its monomers was observed. This was follwed by an allylic cleavage of the isopropyl group to produce the base peak signal at m/z = 93 (**Fig. 5.52**).

The ^{1}H-NMR spectrum of **7** showed three methyl groups at δ 0.91 (d, *J* = 6.9 Hz), 0.92 (d, *J* = 6.6 Hz) and 1.03. Two olefinic proton signals were observed at δ 5.65 (dd, *J* = 10.40, 2.3 Hz) and 5.73 (d, *J* = 10.40 Hz). The other signals were deduced at δ 1.15 (t, *J* = 11.7 Hz, 1H), 1.49 (dd, *J* = 5.6, 11.6, 1H), two multiplets between δ 1.56-1.62 and 1.99-2.02 each corresponding to one proton as well as a singlet at δ 2.03. Although the total of these described signals were added up to a total of 16 hydrogens their integration resulted in 32 protons (**Fig. 5.53**).
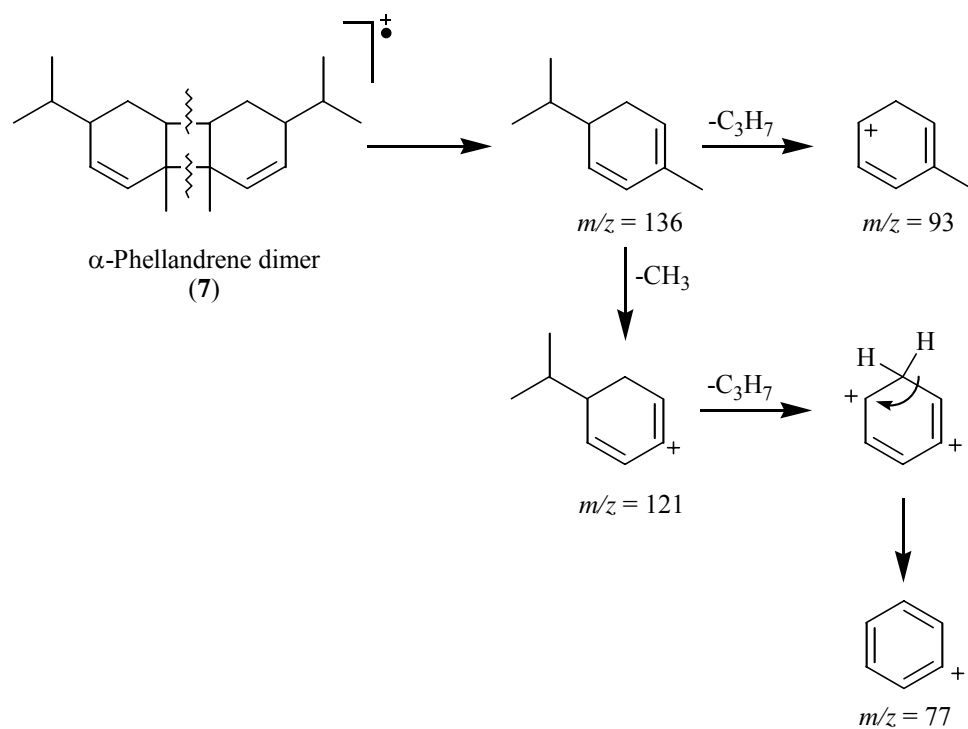
Fig. 5.52. Possible fragmentation of **7**.
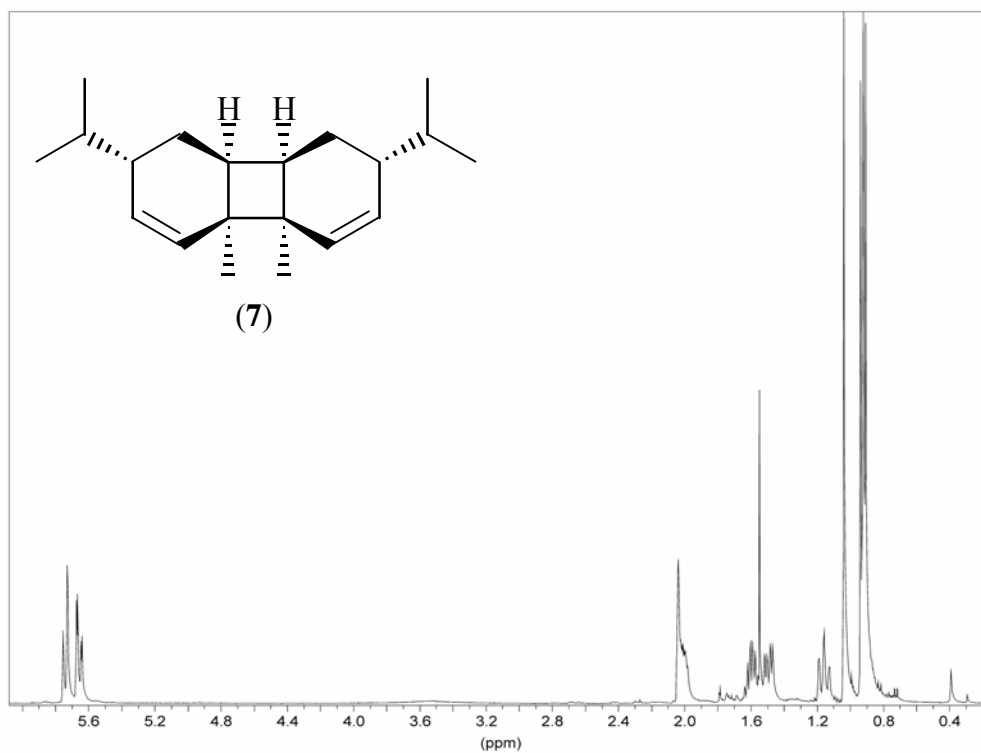
Fig. 5.53. ^{1}H-NMR spectrum of **7**.

The ^{13}C-NMR spectrum of **7** had also indicated only 10 signals where they were classified as three primary carbons at δ 19.48, 19.69, 22.26, one secondary carbon at δ 22.69, five tertiary carbons at δ 32.17, 37.78, 37.96, 129.92, 134.89 and one quaternary carbon at δ 43.84. To the low field shifted carbon signals at δ 129.92, 134.89 indicated a double bond in the molecule (**Fig. 5.54**).

The ^{1}H- and ^{13}C-NMR data pointed to a compound with a molecular formula of $C_{10}H_{16}$ but the molecular ion peak in mass spectrum at *m/z* = 272 indicated $C_{20}H_{32}$ which was exactly the double of what was already observed.

The HMQC spectrum of **7** indicated that the methyl proton signals at δ 0.91, 0.92, 1.03 were correlated with the carbon signals at δ 19.48, 19.69 and 22.26, respectively. The olefinic protons at δ 5.73, 5.65 were found to correlate with the carbons at δ 129.92, 134.89, respectively. The singlet at δ 2.03 were found to couple to the carbon signal at δ 37.96. The protons at δ 1.56-1.62 and 1.99-2.02 were found to correlate with the tertiary carbon signals at δ 32.17, 37.78, respectively (**Fig. 5.55**).
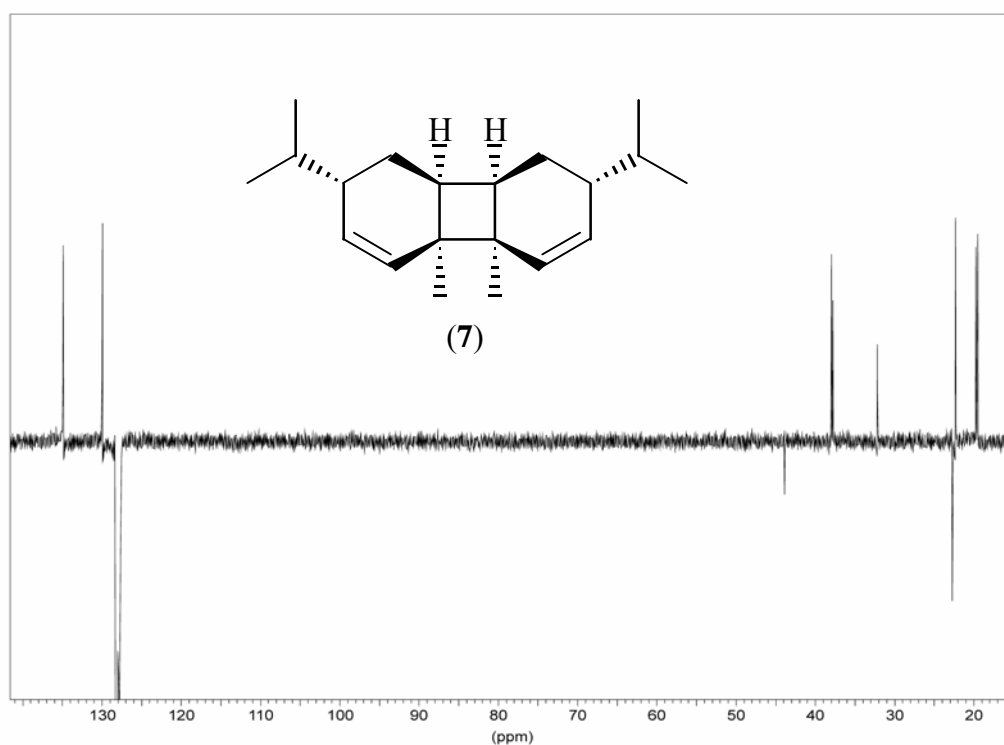
Fig. 5.54. ^{13}C-PENDANT spectrum of **7**.
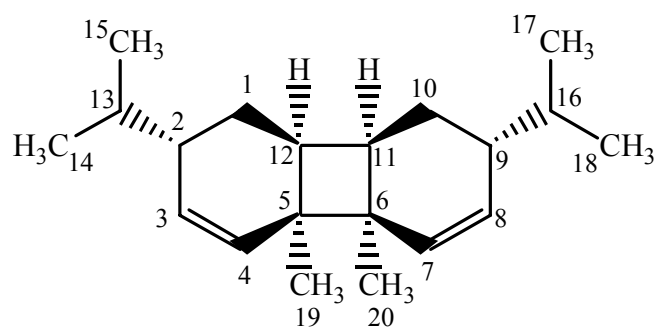
Table 5.6. HMQC correlations of **7**.

No. of C	^{13}C (ppm)	^{1}H (ppm)
1 and 10	22.69	(1.13-1.18), (1.47-1.51)
2 and 9	37.78	(1.99-2.02)
3 and 8	129.92	5.73
4 and 7	134.89	5.65
5 and 6	43.84	
11 and 12	37.96	2.03
13 and 16	32.17	(1.56-1.62)
14 and 18	19.69	0.92
15 and 17	19.48	0.91
19 and 20	22.26	1.03

Fig. 5.55. HMQC correlations of **7**.

The couplings in the HMBC spectrum indicated that two methyl groups CH_3-14 (δ 0.91, 19.48) and CH_3-15 (δ 0.92, 19.69) correlated to each other as well as with two tertiary carbons at δ 32.17 and 37.78. The olefinic proton on the double bond at δ 5.73 coupled with two tertiary carbons at δ 32.17 and 37.78 and the only secondary carbon at δ 22.69 as well as the quaternary carbon at δ 43.84. The other olefinic proton at δ 5.65 coupled only with the methyl group CH_3-19 (δ 1.03, 22.26), the quaternary carbon at δ 43.84 and the tertiary carbon at δ 37.96. The ^{1}H-^{1}H COSY spectrum showed that the three carbons at δ 37.78, 22.69, 37.96 formed a methylene chain through the correlations observed for their coresponding protons (**Fig. 5.56**).
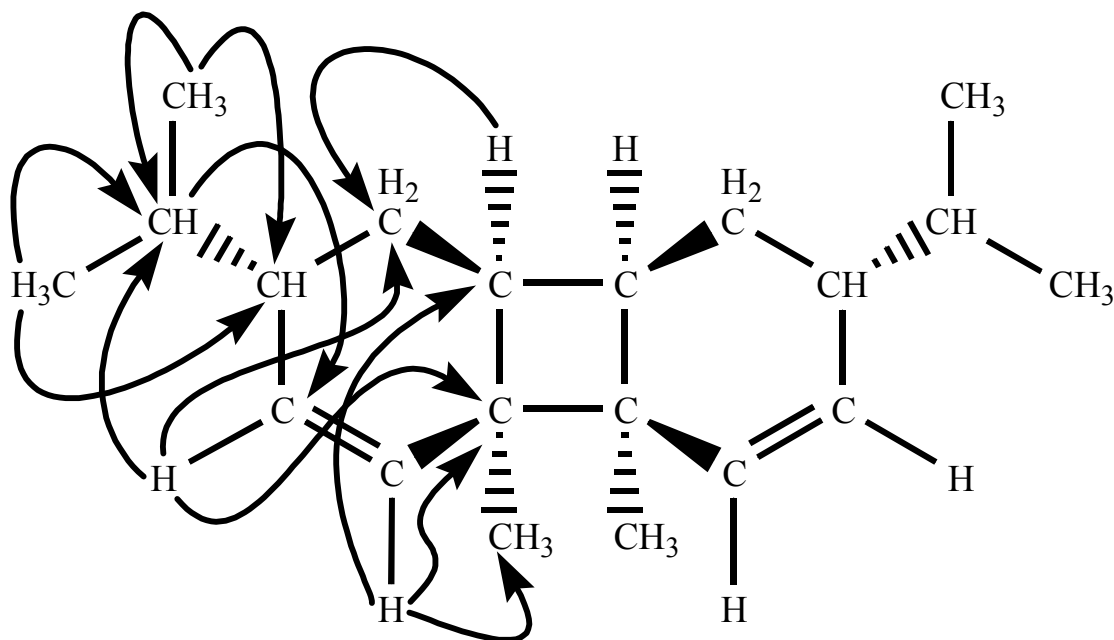
Fig. 5.56. HMBC correlations of **7**.

The relative configuration of the compound was deduced from the NOESY spectrum. The correlations of H-3 (δ 5.73) to H-13 (δ 1.56-1.62) and to H-2 (δ 1.99-2.02) indicated that the isopropyl group was located below the ring system. At this point it should be mentioned that the molecule consisted of two chemically and magnetically equal fragments so that some NOESY correlations seemed to be simply ^{1}H-^{1}H COSY correlations although in reality they reflected the interaction between these two fragments. The correlations between the isopropyl methyl groups to the olefinic proton H-3 (δ 5.73) as well as CH$_3$-19 (δ 1.03, 22.26) to H-4 (δ 5.65) were also deduced. The interactions between H-13 and H-1 (δ 1.47-1.51) showed that this C-1 hydrogen was α oriented (**Fig 5.57**).
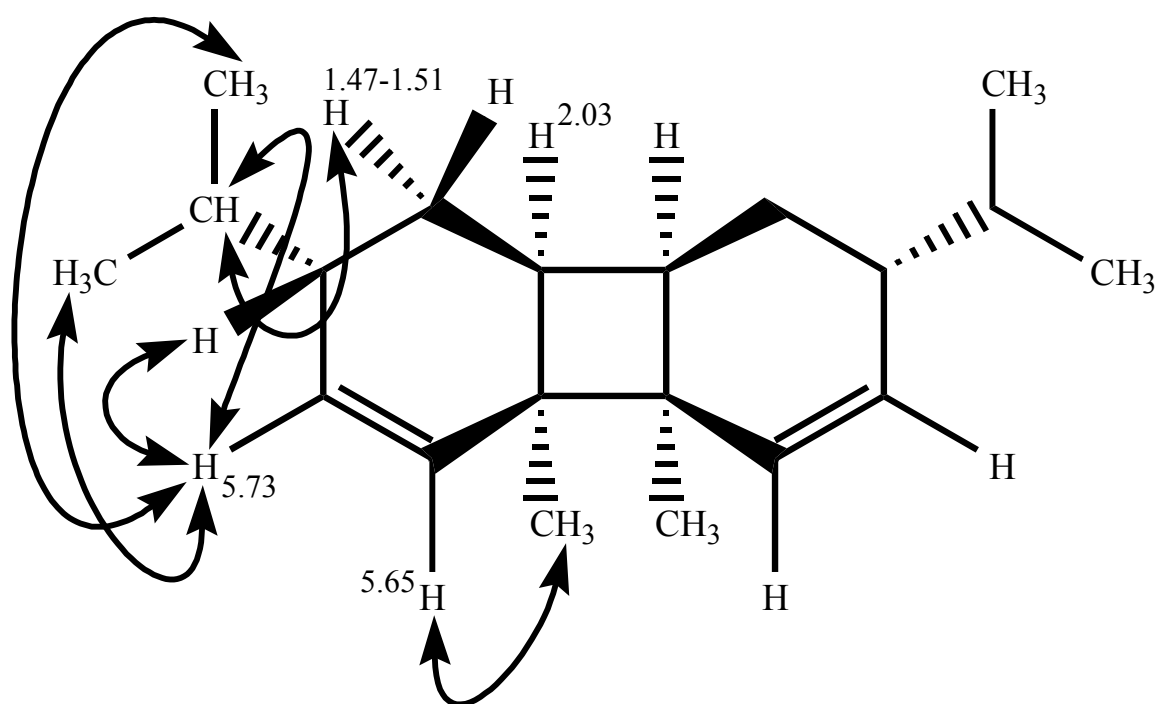
Fig 5.57. NOESY correlations of **7**.

It was assumed that α-phellandrene was the precursor which dimerised into **7**. The essential oil of *B. frereana* contained a small amount of α-phellandrene but it was enough to confirm its absolute configuration by enantioselective GC. A comparative injection of the essential oil and the standard (+/-)-α-phellandrene on 6-methyl-2,3-pentyl-γ-CD showed that (+)-*S*-α-phellandrene was present in the essential oil and dimerised to form compound **7** and other isomers[#] (**Fig. 5.58**).

[#] These isomers were indicated with "*" in the gas chromatogram of the essential oil of *B. frereana* (**Fig. 5.49**).
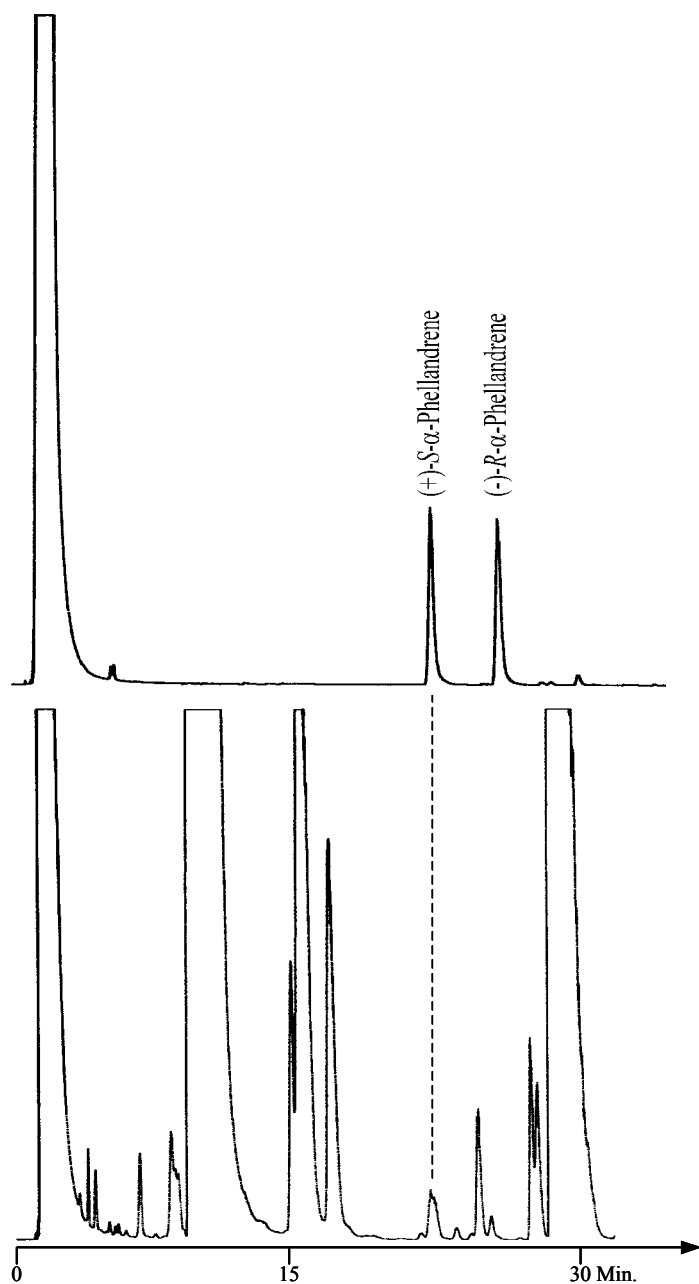
Fig. 5.57. Enantioselective gas chromatograms of (+/-)-α-phellandrene (above) and the essential oil of *B. frereana* (25 m fused silica capillary column with 6-methyl-2,3-pentyl-γ-CD (80% in OV 1701), 50 °C isothermal for 20 min, 1 °C/min up to 100 °C, injector at 200 °C, detector at 250 °C, carrier gas at 0.5 bars H_2).

These dimers were also observed in the *n*-hexane extract of *B. frereana*. This observation led to the conclusion that the dimers of α-phellandrene were not forming as artifacts during hydrodistillation but most probably during the exudation of the latex. It was assumed that the exposure of sunlight on the resin material might cause this dimerisation. *B. frereana* was

recognized as the softest resin of the investigated olibanum types that might provide a suitable medium for the dimerisation process.

A simple experiment was conducted with (-)-α-phellandrene to prove this hypothesis. The hexane solution of α-phellandrene was left to the exposure of sunlight. At the end of five days 13% of the initial concentration of α-phellandrene was predominantly changed into its dimers (**Fig. 5.59**). This cycloaddition reaction was earlier examined[123] and similar results were obtained with (-)-α-phellandrene.
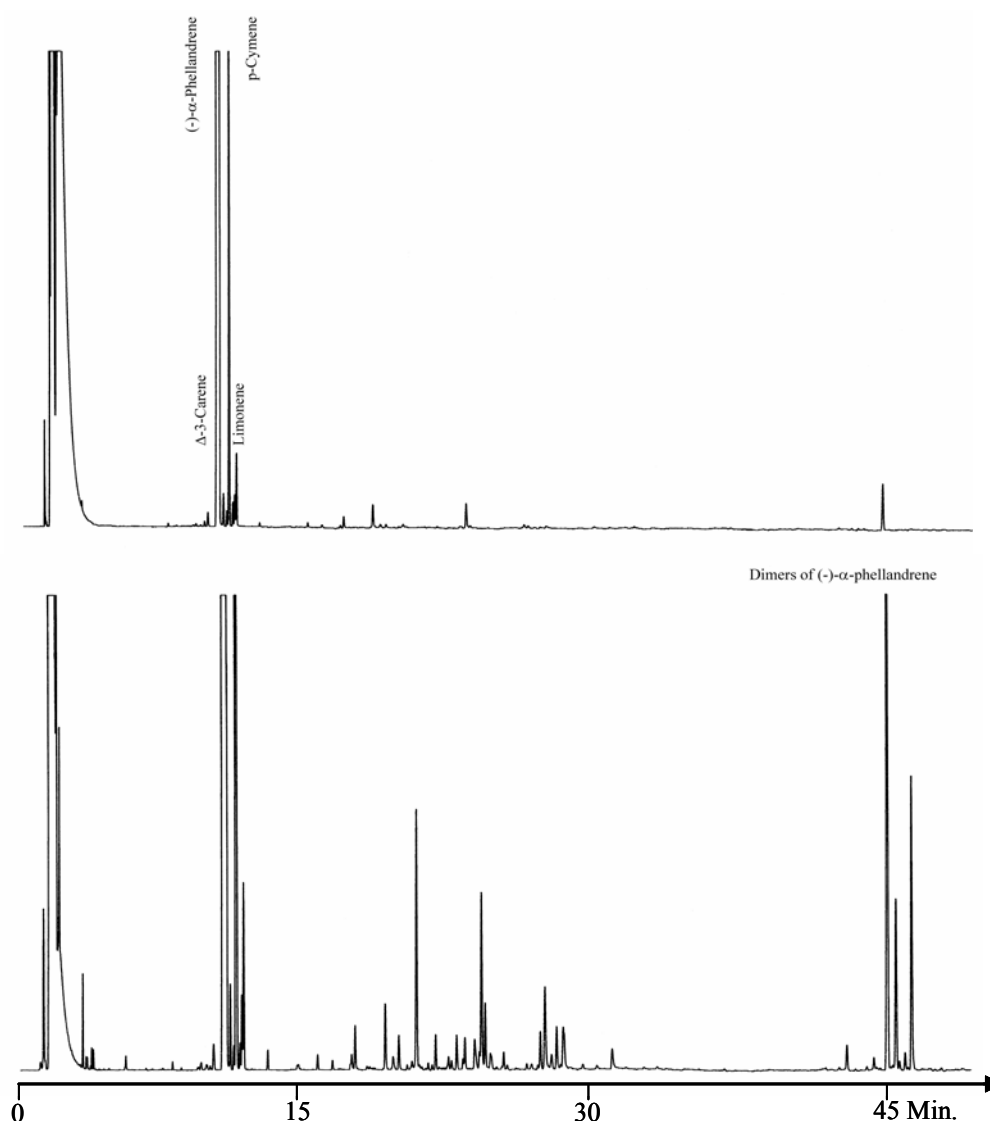
Fig.5.58. Gas chromatogram of (-)-α-phellandrene reference sample (above) and gas chromatogram of the standard sample after 5 days sunlight exposure (25 m fused silica capillary column with CPSil 5 CB, 50 °C, 3 °C/min up to 230 °C, injector at 200 °C, detector at 250 °C, carrier gas 0.5 bars H_2).

90

5.4.4   Essential Oils of *Boswellia neglecta* S. Moore and *Boswellia rivae* Engl.

There is not many results published that concerns the composition of the essential oils of *B. neglecta* and *B. rivae*. A comparative investigation by GC-MS[124] pointed out that *B. neglecta* contained α-thujene, α-pinene and terpinen-4-ol as major constituents whereas *B. rivae* was characterised by limonene and by α-pinene and *trans*-verbenol to a lesser extent.

In this study the essential oils of *B. neglecta* and *B. rivae* were recognized as dark yellow oils in color. Both species produced very similar chromatograms and the GC-MS investigations of the hydrodistillates indicated that both oils were composed of only monoterpenoic compounds (**Fig. 5.60**, **Fig 5.61**).

In the essential oil of *B. neglecta*, α-thujene (21.3%), α-pinene (21.3%), sabinene (1.3%), Δ-3-carene (1.9%), p-cymene (11.8%), terpinene-4-ol (5.3%), verbenone (2.1%) were found to be major constituents whereas in *B. rivae* cara-2,4-diene (1.8%), α-thujene (2.9%), α-pinene (16.7%), o-cymene (3.9%), Δ-3-carene (17.3%), p-cymene (3.2%) and limonene (21.1%) were recognized predominantly.
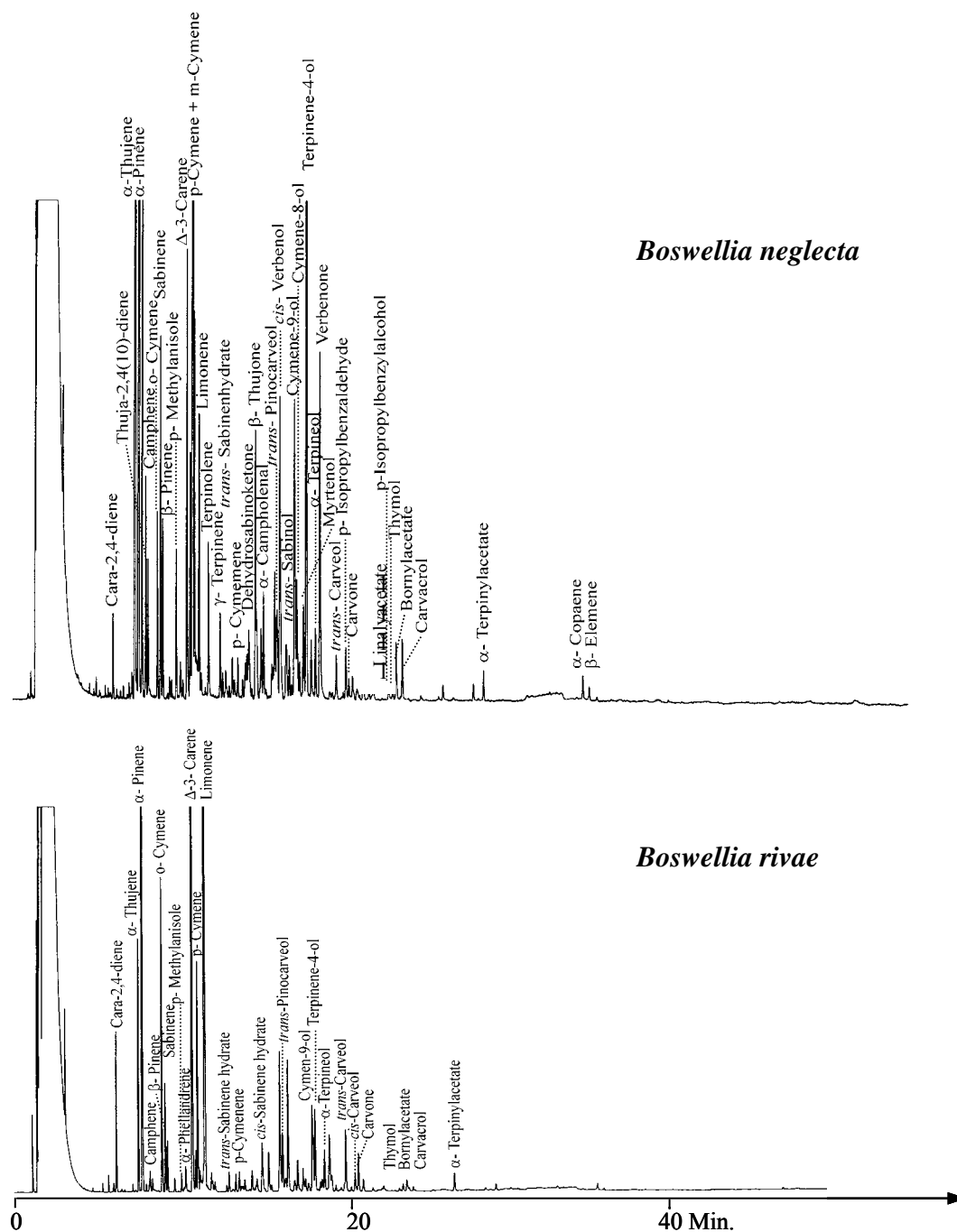
Fig. 5.60. Gas chromatograms of the essential oils of *Boswellia neglecta* and *B. rivae* (25 m fused silica capillary column with CPSil 5 CB, 50 °C, 3 °C/min up to 230 °C, injector at 200 °C, detector at 250 °C, carrier gas 0.5 bars H$_2$).

92
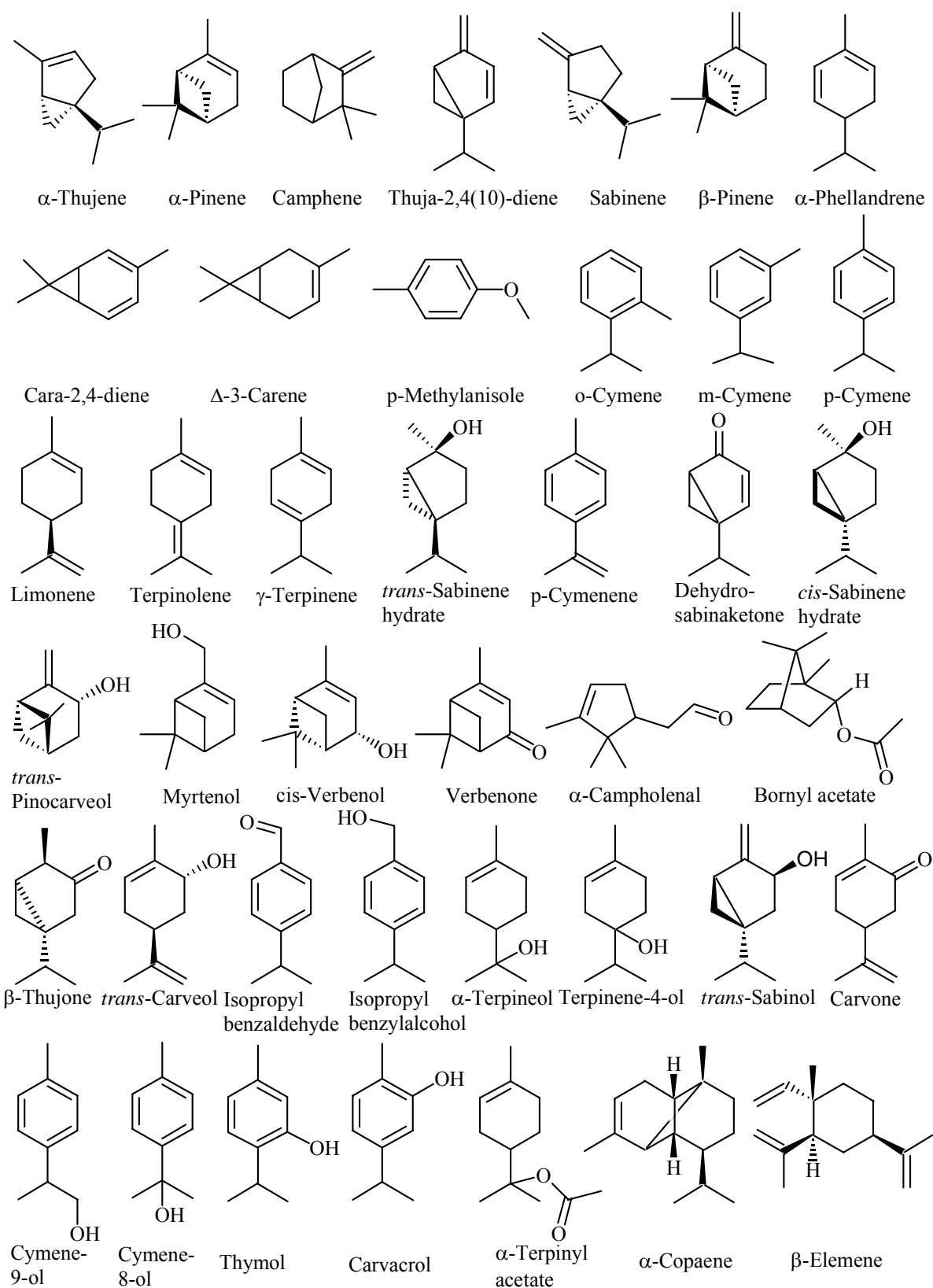
Fig. 5.61. The constituents of the essential oils of *B. neglecta* and *B. rivae*.

5.4.5 Comparison of Essential Oils of *Boswellia* Species

The investigations performed on the essential oils of olibanum species showed important differences between them. The need for the rapid identification of the olibanum species was overwhelmed with a TLC test that indicated these differences more clearly.

Not only the TLC plates but also the GC and GC-MS investigations showed that the olibanum species were mainly differentiated by their diterpenoic constituents. The monoterpenoic composition was found nearly the same in all species with a single exception, the octyl acetate content in the essential oil of *B. carterii*. Besides, some sesquiterpenoids were observed only in the essential oil of *B. serrata*.

Most importantly, the diterpenoic constituents turned out to be diagnostic markers for each species. The presence of incensole, incensyl acetate (**2**), verticilla-4(20),7,11-triene (**1**) as well as cembrene, cembrene A and cembrene C was found to be characteristic for *B. carterii*. On the other hand the presence of m- and p-camphorene (**4** and **5**), cembrene A as well as cembrenol (**6**) was recognized as diagnostic markers of *B. serrata*. Thus, the possibility of testing the purity and authenticity of these two economically and scientifically important species was achieved by TLC (**Fig. 5.62**, **Fig. 5.63**). However, the identification of *B. frereana* samples on TLC plates was only possible by their content of α-phellandrene dimers. For the other species diagnostic constituents could not be found, their absence requiring different investigation methods.
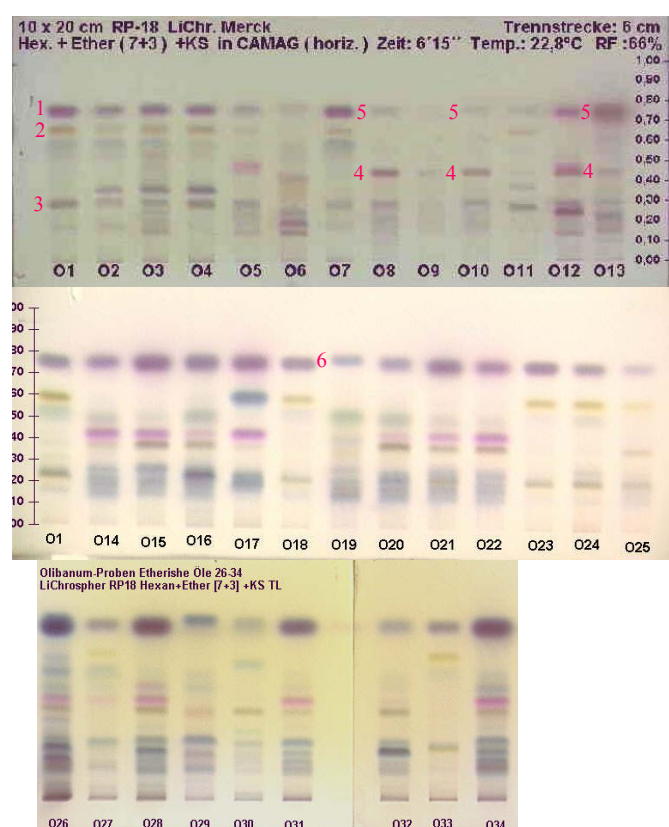
Fig. 5.62. Different examples of essential oils of *B. carterii*, *B. serrata* and *B. frereana*. **1:** Cembrene A, cembrene C, verticilla-4(20),7,11-triene, **2:** Incensyl acetate, **3:** Incensole, **4:** Cembrenol, **5:** m-Camphorene, p-camphorene, cembrene A, **6:** Dimers of α-phellandrene (Lichrosphere RP-18 (Merck), mobile phase: hexane:diethylether (7:3), development distance: 7 cm, detection at daylight after derivatisation with anisaldehyde spray solution and heating at 105 °C).
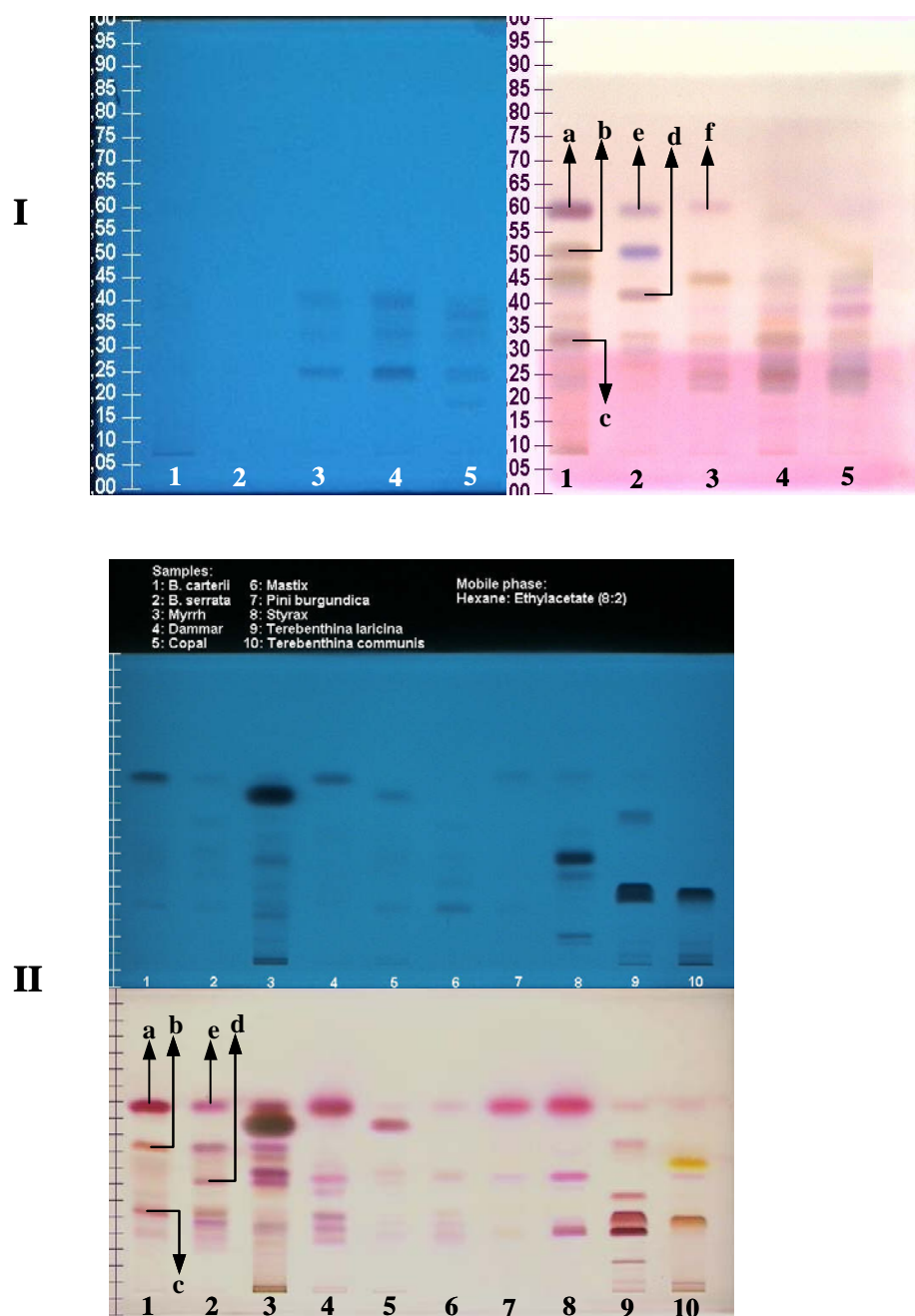
Fig. 5.63. **I:** Essential oils of different olibanum resins. Sample **1:** *B. carterii*, **2:** *B. serrata*, **3:** *B. frereana*, **4:** *B. neglecta*, **5:** *B. rivae*. **II:** Essential oils of different resins. Sample **1:** *B. carterii*, **2:** *B. serrata*, **3:** Myrrh, **4:** Dammar, **5:** Copal, **6:** Mastic, **7:** *Pini burgundica*, **8:** Styrax, **9:** *Terebenthina laricina*, **10:** *Terebenthina communis*. Band **a:** Cembrene A, cembrene C, verticilla-4(20),7,11-triene, **b:** Incensyl acetate, **c:** Incensole, **d:** Cembrenol, **e:** m-Camphorene, p-camphorene, cembrene A, **f:** Dimers of α-phellandrene (Lichrosphere Si 60$_{F254S}$ (Merck), mobile phase: cyclohexane:ethylacetate (8:2), development distance: 7cm, Detection: **I-left, II-above:** at UV $_{254\ nm}$, **I-right, II-below:** at daylight after derivatisation with anisaldehyde spray solution and heating at 105°C).

5.5 Headspace-SPME Studies on *Boswellia* Species

Although SPME (**S**olid **P**hase **M**icroextraction) has been originally developed for the rapid analysis of pollutants in water[125] it has found wide variety of use in the analysis of volatile organic compounds in foods, beverages, flavors, fragrances and essential oils[126, 127]. The components of the vapour phase are considered to be responsible for the odour of these products. Therefore headspace sampling has become the most preferred method in such analysis for the last decade.

Headspace-SPME is identified as a solvent free sample preparation technique in which a fused silica fiber coated with polymeric organic liquid is introduced into the headspace above the sample. The adsorption of the analytes is followed by a thermal desorption process by introducing the SPME fiber into the injection port of a gas chromatograph[128].

It has been a challenging subject to find out the composition of the compounds that created the odour of olibanum since years. The scent of *B. carterii* and *B. serrata* essential oils were described by Obermann[93] as woody, dry, flowery and metallic with slowly increasing balsamic note for *B. carterii* and as a warm balsamic note with a characteristic incense fragrance with a little woody tone for *B. serrata*. Nevertheless, it was not possible to identify the constituents responsible for these fragrant notes.

In this context, the headspace-SPME was considered to be an alternative method to clarify the question about the fragrance of olibanum.

The different utilities of olibanum caused the planning of different experimental conditions. The resin, its oil and the burning process of the resin were studied separately. The optimal equilibrium condition between the SPME fiber and the headspace of the analyte was reached at one hour for the low molecular weight constituents of olibanum at room temperature. In case of detecting the smoke of olibanum this adsorption time was reduced to three minutes and the adsorption of the high molecular weight components on the fiber was also observed.

The experiments were constructed in four different conditions. First, the essential oil headspace was subjected to 7 μm polydimethylsiloxane (PDMS) (bonded) fiber for one hour at room temperature. Secondly, the powdered olibanum resin headspace was subjected to 100 μm PDMS (non-bonded) fiber for one hour at room temperature. Next, the resin was melted at 150 °C for one hour and during this heating process the analytes of the headspace were adsorbed by 100 μm PDMS (non-bonded) fiber. Finally, the resin granules were burned in a muffle oven at 850 °C and the smoke produced was adsorbed on the 100 μm PDMS (non-bonded) fiber for 3 minutes. The fibers were conditioned at 250 °C for 5 minutes each time prior to the experiments. The desorption process was performed on equal conditions for 2 minutes at 200 °C, splitless injection. The results were presented as GC-MS total ion currencies.

5.5.1 Headspace-SPME experiments with *Boswellia carterii* Birdw.

It was observed that the high octyl acetate (**14**) content of *B. carterii* dominated the essential oil and the powdered resin headspace. The powdered resin showed major peaks for 1-octanol (**11**) and bornyl acetate (**16**) whereas in the essential oil headspace α-pinene (**2**) in addition to these compounds was also detected (**Fig. 5.64**, **Table 5.7**).

Fig. 5.63. GC-MS analysis of the headspace-SPME experiments of *B. carterii* (25 m fused silica capillary column with CPSil 5 CB, 80 °C for 2 min, 10 °C/min up to 270 °C).

Table 5.7. Constituents of *B. carterii* identified in the headspace- SPME experiments.

Peak no.	Compound name	Peak no.	Compound name
1	α-Thujene	18	Neryl acetate
2	α-Pinene	19	Geranyl acetate
3	Camphene	20	Decyl acetate
4	Sabinene	21	*E*-Nerolidol
5	β-Pinene	22	Cembrene
6	Myrcene	23	Cembrene A
7	Hexyl acetate	24	Cembrene C
8	p-Cymene	25	Verticilla-4(20),7,11-triene
9	1,8-Cineole + Limonene	26	Unknown
10	*E*-β-Ocimene	27	Incensole
11	1-Octanol	28	Incensyl acetate
12	Linalool	29	α-Terpineol
13	*trans*-Pinocarveol + *trans*-Verbenol	30	Myrtenal
14	Octyl acetate	31	Piperitone
15	3,5-Dimethoxytoluene	32	Decanol
16	Bornyl acetate	33	Hexylhexanoate
17	Citronellyl acetate	34	Isocembrene

In the case of the headspace sampling of *B. carterii* at higher temperatures the resulting chromatograms were found comparable with its hydrodistillate representing both low and high molecular weight constituents of the essential oil. It was also found increasing of temperature of the medium led to the production of some new compounds, which were most probably rearrangement or dehydration products of already identified constituents[†] (**Fig. 5.65**, **Table 5.7**).

[†] Peaks that could not be identified with our library, are indicated with "*" in the chromatograms.

Sample: 1 gr. granules of *B. carterii*
SPME: 100 μm PDMS fiber (non-bonded)
Adsorption: 1 hour at 150 °C
Desorption: 2 minutes at 200 °C
Analysis: GC-MS splitless injection

Sample: 1 gr. granules of *B. carterii* at 850 °C
SPME: 100 μm PDMS fiber (non-bonded)
Adsorption: 3 min. sampling of the smoke
Desorption: 2 minutes at 200 °C
Analysis: GC-MS splitless injection
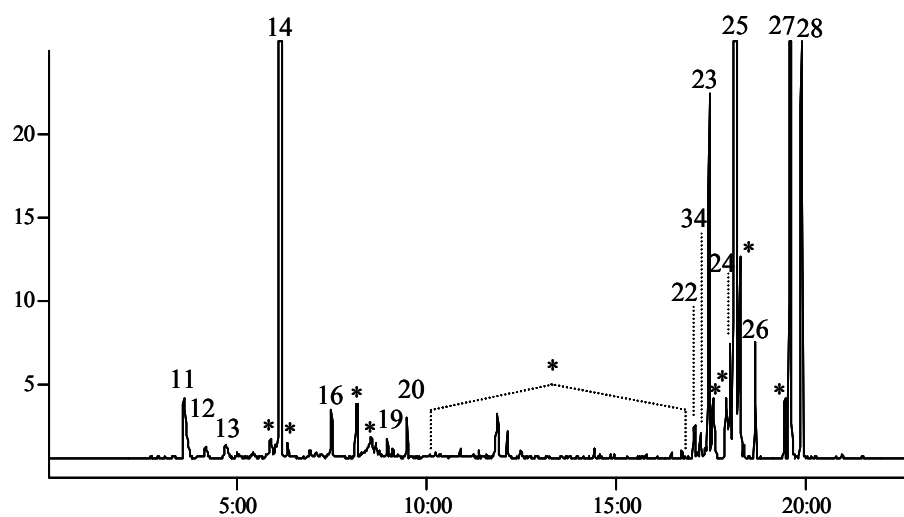
Fig. 5.65. High temperature headspace-SPME investigations of *B. carterii* (25 m fused silica capillary column with CPSil 5 CB, 80 °C for 2 min, 10 °C/min up to 270 °C).

5.5.2 Headspace-SPME experiments with *Boswellia serrata* Roxb.

α-Pinene (**3**), α-thujene (**2**), myrcene (**7**) and methylchavicol (**19**) were detected as the major constituents in the headspace sampling of the essential oil and resin powder of *B. serrata* (**Fig. 5.66, Table 5.8**).
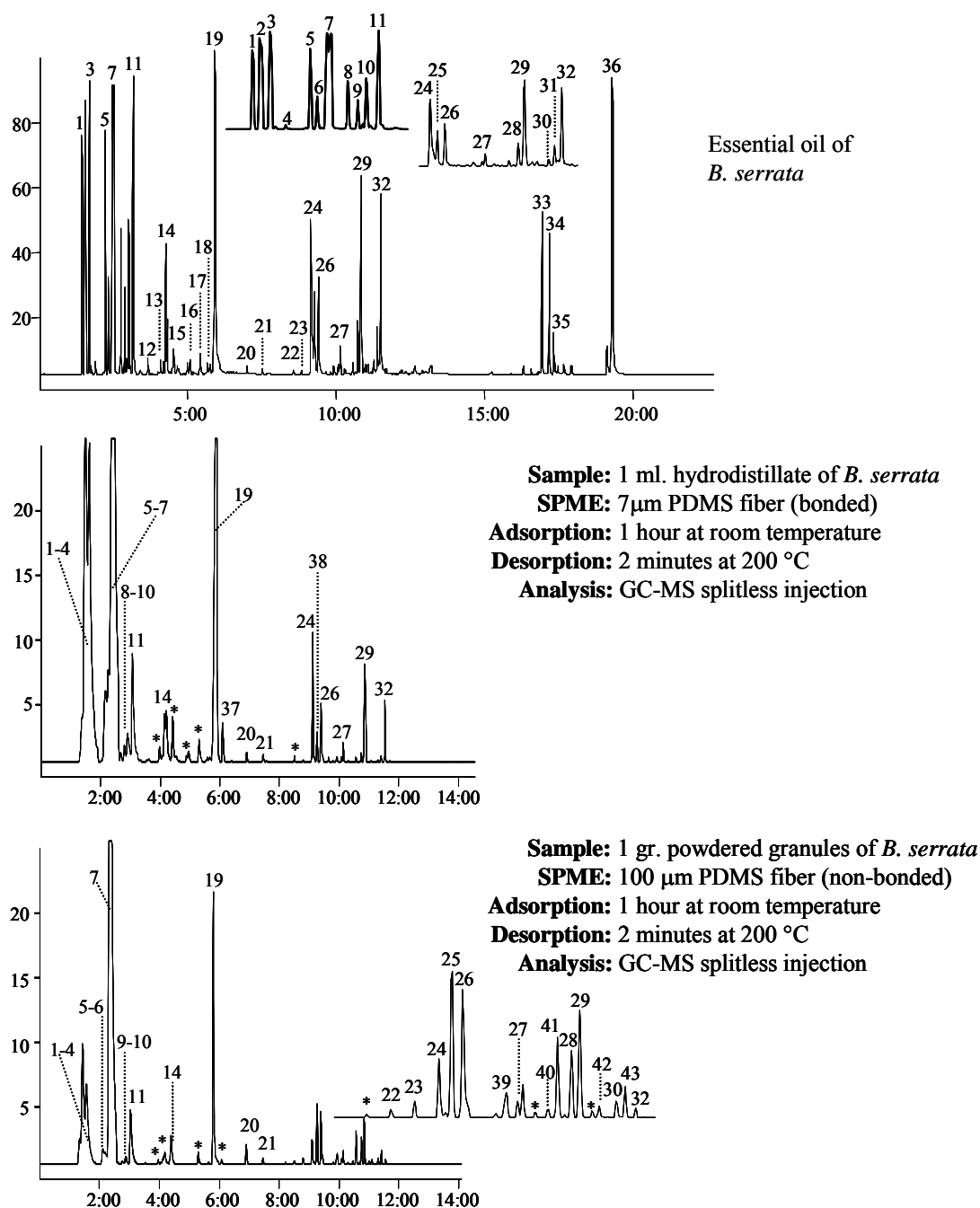
Fig. 5.66. GC-MS analysis of the headspace-SPME experiments of *B. serrata* (25 m fused silica capillary column with CPSil 5 CB, 80 °C for 2 min, 10 °C/min up to 270 °C).

Table 5.8. The identified constituents in headspace-SPME experiments of *B. serrata*.

Peak	Compound name	Peak	Compound name
1	5,5-Dimethyl-1-vinylbicyclo [2.1.1]hexane	28	γ-Muurolene
2	α-Thujene	29	Germacrene D
3	α-Pinene	30	γ-Cadinene
4	Camphene	31	Elemicine
5	Sabinene	32	Kessane
6	β-Pinene	33	m-Camphorene
7	Myrcene	34	Cembrene A
8	α-Phellandrene	35	p-Camphorene
9	Δ-3-Carene	36	Cembrenol
10	p-Cymene + m-Cymene	37	Octyl acetate
11	1,8-Cineole + Limonene	38	α-Ylangene
12	*E*-β-Ocimene + γ-Terpinene	39	*E*-β-Caryophyllene
13	Terpinolene	40	α-Humulene
14	Linalool + Perillene	41	*allo*-Aromadendrene
15	β-Thujone	42	α-Muurolene
16	*trans*- Verbenol	43	γ-Cadinene
17	Unknown	44	Verbenone
18	Terpinene-4-ol	45	p-Anisaldehyde
19	Methylchavicol	46	Perilla alcohol
20	Linalyl acetate	47	Isogermacrene D
21	Bornyl acetate	48	*n*-Pentadecane
22	α-Terpinyl acetate	49	Guaioxide
23	α-Cubebene	50	α-Muurolene
24	Methyleugenol	51	Elemol
25	α-Copaene	52	5-Guaiene-11-ol
26	β-Bourbonene	53	α-Eudesmol
27	β-Ylangene,β-Copaene, *trans*-α-Bergamotene	54	Verticilla-4(20),7,11-triene

The results of headspace analysis of *B. serrata* resin at high temperatures also resembled those of its essential oil (**Fig. 5.67**, **Table 5.8**).

Sample: 1 gr. granules of *B. serrata*
SPME: 100 µm PDMS fiber (non-bonded)
Adsorption: 1 hour at 150 °C
Desorption: 2 minutes at 200 °C
Analysis: GC-MS splitless injection
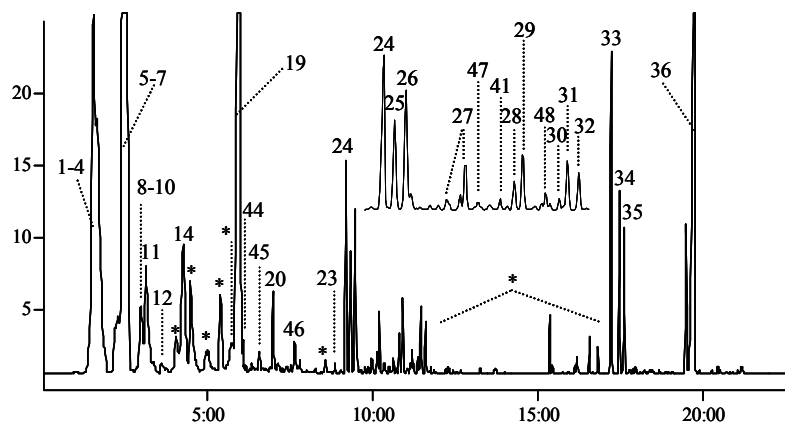
Sample: 1 gr. granules of *B. serrata* at 850 °C
SPME: 100 µm PDMS fiber (non-bonded)
Adsorption: 3 min. sampling of the smoke
Desorption: 2 minutes at 200 °C
Analysis: GC-MS splitless injection
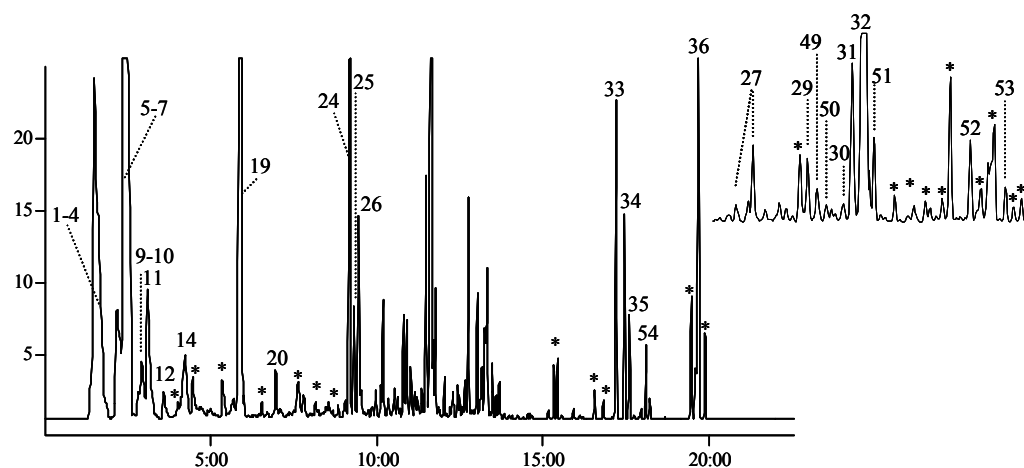
Fig. 5.67. High temperature headspace-SPME experiments of *B. serrata* by GC-MS (25 m fused silica capillary column with CPSil 5 CB, 80°C for 2 min, 10 °C/min up to 270 °C).

5.5.3 Headspace-SPME experiments with *Boswellia frereana* Birdw.

α-Pinene (**2**), p-cymene (**7**), bornylacetate (**25**) were the constituents observed primarily in the *B. frereana* headspace analysis of its essential oil and resin powder (**Fig. 5.68**, **Table 5.9**).
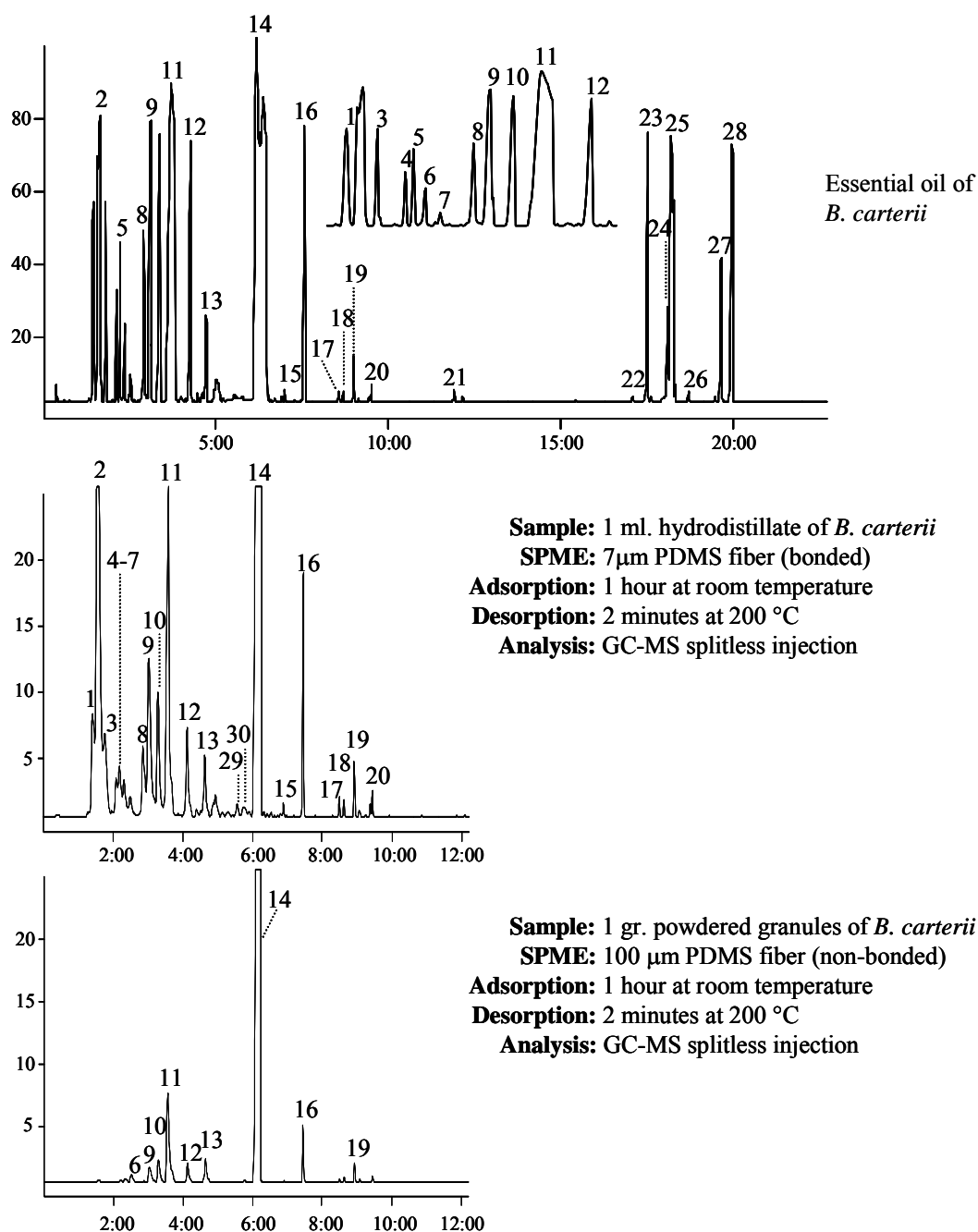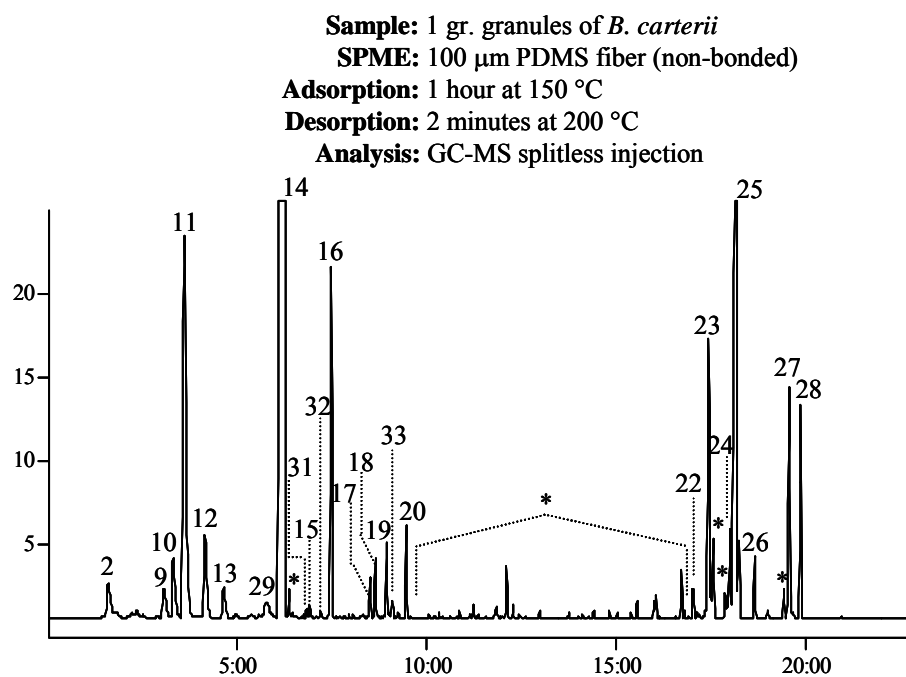
103
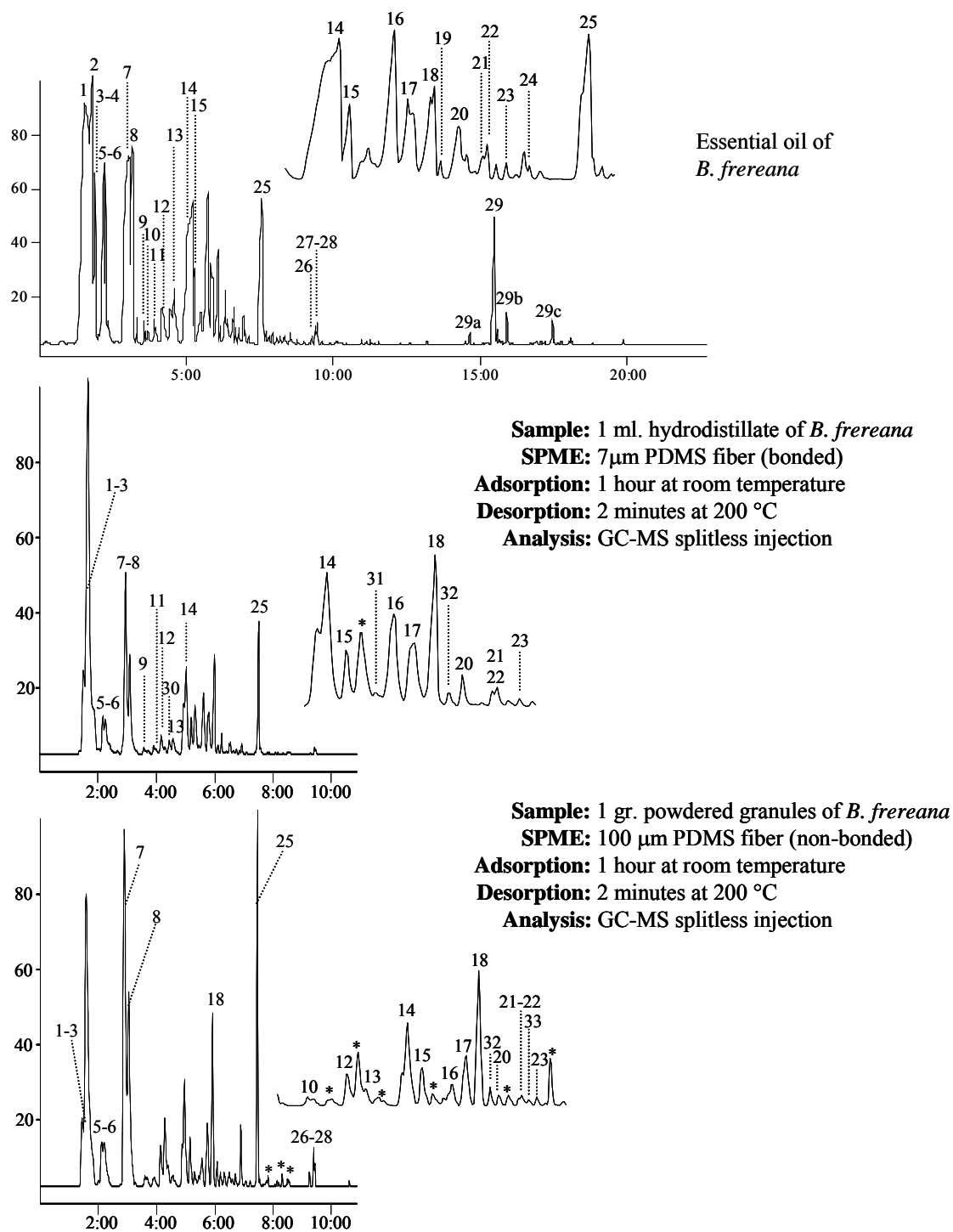
Fig. 5.68. GC-MS analysis of the headspace-SPME experiments of *B. frereana* (25 m fused silica capillary column with CPSil 5 CB, 80 °C for 2 min, 10°C/min up to 270 °C).

Table 5.9. The constituents identified in the headspace-SPME experiments of *B. frereana*.

Peak no.	Compound name	Peak no.	Compound name
1	α-Thujene	24	Isopiperitenone
2	α-Pinene	25	Bornyl acetate
3	Camphene	26	α-Copaene
4	Thuja-2,4(10)-diene	27	β-Bourbonene
5	Sabinene	28	β-Elemene
6	β-Pinene	29	α-Phellandrene dimer
7	p-Cymene	30	Dehydrosabinaketone
8	1,8-Cineole + Limonene	31	p-Methylacetophenone
9	γ-Terpinene	32	Octyl acetate
10	*trans*-Sabinene hydrate, *trans*-Linalool oxide	33	Carvotanacetone
11	p-Cymenene	34	α-Phellandrene
12	Linalool	35	Linalyl acetate
13	β-Thujone + α-Campholenal	36	Methyleugenol
14	*trans*-Pinocarveol + *trans*-Verbenol	37	α-Ylangene
15	Pinocarvone	38	β-Bourbonene
16	Terpinene-4-ol	39	Germacrene D
17	Myrtenal	40	Cymene-8-ol
18	Verbenone	41	α-Terpineol
19	*trans*-Piperitol	42	Carvacrol
20	*trans*-Carveol	43	Verticilla-4(20),7,11-triene
21	p-Isopropyl benzaldehyde	44	Incensole
22	Carvone	45	Incensyl acetate
23	Piperitone		

.

As *B. frereana* was subjected to higher temperatures, an increase in the concentration of α-phellandrene dimers was detected. It was also observed that *B. frereana* was the only olibanum species which showed the most alterations in its monoterpenoic fraction during these high temperature headspace analyses (**Fig. 5.69, Table 5.9**).

Sample: 1 gr granules of *B. frereana*
SPME: 7μm PDMS fiber (bonded)
Adsorption: 1 hour at 150 °C
Desorption: 2 minutes at 200 °C
Analysis: GC-MS splitless injection

Sample: 1 gr. powdered granules of *B. frereana* at 850 °C
SPME: 100 μm PDMS fiber (non-bonded)
Adsorption: 3 min. sampling of the smoke
**Desorption:** 2 minutes at 200 °C
Analysis: GC-MS splitless injection
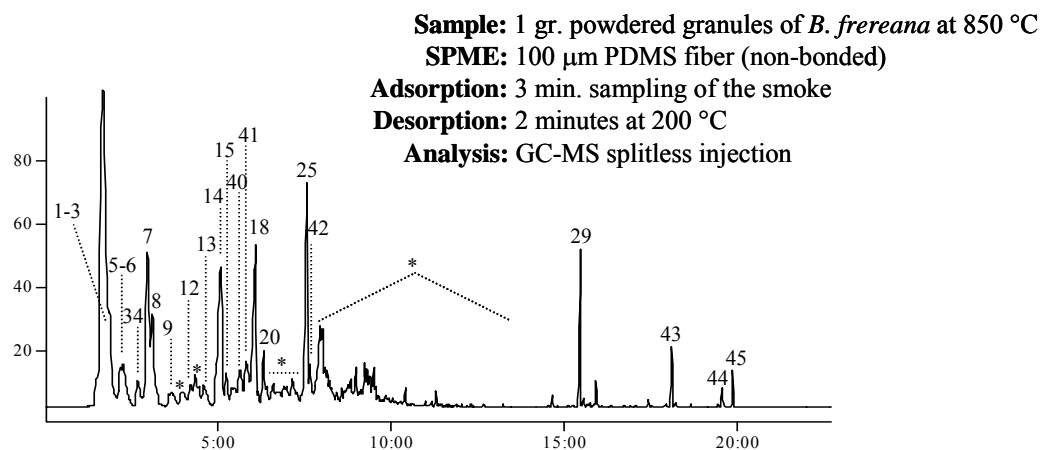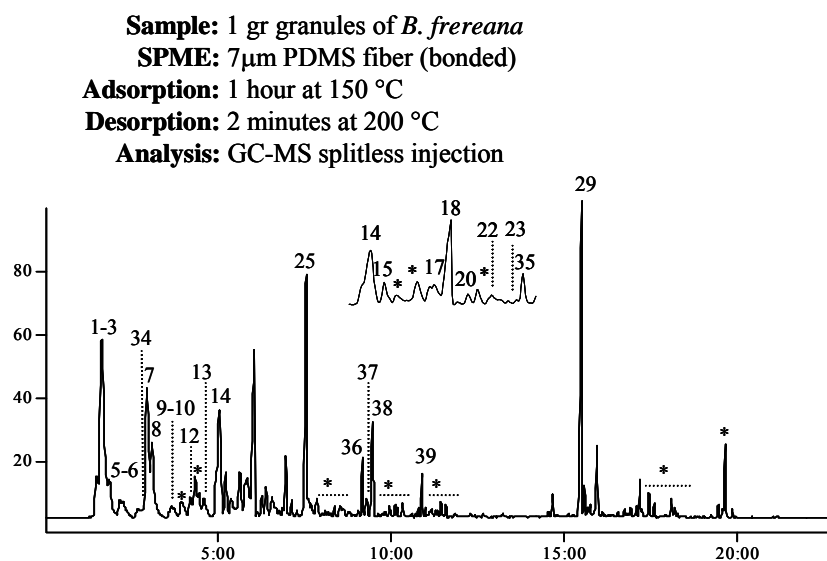
Fig. 5.69. High temperature headspace-SPME investigations of *B. frereana* by GC-MS (25 m fused silica capillary column with CPSil 5 CB, 80 °C for 2 min, 10 °C/min up to 270 °C).

In conclusion, the results determined from the SPME analysis performed on *Boswellia* species did not really show a great deviation from the results of the essential oil analysis of the same samples. However, it was possible to observe the constituents composing the odor of these species with this analysis technique. Especially, the odour of the resin samples was found to be due mainly to the mixture of the major constituents of the oils. Octyl acetate, 1-octanol, bornyl acetate and geranyl acetate composition for *B. carterii*, myrcene and methylchavicol composition for *B. serrata*, camphene, p-cymene and bornyl acetate composition for *B. frereana* were detected.

106

5.6 Comparative Studies on the Acid Fraction of Olibanum

All through the history olibanum was recognized as one of the powerful and expensive medicines because of its well known effects. In the Antiquity it had been used in the treatment of wounds, as a styptic agent and against rheumatism by many therapists especially by Hippokrates and Dioskarides. Additionally in the Middle Ages it had found application against cough, vomit, dysentery and for a number of dermatological illnesses.

In the traditional Indian medicine, Ayurveda, it has been a convenient material in the treatment of cough, articularic pains, diarrhoea, colored stool as well as insanity for centuries.

All these led the western medicine to consider and research on the effects against chronical intestinal diseases, asthma and rheumatism, recently[129, 130].

The concern of this study was to identify the acidic constituents of the olibanum species which were proved to be the decisive constituents responsible of these pharmacological effects. The survey of the earlier works indicated that there exist several methods for the isolation of acid fraction from the resin. However, the identification of the acid fractions determined with these methods was not consistent. Therefore primarily, the methods were compared to find out the most suitable procedure to extract the acid fractions from olibanum species.

Secondly, the determined method of isolation was performed on each olibanum resin to identify the composition of their acid fractions and the characteristic constituents in these fractions.

The inconsistency in the results of the different extraction methods indicated that one or more constituents were labile to the extraction conditions. Therefore, the stability of these compounds were examined with different "*stress tests*"[#] to determine in which step of these methods the change occured and what kind of artifacts were formed.

5.6.1 Boswellic Acids

Sallaki[®] (Gufic Company/India) which was known as a phytoparmacetical prepared from the dried ethanolic extracts of *Boswellia serrata* was used in the Ayurvedic medicine against inflammatory diseases. A study performed in Germany at the end of 1980's pointed out for the first time that *B. serrata* alcoholic extracts contain compounds exerting inhibitory action on the production of leukotriene-type mediators of inflammation *in vitro*[131].

[#] Stress tests are used in pharmaceutical investigations to prove the stability of the compounds. They are performed by treating the compounds with acids, bases or exposing them to high temperatures or UV light.

Further studies showed that the ether or alcohol soluble part of the olibanum resin was found to contain higher terpenoic compounds including triterpenoic carboxylic acids which were called as "*Boswellic acids*" (BA) in common[130]. In addition to these some tetracyclic triterpenoic acids having tirucallane skeleton (tirucallic acids (TA)) were also detected in the extracts of olibanum.

After *Winterstein and Stein*[86] isolated and characterised the boswellic acid as a monohydroxy acid with an elemental composition of $C_{30}H_{48}O_3$, further studies[132(I-VIII)] clarified that boswellic acids correspond to the triterpenes of the amyrin series with hydroxy group at 3-α and carboxylic acid function at 4-β position.

Recently, boswellic acids were defined as pentacyclic triterpenoic acids of which β-boswellic acid {(3α,4β)-3-hydroxyurs-12-en-23-oic acid} and its derivatives were found to be derived from ursane type triterpenoids whereas α-boswellic acid {(3α,4β)-3-hydroxyolean-12-en-23-oic acid} and its derivatives based on the oleanane skeleton[133] (**Fig. 5.70**).

Research results on the structure-activity relationship between antiinflammatory activity and natural triterpenoids indicated that an acid functional group increased the effect[134]. This result was found to be consistent with antiinflammatory effect of the alcohol extract of *B. serrata* regarding the boswellic acids.

5.6.1.1 Leukotriene Biosynthesis, The Inhibitiory Role of Boswellic Acids and Their Additional Medicinal Effects

The production of leukotrienes in the body with prostaglandins and lipoxines, generally called eicosanoides, are induced by arachidonic acid in the metabolism. The leukotriene (LT) biosynthesis in human body is initiated with the increase in the Ca^{+2} concentration in the cell to 350-400 nM that further activates the phospholipase A_2 (PLA$_2$) which will involve in the relaese of arachidonic acid from the phospholipids of the cell membrane. With the liberation of arachidonic acid in the cell several enzymatic reactions take place via different type of enzymes such as 12-lipoxygenase (12-LO), 5-lipoxygenase (5-LO), 15-lipoxygenase (15-LO) and cyclooxygenases each leading to different type of inflammation mediators. Boswellic acids are found to be specific inhibitors of 5-lipoxygenase. Therefore in the further steps of leukotriene biosynthesis the reactions via 5-lipoxygenase will be mainly considered.

Arachidonic acid is converted to the labile 5,6-epoxide LTA$_4$[#] via 5-HPETE (5S-hydroperoxy-6,8,11,14-eicosatetraenoic acid) by 5-lipoxygenase as well as 5-HETE (5-hydroxy-eicosatetraenoic acid). By enzymatic action of LTA$_4$ hydrolase, LTB$_4$ (5S, 12R-dihydroxy-6,8,10,14-eicosatetraenoic acid) is formed.

[#] For the symbolisation of the different leukotriene (LT) types the capitals A-E stand for the structurally different leukotrienes whereas the subscript following the capital indicates the number of double bonds in the molecule.

On the other hand the enzymatic conjugation of LTA$_4$ with glutathione catalyzed by LTC$_4$ synthase (glutathion-S-transferase) resulted in the formation of LTC$_4$, the primary cysteinyl leukotriene. Further cleavages of glutamate and glycine from LTC$_4$ by γ-glutamyltransferase and dipeptidase followed by enzymatic action of N-acetyltransferase resulted in the formation of LTD$_4$, LTE$_4$ and N-acetyl-LTE$_4$, respectively[135, 136] (**Fig. 5.71**).

β-Boswellic acid

α-Boswellic acid

Tirucallic acid
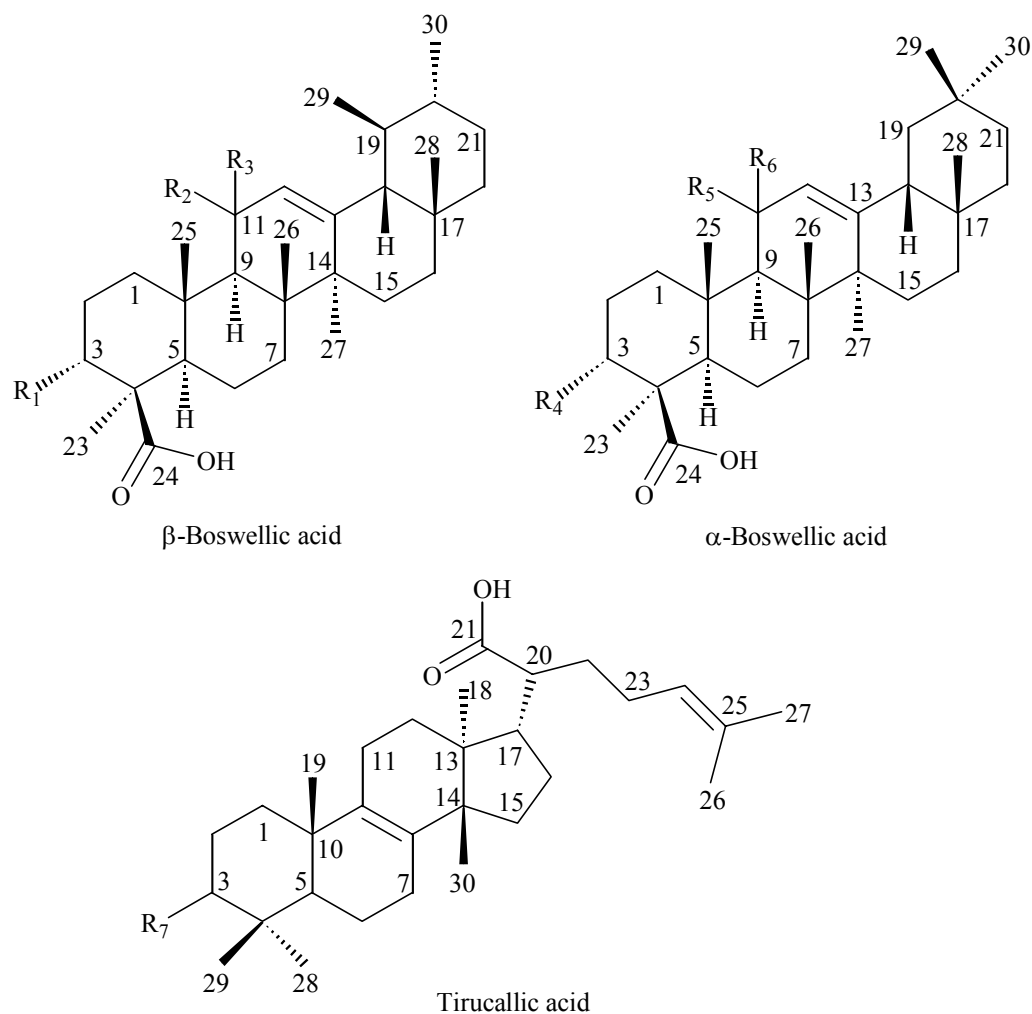
R$_1$= OH	R$_2$= H	R$_3$= H	β-Boswellic acid (β-BA)
R$_1$= OAc	R$_2$= H	R$_3$= H	3-*O*-Acetyl-β-boswellic acid (ABA)
R$_1$= OH	R$_2$= R$_3$= O	------	11-Keto-β-boswellic acid (KBA)
R$_1$= OAc	R$_2$= R$_3$= O	------	3-*O*-Acetyl-11-keto-β-boswellic acid (AKBA)
R$_1$= OH	R$_2$= OH	R$_3$= H	11-Hydroxy-β-boswellic acid
R$_1$= OAc	R$_2$= OCH$_3$	R$_3$= H	3-*O*-Acetyl-11-methoxy-β-boswellic acid
R$_1$= OAc	R$_2$= OH	R$_3$= H	3-*O*-Acetyl-11-hydroxy-β-boswellic acid

R$_1$= OH	R$_2$= ---	R$_3$= ---	9,11-Dehydro-β-boswellic acid
R$_1$= OAc	R$_2$= ---	R$_3$= ---	3-*O*-Acetyl-9,11-dehydro-β-boswellic acid
R$_4$= OH	R$_5$= H	R$_6$= H	α-Boswellic acid
R$_4$= OAc	R$_5$= H	R$_6$= H	3-*O*-Acetyl-α-boswellic acid
R$_4$= OH	R$_5$= OH	R$_6$= H	11-Hydroxy-α-boswellic acid
R$_4$= OH	R$_5$= ---	R$_6$= ---	9,11-Dehydro-α-boswellic acid
R$_4$= OAc	R$_5$= ---	R$_6$= ---	3-*O*-Acetyl-9,11-dehydro-α-boswellic acid
R$_7$= OH			3-Hydroxy-8,9,24,25-tetradehydro-tirucallic acid
R$_7$= OAc			3-*O*-Acetyl-8,9,24,25-tetradehydro-tirucallic acid
R$_7$= O			3-Oxo-8,9,24,25-tetradehydro-tirucallic acid

Fig. 5.70. Boswellic and tirucallic acid derivatives reported from *Boswellia* species.
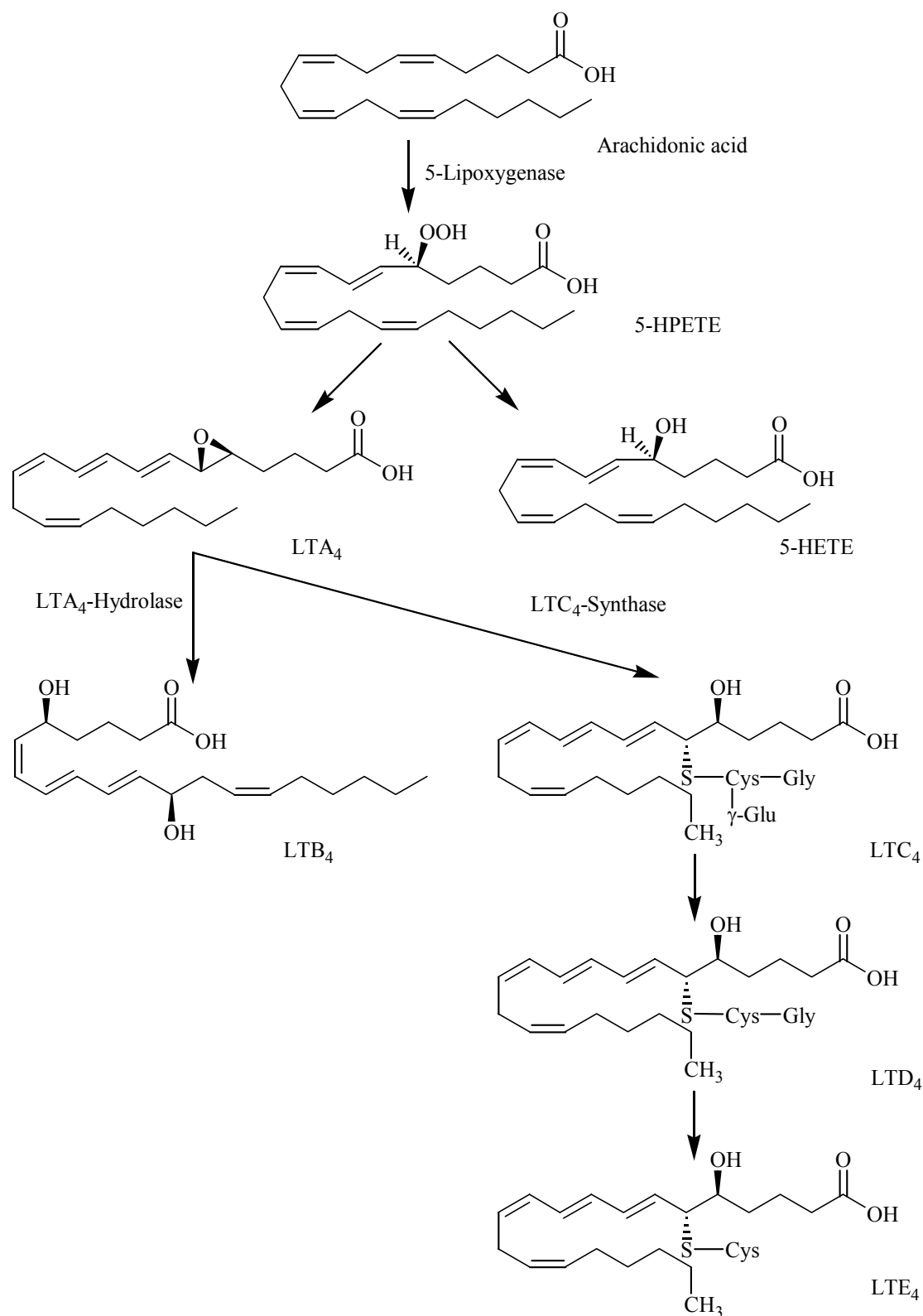
Fig. 5.71. Biosynthesis of leukotrienes from arachidonic acid via 5-lipoxygenase pathway.

Although all leukotrienes are called as the inflammation mediators the type of diseases they cause in the body are different. The cysteinyl leukotrienes, LTC_4, LTD_4, LTE_4, were found to have a decisive role on the lung diseases such as acute asthma, allergic rhinitis, aspirin-sensitive and exercise-induced asthma since the inflammatory cells, basophiles, mast cells and eosinophiles, in the respiratory tracts, can synthesize these type of leukotrienes. They cause vasoconstruction, increase in vascular permeability in postcapillary venules, broncho-constriction, stimulation of mucus secretion and many other biological effects.

On the other hand for the LTB_4 type of leukotrienes which are produced in the macrophages and neutrophiles, are responsible from aggregation, chemokinesis, chemotaxis, release of lysosomal enzymes, stimulation of the superoxide anion production, adhesion and transendothelial migration of neutrophiles, etc. causing dieseases like rheumatoide arthritis, psoriasis and gastrointestinal diseases like Morbus Crohn and colitis ulcerosa.

Scientists have been trying to develop strategies to block the arachidonic acid metabolism in many different ways such as inhibiting the release of arachidonic acid and preventing its conversion to LTA_4 via 5-lipoxygenase (5-LO) inhibitors, blocking the synthesis of LTB_4, LTC_4 and LTD_4, inhibiting the release of LTA_4 or by blocking the uptake of LTA_4.

3-*O*-Acetyl-11-keto-β-boswellic (AKBA) acid which was isolated from the ethanolic extract of *B. serrata* was proved to be the most efficient member in the group of boswellic acids having this inhibitory activity against 5-LO. It was found that AKBA was an enzyme-directed, non-redox based leukotriene biosynthesis inhibitor (IC_{50} = 1.5 μM) that reacted with 5-LO via a pentacyclic triterpene selective binding site that was different from the arachidonic acid substrate binding site[137].

In another study, where the structure-activity relationship was compared between the compounds from ursane series and boswellic acids against 5-LO, it was reported that the pentacyclic triterpene ring system was crucial to bind the inhibitor to the highly selective effector site. Besides the presence of various functional groups on the ring system, especially 11-keto function in addition to a hydrophilic group on C-4 of ring A were found essential for 5-LO inhibitory activity [138]. Recently, a further hypothesis was proposed claiming that AKBA was bound in the presence of calcium (Ca^{+2}) to a site which was distinct from the substrate binding site of 5-LO, that was most likely to be identical with a regulatory, second arachidonate binding site of the enzyme[139, 140].

The inhibitory activity of boswellic acids, especially AKBA, or the medical preparations of olibanum (e.g. H15, Sallaki, Boswellin) was thought to be a phytomedical solution for the diseases where the main reason was the high leukotriene synthesis such as, chronic polyatrhritis[141], chronic cholitis[142], Morbus Crohn[143, 144], inflammatory bowel disease[145], colitis ulcerosa and bronchial asthma[146]. Because the preliminary clinical studies gave hopeful results with less side effects in comparison to the medical therapie with sulfasalazine or mesalazine with the patients suffering from these diseases. Nevertheless, the use of complex extracts showed in some cases biphasic potentiating inhibitory effects in contrast to the

purified compounds (e.g. AKBA) from these extracts. Therefore it was clearly mentioned that the standardization of the complex pharmaceutical products from *Boswellia* was needed[147].

The alterations in the results of the clinical tests between the crude extract and the isolated pure compounds led the investigation of the analogues of boswellic acids that were present in the *Boswellia* extracts to a deeper level[148]. However, a better result than the inhibitory effect of AKBA was not determined. On the contrary, the tirucallic acids that were identified in the extract of *B. serrata* were found to enhance the 5-LO product formation. Especially, 3-oxo-tirucallic acid and 3-*O*-acetyl-tirucallic acid were found to involve in the production of LTB_4 which was identified as the strongest mediator in the leukotriene biosynthesis causing the diseases mentioned above[149].

While screening the additional effects of boswellic acids it was detected that they did not only block the leukotriene biosynthesis but inhibited proinflammatory pathways such as decreasing the human leukocyte elastase (HLE). This enzyme was identified as a serine protease produced and released by polymorpho human leukocytes (PMNL). Considering the aggressive destructiveness of this enzyme some researchers suggested it might play an important role in some diseases like chronic bronchitis, cyctic fibrosis, acute respiratory distress syndrome and rheumatic arthritis. The data showed that the dual inhibition of 5-LO and HLE was unique only to boswellic acids[150].

Antileukemic activity was another effect of boswellic acids[151]. Two human leukemic cell lines, HL-60 and CCRF-CEM, which have no capability of producing 5-LO metabolites were tested against AKBA and with its structural analogue α-amyrin. In both cell lines AKBA was found to inhibit the cell growth and induce apoptosis[152].

Acetyl-boswellic acids were detected as the catalytic inhibitors of human topoisomerase I and IIα. Topoisomerase is an enzyme that makes a sequential breakage and then allows the reunion of the DNA strand. Their pharmacological inhibition has made them targets of antitumor and antimicrobial drugs. The drugs may act in two different ways, either as topoisomerase poisons or as catalytic inhibitors. The former one stabilize the enzyme-DNA complex and block the rejoining but as a result damaged DNA accumulation occurs in the cell and the mutagenetic potential increases. But catalytic inhibitors prevent the binding of enzyme to DNA as in the case of acetyl-boswellic acids. The three acetyl derivatives of boswellic acids were proved to have this effect with a decreasing order of activity as acetyl-α-BA, acetyl-β-BA and AKBA[153].

Recent studies on the reduction of edema in the cases of peripheral brain tumors and the regression of the brain tumors[146], on the cyctotoxic activity on meningioma cells (central nervous system tumors) of AKBA[154] as well as the antiproliferative and apoptopic effects of AKBA and 11-keto-β-BA on colon cancer HT-29 cells[155] were found as promising results in the field of cancer research.

5.6.2 Comparison of the Extraction Methods of Boswellic Acids

The already mentioned pharmacological studies on boswellic acids were performed either on the alcohol extracts of olibanum or on their acid fractions prepared from these resins. However, in most studies either the origin of the resin or the procedures to prepare the extracts were not properly mentioned. *Winterstein and Stein*[86] were the first scientists who tried to determine a fraction of boswellic acids from olibanum by treating its diethylether extract with Ba(OH)$_2$. This simple idea, determining the salt of the acids by treating a fraction with a basic solution and after the separation of this salt mixture acidifying it to gain back the acidic compounds, was repeated later by other researchers.

In variation of the method of *Winterstein and Stein*[86], in 1983 *Fattoruso et al.*[156] used 2 M NaOH to determine the salt of the acids. Later in 1989 *Hairfield et al.*[157] tried extractions on a microscale level with 1% and 10 % KOH but observed no differences in the results. This group also tried extraction with NaHCO$_3$ but they reported very low yields. Similarly *Shao et al.*[151] in 1998 used 2 % KOH. Extraction of a polar fraction of olibanum resin with Mg(OH)$_2$ was the standard method applied by *Ammon et al.*[158].

The comparison of the results of these studies points out that the description of the acidic fraction of olibanum is ambiguous. Considering the stability problems of the acid fraction of olibanum in pharmacological studies and the inconsistency of the published results of these five methods with KOH (2% and 10%), NaOH, Mg(OH)$_2$ and Ba(OH)$_2$, the procedures were simply applied to the polar fractions of *B. carterii* and *B. serrata* as indicated. Although the pharmacological studies were performed mostly on *B. serrata* resin, it was recognized that boswellic acids were present with the same proportion in *B. carterii* as well.

5.6.2.1 Detection of the Boswellic Acids

Investigations by GC, GC-MS and TLC were considered to be the most rapid way of analysis of the acid fractions. However, the constituents in question are not suitable substances for direct GC analysis, and therefore derivatisation of the acid fractions was performed. The optimal result was achieved by the silylating these acid fractions with N-methyl-N-trimethylsilyl-trifluoroacetamide (MSTFA) (**Fig. 5.72**).

MSTFA was used trimethylsilyl (TMS) donor for the silylation of various functional groups especially of carboxylic acids, steroids, N-nitrosoamino acids, β-ketoesters, ureas, nucleic acids and many other polar compounds. Its capability of resolving even highly polar substances and its use without any solvent make MSTFA an adventageous silylating agent[159].
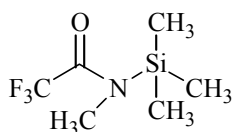
N-Methyl-N-trimethylsilyl-trifluoroacetamide
(MSTFA)

Fig. 5.72. The silylating agent N-methyl-N-trimethylsilyl-trifluoroacetamide.

Analysis of the acid fraction of olibanum after silylation by GC and GC-MS was performed for the first time. The detection of their methylester derivatives had already been performed by *Hairfield et al.*[157]. However, they only detected β-BA and 3-*O*-acetyl-β-BA.

There are 17 triterpenoic acidic constituents (**Fig. 5.70**) reported from *Boswellia* species which are also expected to be found in the GC, GC-MS investigations of the silylated acid fractions.

The assignment of the GC-MS peaks of the silylated derivatives of these acidic components, was done by considering the changes in their molecular ion signal (**Table 5.10**) or in their fragmentation pattern. The GC, GC-MS investigations of some reference substances, oleanolic acid, ursolic acid, lupeol and baurenol that have comparable structural properties to boswellic acids (**Fig. 5.73**) gave satisfactory results in the GC, GC-MS analysis after silylation. Contrarily to the published data on the separation of single constituents by HPLC, the detection of the α- and β-BA as well as their 3-*O*-acetyl derivatives as single peaks was only possible by GC after this derivatisation.

Isolation of some constituents, AKBA, KBA, 3-oxo-8,9,24,25-tetradehydro-TA and 3-*O*-acetyl-8,9,24,25-tetradehydro-TA was accomplished by TLC. Mixtures of α-BA and β-BA, 3-*O*-acetyl-α-BA and 3-*O*-acetyl-β-BA were also obtained by preparative TLC separations.

Oleanolic acid

Ursolic acid

Baurenol

Lupeol
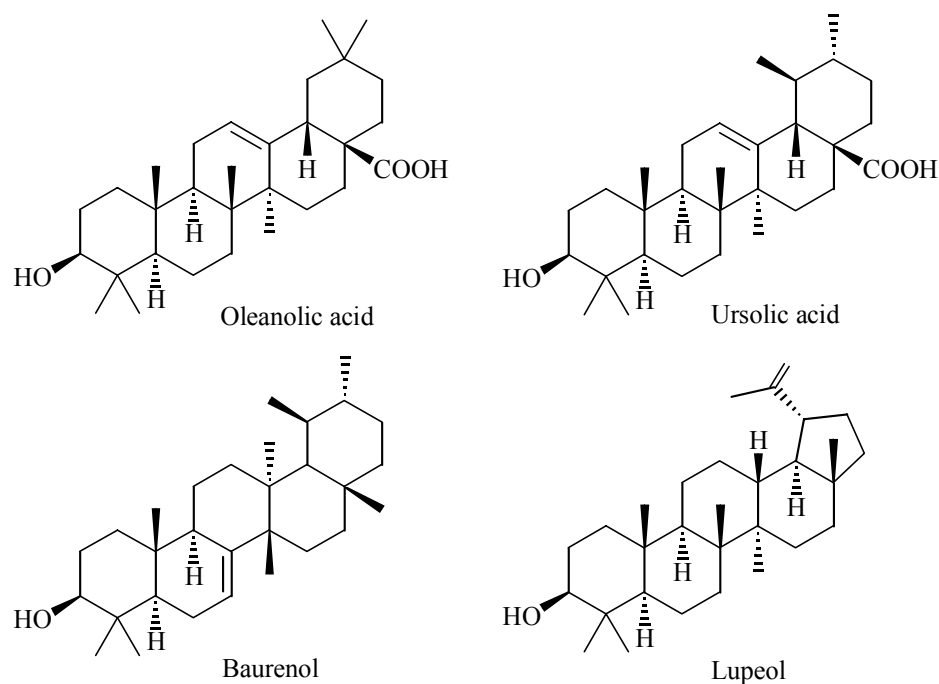
Fig. 5.73. The reference compounds used in derivatisation with TMS.

Table 5.10. The molecular ion calculations of the boswellic acids, tirucallic acids and their TMS derivatives.

Name of the acid	Molecular Formula	[M$^+$]	[M$^+$] of TMS derivative
β-Boswellic acid (β-BA)	$C_{30}H_{48}O_3$	456	600
3-*O*-Acetyl-β-boswellic acid (ABA)	$C_{32}H_{50}O_4$	498	570
11-Keto-β-boswellic acid (KBA)	$C_{30}H_{46}O_4$	470	614
3-*O*-Acetyl-11-keto-β-boswellic acid (AKBA)	$C_{32}H_{48}O_5$	512	584
11-Hydroxy-β-boswellic acid	$C_{30}H_{48}O_4$	472	688
3-*O*-Acetoxy-11-methoxy-β-boswellic acid	$C_{33}H_{52}O_5$	528	600
3-*O*-Acetyl-11-hydroxy-β-boswellic acid	$C_{32}H_{50}O_5$	514	658
9,11-Dehydro-β-boswellic acid	$C_{30}H_{46}O_3$	454	598
3-*O*-Acetyl-9,11-dehydro-β-boswellic acid	$C_{32}H_{48}O_4$	496	568
α-Boswellic acid	$C_{30}H_{48}O_3$	456	600
3-*O*-Acetyl-α-boswellic acid	$C_{32}H_{50}O_4$	498	570

11-Hydroxy-α-boswellic acid	$C_{30}H_{48}O_4$	472	688
9,11-Dehydro-α-boswellic acid	$C_{30}H_{46}O_3$	454	598
3-O-Acetyl-9,11-dehydro-α-boswellic acid	$C_{32}H_{48}O_4$	496	568
3-Hydroxy-8,9,24,25-tetradehydro-tirucallic acid	$C_{30}H_{48}O_3$	456	600
3-O-Acetyl-8,9,24,25-tetradehydro-tirucallic acid	$C_{32}H_{50}O_4$	498	570
3-Oxo-8,9,24,25-tetradehydro-tirucallic acid	$C_{30}H_{46}O_3$	454	526

Generally, for structure determination of target compounds mass spectra alone were found insufficient. However, in the case of boswellic acids, especially for the assignment of peaks which could not be properly isolated, the interpretation of the mass spectra was found to be very useful. Interpretation of mass spectra of the silylated boswellic and tirucallic acids not only yield structures for unknown peaks but also furnished some interesting results in the mass spectroscopy of pentacyclic triterpenoids.

The studies performed on the fragmentation patterns of pentacyclic triterpenoid compounds indicated that if the compound has a double bond at position 12 the Retro-Diels-Alder (RDA) reaction is primarily observed[160]. Members of 12-ursene and 12-oleanene series showed, therefore, very similar patterns in the mass spectra. Further cleavage reactions also took place after the formation of RDA fragments. It was detected that the RDA fragment containing the C-D-E ring system preferably loses first the functional group at position 17 in both types of triterpenes. This observation was made during the analysis of compounds with different functional groups at C-17, C-19 and C-20[160]. No results were presented when three of these substituents were methyl groups as in the case of boswellic acids.

Additionally, it was reported that ursane and oleanane type triterpenes could be distinguished by the order of elution during gas chromatography. The compounds of ursane series had longer retention times than the coresponding oleanane compounds. This was explained by the shift of the CH_3 group from an axial conformation at C-20 in oleanane structures, to an equatorial conformation at C-19 in ursane type compounds which caused an increase in the planarity of the molecules that related to their retention time[161].

The most challenging problem in the GC-MS analysis of the silylated acid fractions of olibanum was the structure assignment of the compounds with very similar structures and, therefore, similar mass spectra as in the case of α- and β-BA. Regarding the mentioned fragmentation related to $^{12}\Delta$- ursane or oleanane triterpenes, the silylated derivatives of α- and β-BA were assigned according to their MS in which the molecular ion peak was $m/z = 600$, and the only observable difference between the two compounds was the intensity of the fragment ion signal at $m/z = 203$ (**Fig. 5.74**).
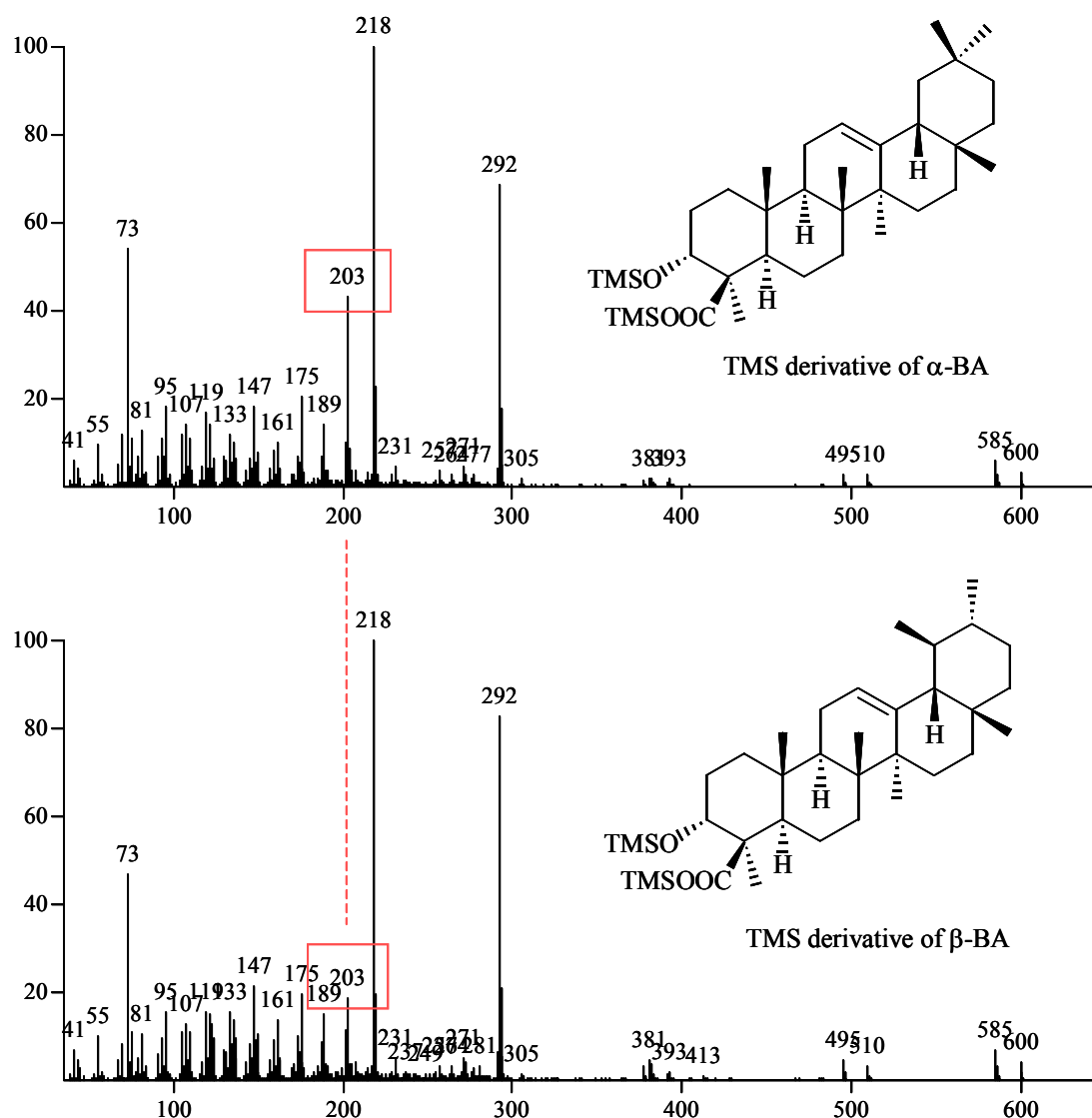
Fig. 5.74. Mass spectra of the TMS derivatives of α-BA and β-BA.

The fragment ion signals $m/z = 585$ represented the loss of a methyl group ($[M-CH_3^+]$), $m/z = 510$ elimination of TMS-OH ($[M-TMSOH^+]$) followed by the loss of a methyl group forming $m/z = 495$ ($[M-(TMSOH + CH_3)^+]$) for both α- and β-BA. However, the most intensive signals are formed upon a RDA reaction. The RDA fragment including ring A and B produced the signal at $m/z = 292$ by elimination of TMSOH. The other RDA fragment signal at $m/z = 218$ included the ring C-D-E. At this point, the mass spectrum of α-BA become different than the β-BA. The latter RDA fragment $m/z = 218$ lost a methyl group and produced the signal at $m/z = 203$ for both compounds. However, this fragment was more

abundant in the mass spectrum of α-BA than β-BA. The higher intensity of the signal may be due to the more stable ion it formed from α-BA (**Fig. 5.75**).
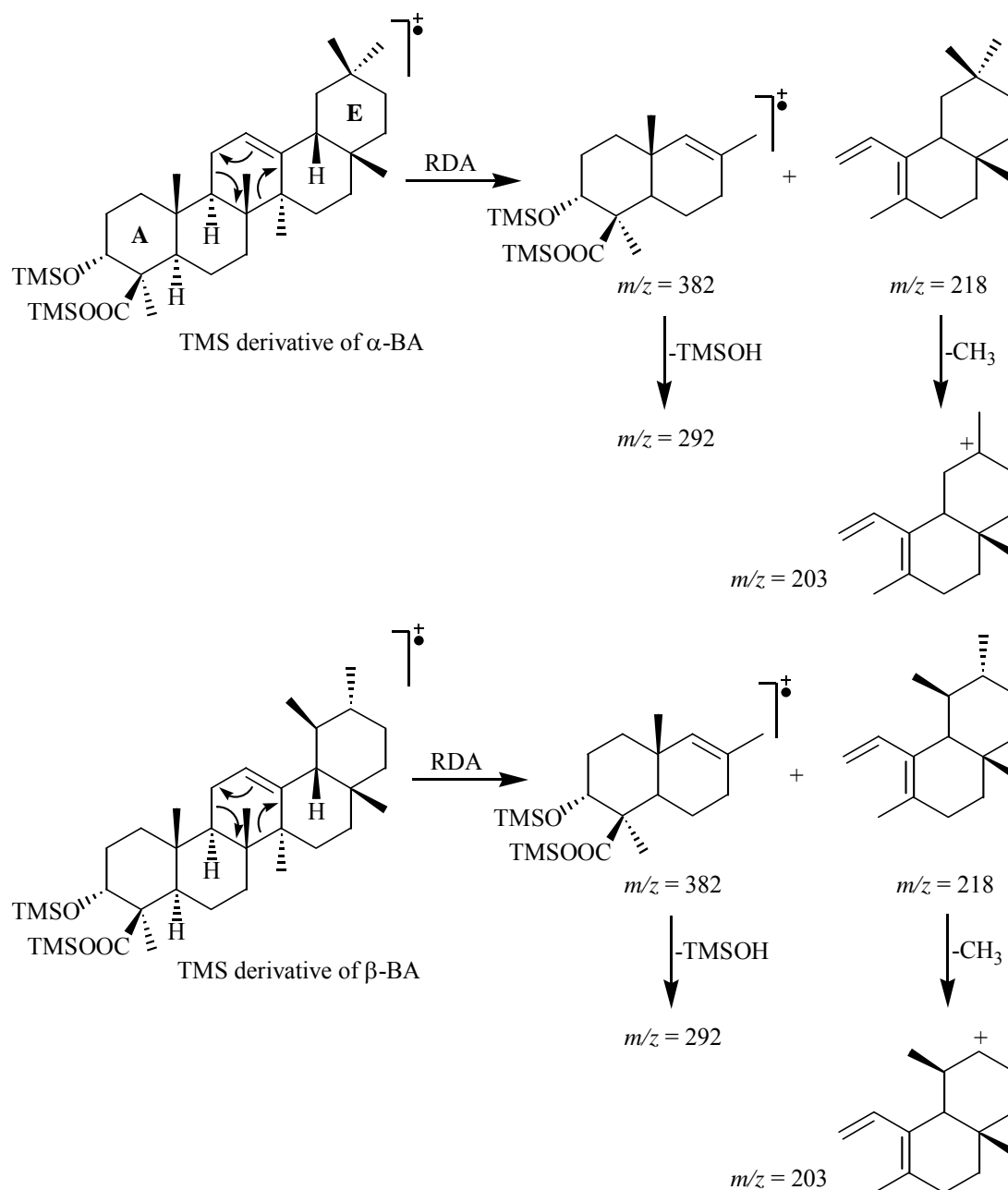
Fig. 5.75. Possible fragmentation of the TMS derivatives of α- and β-BA.

In contrast to an expected cleavage at C-17[160], the decisive fragmentation happened at C-20 in case of three equal functional groups on ring E of α- and β-BA. This hypothesis, the differentiation of α-BAs from β-BAs with a single fragment ion signal was proved with the standard samples of α- and β-amyrin without derivatisation of the samples. The GC

investigations indicated that β-amyrin had shorter retention time than α-amyrin which was consistent with the earlier results[161] (**Fig. 5.76**). The mass spectra of α- and β-amyrin determined by GC-MS investigations were found to be consistent with the observed fragmentation behaviour of α- and β-BA (**Fig. 5.77**).
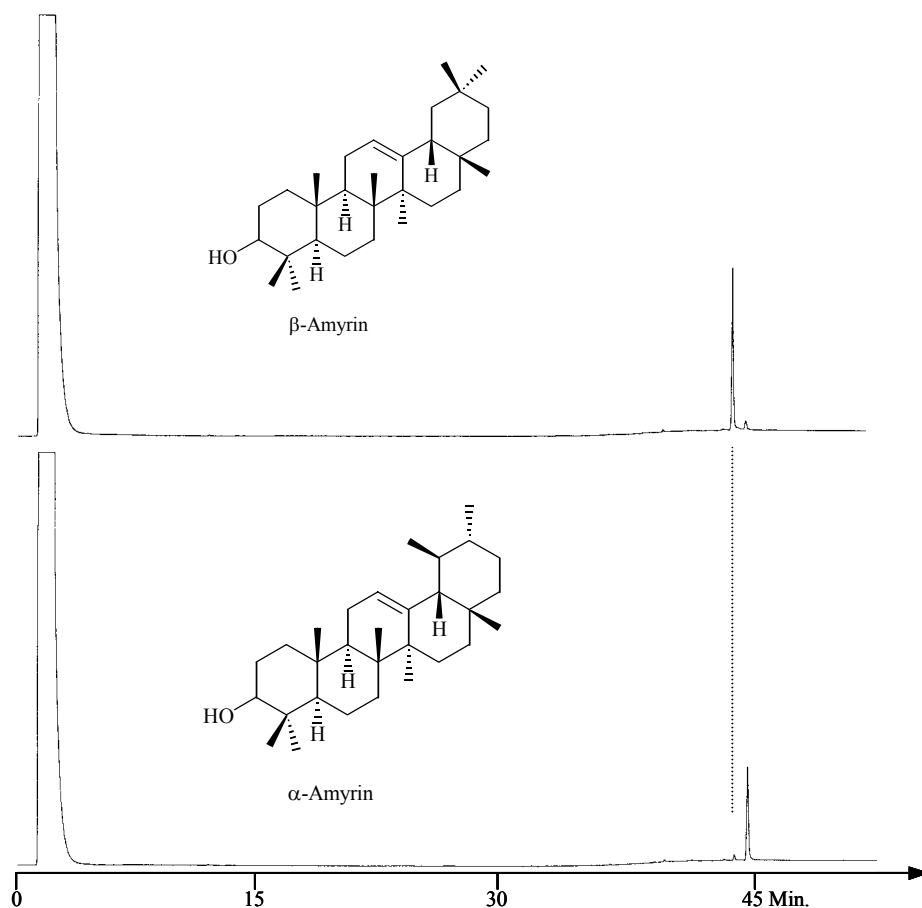
Fig. 5.76. Gas chromatograms of α-and β-amyrin (25 m fused silica capillary column with CPSil 5 CB, 100 °C, 5 °C/min up to 300 °C, injector at 250 °C, detector at 320 °C, carrier gas 0.5 bars H_2).
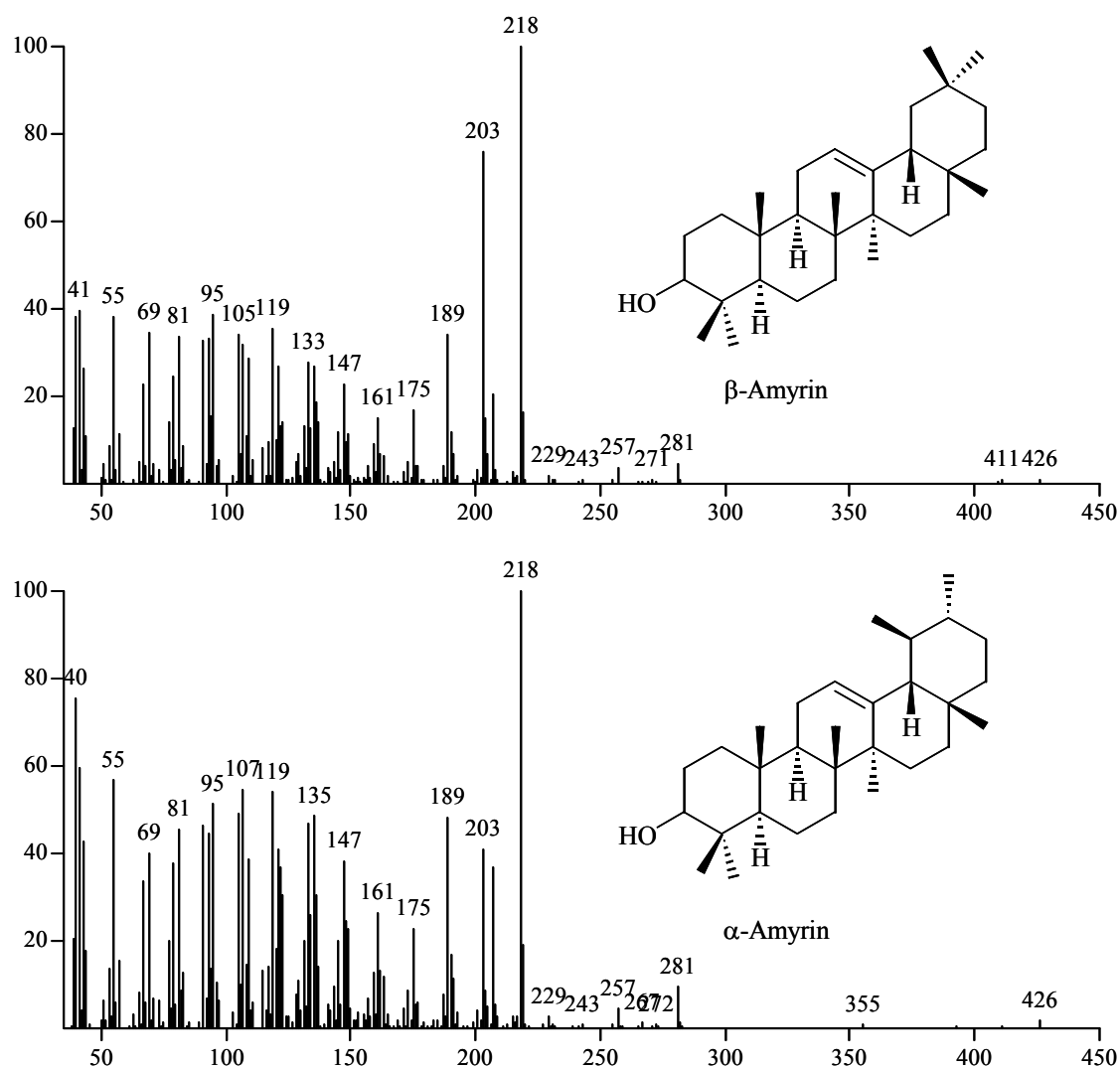
Fig. 5.77. Mass spectra of α- and β-amyrin.

Analogue compounds to α- and β-amyrin were prepared having the same substitution pattern at ring E but different functional groups on C-3. The oxidation of α- and β- amyrin with pyridinium dichromate[162, 163] resulted in the corresponding ketones. During the GC-MS analysis these two compounds also reproduced similar mass spectra indicating that the stability difference between the secondary and tertiary carbenium ion formed on C-20 of both compounds caused an increase in the intensity of the corresponding signal up to 60% (**Fig. 5.78**).
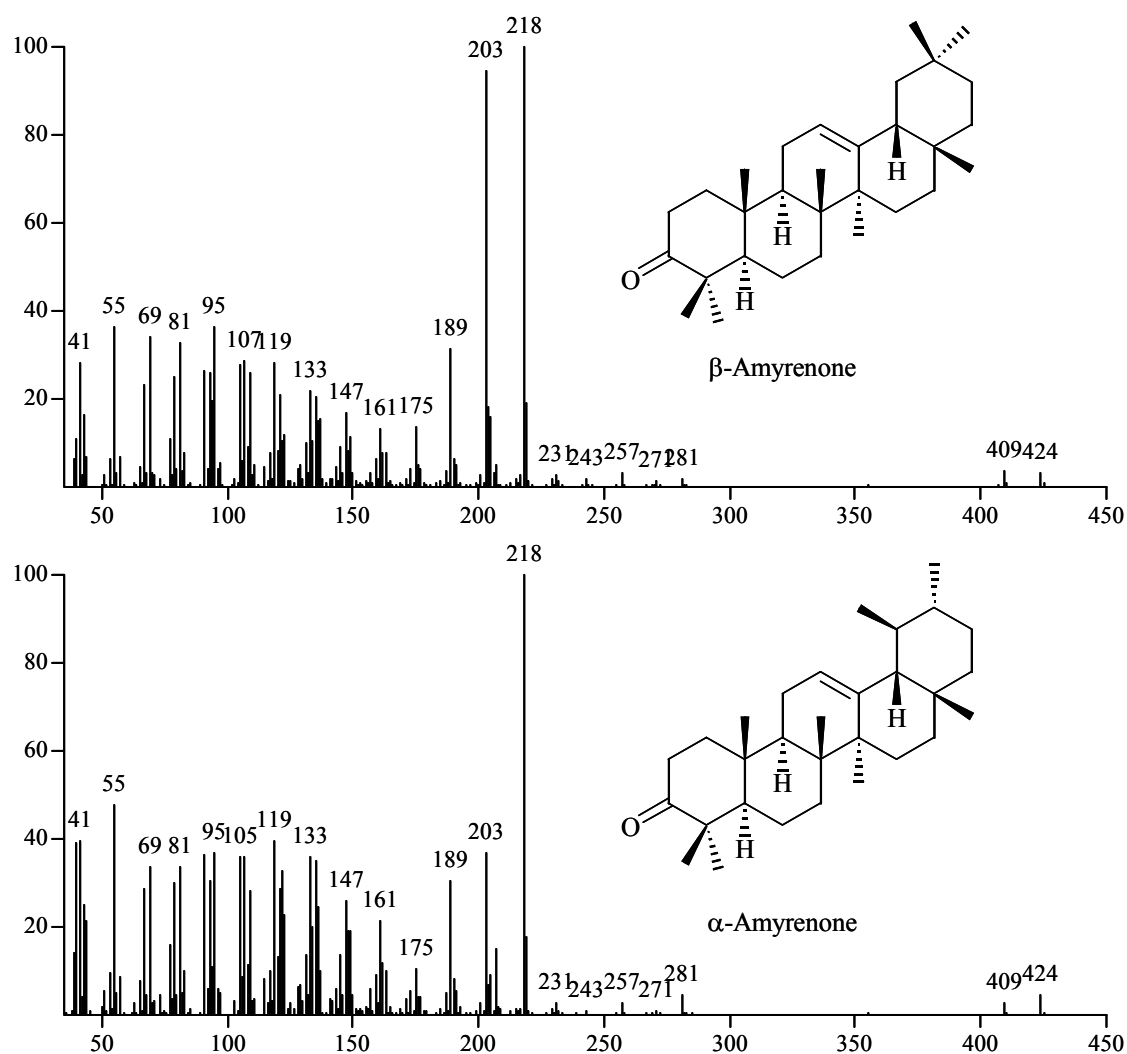
Fig. 5.78. Mass spectra of α- and β-amyrenone.

The same fragmentation pattern was observed in the case of the TMS derivatives of 3-*O*-acetyl-α-BA and 3-*O*-acetyl-β-BA. The mass spectra of both acids showed a molecular ion peak m/z = 570. Loss of a methyl group produced the signal m/z = 555, while elimination of acetic acid produced m/z = 510 which upon loss of a methyl group produced m/z = 495. The RDA fragment containing ring D and E was observed as the base peak at m/z = 218. After loss of a methyl group, the diagnostic signal at m/z = 203 was observed again to be 50% more abundant in 3-*O*-acetyl-α-BA. The other RDA fragment containing rings A and B produced a signal at m/z = 352 which preferably lost acetic acid to produce m/z = 292 (**Fig 5.79**).
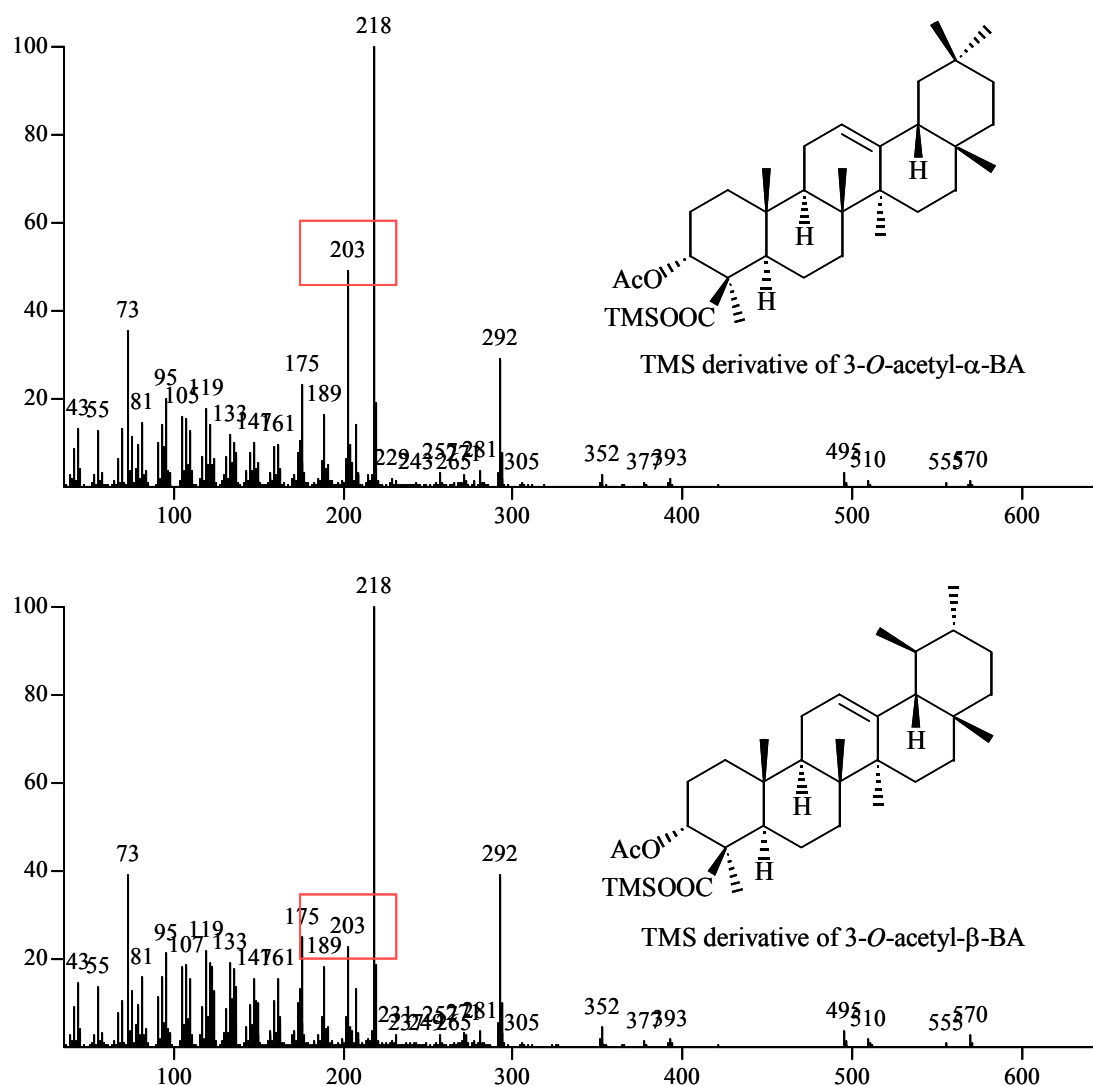
Fig. 5.79. Mass spectra of the TMS derivatives of 3-*O*-acetyl-α-BA and 3-*O*-acetyl-β-BA.

Surprisingly no 11-keto derivatives of α-BA were observed in the acid fractions of olibanum. Both 11-keto-β-BA (KBA) and 3-*O*-acetyl-11-keto-β-BA (AKBA) were distinguishable by their molecular ion signals after silylation (**Fig. 5.80**).

KBA produced a molecular ion signal at $m/z = 614$ whereas for AKBA at $m/z = 584$ was observed. Fragment ion signals of KBA at $m/z = 599$ showed loss of a methyl group, followed by loss of TMSOH to produce $m/z = 509$. The signal at $m/z = 524$ was produced upon loss of TMSOH whereas $m/z = 496$ was observed for the loss of TMSOOCH. Additionally, the fragment that was formed upon RDA cleavage ($m/z = 382$) produced a signal ($m/z = 367$) by loss of a methyl group.

The fragment ion signals observed for AKBA showed slight changes as compared to KBA. The signal for the loss of a methyl group at $m/z = 569$ followed by elimination of acetic acid ($m/z = 509$) as well as elimination of TMSOH ($m/z = 494$) and the extrusion of acetate producing $m/z = 525$ followed by loss of TMSOH ($m/z = 435$) or as well as loss of TMSOH + CO ($m/z = 407$) represent the heaviest fragments in its mass spectrum.
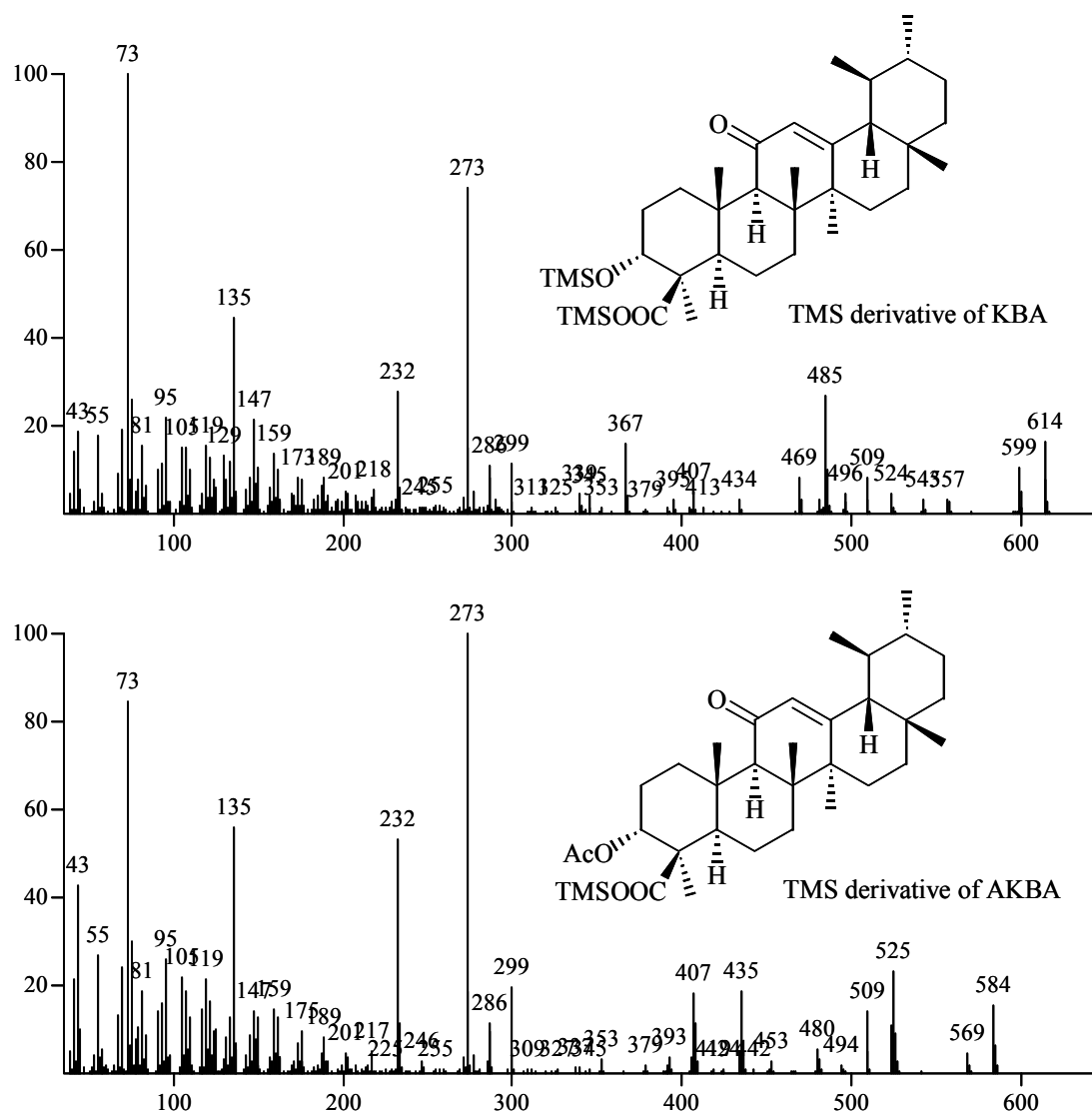
Fig. 5.80. Mass spectra of the silylated derivatives of KBA and AKBA.

However, in the MS of TMS derivatives of KBA and AKBA some common signals were also observed which were produced upon the RDA reaction and McLafferty rearrangement that took place in the ring C (**Fig 5.81**). Earlier work indicated that the presence of a keto group at

C-11 of 12-oleanene and 12-ursene triterpenes causes McLafferty rearrangement to be enhanced rather than RDA reaction[164].
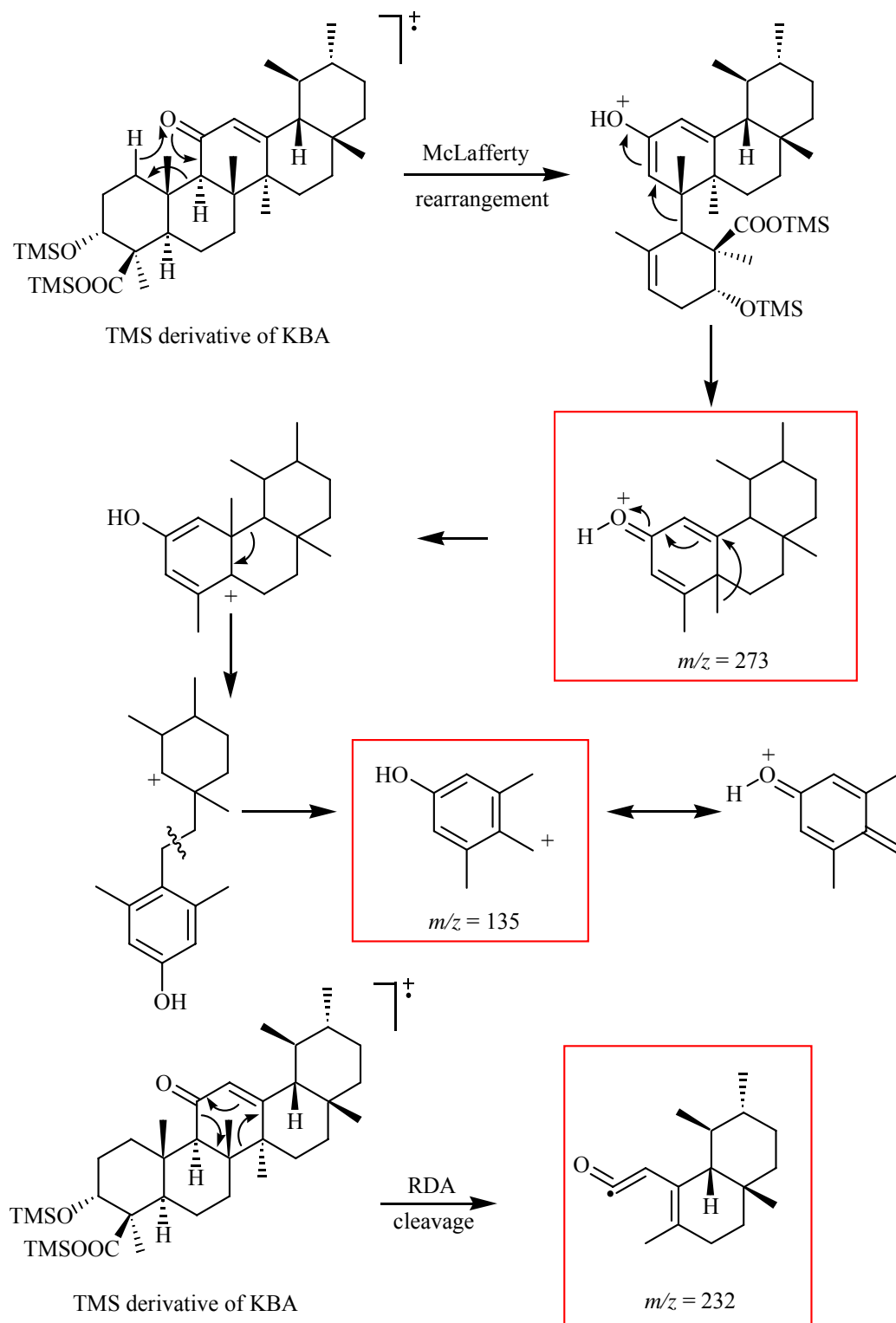
Fig. 5.81. Possible fragmentation of TMS derivative of KBA.

11-OH, 11-OMe and their 3-O-acetyl derivatives were also observed in the group of boswellic acids (**Fig. 5.82**). The molecular ion signals for the TMS derivatives of 11-hydroxy-β-BA, 3-O-acetyl-11-hydroxy-β-BA and 3-O-acetyl-11-methoxy-β-BA were observed at m/z = 688, 658 and 600, respectively.

For BA derivatives it was observed that the change from 11-keto to the TMS derivative of 11-hydroxy triggered the RDA reaction in ring C. As a result a characteristic signal for the RDA fragment was observed at m/z = 306 (**Fig. 5.83**). In addition, in the mass spectrum of 11-OH-β-BA loss of a methyl group (m/z = 673), and two subsequent TMSOH eliminations formed fragment signals at m/z = 598 and m/z = 508 both of which lost a methyl group (m/z = 583 and m/z = 493).

In 3-O-acetyl-11-hydroxy-β-BA the loss of a methyl group at m/z = 643, elimination of acetic acid (m/z = 598) and the loss of a TMSOH group (m/z = 568) were predominantly recognized.

Replacement of the hydroxy group by a methoxy group at C-11 in 3-O-acetyl-11-methoxy-β-BA surprisingly suppressed the RDA cleavage. Instead, elimination of methanol was observed with a fragment ion signal at m/z = 568 [M^+-32] producing a conjugated double bond system in ring C. The signals were to represent, m/z = 518 as the loss of the acetic acid, m/z = 495 as elimination of TMSOH from the fragment m/z = 585 formed by the loss of a methyl group (m/z = 467) as the loss of CO followed by another TMSOH elimination releasing m/z = 377.

The 11-hydroxy-α-BAs were identified in trace amounts in the acid fractions of olibanum resins. Their assignment was mainly depended on the retention times in GC analysis compared to their β-BA analogues.
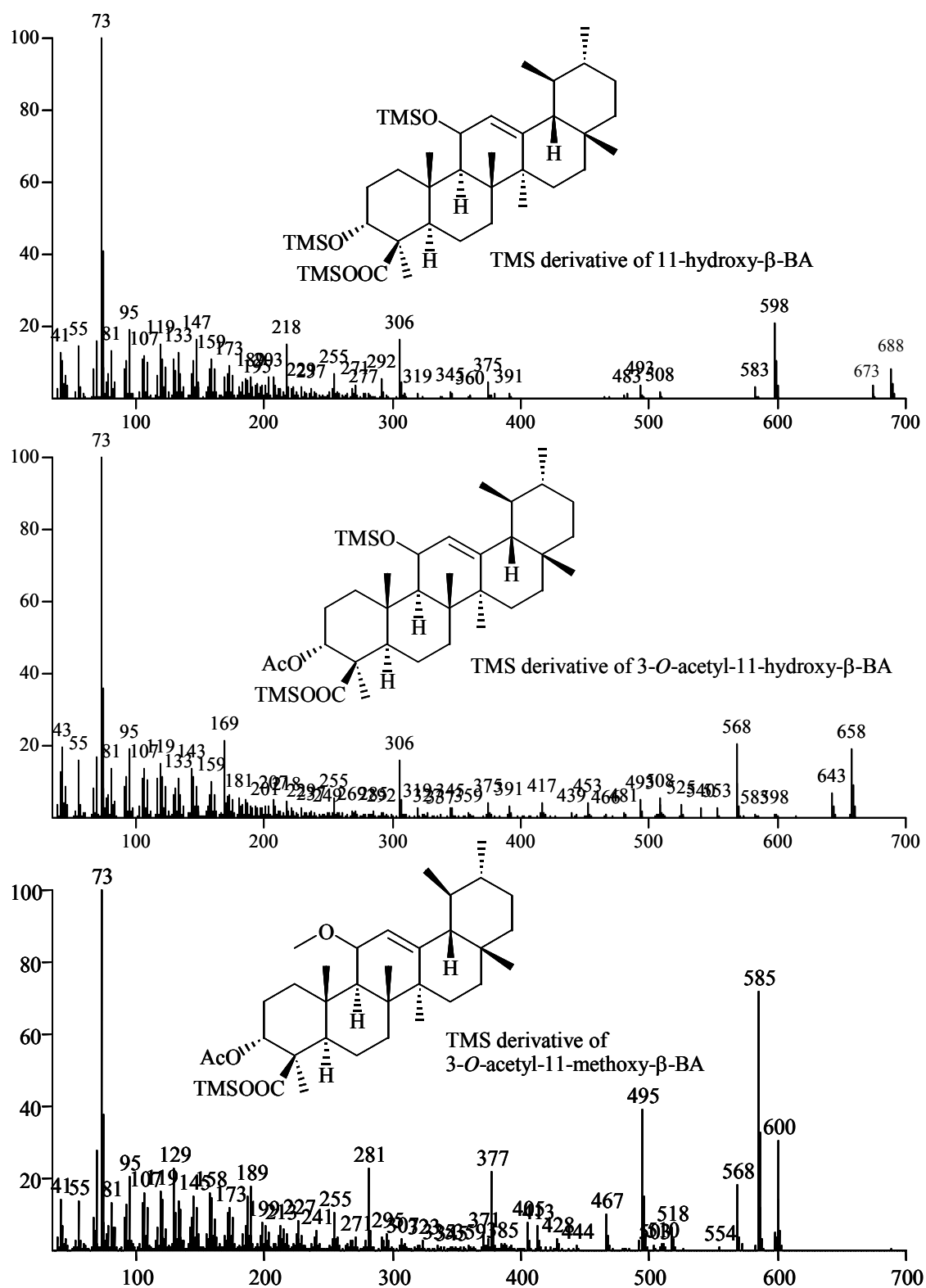
Fig. 5.82. Mass spectra of the TMS derivatives of 11-hydroxy-β-BA, 3-*O*-acetyl-11-hydroxy-β-BA and 3-*O*-acetyl-11-methoxy-β-BA.
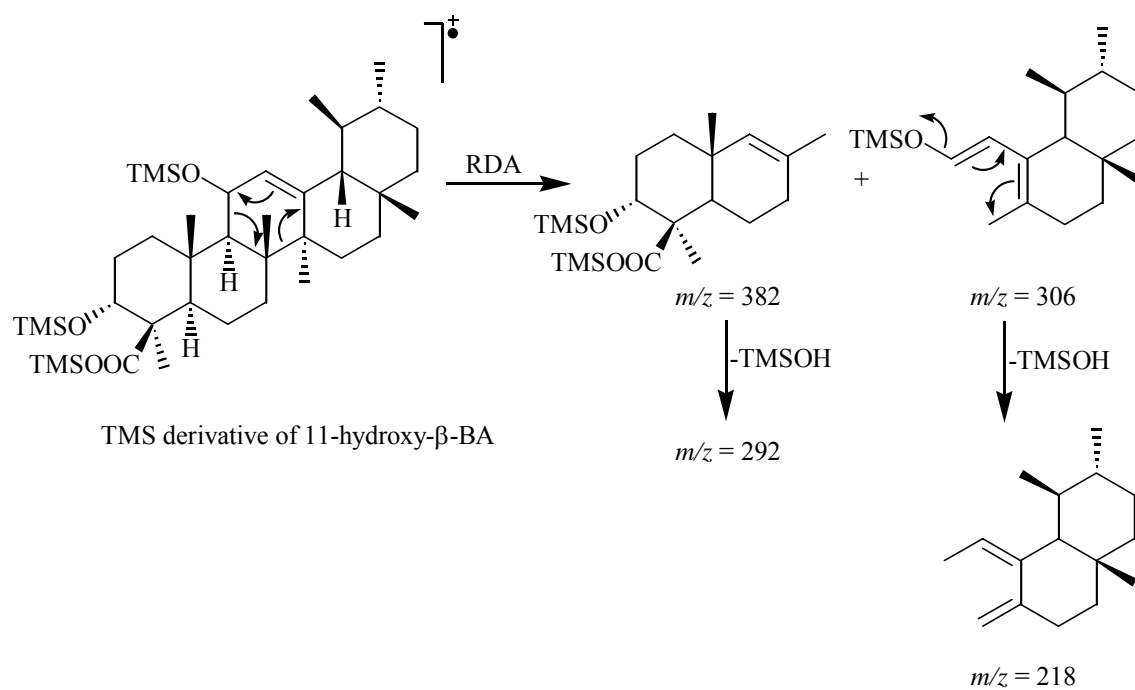
Fig. 5.83. Possible fragmentation of the TMS derivative of 11-hydroxy-β-BA.

9,11-Dehydro-β-BA and its 3-*O*-acetyl derivative showed unique fragmentation patterns. The fragment ion signal at $m/z = 255$ could not be explained with the known information. But nevertheless, this fragment turned out to be a diagnostic signal in the assignment of structures having conjugated double bond system in ring C (**Fig. 5.84**).
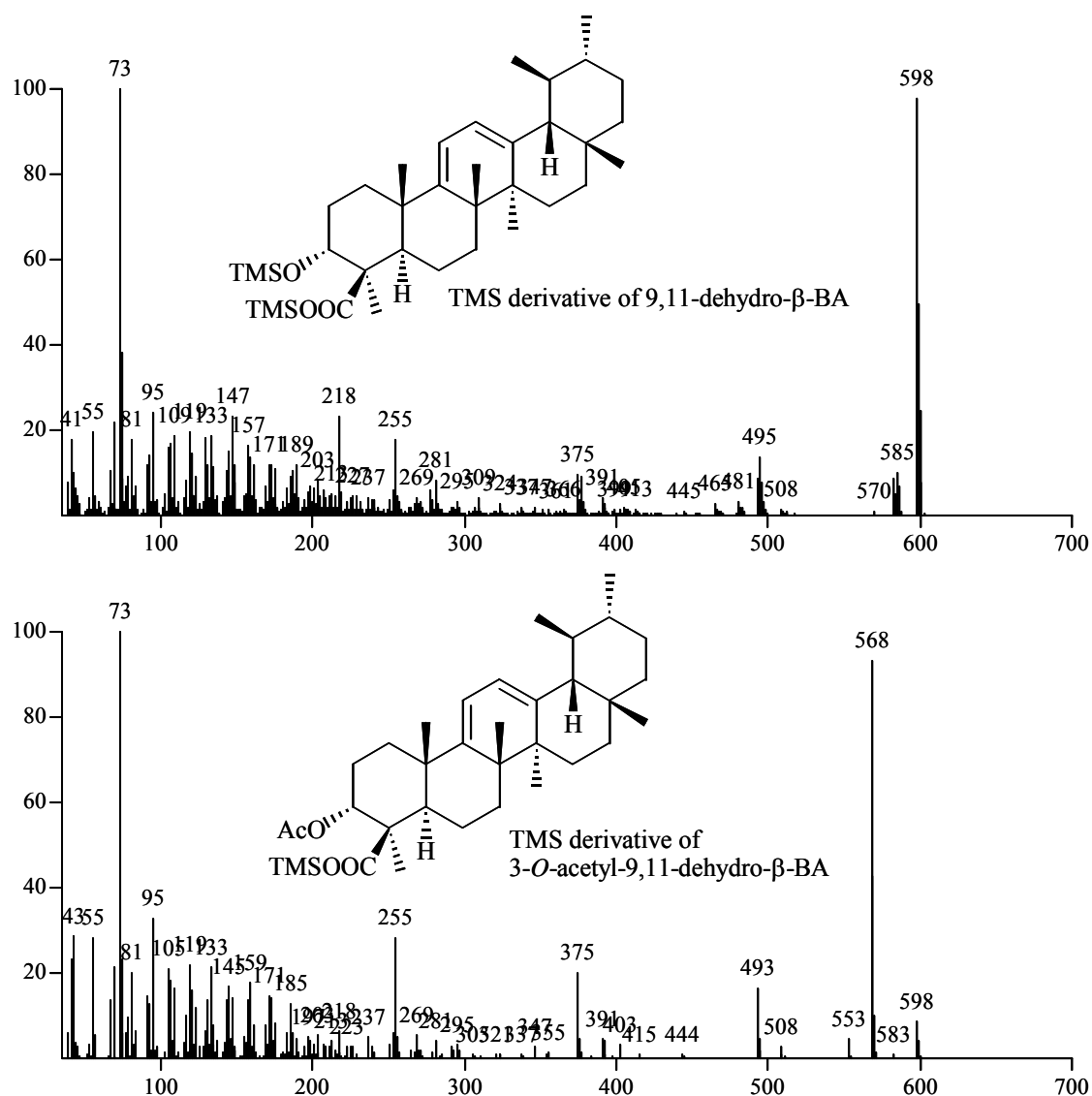
Fig. 5.84. Mass spectra of the TMS derivatives of 9,11-dehydro-β-BA and its 3-*O*-acetyl derivative.

In the silylated fractions of olibanum the tirucallic acids (TA) were also observed. Their mass spectra show consistency. Therefore, the molecular ions at *m/z* = 600 and 570 calculated for the TMS derivatives of 3-hydroxy-TA and 3-*O*-acetyl-TA, respectively, were easily distinguished from β-BA and 3-*O*-acetyl-β-BA (**Fig. 5.85**).
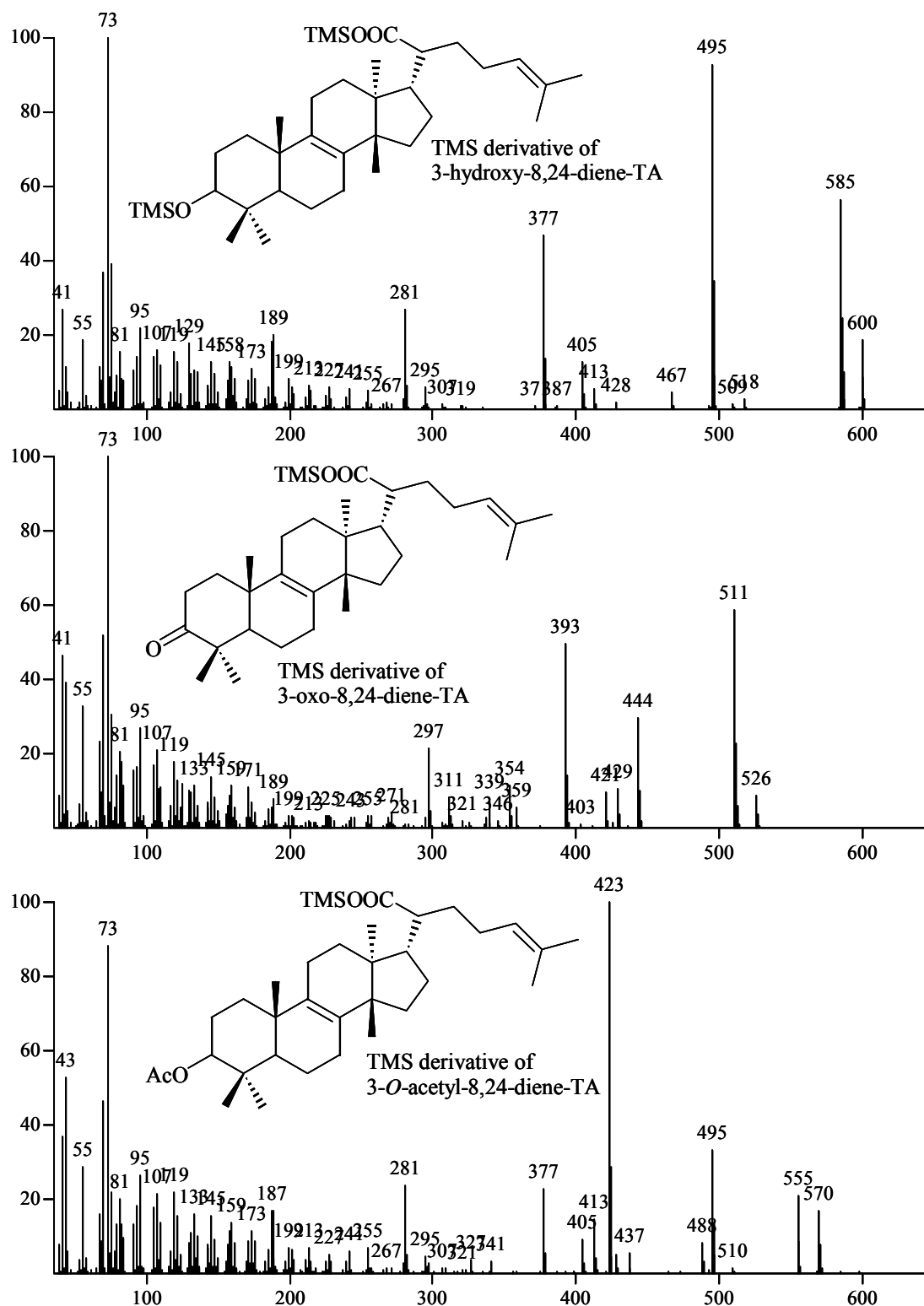
Fig. 5.85. Mass spectra of the TMS derivatives of tirucallic acids in olibanum resin.

The fragmentation patterns of TAs showed typical differences as compared to boswellic acids. The 3-hydroxy-TA and 3-*O*-acetyl-TA showed similar mass spectra. The splitting of methyl groups, TMS groups and allylic cleavages were clearly observed with 3-hydroxy-TA (**Fig. 5.86a**) whereas its acetyl derivative showed elimination of acetic acid in addition. The 3-oxo-TA compared to the other derivatives of tirucallic acids showed differences (**Fig 5.86b**).
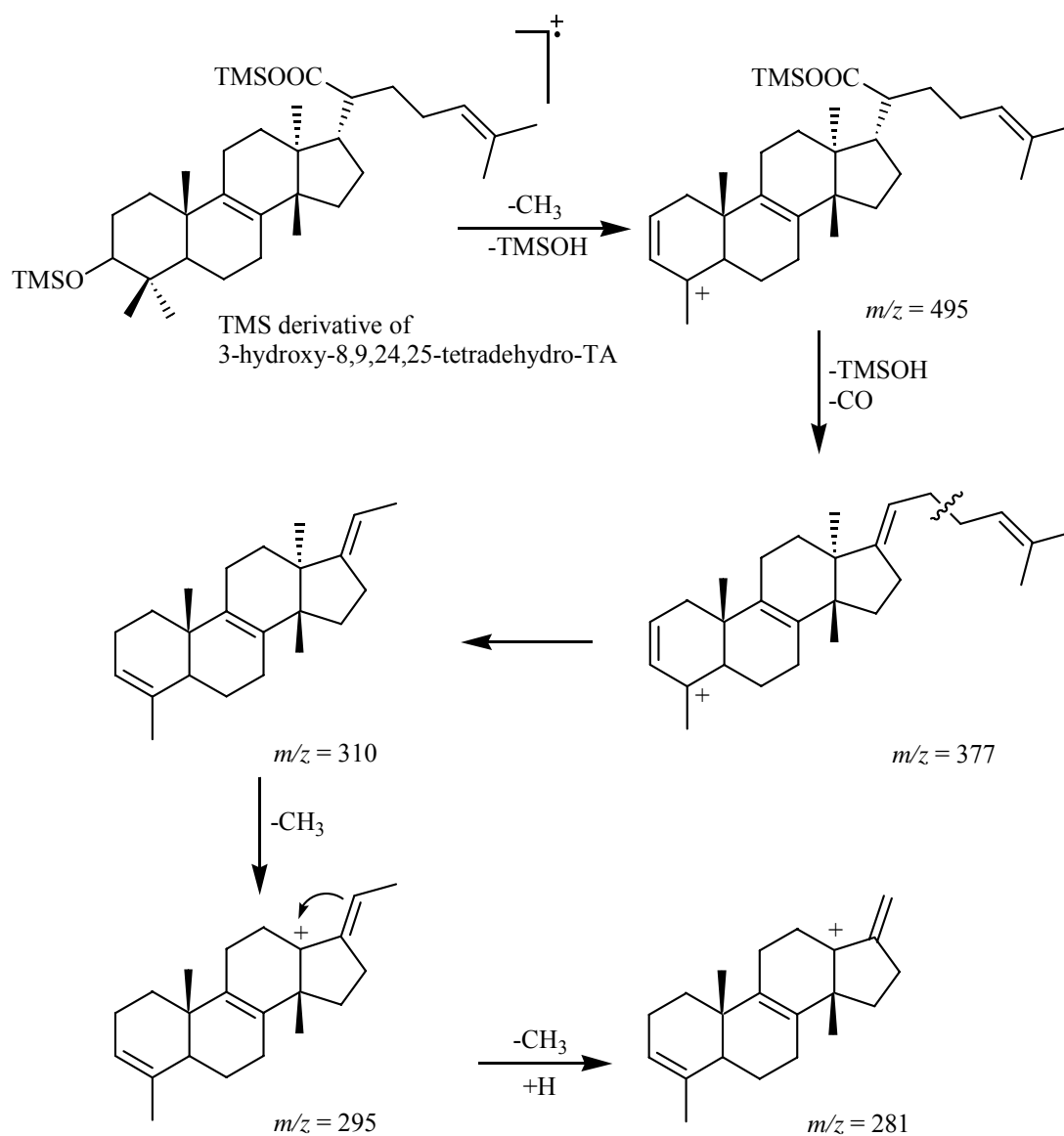
Fig. 5.86a. Possible fragmentation of the TMS derivative of 3-hydroxy-8, 9, 24, 25-tetradehydro-TA.

131
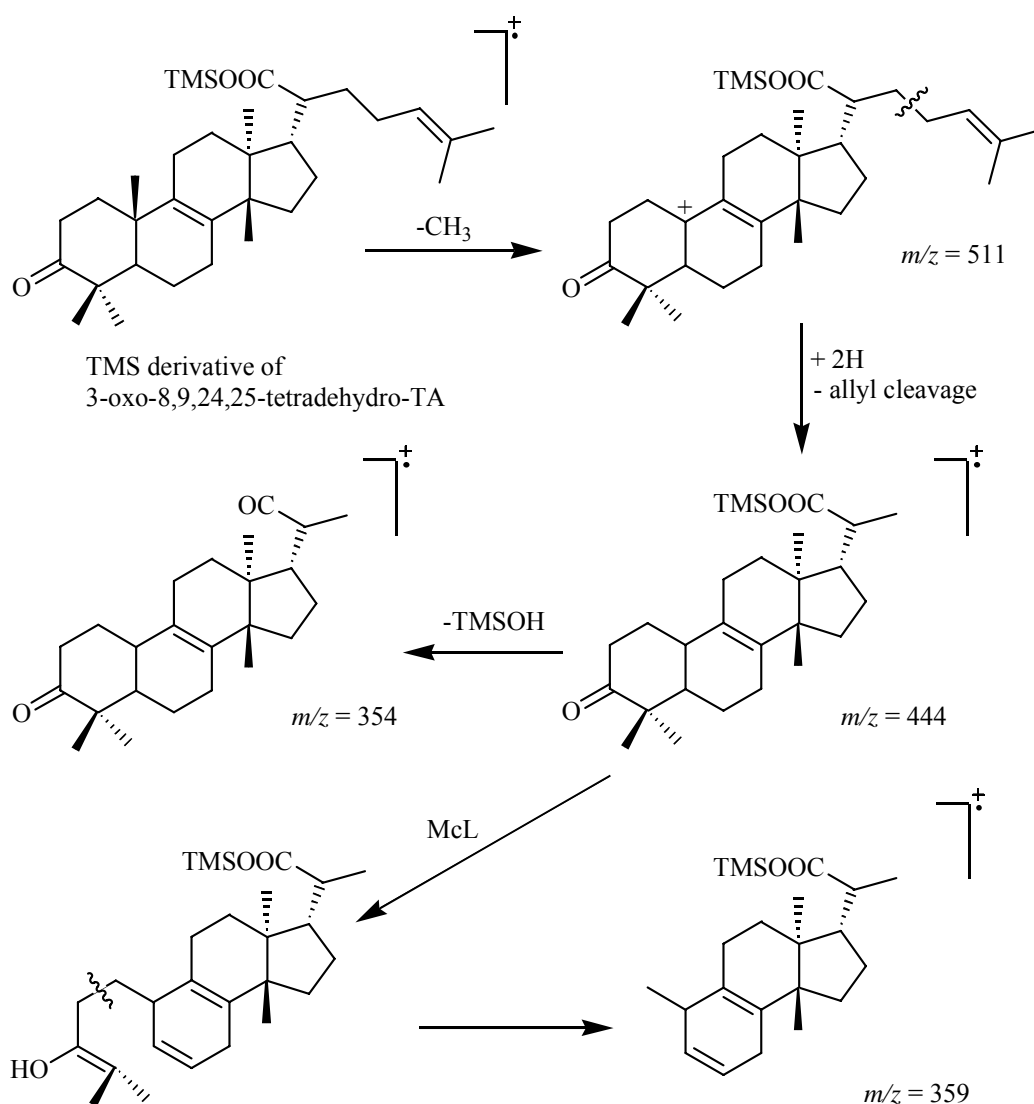
Fig. 5.86b. Possible fragmentation of theTMS derivative of 3-oxo-8, 9, 24, 25-tetradehydro-TA.

5.6.2.2 Analysis of Acid Fractions of B. carterii and B. serrata Determined by The Use of Different Basic Extractions

For the determination of the constituents of the acid fractions *n*-hexane extracts were prepared from the powdered resins of *B. carterii* and *B. serrata*. The residue was then further extracted with polar solvents (diethylether, ethylacetate or ethanol) after the filtration of *n*-hexane. Thereafter the polar extracts were treated with five aqueous basic solutions of KOH (2% and 10%), NaOH, $Mg(OH)_2$, $Ba(OH)_2$ as it has been described before. The separation of the salt of the acids from the reaction medium, acidification of this mixture and extraction with an organic solvent to regain the acids represented the final steps in this procedure. The acid

fractions were then silylated to be analysed by GC and GC-MS. A parallel investigation was performed by TLC from the acid fractions without any derivatisation.

Both *B. carterii* (**Fig. 5.87, Fig. 5.88, Fig. 5.89**) and *B. serrata* (**Fig. 5.90, Fig. 5.91, Fig. 5.92**) acid fractions afforded similar results. The inconsistency in these results was observed between five different methods in the concentration of the single constituents although the experiments were performed with equal amount of resin in each case.
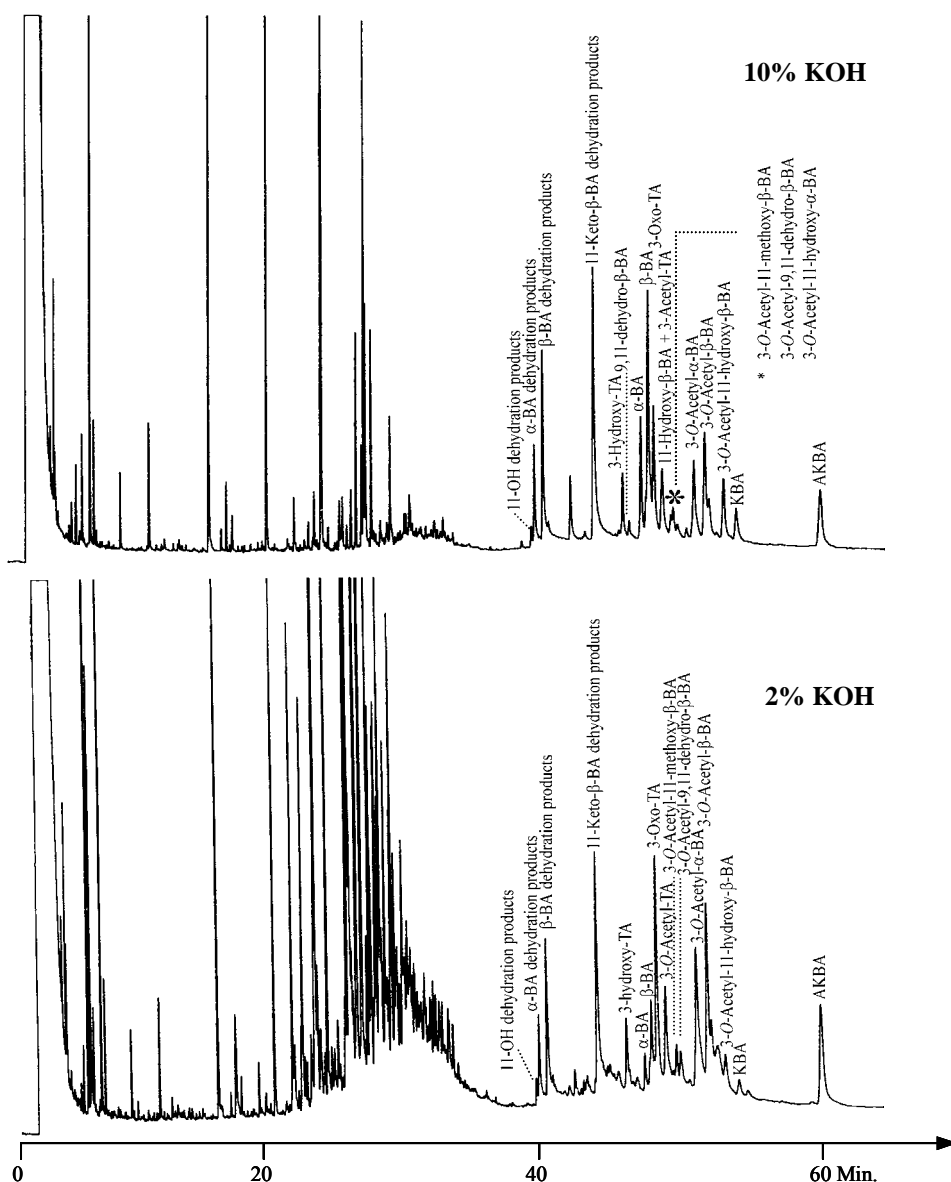
Fig. 5.87. Gas chromatograms of the silylated acid fractions determined by 10% KOH extraction (above) and 2% KOH extraction from *B. carterii* (25 m fused silica capillary column with CPSil 5CB, 100 °C, 5 °C /min up to 300 °C, injector at 250 °C, detector at 320 °C, carrier gas 0.5 bars H_2).

133
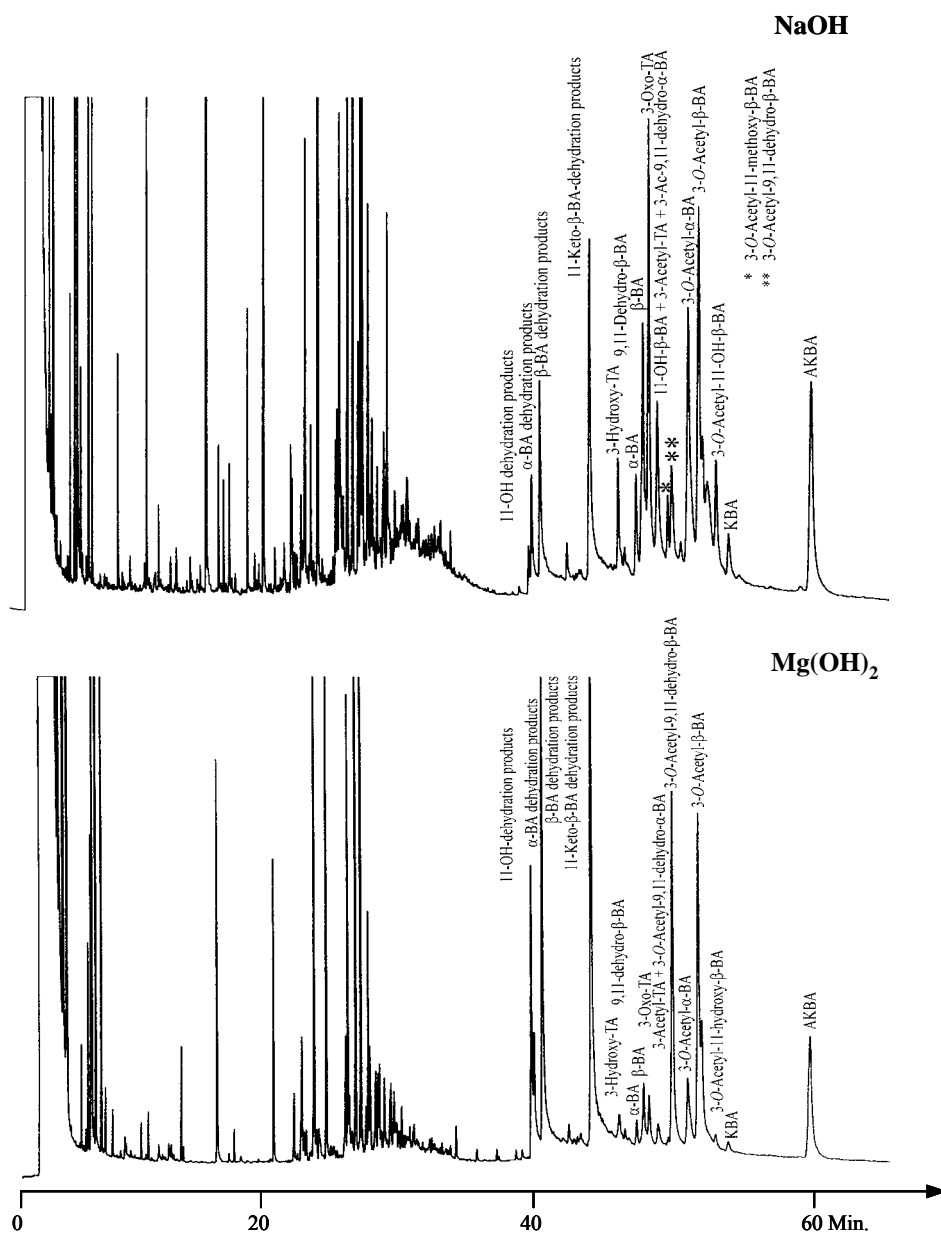
Fig. 5.88. Gas chromatograms of the silylated acid fractions determined by NaOH extraction (above) and Mg(OH)$_2$ extraction from *B. carterii* (25 m fused silica capillary column with CPSil 5CB, 100 °C, 5 °C /min up to 300 °C, injector at 250 °C, detector at 320 °C, carrier gas 0.5 bars H$_2$).
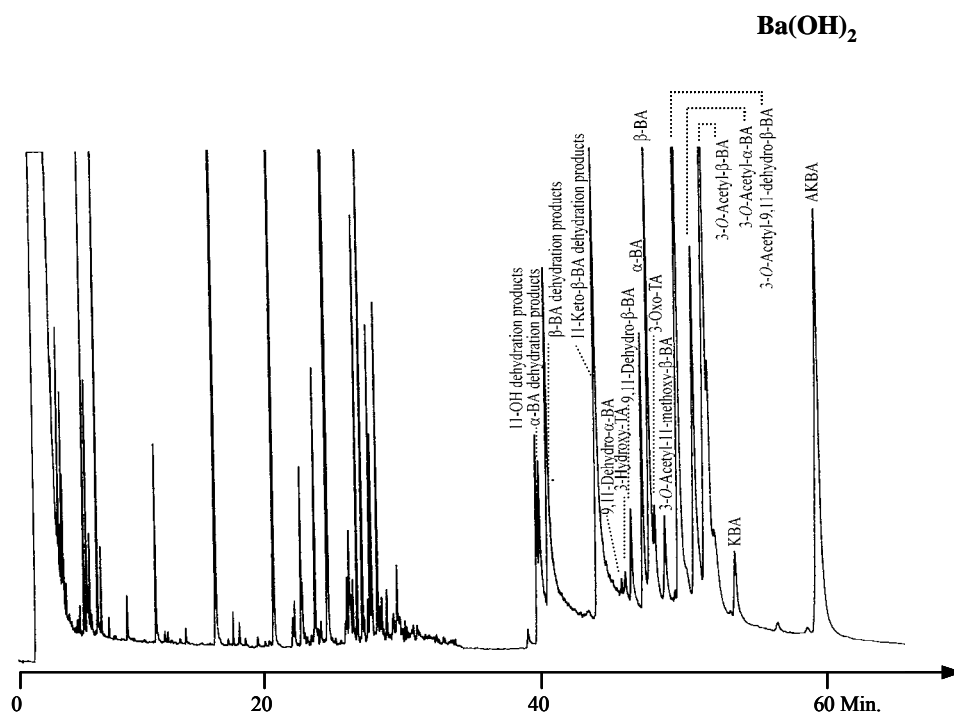
Fig. 5.89. Gas chromatogram of the silylated acid fraction determined by Ba(OH)$_2$ extraction from *B. carterii* (25 m fused silica capillary column with CPSil 5CB, 100 °C, 5 °C /min up to 300 °C, injector at 250 °C, detector at 320°C, carrier gas 0.5 bars H$_2$).

During the preparation of acid fractions the use of concentrated acid solutions and high temperatures was avoided in order to prevent decomposition or any possible rearrangement although some reported procedures did not consider this. Nevertheless, some dehydration products were observed in gas chromatograms due to the high temperatures during the injection of the samples.

For the acid fractions of *B. carterii* the best results were obtained by using 10% KOH extraction. Both 2% KOH and Mg(OH)$_2$ extractions gave unsatisfactory results.

The five extractions performed with *B. serrata* (**Fig. 5.90-5.92**) were similar in most cases with those of *B. carterii*. In addition, it was recognized that nearly all these acid fractions contained other members of oleanane and ursane series that do not bear an acid functional group. The possible synergistic effects of these triterpenoic constituents on the pharmacological activities of *B. serrata* could be an intriguing area to study.
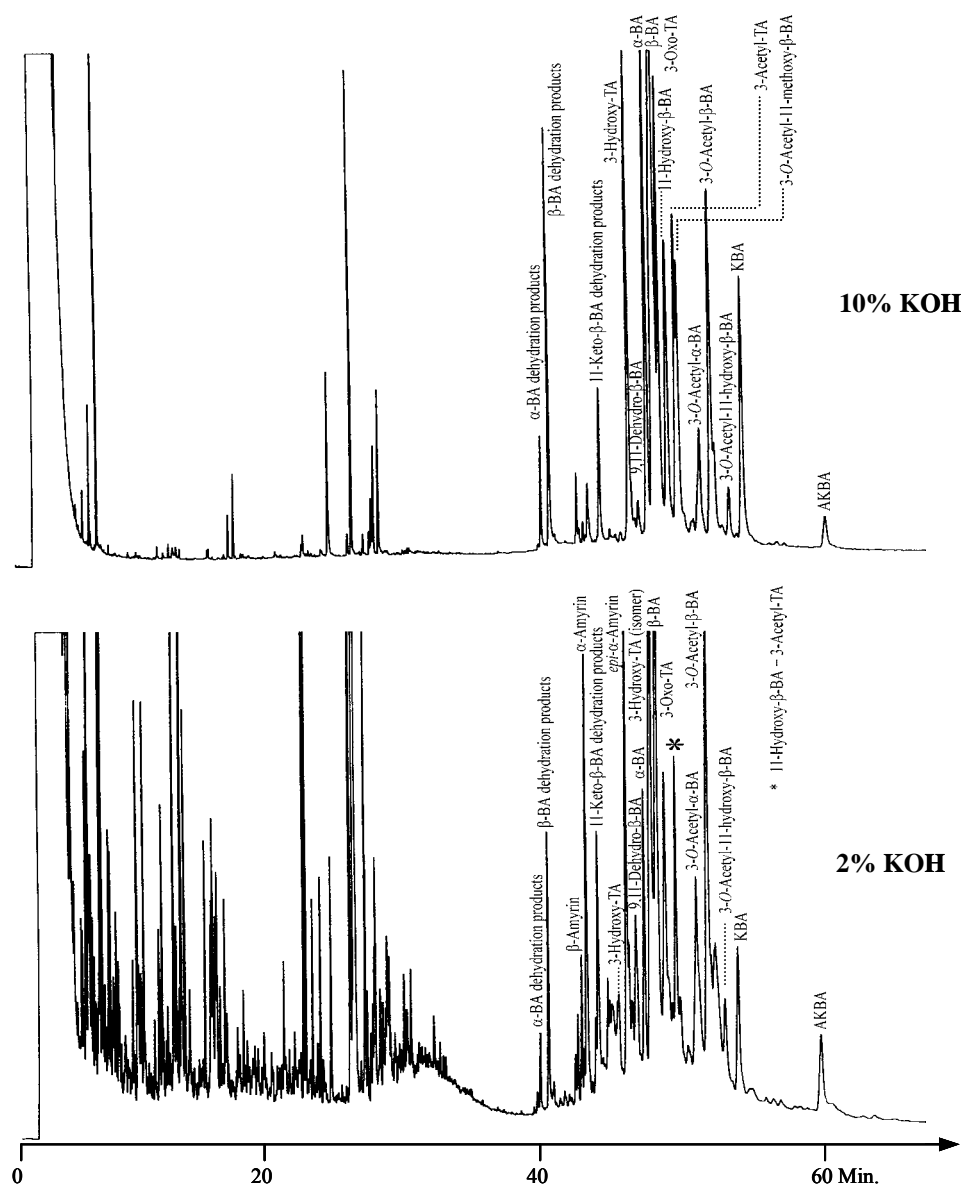
Fig. 5.90. Gas chromatograms of the silylated fractions determined by 10% KOH extraction (above) and 2% KOH extraction from *B. serrata* (25 m fused silica capillary column with CPSil 5CB, 100 °C, 5 °C /min up to 300 °C, injector at 250 °C, detector at 320°C, carrier gas 0.5 bars H$_2$).
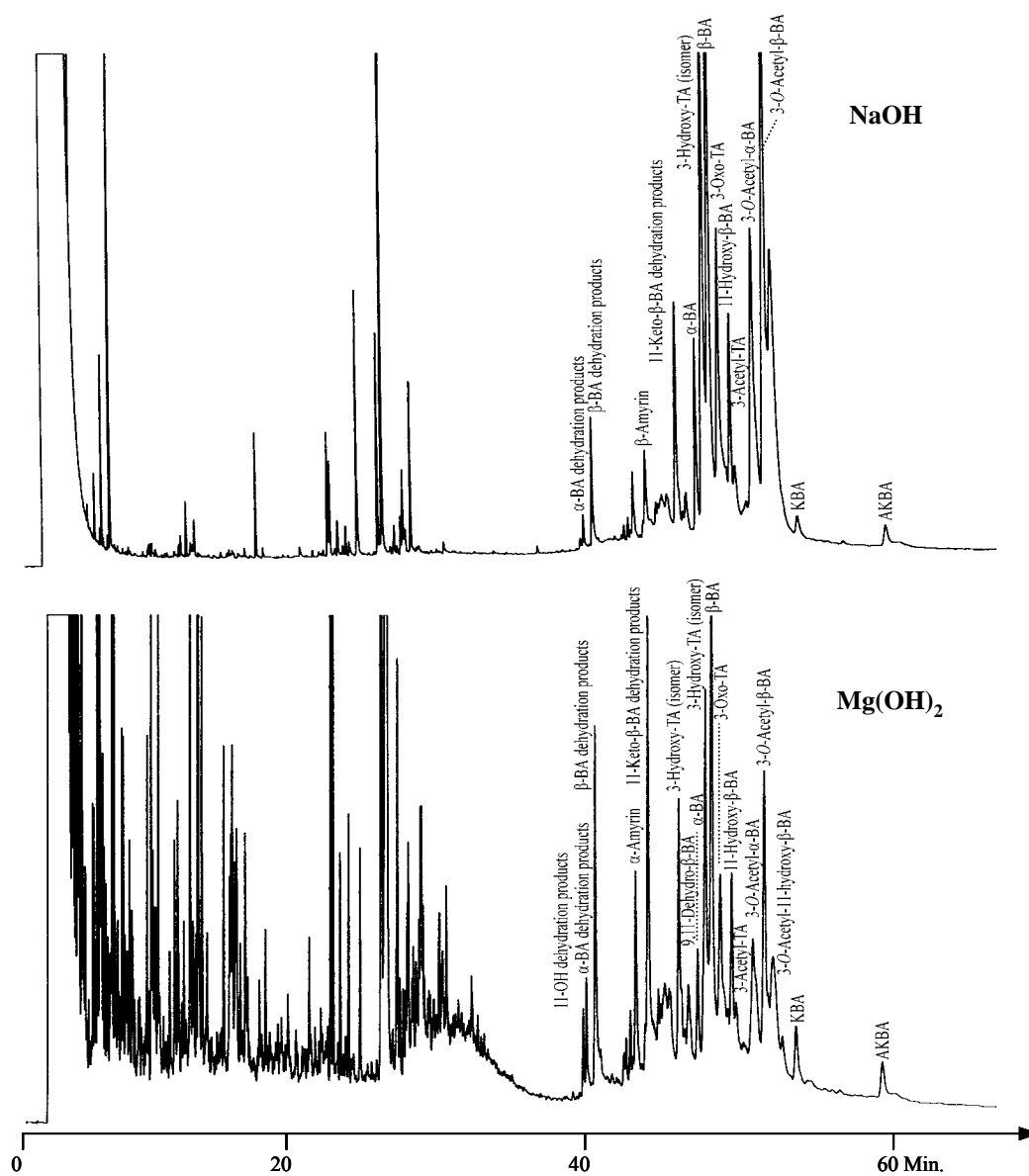
Fig. 5.91. Gas chromatograms of the silylated fractions determined by NaOH extraction (above) and Mg(OH)$_2$ extraction from *B. serrata* (25 m fused silica capillary column with CPSil 5CB, 100 °C, 5 °C /min up to 300 °C, injector at 250 °C, detector at 320 °C, carrier gas 0.5 bars H$_2$).
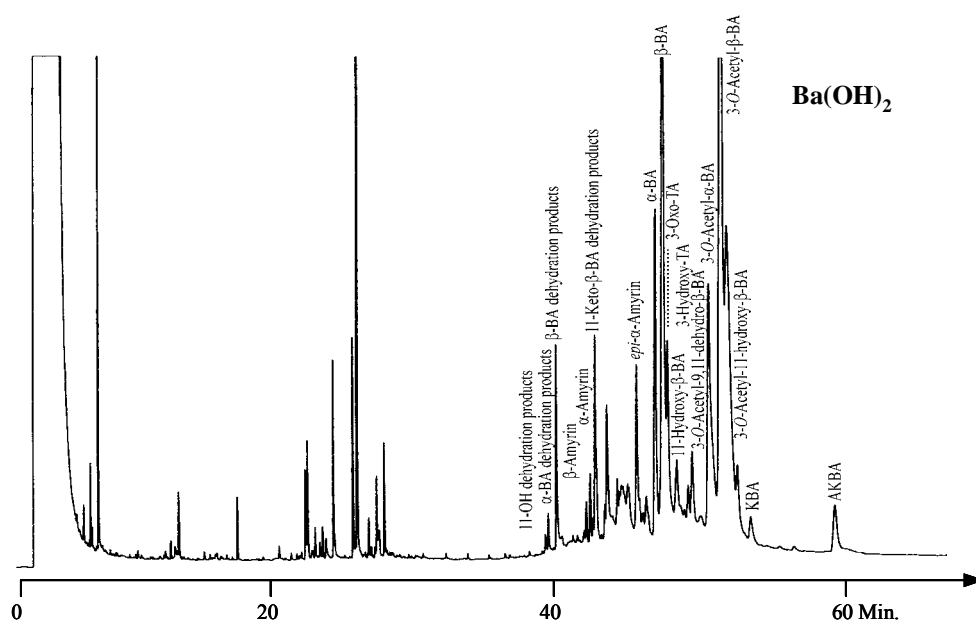
Fig. 5.92. Gas chromatogram of the silylated fraction determined by Ba(OH)$_2$ extraction from *B. serrata* (25 m fused silica capillary columkn with CPSil 5CB, 100 °C, 5 °C /min up to 300 °C, injector at 250 °C, detector at 320 °C, carrier gas 0.5 bars H$_2$).

Both GC, GC-MS investigations and TLC experiments showed differences in the acid fractions of *B. carterii* and *B. serrata* determined with various basic extracts (**Fig. 5.93**). The advantage of TLC experiments in comparison to GC investigations relies on the direct application of the samples whereby decomposition and the formation of dehydration products is avoided caused by the high temperatures at the injection port. On the other hand it was not possible to detect α-BA and β-BA as well as 3-*O*-acetyl-α-BA and 3-*O*-acetyl-β-BA separately as two different spots.
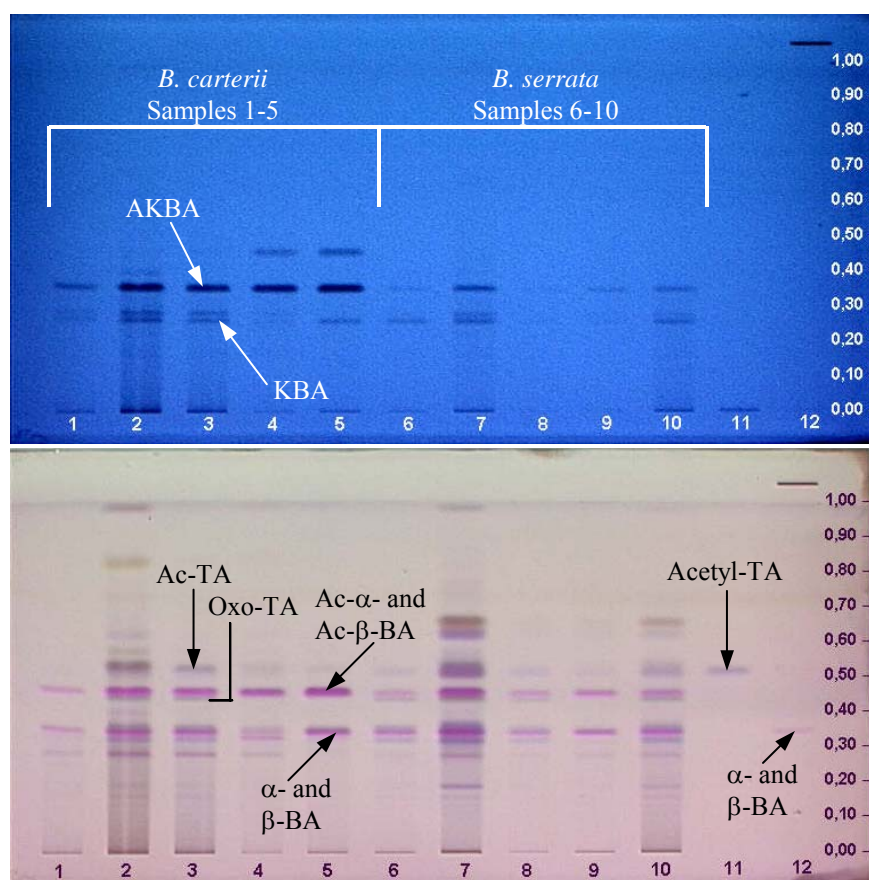
Fig. 5.93. TLC documentation of the acid fractions of *B. carterii* (samples 1-5) and *B. serrata* (samples 6-10) determined by different bases. Sample **1** and **6**: 10% KOH, **2** and **7**: 2% KOH, **3** and **8**: NaOH, **4** and **9**: $Mg(OH)_2$, **5** and **10**: $Ba(OH)_2$, **11**: 3-Acetyl-TA, **12**: α-BA and β-BA. (LiChrosphere Si 60_{F254S} plate (Merck), mobile phase: toluol: ethylacetate: heptane: formic acid (8:2:1:0.3). Development distance: 8 cm. Detection: above: UV $_{254\,nm}$. Below: Daylight detection after derivatisation with anisaldehyde spray reagent with subsequent heating at 105 °C).

5.6.3   Stability Testing of Boswellic acids

GC and TLC investigations revealed a variety of differences in the composition of the acid fractions of *B. carterii* and *B. serrata*. It was assumed that, the variability of the results can be attributed to the reagents used in one of the reaction steps in which first the salt of these acids with different basic aqueous solutions (KOH, NaOH, $Mg(OH)_2$, $Ba(OH)_2$) were prepared, then this salt mixture was acidified with dilute HCl and finally the acidic components were extracted back with an organic solvent. Therefore, it became crucial to monitor the factor which affects this change.

An artifact formation was first detected by a multi-wave scanning of the lanes of TLC plates[165] (**Fig. 5.94**) showed differences in its UV spectra at 245 nm (light blue line) and 285 nm (purple line). The olibanum sample treated with HCl vapour and heat separately and

compared with the original sample. The formation of new absorption bands proved that high temperatures and acidic conditions caused conversions on the constituents of olibanum fractions into artifacts. This could also explain the unidentified bands that were observed on the TLC plate prepared for the detection of acid fractions determined by different basic extractions (**Fig. 5.95**).
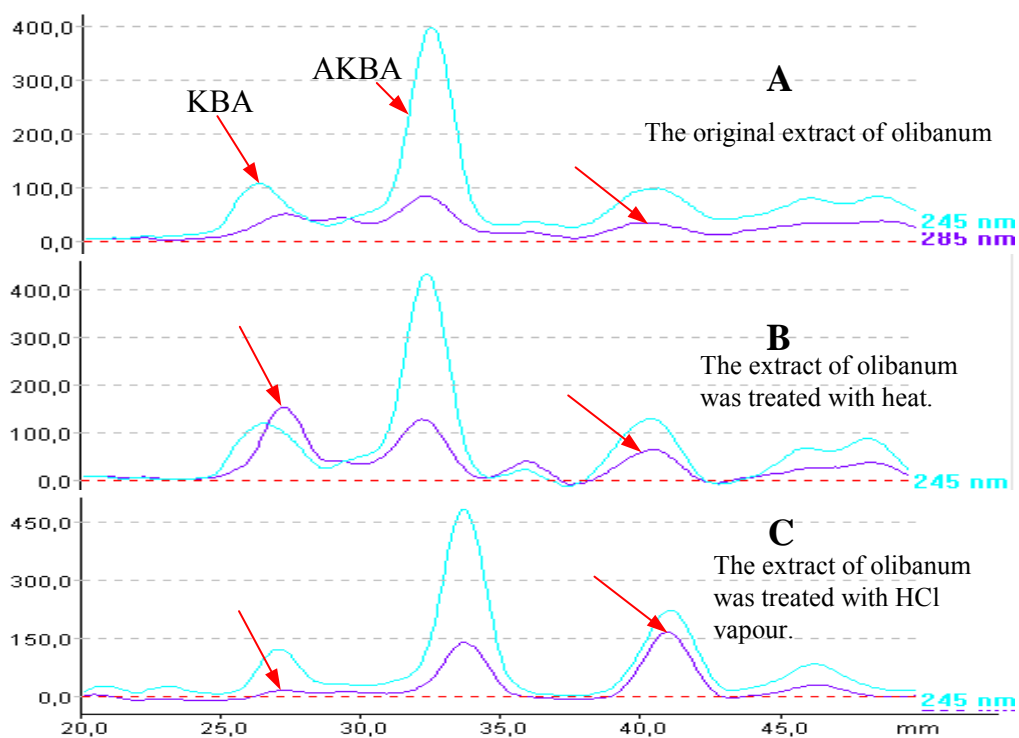
Fig. 5.94. Multi-wave scans of olibanum extracts at 245 nm (light blue line) and 285 nm (purple line). **A:** Scans of olibanum extract after the development of the plate. **B:** Scans of olibanum extract, heat (120 °C) treatment after the development of the plate. **C:** Scans of olibanum extract, treatment with HCl vapour after the development of the plate.
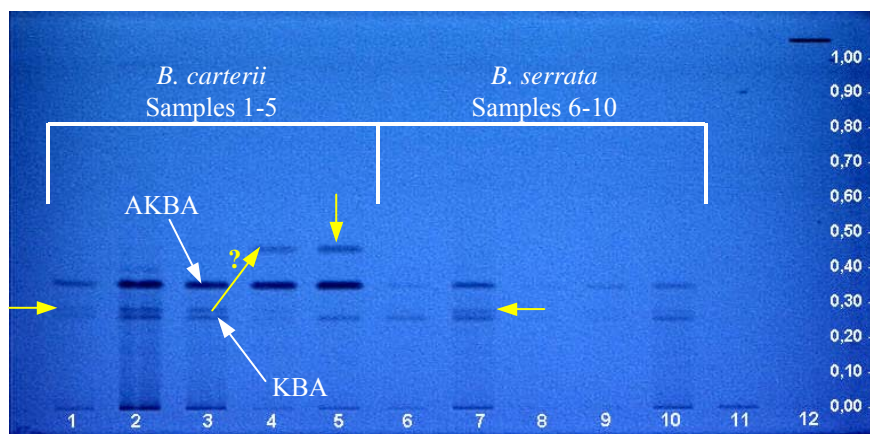
Fig. 5.95. TLC plate prepared with the samples of acid fractions of *B. carterii* (samples 1-5) and *B. serrata* (samples 6-10) extracted by different bases. The possible artifact formation indicated with yellow arrows. Sample **1** and **6**: 10% KOH, **2** and **7**: 2% KOH, **3** and **8**: NaOH, **4** and **9**: Mg(OH)$_2$, **5** and **10**: Ba(OH)$_2$, **11**: 3-*O*-Acetyl-TA, **12**: α-BA and β-BA. (LiChrosphere Si 60$_{F254S}$ plate (Merck), mobile phase: toluol: ethylacetate: heptane: formic acid (8:2:1:0.3). Development distance: 8 cm. Detection: above: UV $_{254\ nm}$. below: Daylight detection after derivatisation with anisaldehyde spray reagent with subsequent heating at 105 °C)

The acidic constituents of *B. carterii* and *B. serrata* were determined with another method to compare the effect of extraction with bases on these components. The point of using the ion-exchange resin as an adsorption material was to advantage from the ionic forces which would form between the carboxylate ion of the acidic components of olibanum and the resin only[166] (**Fig. 5.96**). Therefore the resin extract was expected to be purified from the other compunds which were involved in the former extraction procedures.

The ion-exchange resin (Amberlite$^©$ 900) was conditioned with 10 % aqueous NaOH solution. This conditioning step provided the exchange of the hydroxyl (OH$^-$) with chloride (Cl$^-$) ion. The resin was eluted with a gradient of deionized water: ethanol (from 1:1 to 0:1) until the pH of the decantate was neutralised. The application of the sample was followed by the elution of the resin with ethanol until all constituents other than BAs were separated. The acidic constituents were determined by the elution of the ion-exchange resin with 10% acetic acid in ethanol.

141
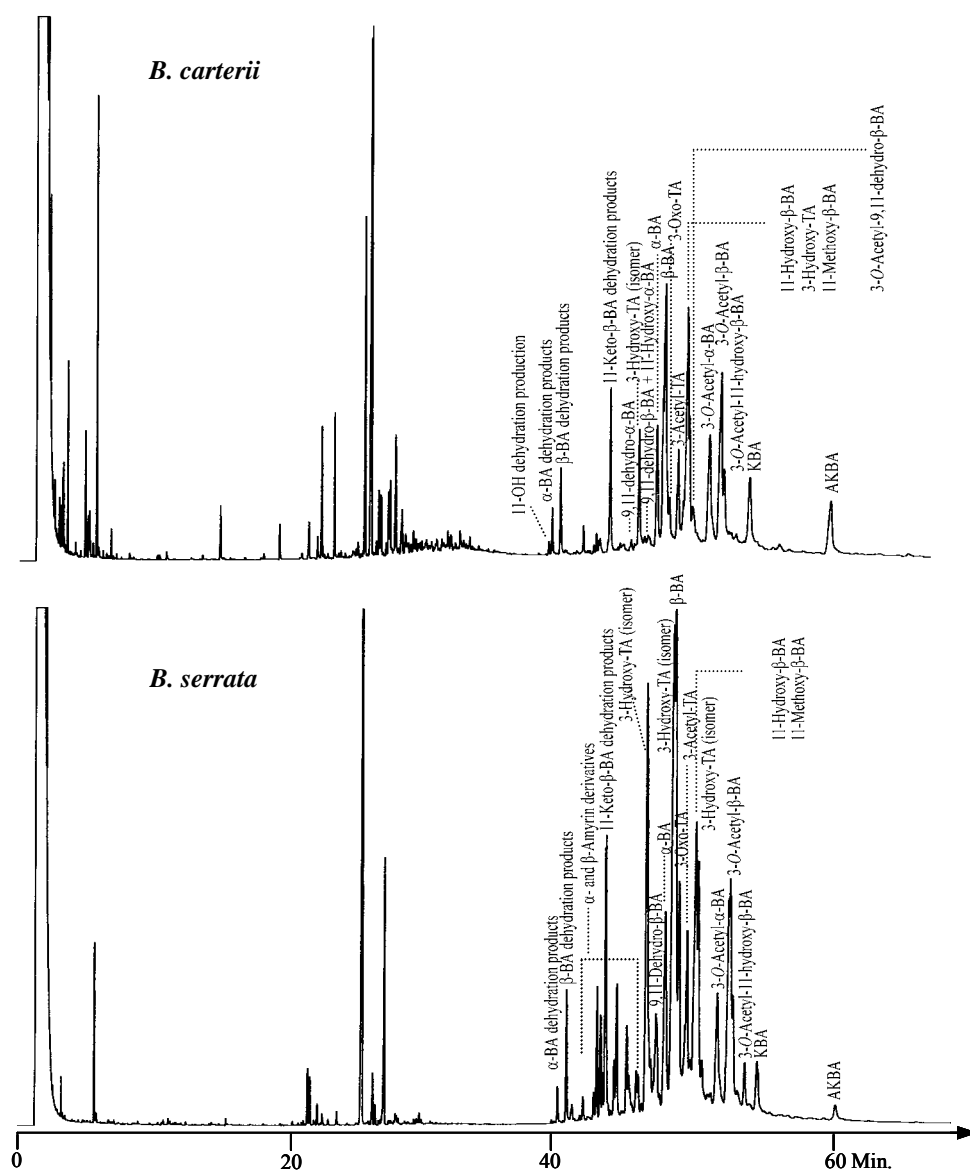
Fig. 5.96. Gas chromatograms of the silylated acid fractions determined by ion-exchange column from *B. carterii* (above) and *B. serrata* (25 m fused silica capillary column with CPSil 5CB, 100 °C, 5 °C/min up to 300 °C, detector at 320 °C, injector at 250 °C, carrier gas 0.5 bars H₂).

As shown in the chromatograms (**Fig. 5.96**), both olibanum species produced purer acid fractions with the ion-exchange method compared to the methods depending on base extraction. Additionally, *B. serrata* was recognized to contain a high amount of α- and β-amyrin type of triterpenoids other than boswellic acids.

A series of "stress tests" were planned on TLC plates to demonstrate the reaction step in which the artifact formation occured. "*Stress tests*" were used often in pharmaceutical

analysis to prove the stability of the compounds in question. For this reason the samples were analysed under various conditions in which exposing the sample to acid, base vapour or heat could also be counted[167].

To test the stability of the constituents of olibanum and define the reaction step in which the artifact formation occurred the polar extracts of *B. carterii* and *B. serrata* were applied on the TLC plate. The applied samples were treated with HCl vapour and the aqueous solutions of different bases (KOH, NaOH, $Mg(OH)_2$, $Ba(OH)_2$) and exposed to heat (120 °C) to observe the changes. These applications were actually reflecting the reaction steps in the extraction method with different bases. All the samples, original polar fraction of olibanum and the stressed samples were finally compared to the acid fractions obtained from the ion-exchange method (**Fig. 5.97**).

The HCl vapour exposure to the samples 1 and 2 produced a new band at R_f: 0.43[#] (**Fig. 5.97. I**). On the other hand, the application of heat revealed a band at R_f: 0.26 in samples 3 and 4. There were no considerable changes observed with the traetment of the polar extracts with different basic solutions but further heat application on these samples revealed the band at R_f: 0.26 (**Fig. 5.97.II**).

[#] R_f = the distance of the sample from the application zone/development distance. The indicated scales in this work were not showing the real R_f values. Since different detection methods were performed for detection the frontline was not recognized in some cases. Therefore they were given only for practical reasons as a scale from top to bottom of the plate. The similarity of the R_f values to the given scale is only a coincidance.
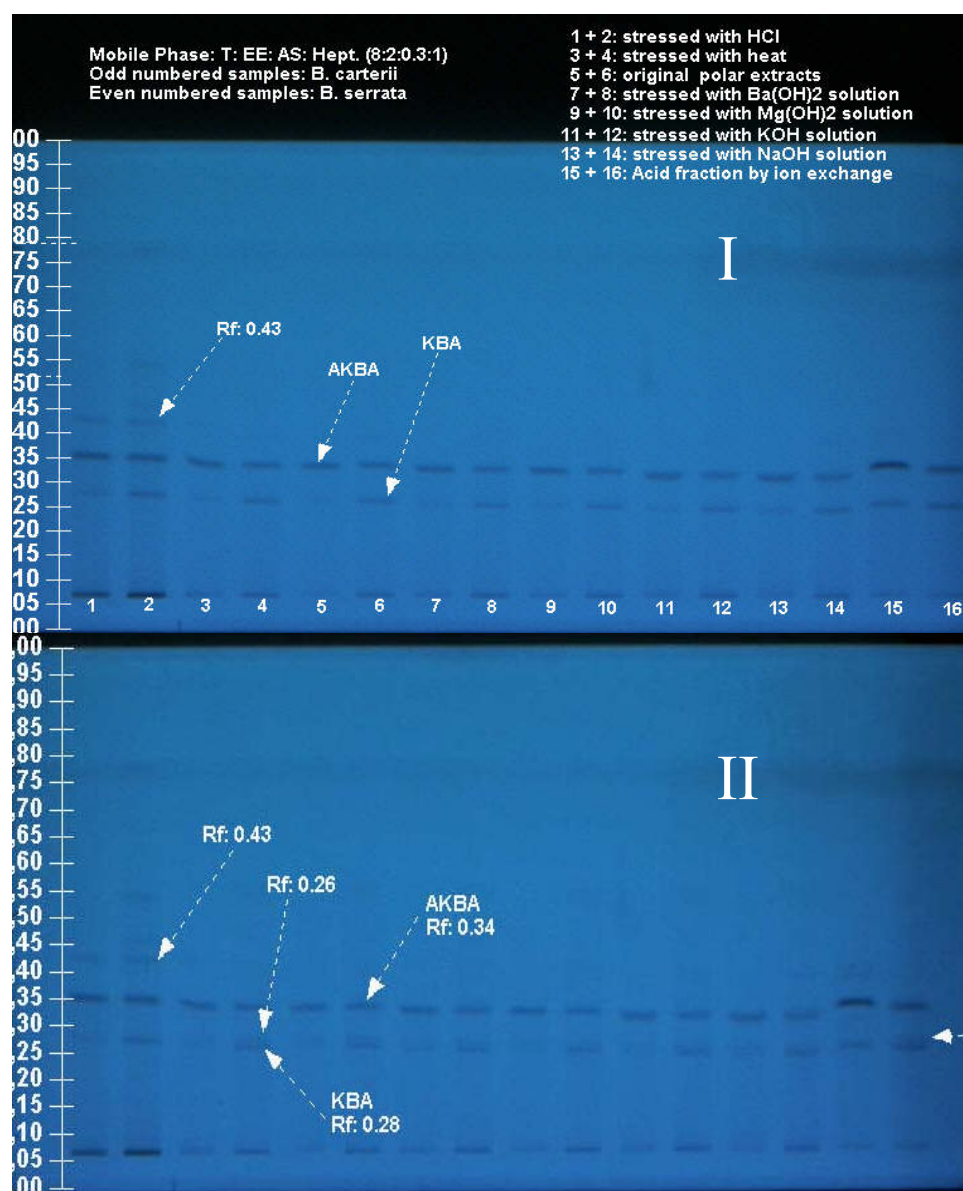
Fig. 5.97. TLC plate prepared with *B. carterii* (odd numbered samples) and *B. serrata* (even numbered samples) polar extracts for the detection of the changes on boswellic acids with different conditions. Samples **1** and **2**: exposed to HCl vapour, **3** and **4**: heat application, **5** and **6**: original extracts, **7** and **8**: exposed to 10% Ba(OH)$_2$, **9** and **10**: exposed to 10% Mg(OH)$_2$, **11** and **12**: exposed to 10% KOH, **13** and **14**: exposed to 10% NaOH, **15** and **16**: acid fractions from ion-exchange elutions (Merck HPTLC-LiChrosphere Si 60$_{F254S}$ plates, mobile phase: toluol: ethylacetate: heptane: formic acid (8:2:1:0.3), elution distance: 7 cm., detection: UV $_{254 nm}$).

It was assumed that a dehydration reaction occurred during the treatment of HCl vapour and application of heat on the samples which could be assigned to the boswellic acids with hydroxyl or equivalent functionality at 11th position. Because of a possible dehydration that took place in ring C the conjugation would increase and therefore the artifacts have become

detectable with UV at 254 nm. Besides, in the multiwave scans of these artifacts, a bathochromic shift in their UV spectra was observed which also pointed out a conjugated system (**Fig. 5.94**).

The separation of the boswellic acids from an olibanum extract needed the use of an acid in each method, either the extractions with basic solutions or the ion exchange elutions. Because the effect of HCl vapour had been clearly observed, the other acidic reagents used as mobile phase or in chromatographic processes during these experiments should also be compared to find out whether an additional change occur with their utilisation. Therefore a TLC plate was prepared to test the effects of different acids on *B. serrata* extracts (**Fig. 5.98**).
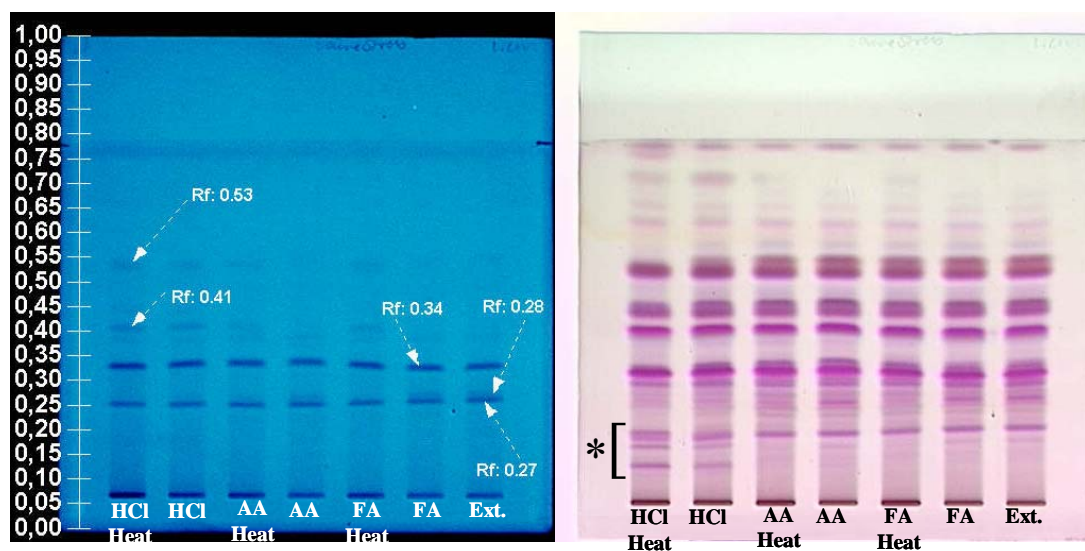
Fig. 5.98. TLC plate to test the effect of different acids on *B. serrata* polar extract. **AA**: Acetic acid, **FA**: Formic acid. Samples 1, 3, 5 were exposed to heat after the acid treatment (Merck HPTLC-LiChrospher Si 60_{F254S}, mobile phase:toluol: ethylacetate: heptane: formic acid (8:2:1:0.3), development distance:7 cm., detection: 1. UV $_{254\,nm}$ 2. Daylight detection after derivatisation with anisaldehyde spray solution and heating at 105 °C).

Double samples of the polar extract of *B. serrata* were exposed to the vapour of HCl, acetic acid (AA) and formic acid (FA). One sample from each set was additionally subjected to heat. The strongest change was detected with the samples treated with HCl vapour. The band at R_f: 0.41 appeared in both of the samples of HCl treatment. Moreover with HCl treatment some other bands (*) were detected after the derivatisation of the plate with anisaldehyde between R_f: 0.1-0.2. The effect of AA and FA were found negligible but heating the plate after acid vapour exposure a new band appeared at R_f: 0.28 slightly above KBA (R_f: 0.27) in samples 4,

6 and 7 as well. Contrarily, the samples 3 and 5 showed the presence of a band at R_f: 0.41 after the heating of the plate. This observation indicated a possible relationship between these two bands appearing at R_f: 0.41 and R_f: 0.28 which was further proved with a 2-D TLC experiment (**Fig. 5.99**).

For the proof of this hypothesis *B. carterii* was used as the formation of these two artifact bands was more obvious with its extracts.
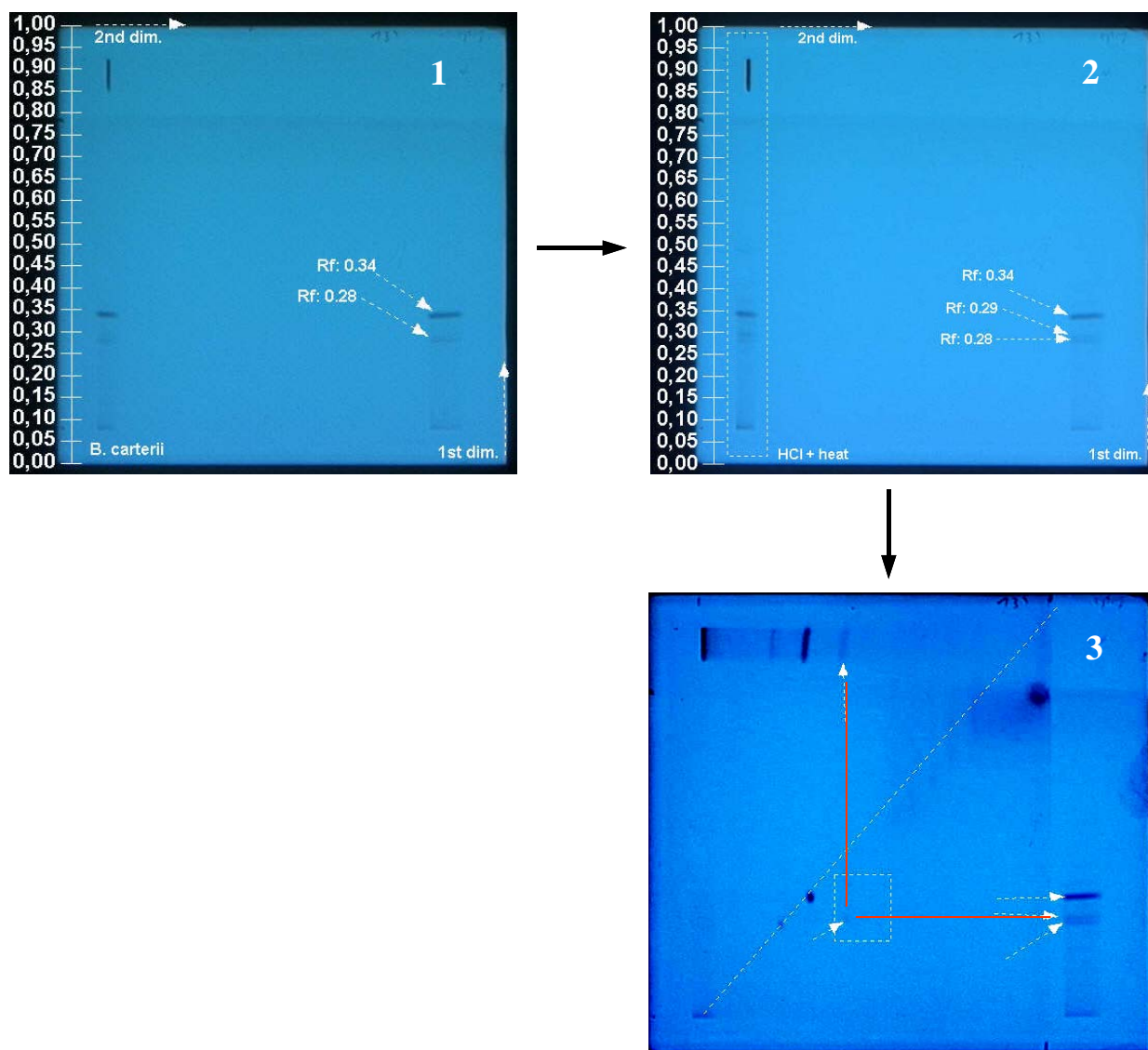
Fig. 5.99. View 1, 2, 3: Proof of the relation between the artifact bands at R_f: 0.41 and R_f: 0.29 by a 2-D TLC experiment (Merck HPTLC-LiChrS, mobile phase: toluol: ethylacetate: heptane: formic acid (8:2:1:0.3), development distance: 7 cm., detection: UV $_{254\,nm}$).

The experiment with 2-D TLC was composed of mainly three steps (**Fig. 5.99**). To obtain the first view (**1**) *B. carterii* extract was applied on two zones linearly and the plate was eluted in one direction. In both lanes the bands for AKBA (R_f: 0.34) and KBA (R_f: 0.28) were detected.

The second view (**2**) was determined after the performance of three substeps. First the refence sample, which was the same *B. carterii* extract, was applied on the second dimension. Secondly, the whole track, the eluted *B. carterii* extract in **1** and the refence sample, was treated with HCl vapour. Finally the whole plate was heated so that the band at R_f: 0.29 above KBA (R_f: 0.28) were also detectable in the second track of *B. carterii* in **1**.

The experiment was finished by the elution of the plate in the second dimension which was shown in the final view (**3**). In 2-D TLC experiments if no decomposition occurs then the compounds were detected on a diagonal. In this case it was clearly observed that the band at R_f: 0.41, that was revealed after the acid treatment and heat application, corresponded to the band at R_f: 0.29, that appeared after the application of heat (red lines) and their cross peak lay obviously apart from the diagonal.

The stability tests of boswellic acids showed which bands were formed under the treatment of acids or exposure to heat. The detection of these bands in the extracts of the phytopharmaceuticals prepared from olibanum can be considered as a method for testing their stability and the procedures that the drug has undergone.

5.6.4 Acid fractions of *Boswellia frereana*, *Boswellia neglecta* and *Boswellia rivae*

While the acid fractions of *B. carterii* and *B. serrata* contained a series of boswellic and tirucallic acid derivatives, the other *Boswellia* species did not show this diverse composition in their acid fractions. More commonly, different α- and β-amyrin derivatives could rather be detected than their triterpenoic constituents.

Lupeol and epi-lupeol were identified for *B. frereana* in earlier works. The preparation of an acid fraction of *B. frereana* with a basic extraction with 10% KOH was investigated by GC and GC-MS after silylation. Lupeol and *epi*-lupeol were detected and compared with a reference sample. Moreover, α-BA, β-BA, 3-*O*-acetyl-11-methoxy-β-BA and KBA were detected in small amounts. 3-Oxo-8,9,24,25-tetradehydro-TA was the only tirucallic acid derivative detected in this species (**Fig. 5.100**).

Fig. 5.100. Gas chromatogram for the silylated acid fraction of *B. frereana* (25 m fused silica capillary column with CPSil 5CB, 100 °C, 5 °C/min up to 300 °C, injector at 250 °C, detector at 320 °C, carrier gas 0.5 bars H_2).

Using the extraction method with 10% KOH, the acid fraction prepared from *B. neglecta* showed from the series of boswellic acids only trace amounts of α- and β-BAs. The peaks observed in this silylated acid fraction showed the characteristic signals for α- and β-amyrin, their diol or acid derivatives in their fragmentation patterns (**Fig. 5.101**).

Fig. 5.101. Gas chromatogram for the silylated acid fraction of *B. neglecta* (25m fused silica capillary column with CPSil 5CB, 100 °C, 5 °C/min up to 300 °C, injector at 250 °C, detector at 320 °C, carrier gas 0.5 bars H_2).

In the case of *B. rivae*, the acid fraction was found to contain fewer amounts of amyrin derivatives, but more α- and β-BA derivatives in comparison to *B. neglecta*. The acid fraction of *B. rivae* was also prepared from the 10% KOH basic extraction (**Fig. 5.102**).

Fig. 5.102. Gas chromatogram for the silylated acid fraction of *B. rivae* (25 m fused silica capillary column with CPSil 5CB, 100 °C, 5 °C/min up to 300 °C, injector at 250 °C, detector at 320 °C, carrier gas 0.5 bars H_2).

The acid fractions of the three species of *Boswellia* simply proved that olibanum resins do not always contain the pharmacologically important boswellic acid constituents. Therefore, the quality control of phytopharmaceuticals prepared from olibanum resin should be performed carefully.

The acid fractions prepared from *Boswellia species* with 10% KOH basic extraction were also compared by TLC investigation (**Fig. 5.103**).
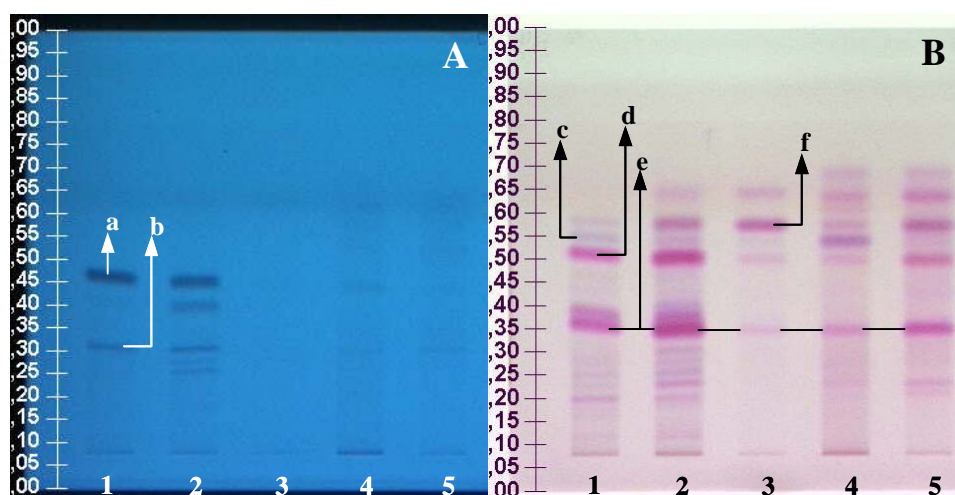
Fig. 5.103. TLC investigation for the acid fractions of olibanum. Samples **1**: *B. carterii*, **2**: *B. serrata*, **3**: *B. frereana*, **4**: *B. neglecta*, **5**: *B. rivae*. HPTLC LiChrospher® Si 60F$_{254S}$ (Merck) plates, mobile phase: chloroform: diisopropylether : methanol (7:2.5:0.5), development distance : 7 cm. **A**: UV detection at 254 nm., **B**: Detection at daylight after derivatisation with anisaldehyde spray solution with subsequent heating the plate at 105°C. Bands **a**: AKBA, **b**: KBA, **c**: 3-Oxo-TA, **d**: α- and β-Acetyl-BA, **e**: α- and β-BA, **f**: Lupeol.

5.7 Pyrolysis of Olibanum

The investigation of the pyrolysate of olibanum was found to be a challenging topic in two aspects. First, the chemical composition of the scent of olibanum was not completely described when it comes in contact with the red-hot charcoal. Secondly, it was assumed that in the pyrolysis process the resin produces hallucinogenic[82] or carcinogenic compounds, especially polyaromatic hydrocarbons (PAHs) if the incense mixtures are burned intensively in temples or churches[168].

It is, however, difficult to capture the smoke of olibanum and turn it into an analysable material. Most probably, this is the main reason why only a single publication exists on the pyrolysates of *B. carterii* performed by *Pailer et al.*[169] who collected the pyrolysates by vacuum distillation at 0.5-2 mbars from the ether extract of the resin. As a result, α-campholenaldehyde, cuminaldehyde, carvotanacetone, phellandral, *o*-methylacetophenone, carvone, perillaaldehyde, eucarvone, 1-acetyl-4-isopropenylcyclopentene, piperitone, nopinone, cryptone, verbenone, γ-campholenaldehyde, thujone, myrtenoic acid, *p*-menth-4-en-3-one, 3,6,6-trimethylnorpinan-2-one, myrtenal, 2,4-dimethylacetophenone, pinocamphone, isopinocamphone, 5-hydroxy-*p*-menth-6-en-2-one, 10-hydroxy-4-cadinen-3-one, 1,2,4-trihydroxy-*p*-menthane, α-amyrenone, 11-keto-α-amyrenone were reported as

constituents identified in the pyrolysate of olibanum. The results, nevertheless, of this study are not found to be applicableon the conditions observed in daily rituals.

It is known that the scent of the incense used in churches or temples is formed as a result of mixing different ingredients but mainly olibanum and myrrh. Therefore, it is important to identify primarily the pyrolysate of single components rather than the incense mixture.

In this context the pyrolysates of olibanum species were determined by solid phase adsorption (SPA) technique and investigated by GC and GC-MS. The isolation of novel compounds was achieved by chromatographic means, particularly by CC and TLC. The structures of these compounds were elucidated by mass, 1- and 2-D NMR spectroscopic techniques. The pyrolysate of olibanum was finally determined by a conventional pyrolysis-GC/MS technique to compare the validity of the results obtained with the newly designed SPA set-up.

5.7.1   The SPA Set-up for The Determination of Pyrolysates of *Boswellia* Resins

In this method it was primarily considered to adsorb the pyrolysates of olibanum on a solid phase as it comes in contact with red-hot charcoal and then elute them back with an organic solvent which could be later investigated by analytical means.

Glass cartidges filled with Super Q$^{®}$ (Alltech Chemicals) adsorbent were prepared for the adsorption of the pyrolysates under vacuum. These cartidges were placed across the openings of the censer. Nevertheless, all openings of the censer were not closed to allow the oxygen circulation in the censer. The other end of these adsorption cartidges were connected to the vacuum (**Fig. 5.104**).

First the charcoal was heated up until it became red-hot. Next, it was placed in the censer and then the resin granules were distributed on the charcoal. The smoke formation was observed immediately. The vacuum application led the smoke to be sucked in the cartidges and it was continued until no smoke formation was observed in the censer. The final step of the experiment included disconnecting the glass cartidges from the vacuum and extracting the adsorbent to be investigated by GC and GC-MS.
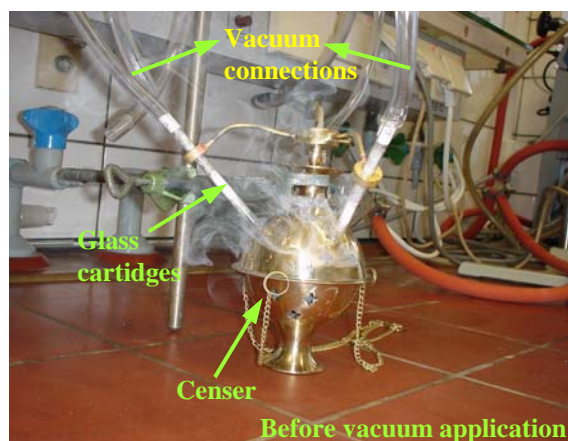
Fig. 5.104. The set-up designed for the determination of the pyrolysate of olibanum.

Incense mixtures are burned in churches in a very similar way; therefore it is believed that the results obtained from these experiments would reflect the most realistic results for the first time about the pyrolysates of olibanum resins.

5.7.2 The Pyrolysate of *Boswellia carterii*

The pyrolysis products of *B. carterii* were determined by the SPA technique. The GC and GC-MS investigations of the pyrolysate revealed six new triterpenoic constituents, 24-norursa-3,12-diene (**8**) (3.3%), 24-noroleana-3,12-diene (**9**) (1.6%), 24-norursa-3,9(11),12-triene (**10**) (1.3%), an unidentified triterpene (**11**) (0.2%), 24-noroleana-3,9(11),12-triene (**12**) (0.3%) and 24-norursa-3,12-dien-11-one (**13**) (2.9%).

Particularly intriguing was the detection of the diagnostic markers of *B. carterii*, its diterpenoic constituents, cembrene A (3.7%), cembrene C (1.5%), verticilla-4(20),7,11-triene (9.3%), incensole (22.8%) and incensyl acetate (15.5%). These compounds were found without any alteration in their structures and in relatively high concentrations. Besides these, 1-octanol (4%) and octyl acetate (10%) were identified which cause an acrid smell during the pyrolysis (**Fig. 5.105**).
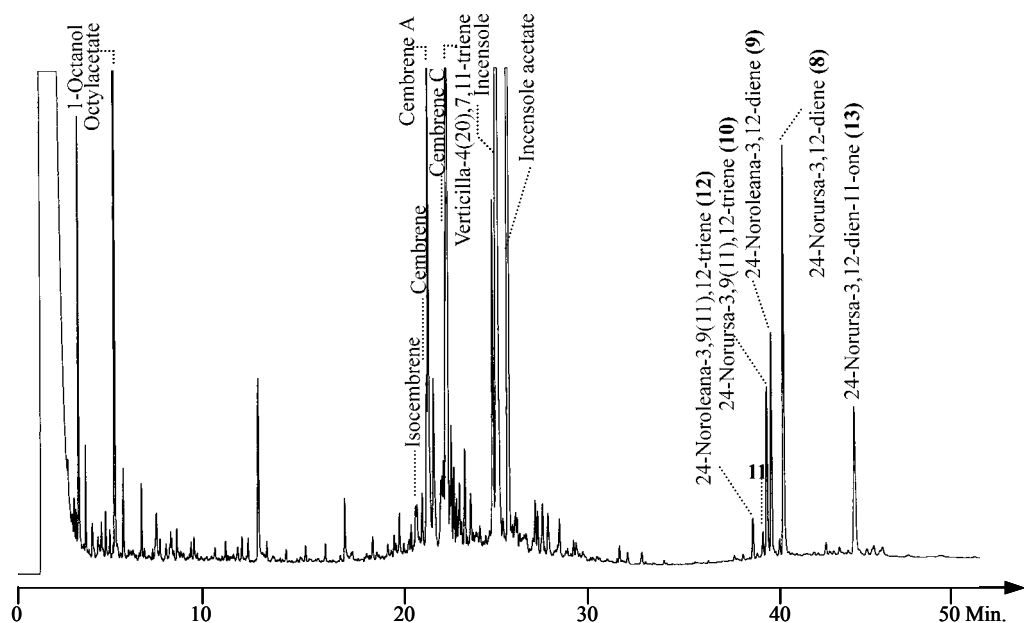
Fig. 5.105. Gas chromatogram of the pyrolysate of *B. carterii*. (25 m fused silica capillary column with CPSil 5 CB, 100 °C, 5 °C/min up to 300 °C, detector at 320 °C, injector at 250 °C, carrier gas 0.5 bars H_2).
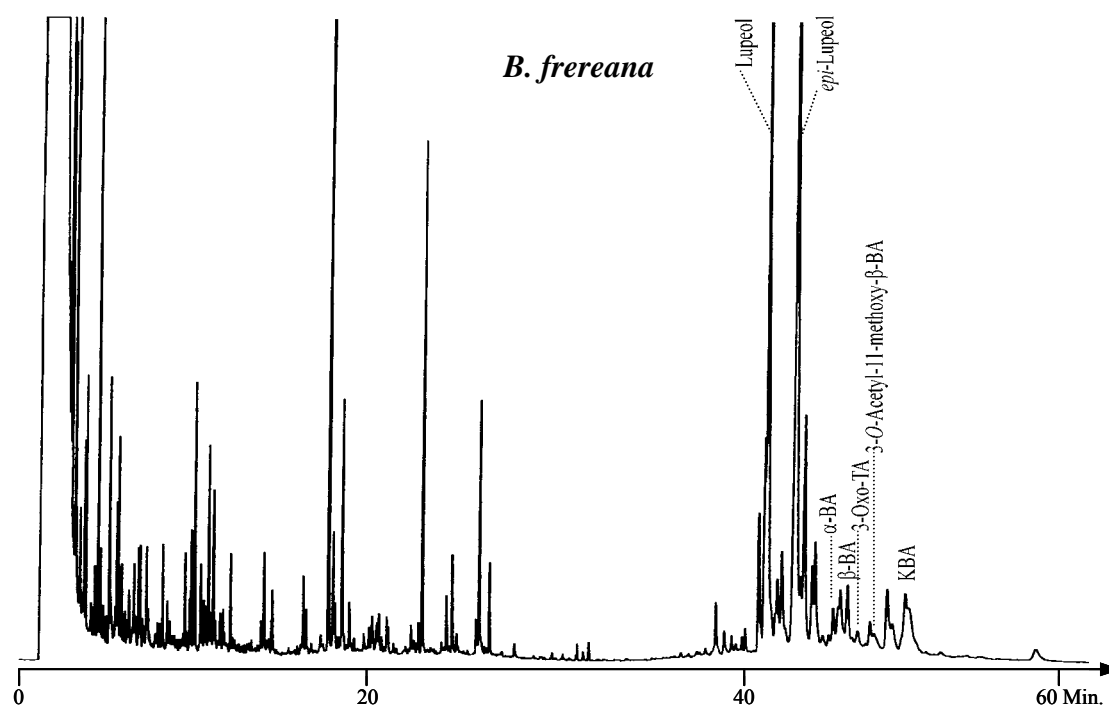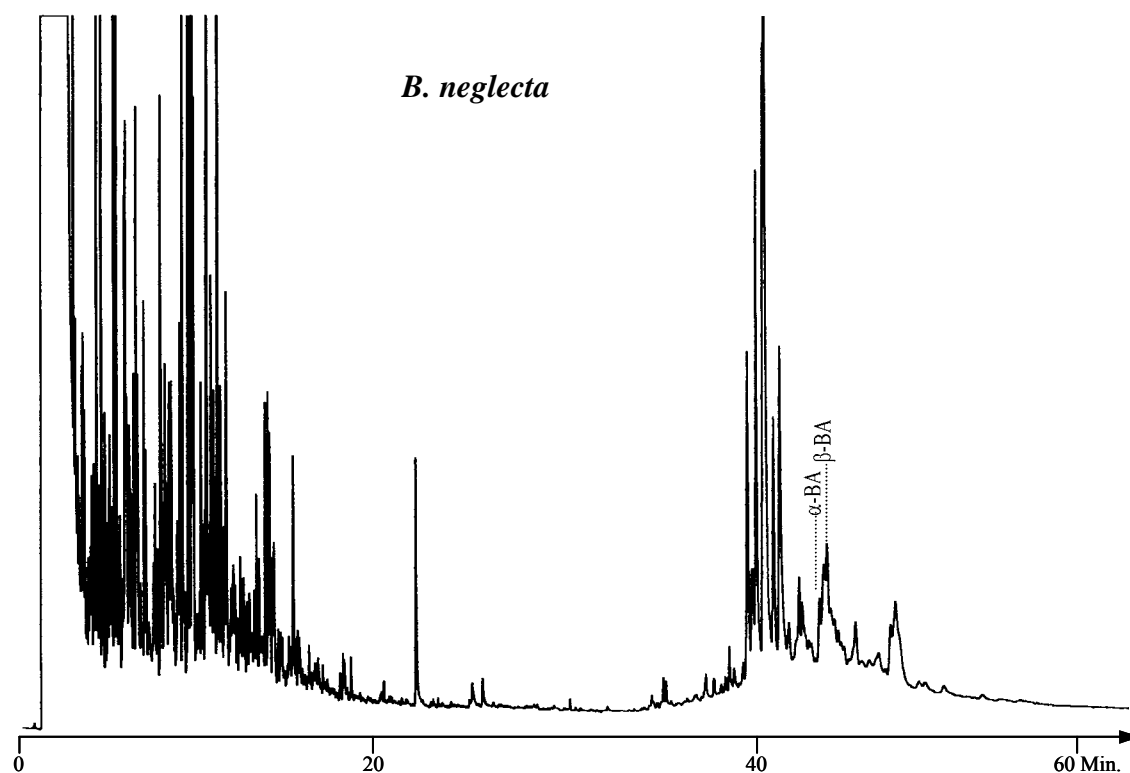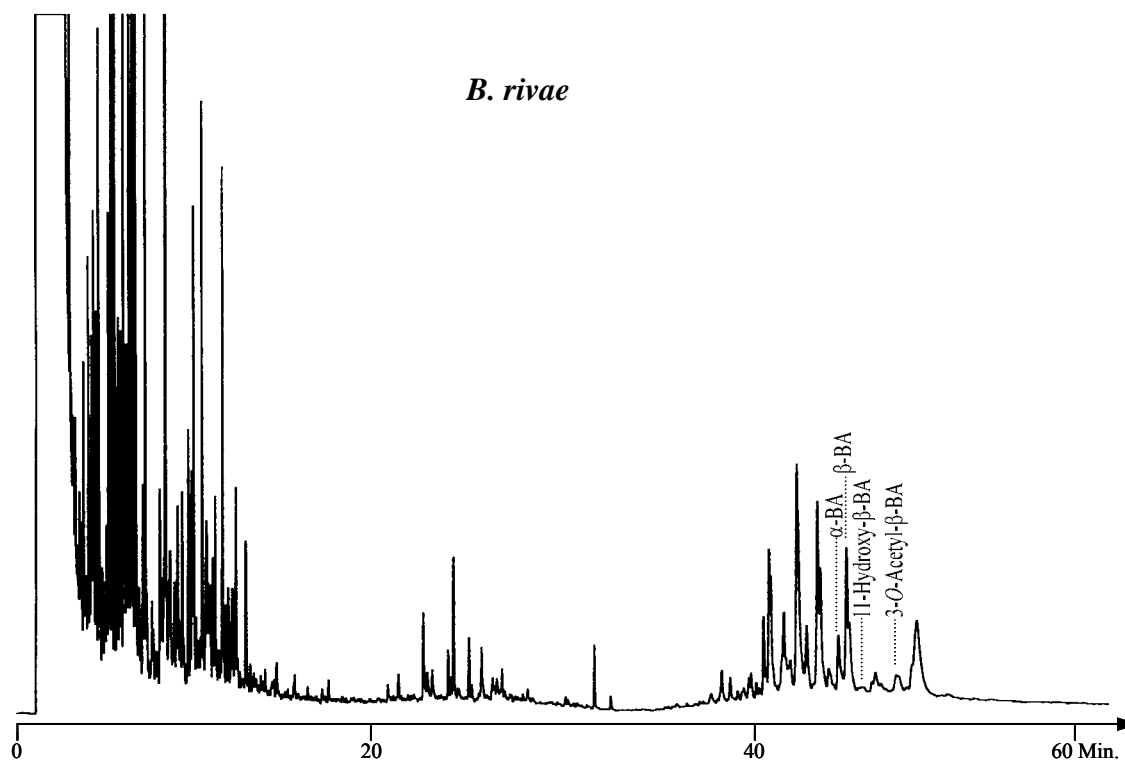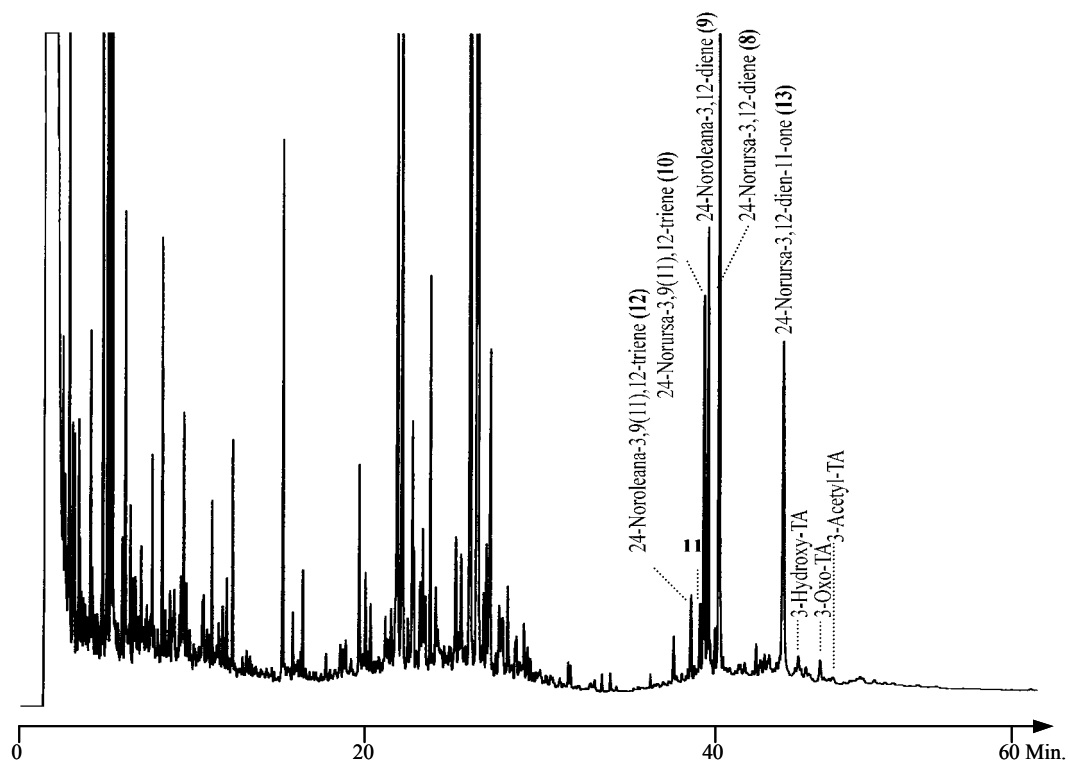

Fig. 5.106. Gas chromatogram of the silylated pyrolysate of *B. carterii*. (25 m fused silica capillary column with CPSil 5 CB, 100 °C, 5 °C/min up to 300 °C, detector at 320 °C, injector at 250 °C, carrier gas 0.5 bars H_2).

154

The pyrolysate of *B. carterii* was silylated to detect the fate of the boswellic and tirucallic acids in these experimental conditions. The GC-MS investigation of the silylated fraction indicated trace amounts of tirucallic acids[‡] but none of the boswellic acid derivatives (**Fig. 5.106**).

The nortriterpenes (**8-10, 12, 13**) were recognized as the decarboxylation and either dehydration or deacetylation products of α- and β-boswellic acids and their derivatives because of the similar fragmentation patterns in their mass spectra (**Fig. 5.107**).

[‡] The tirucallic acid derivatives were observed in trace amounts in GC and GC-MS investigations of the silylated pyrolysate of *B. carterii*. Considering the real amount of these constituents in comparison to boswellic acids in the acid fraction of *B. carterii* and the amount of resin pyrolysed in one experiment (2-3 granules), the observed result can be regarded as consistent.
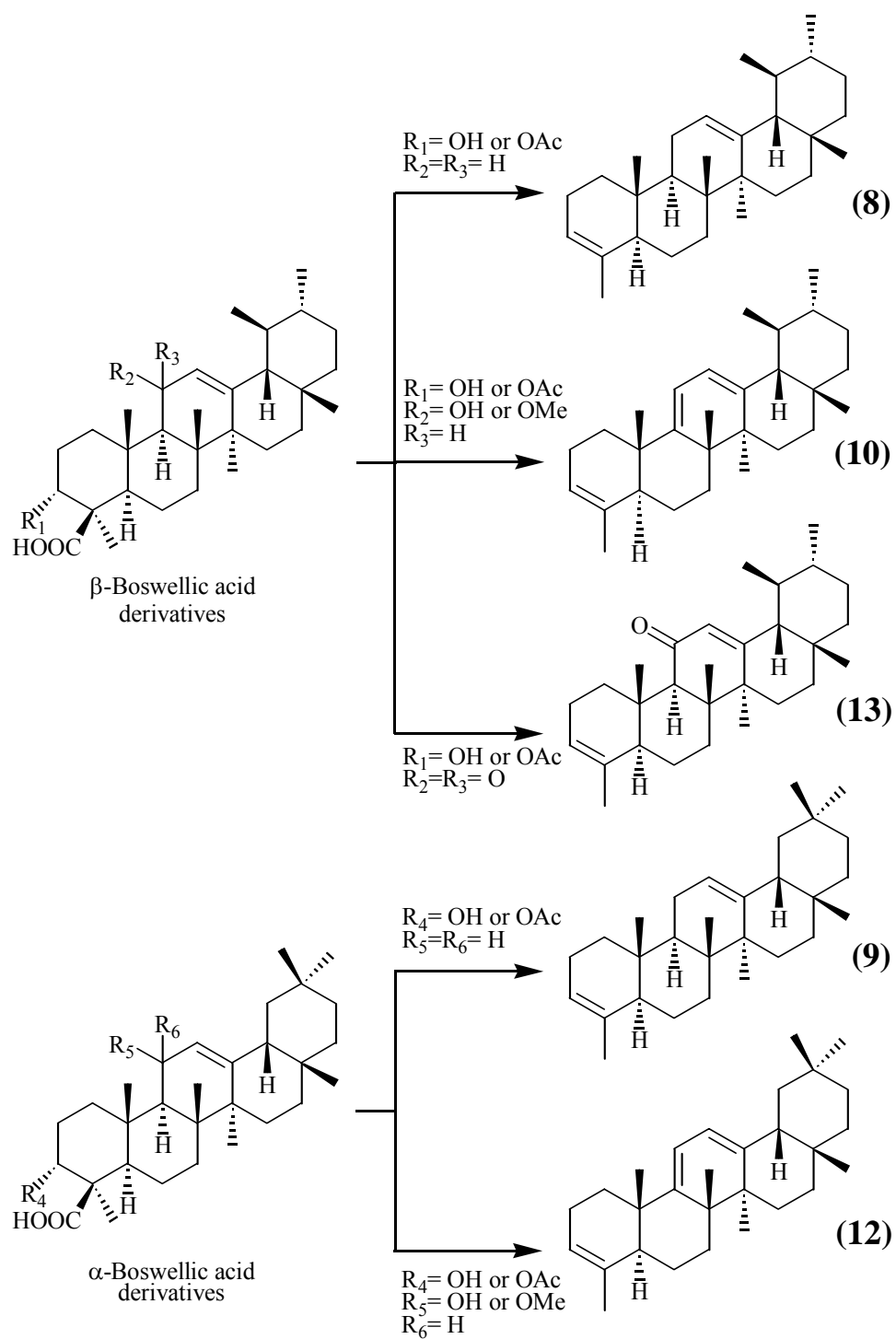
Fig. 5.107. Schematic expression of the nortriterpenes detected in the pyrolysate of *B. carterii* and their possible boswellic acid precursors.

To confirm this relationship between the boswellic acids and the nortriterpenoic constituents[§] of the pyrolysate, the acid fraction of *B. carterii* was pyrolysed. The nortriterpenes were clearly observed also in this pyrolysate (**Fig 5.108**).
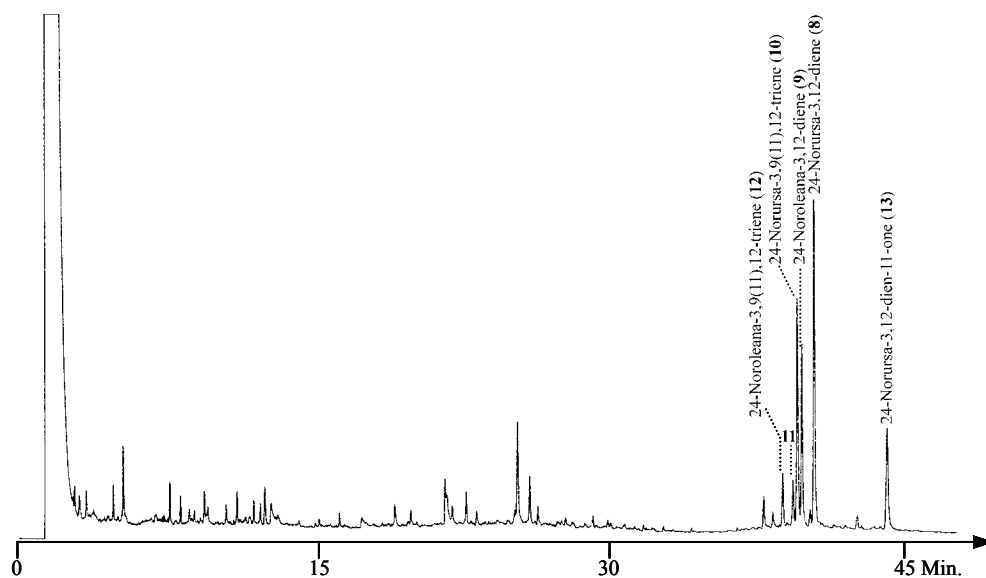
Fig. 5.108. The pyrolysed acid fraction of *B. carterii* (25 m fused silica capillary column with CPSil 5 CB, 100 °C, 5 °C/min up to 300 °C, injector at 250 °C, detector at 320 °C, carrier gas 0.5 bars H_2).

Two of these nortriterpenes were identified previously as constituents detected in the archaeological frankincense[170]. The solvent soluble part of the ancient material was investigated by conventional GC-MS whereas the insoluble residue by pyrolysis-GC/MS. α- and β-boswellic acids and their acetates were identified in the soluble part. 24-Norursa-3,12-diene (**8**) and 24-noroleana-3,12-diene (**9**) predominated the result of *Curie*-point (610 °C) pyrolysis-GC/MS. Their structural identification was confirmed further by synthetic methods.

In this study 24-norursa-3,12-diene (**8**) and 24-norursa-3,12-dien-11-one (**13**) were isolated from the pyrolysate of *B. carterii* and investigated by 1- and 2-D NMR techniques for their structure elucidation. 24-Norursa-3,12-dien-11-one (**13**) was isolated and identified for the first time.

[§] These nortriterpenes were observed in the previous section of this study, during the analysis of acid fractions of olibanum resins named as dehydration products of boswellic acids as well. However, they were detected as a result of partial dehydration products of boswellic acids at the injection port of the gas chromatogram.

5.7.2.1 Isolation and Identification of 24-norursa-3,12-diene (8)

The pyrolysate of *B. carterii* was fractionated by CC on silica gel with a gradient of an *n*-pentane: ethylacetate solvent mixture. The GC investigation of the fraction received with 100% *n*-pentane elution contained cembrene A, verticilla-4(20),7,11-triene (**1**), **8**, and additionally four triterpenoic compounds (**9-12**) as major constituents (**Fig. 5.109**).

Subsequently, this fraction was applied preparatively to TLC plates and developed at −25°C with *n*-pentane. A high efficiency was observed in the separation of the components at this temperature (**Fig. 5.110**).
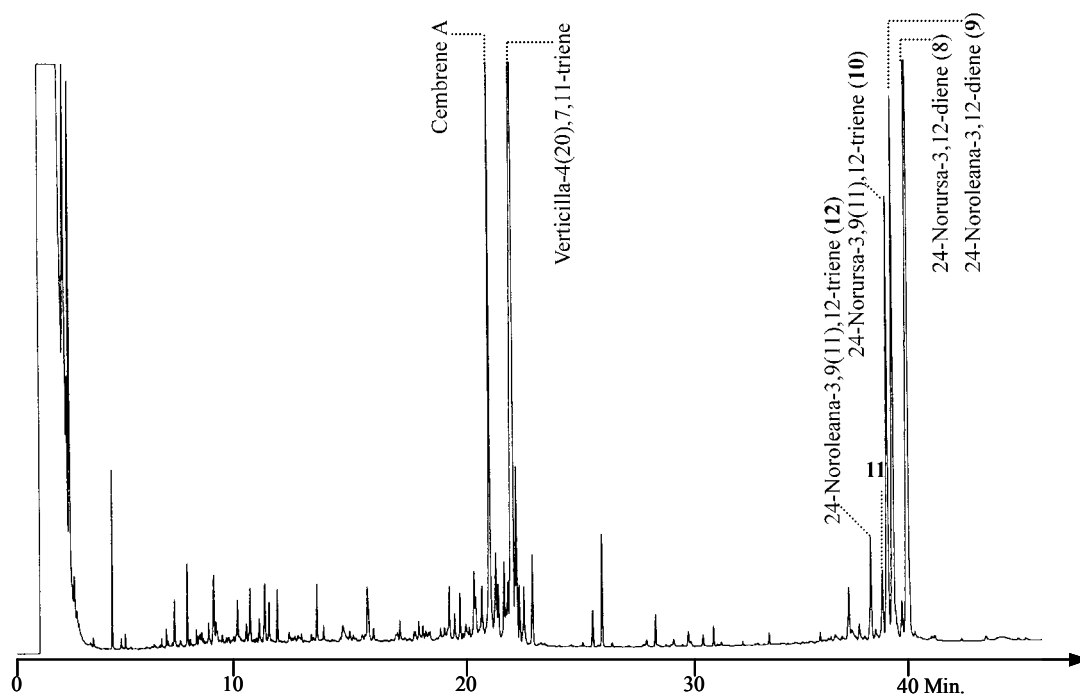
Fig. 5.109. Gas chromatogram of the 100% *n*-pentane fraction of the pyrolysate of *B. carterii*. (25 m fused silica capillary column with CPSil 5 CB, 100 °C, 5 °C/min up to 300 °C, injector at 250 °C, detector at 320 °C, carrier gas 0.5 bars H$_2$).

158

TLC of the isolated
n-pentane fraction at -25 °C.

TLC of the pyrolysate
of *B. carterii* at room
temperature.

100%
Pentane
fraction

24-Norursa-3,12-diene (**8**)
24-Noroleana-3,12-diene (**9**)
24-Norursa-3,9(11),12-triene (**10**)
Compound (**11**)
24-Noroleana-3,9(11),12-triene (**12**)

Verticilla-4(20),7,11-triene

Cembrene A
Cembrene C
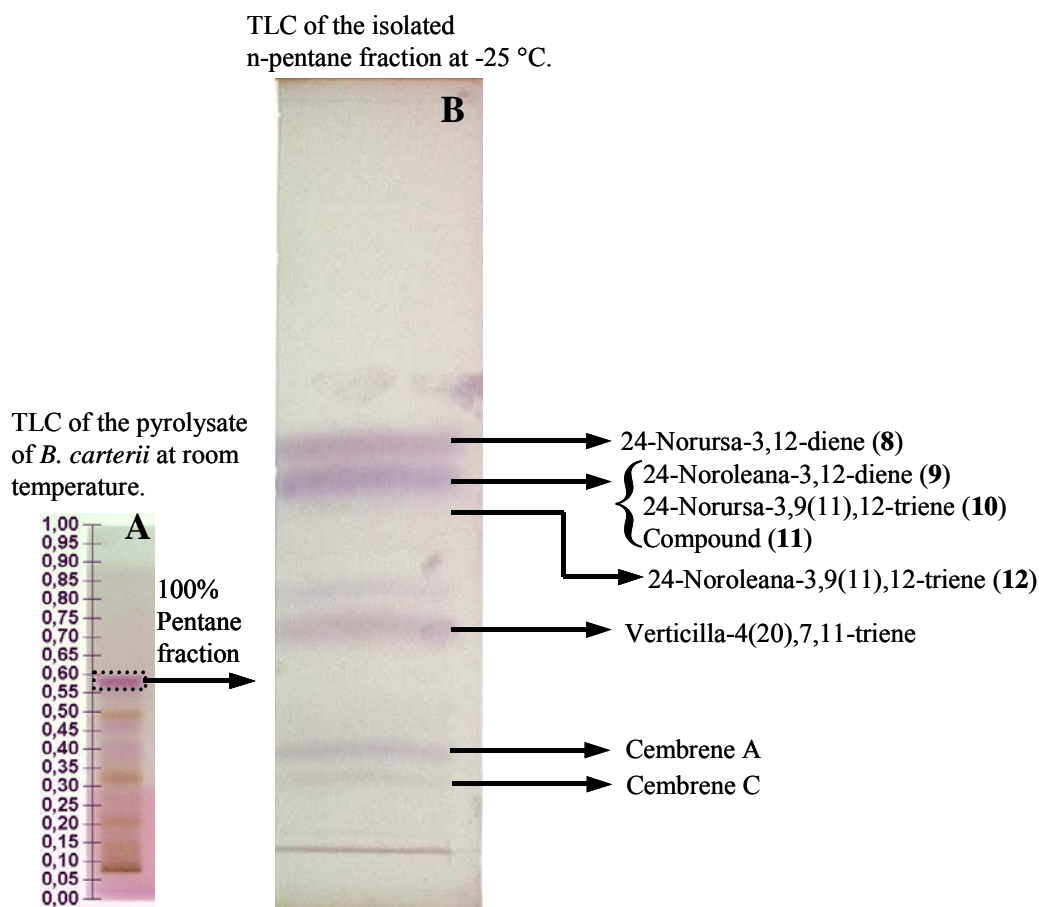
Fig. 5.110. TLCs the *B. carterii* pyrolysate developed at room temperature (**A**) and its 100% pentane fraction developed at –25 °C (**B**). **A**: Silica gel 60_{F254} plates (Merck), mobile phase: cyclohexane: diethylether (8:2), development distance: 7 cm., detection with anisaldehyde spray solution, subsequent heating at 105 °C. **B**: Silica gel 60_{F254} plates (Merck), mobile phase: *n*-pentane, development distance: 18 cm, detection with anisaldehyde spray solution, subsequent heating at 105 °C.

The GC-MS investigations revealed a molecular ion signal at m/z = 394 for 24-norursa-3,12-diene (**8**) which corresponded to an elemental composition of $C_{29}H_{46}$ (**Fig. 5.111**).

The mass spectrum of **8** showed the typical fragmentation pattern for ursane type of triterpenes having a double bond at position 12. The RDA reaction that was triggered by this double bond revealed a fragment ion signal m/z= 218 and a further methyl cleavage from this fragment formed the signal m/z= 203 (**Fig. 5.112**).
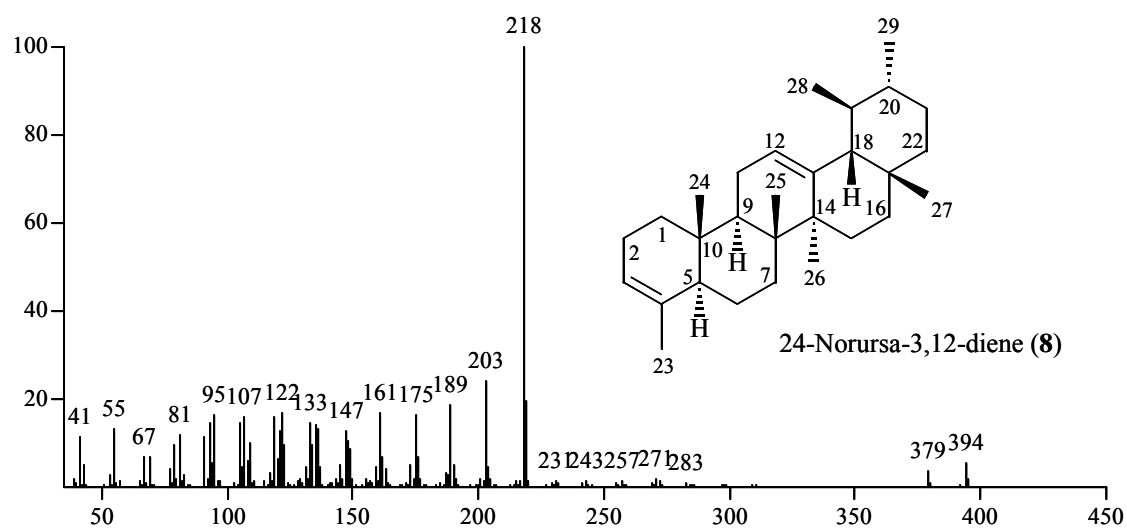
Fig. 5.111. Mass spectrum of 24-norursa-3,12-diene (**8**).
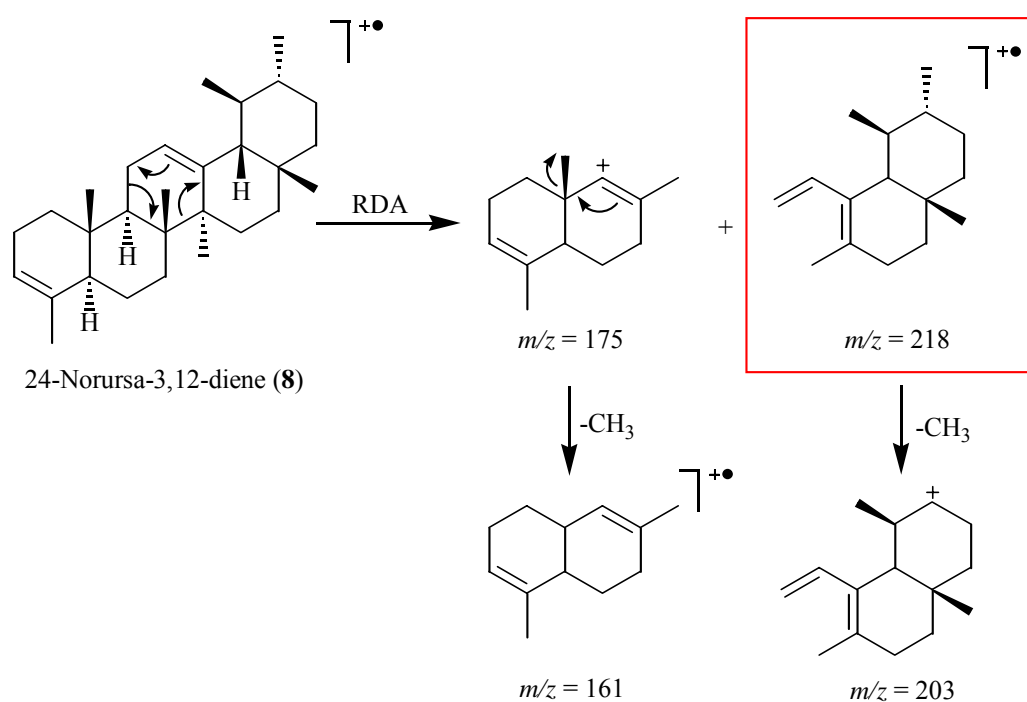
Fig. 5.112. Possible fragmentation of **8**.

The ^{1}H-NMR spectrum of **8** showed five singlets at δ 0.92, 0.96, 1.15, 1.16, 1.68 and two doublets at δ 0.97 (d, *J* = 6.6 Hz, 3H), 0.98 (d, *J* = 6.6 Hz, 3H) for seven methyl group

signals. Additionally two olefinic protons were observed at δ 5.26 (bs, 1H) and 5.34 (dd, $J =$ 6.8, 2.8 Hz, 1H) (**Fig. 5.113**).
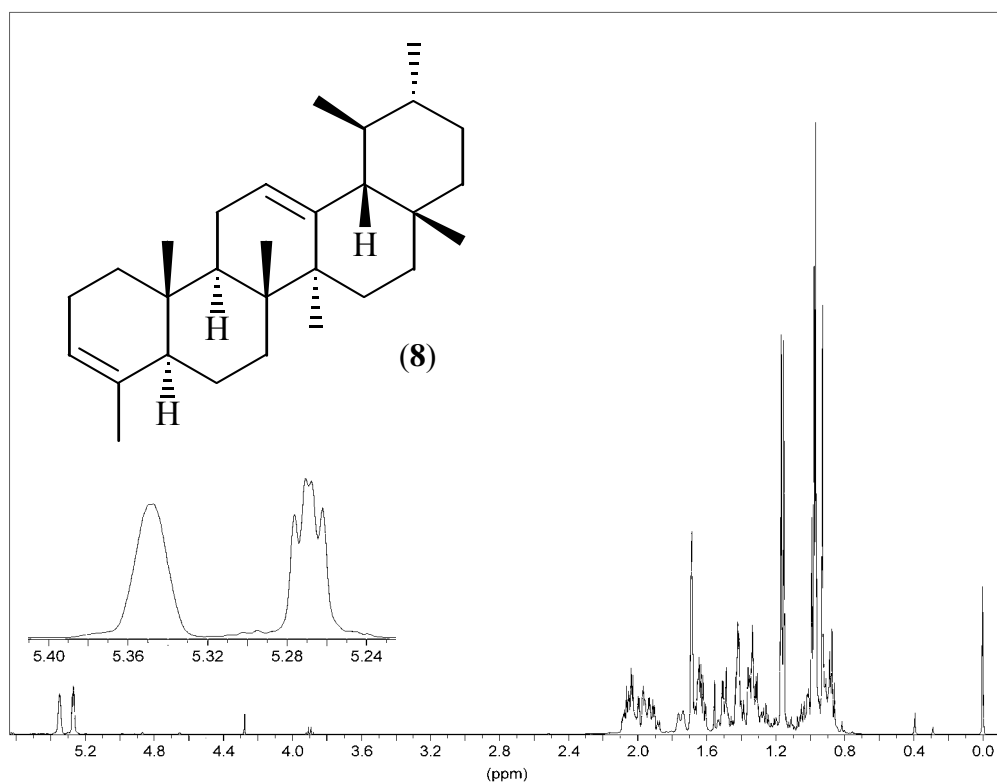
Fig. 5.113. ^{1}H-NMR spectrum of **8**.

Seven primary carbons at δ 13.22, 17.92, 18.18, 21.89, 22.08, 23.85, 29.38, nine secondary carbons at δ 20.99, 23.49, 24.58, 27.20, 28.79, 31.91, 33.10, 36.85, 42.19, seven tertiary carbons at δ 40.22, 40.33, 44.97, 49.32, 59.89, 121.00, 125.72, six quaternary carbons at δ 34.39, 35.81, 40.75, 42.96, 135.34, 140.54 were assigned for **8** from its ^{13}C-PENDANT spectrum. Four carbon signals which were recognized at low field at δ 121.00, 125.72, 135.34, 140.54 indicated two double bonds in the molecule (**Fig. 5.114**).

The correlations of the olefinic protons at δ 5.26, 5.34 to the carbons at δ 125.72, 121.00, respectively, were detected from HMQC spectrum of **8**. Additionally, the methyl protons at δ 0.92, 0.96, 0.97, 0.98, 1.15, 1.16, 1.68 were found to correlate to the carbon signals at δ 13.22, 29.38, 17.92, 21.89, 18.18, 23.85, 22.08, respectively (**Table 5.11**, **Fig. 5.115**).
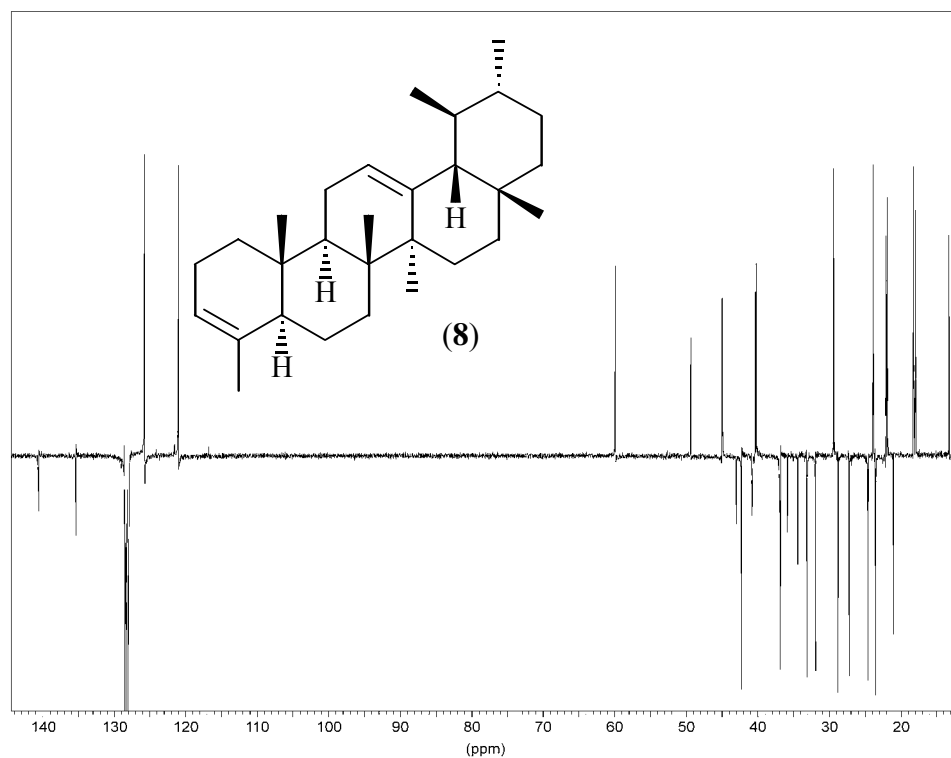
Fig. 5.114. ^{13}C-PENDANT spectrum of **8**.

Table 5.11. HMQC correlations of **8**.
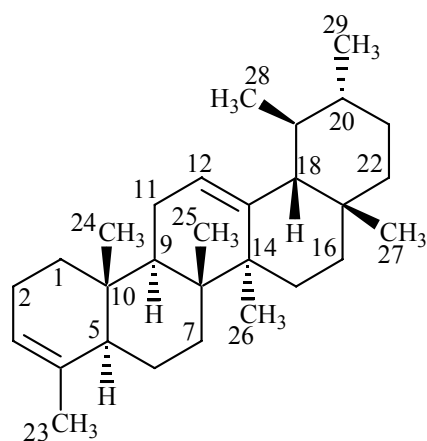
Fig. 5.115. Numbered structure of **8**.

No.	^{13}C (ppm)	^{1}H (ppm)	No.	^{13}C (ppm)	^{1}H (ppm)
1	36.85	(1.00-1.02), (1.60-1.66)	16	28.79	(0.87-0.89), (2.02-2.06)
2	23.49	(1.95-1.97), 2H	17	34.39	
3	121.00	5.34	18	59.89	(1.40-1.44)
4	135.34		19	40.33	(1.40-1.44)
5	49.32	(1.73-1.76)	20	40.22	(0.87-0.89)
6	20.99	(1.27-1.38), 2H	21	31.91	(1.30-1.37), (1.40-1.44)
7	33.10	(1.30-1.37), (1.48-1.52)	22	42.19	(1.30-1.37), (1.48-1.52)
8	40.75		23	22.08	1.68
9	44.97	(1.60-1.66)	24	13.22	0.92
10	35.81		25	23.85	1.16
11	24.58	(2.02-2.04), (1.95-1.97)	26	18.18	1.15
12	125.72	5.26	27	29.38	0.96
13	140.54		28	21.89	0.98
14	42.96		29	17.92	0.97
15	27.20	(0.96-1.00), (1.87-1.90)			

Six main fragments were established from the couplings in the HMBC and ^{1}H-^{1}H COSY spectra of **8** (**Fig. 5.116**). The first fragment was recognized by the coupling of the olefinic proton H-3 (δ 5.34) to the olefinic quaternary carbon C-4 (δ 135.34) so that the first double bond was identified in the molecule. The methyl group CH$_3$-23 (δ 1.68, 22.08) was found to couple first with C-4 and further with a tertiary carbon C-5 (δ 49.32).
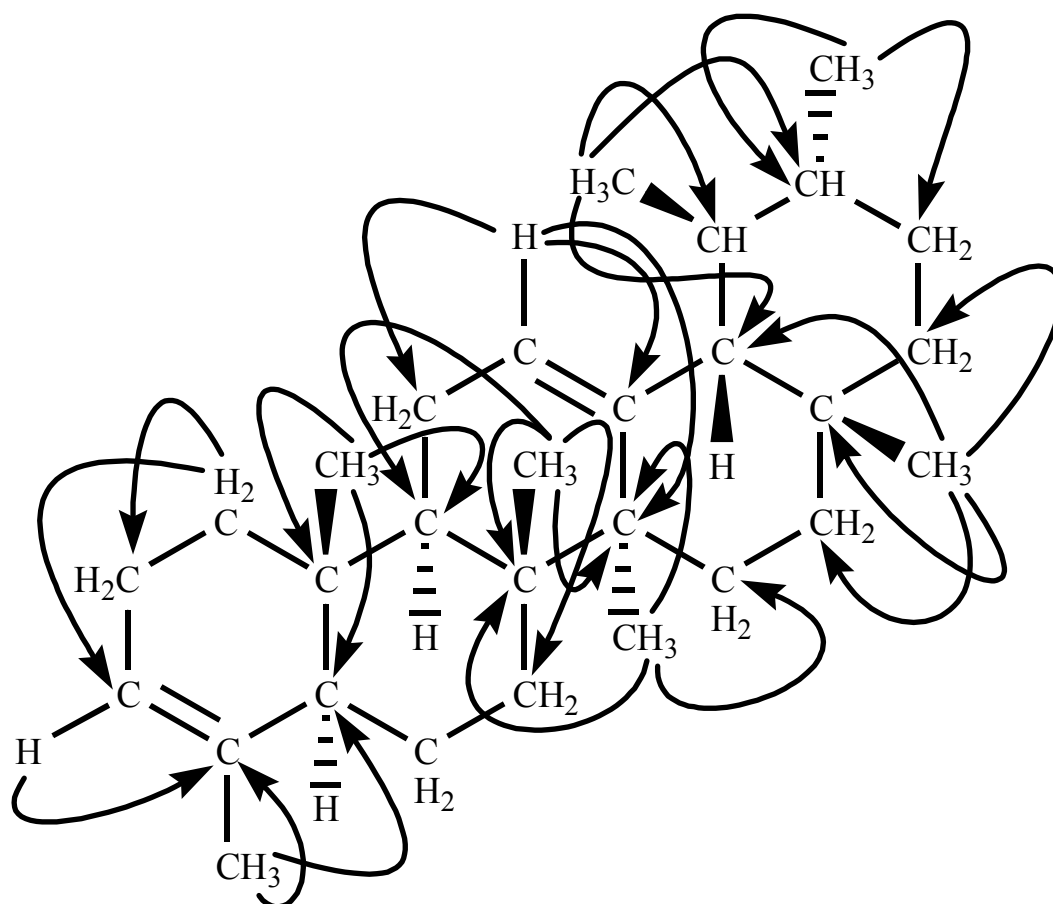
Fig. 5.116. HMBC correlations of **8**.

A second fragment was deduced from the couplings of two methyl singlets CH$_3$-25 (δ 1.16, 23.85) and CH$_3$-26 (δ 1.15, 18.18) with two quaternary carbons C-8 (δ 40.75) and C-14 (δ 42.96), respectively. A connection was detected between C-8 and C-14 as a result of the couplings of CH$_3$-25 with C-14 and CH$_3$-26 with C-8. CH$_3$-25 was further coupled with two carbons one of which was secondary C-7 (δ 33.10) and the other was a tertiary carbon C-9 (δ 44.97). On the other hand CH$_3$-26 was found to couple with a secondary carbon C-15 (δ 27.20).

The third fragment was observed as a junction between the previously interpretated fragments. The couplings between the methyl group CH_3-24 (δ 0.92, 13.22) with C-9 (δ 44.97) and C-5 (δ 49.32) as well as with the quaternary carbon C-10 (δ 35.81) provided this connection.

The second double bond was deduced from the couplings of the olefinic proton H-12 (δ 5.26) with the olefinic quaternary carbon C-13 (δ 140.54). This proton was further coupled with C-14 (δ 42.96) and a secondary carbon C-11 (δ 24.58). The neighbouring of C-11 protons (δ 2.03-2.02, 1.97-1.95, 2H) with H-9 (δ 1.60-1.66, 1H) which was deduced from ^{1}H-^{1}H COSY spectrum of **8**, established a further connection between the fragments.

A further fragment was interpreted including the methyl groups CH_3-28 (δ 0.98, 21.89) and CH_3-29 (δ 0.97, 17.92) which were resonating as doublets. Both of these methyl groups coupled with tertiary carbons C-19 (δ 40.33) and C-20 (δ 40.22), respectively. CH_3-28 was further coupled with C-13 (δ 140.54), C-20 and C-18 (δ 59.89). On the other hand the couplings of CH_3-29 with C-21 (δ 31.91) and C-19 were also deduced. The coupling of the neighbouring protons H-20 (δ 0.89-0.87, 1H) and H-21 (δ 1.44-1.40, 1.37-1.30, 2H) observed in the ^{1}H-^{1}H COSY spectrum, had confirmed this connectivity.

The last fragment was deduced from the couplings of CH_3-27 (δ 0.96, 29.38) with the quaternary carbon C-17 (δ 34.39), tertiary carbon C-18 (δ 59.89), and two secondary carbons C-22 (δ 42.19) and C-16 (δ 28.79). No correlations were detected between the protons of C-22 (δ 1.37-1.30, 1.48-1.52, 2H) and C-16 (δ 0.89-0.87, 2.06-2.02, 2H) in the ^{1}H-^{1}H COSY spectrum. Therefore it was concluded that these secondary carbons were not the part of the same methylene chain.

The NOESY spectrum of **8** indicated couplings of H-5 (δ 1.73-1.76) with CH_3-26 (δ 1.15, 18.18), H-9 (δ 1.60-1.66), H-1α (δ 1.00-1.02), H-7α (δ 1.48-1.52). No crosspeaks were observed for the connectivity of H-5 and CH_3-24 (δ 0.92, 13.22). However, CH_3-24 was found to couple with H-1β (δ 1.60-1.66) and CH_3-25 (δ 1.16, 23.85) which further coupled to H-18 (δ 1.40-1.44) indicating that their connectivity through-space was above the plane of the ring system.

CH_3-25 was further related to H-11β (δ 1.95-1.97) whereas H-11α (δ 2.02-2.04) was coupling with CH_3-26. The only methyl groups that were absorbing below the plane of the ring system CH_3-26 and CH_3- 29 (δ 0.97, 17.92) also showed a crosspeak in the spectrum. CH_3-26 was further correlated to H-16α (δ 2.02-2.06) whereas H-16β (δ 0.87-0.89) was correlated to H-18. Finally the coupling observed between H-18 and CH_3-27 (δ 0.96, 29.38) indicated the *cis* configuration between ring D and E (**Fig. 5.117**).

Fig. 5.117. NOESY correlations of **8**.

5.7.2.2 The Identification of 24-Noroleana-3,12-diene (*9*), 24-Norursa-3,9(11),12-triene (*10*), 24-Noroleana-3,9(11),12-triene (*12*) and Compound (*11*)

The band at R_f: 0.48 was separated from the preparative TLC plates developed at –25 °C during the isolation of compound **8** (**Fig. 5.95**). The GC and GC-MS investigations of this fraction indicated two of the nortriterpenes 24-noroleana-3,12-diene (**9**) and 24-norursa-3,9(11),12-triene (**10**) as well as another triterpenoic compound **11** (**Fig. 5.118**). It was recognized that **11** was not an analogue of the nortriterpenes **8**-**10** when its mass spectrum was considered. Additionally 24-noroleana-3,9(11),12-triene (**12**) was found as a diffused band at R_f: 0.48-0.44 on the same TLC plates.

Fig. 5.118. Gas chromatogram of the band at R_f: 0.48 isolated by preparative TLC at −25 °C (25m fused silica capillary column with CPSil 5CB, 100°C, 5°C/min. up to 300 °C, injector at 250 °C, detector at 320 °C, carrier gas 0.5 bars H_2).

The isolation of the triterpenes **9-12** as pure substances was not achieved in preparative scale by conventional methods such as preparative TLC, preparative GC, CC either on silicagel or AgNO$_3$ impregnated silica gel. Nevertheless, analytical separations by two different methods were observed between the compounds **9**, **10**, **11**. Compound **12** was detected in GC-MS but could not be purified for NMR spectroscopic analysis.

The first separation was achieved on a modified cyclodextrin (CD) column (2,6-methyl-3-pentyl-γ-CD) with an isothermal injection at 200 °C. Unfortunately, the same parameters were not achievable with the preparative column of the same CD phase (**Fig. 5.119**).
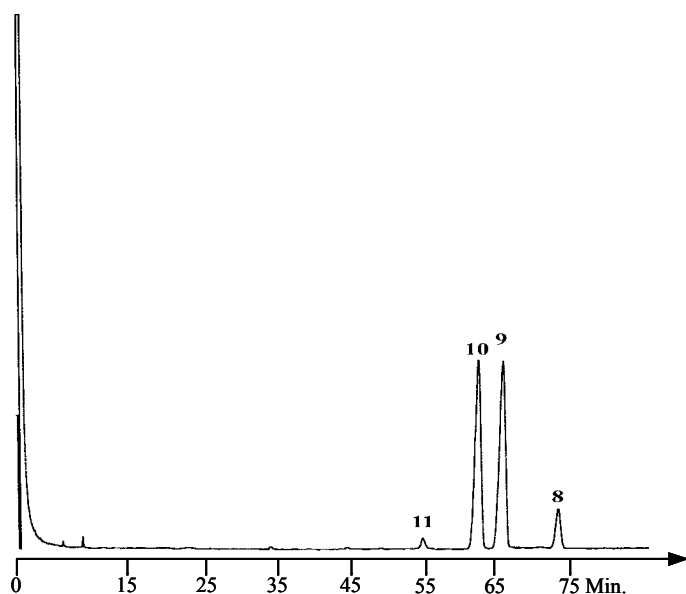
Fig. 5.119. Separation of the triterpenes **9-11** on 2,6-methyl-3-pentyl-γ-CD column. (15m fused silica capillary column with 2,6-methyl-3-pentyl-γ-CD (1:1 OV1701), 200 °C isothermal, detector at 300 °C, injector at 250 °C, carrier gas 0.5 bars H$_2$).

Another separation in analytical scale was achieved by HPLC with AgNO$_3$ loaded cation-exchange column. Argentation chromatography has been applied to HPLC to separate the fatty acid methyl esters, prostaglandins, arachidonic acid and its biological products. One big advantage of this method was its capability of separating the compounds according to their degree of unsaturation and geometry of the double bonds[171, 172].

The triterpenes **9** and **10** showed a separation on the silver modified cation exchange column with 100% *n*-hexane. The UV spectra of these two peaks showed that **10** had an maximum absorption at a longer wavelength than **9**. This bathochromic shift in its absorption maximum was considered to be a result of the conjugated double bond system in the C ring of the molecule (**Fig. 5.120**).

167
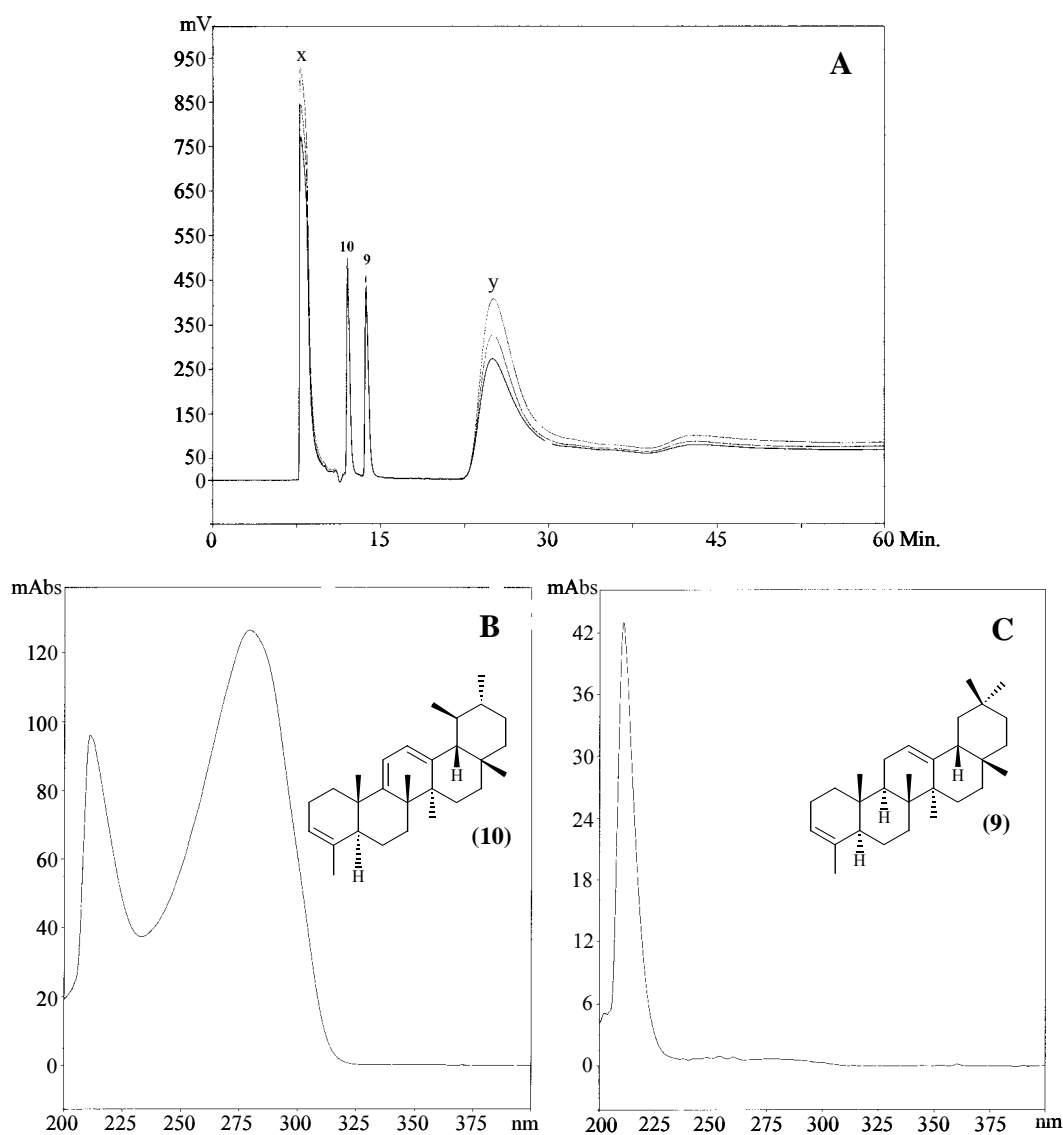
Fig. 5.120. Above: separation observed on the AgNO3 loaded cation-exchange HPLC column. Below: UV spectra of **9** and **10**.

The identification of the compounds **9**, **10**, **12** was achieved by the interpretation of their MS. **9** showed a similar fragmentation as **8** in its MS with a molecular ion peak at $m/z = 394$ which corresponded to an elemental composition of $C_{29}H_{46}$. A base peak at $m/z = 218$ and a typical ion signal at $m/z = 203$ indicated that **9** had also undergone a RDA reaction like **8**.

It was already discussed that oleanane type triterpenes having a double bond at position 12 form more stable ions during the cleavage of a methyl group from the RDA fragment $m/z = 218$ in comparison to their ursane analogues. The relative abundance of this signal $m/z = 203$ was found to be at least 50% more for oleananes than ursanes.

168

In the case of **9** the fragment ion signal $m/z = 203$ was detected around 60% whereas this value was detected almost 30% abundancy in **8** (**Fig. 5.121, Fig. 5. 122**). Therefore it was concluded that **9** was formed as a result of the dehydration, deacetylation and decarboxylation of α-BA and 3-*O*-acetyl-α-BA during the pyrolysis experiments.
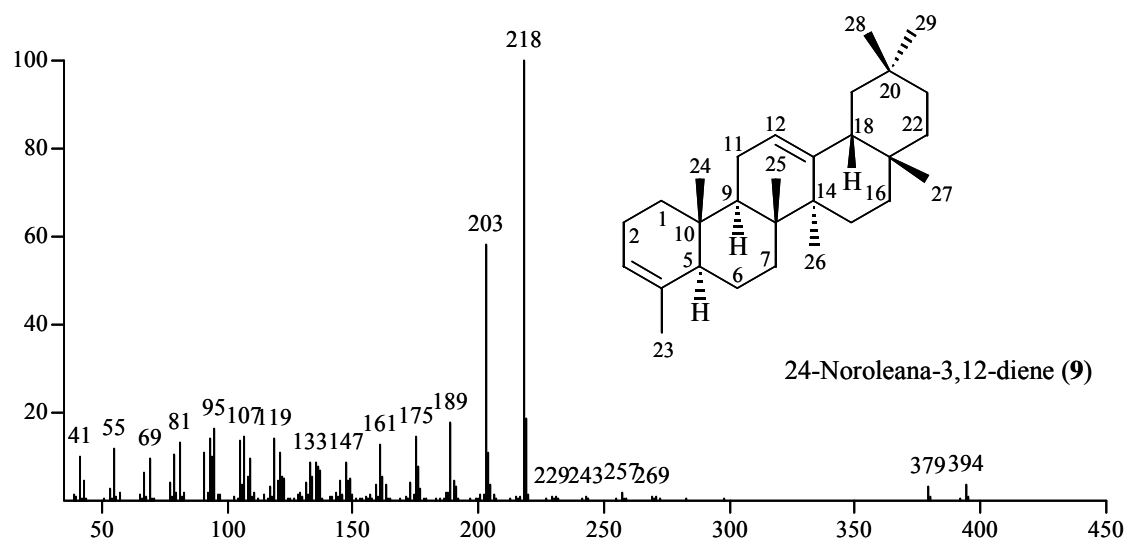
Fig. 5.121. Mass spectrum of 24-noroleana-3,12-diene (**9**).
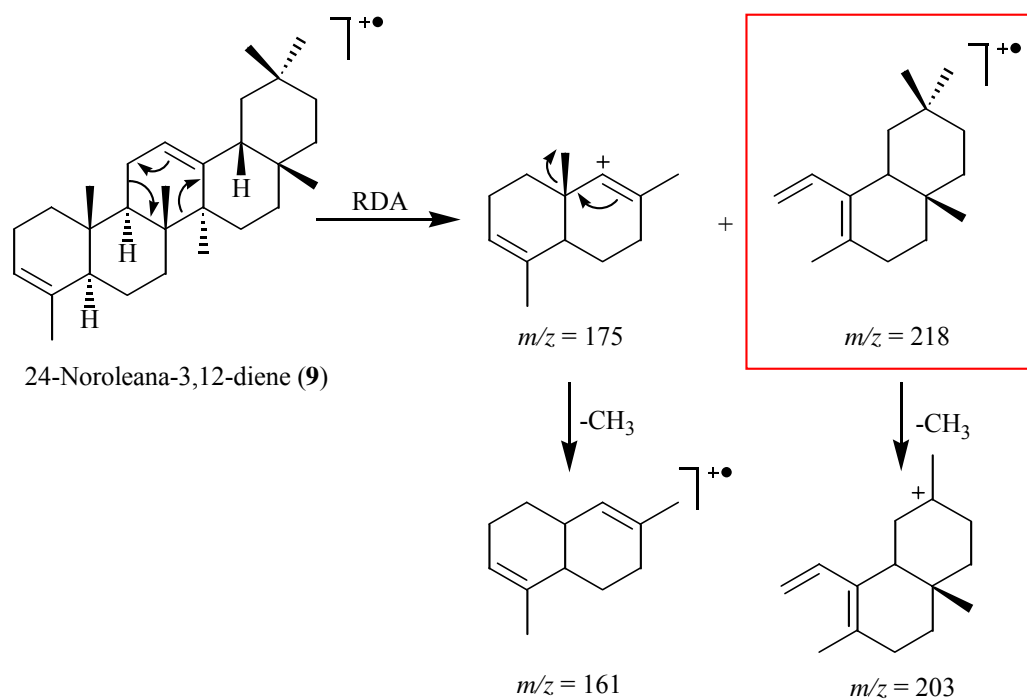
Fig. 5.122. Possible fragmentation pattern of **9**.

On the other hand 24-norursa-3,9(11),12-triene (**10**) and 24-noroleana-3,9(11),12-triene (**12**) showed a similar relationship in their MS. Both compounds showed a typical fragment ion signal at $m/z = 255$ and a molecular ion signal at $m/z = 392$ corresponding to an elemental composition of $C_{29}H_{44}$ (**Fig. 5.123**).
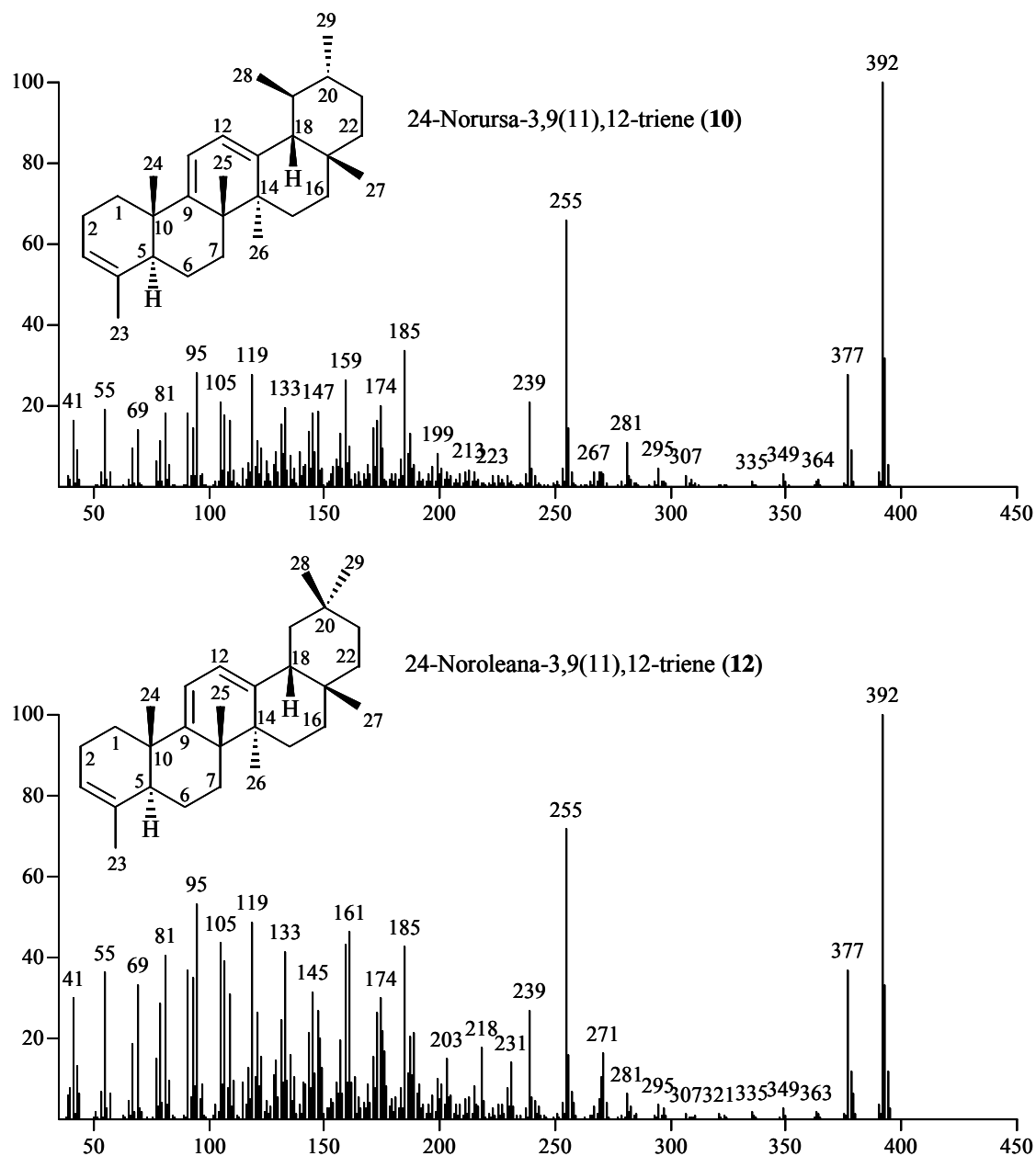
Fig. 5.123. Mass spectra of **10** and **12**.

The compounds **10** and **12** were primarily assigned according to the order of elution on GC investigations. The fragment ion signal $m/z = 255$ in their mass spectra indicating that they could have similar fragmentation patterns as the 9, 11-dehydro-β-BA and their derivatives.

Compound **11** has already mentioned as not being an anologue of the nortriterpenes **8-13**. However, its mass spectrum showed a molecular ion signal at $m/z = 394$ that corresponded to an elemental composition of $C_{29}H_{46}$ which confirmed a triterpenoic character (**Fig. 5.124**).
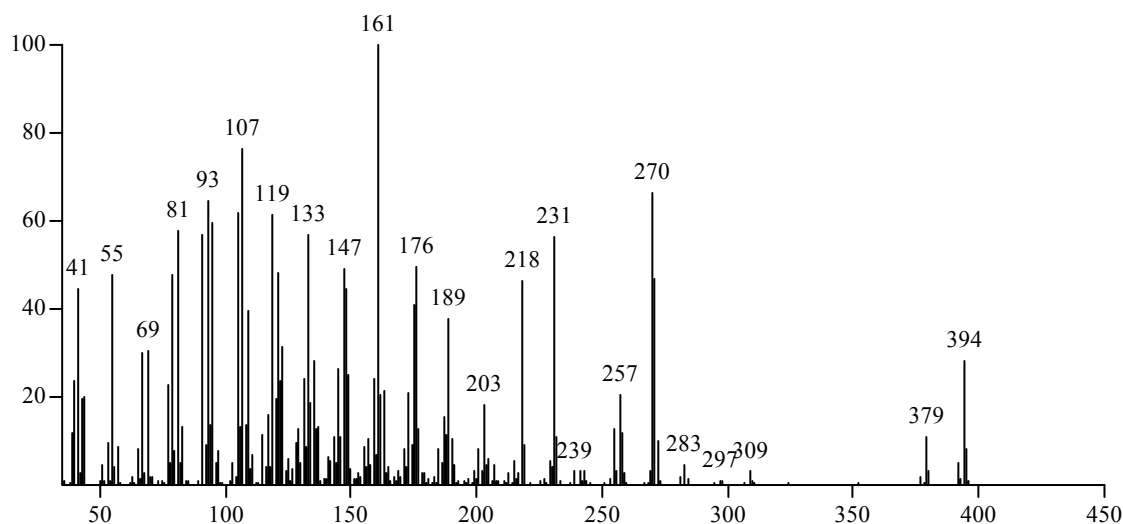
Fig. 5.124. Mass spectrum of compound **11**.

5.7.2.3 Isolation and Identification of 24-Norursa-3,12-dien-11-one (*13*)

24-Norursa-3,12-dien-11-one (**13**) was isolated from the pyrolysate of *B. carterii* by preparative TLC. Two consecutive preparative TLC separations in which the plates were developed first with toluene: ethylacetate (9.5:0.5) and then with pentane:ethylacetate (9:1) resulted in the 80% pure **13**.

The mass spectrum of **13** showed a molecular ion signal at $m/z = 408$ corresponding to an elemental composition of $C_{29}H_{44}O$ (**Fig. 5.125**).
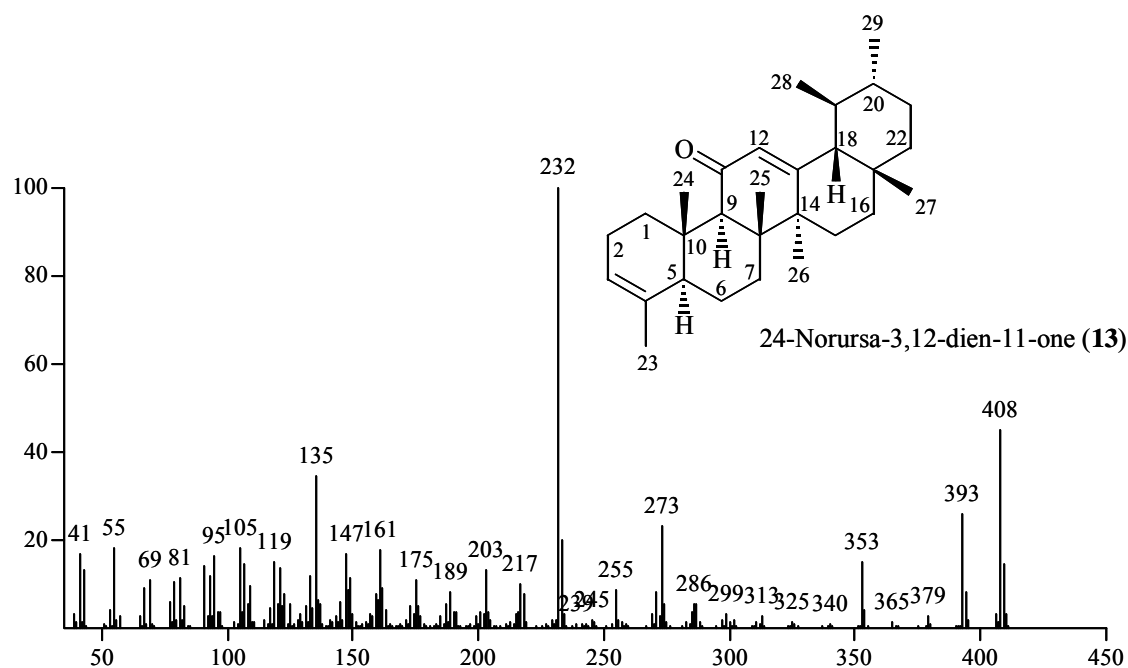
Fig. 5.125. Mass spectrum of 24-norursa-3,12-dien-11-one (**13**).

According to the fragmentation pattern in the mass spectrum of **13** it was recognized that two different types of processes, RDA reaction and McLafferty rearrangement took place in the molecule. In contrast to the mass spectra of its precursors, AKBA and KBA, in the spectrum of **13** it was observed that RDA reaction products were preferred over McLafferty rearrangement products (**Fig. 5.126**).
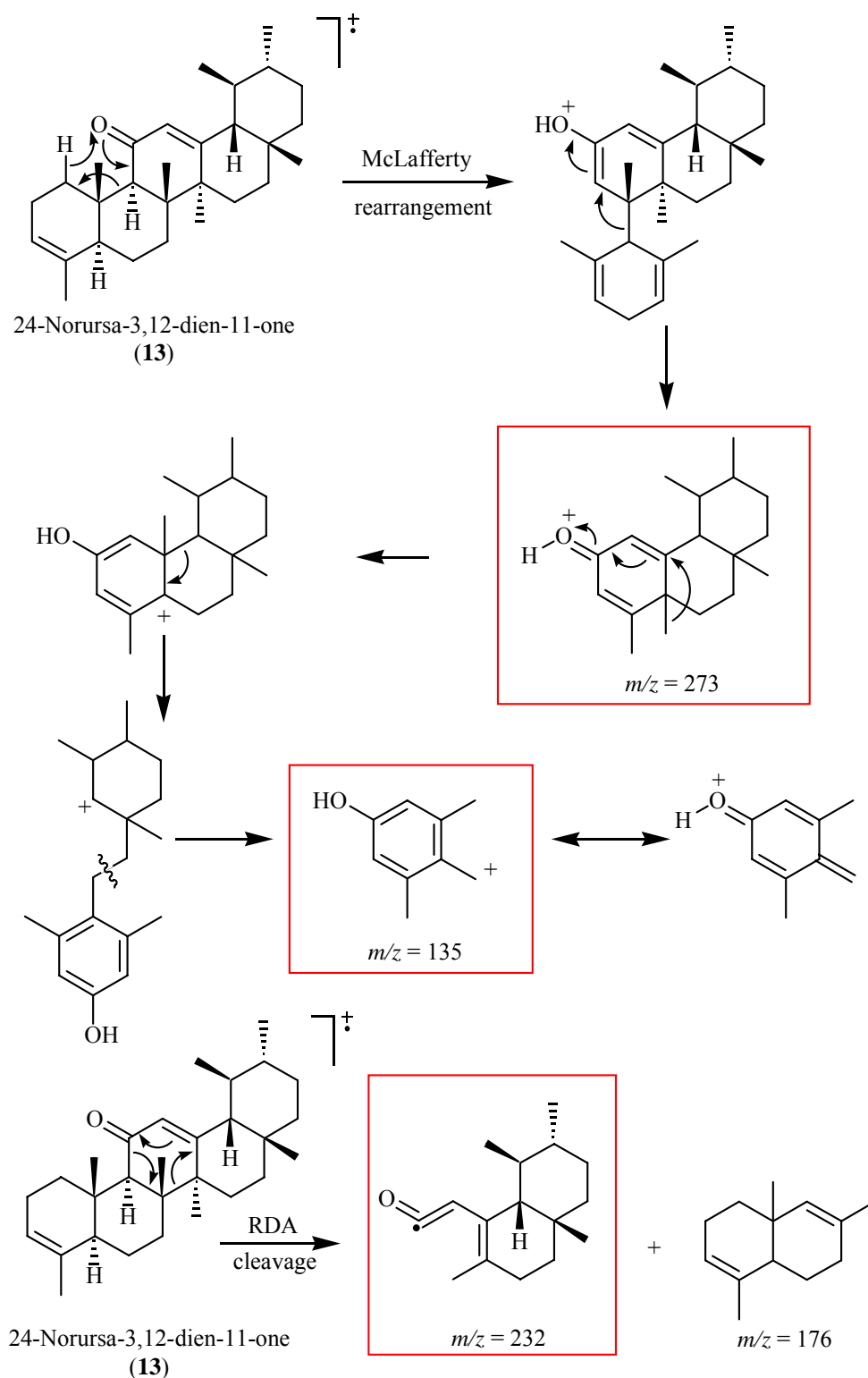
Fig. 5.126. Possible fragmentation of **13**.

The ^{1}H- NMR spectrum of **13** indicated two doublets at δ 0.73 (d, *J* = 6.3 Hz, 3H), 0.86 (d, *J* = 6.6 Hz, 3H) and five singlets at δ 0.75, 1.13, 1.18, 1.40, 1.66 for seven methyl groups. Two olefinic proton singlets were observed at δ 5.39 and 5.75. Additionaly two proton signals at δ 2.45 as a singlet and at δ 3.04-3.08 (dd, *J* = 5.7, 12.6, 1H) were detected (**Fig. 5.127**).
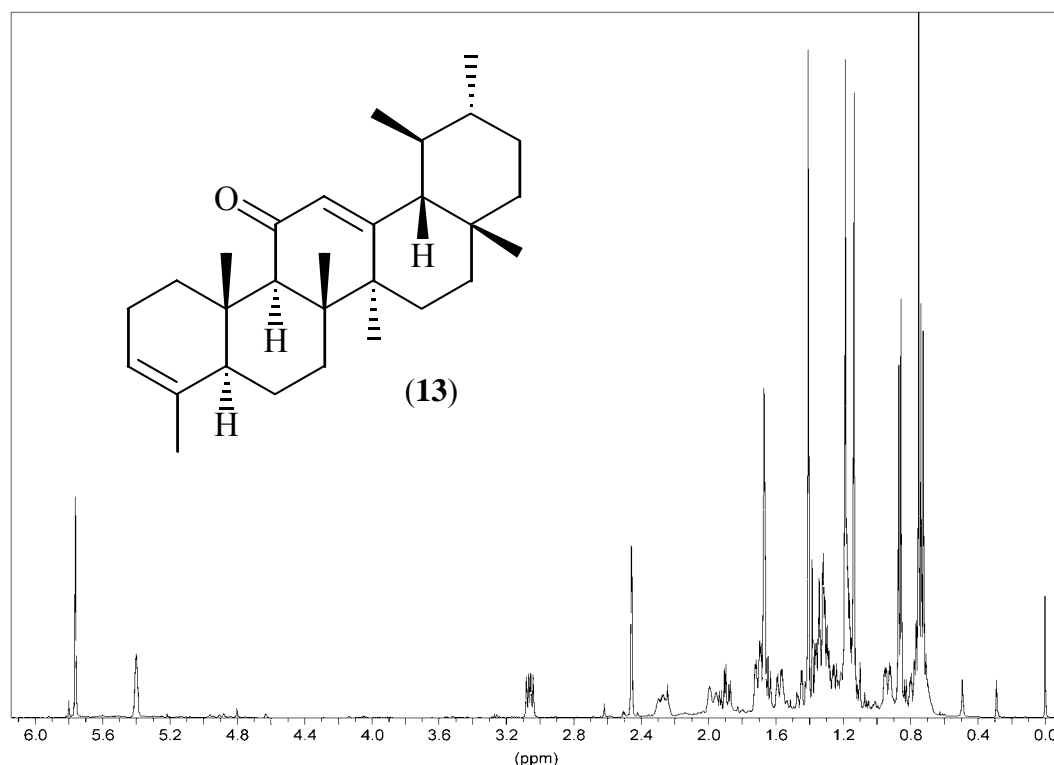
Fig. 5.127. ^{1}H-NMR spectrum of **13**.

The ^{13}C-PENDANT spectrum of **13** indicated seven primary carbons at δ 13.21, 17.73, 19.55, 20.98, 21.53, 22.19, 29.17, eight secondary carbons at δ 20.26, 23.60, 27.71, 28.07, 31.46, 32.80, 37.34, 41.44, seven tertiary carbons at δ 39.58, 39.60, 49.36, 58.90, 59.14, 122.49, 131.37, seven quaternary carbons at δ 34.20, 35.62, 44.15, 45.34, 134.05, 163.23, 198.61. The carbon signals that were shifted to the low field to δ 122.49, 131.37, 134.05, 163.23 indicated two double bonds whereas the signal at δ 198.61 indicated a carbonyl function in the molecule (**Fig. 5.128**).

HMQC spectrum indicated that the methyl group protons at δ 0.73, 0.75, 0.86, 1.13, 1.18, 1.40, 1.66 were correlating to the carbon signals at δ 17.73, 29.17, 21.53, 20.98, 19.55, 13.21, 22.19, respectively. Additionally the correlation between the olefinic protons at δ 5.39, 5.75 and the carbons at δ 122.49, 131.37 were also detected (**Table 5.12, Fig. 5.129**).

174
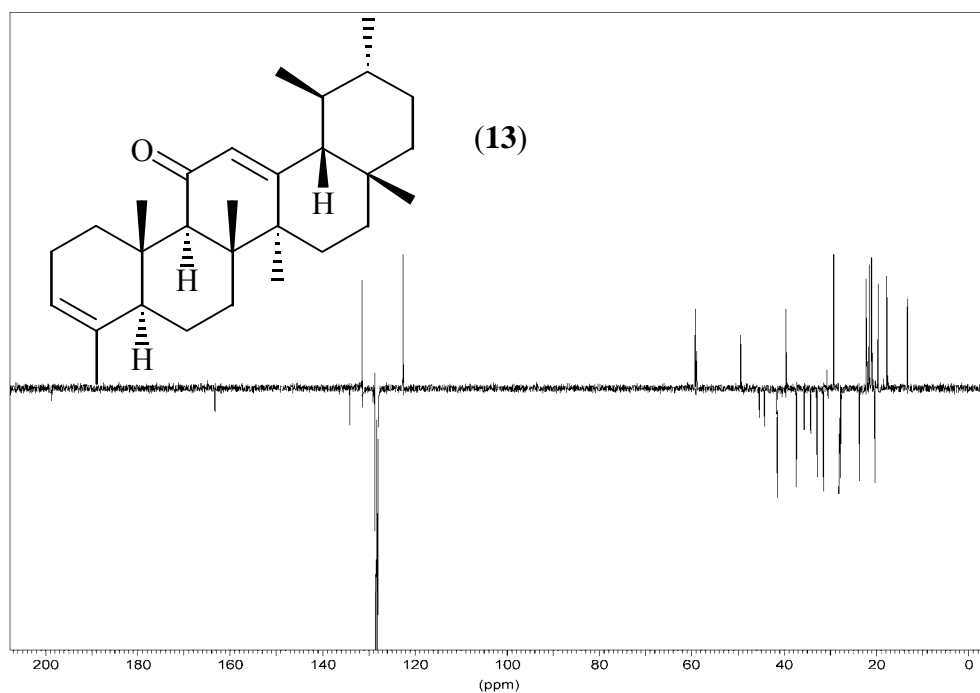
Fig. 5.128. ^{13}C-PENDANT spectrum of **13**.

Table 5.12. HMQC correlations of **13**.

No.	^{13}C (ppm)	^{1}H (ppm)	No.	^{13}C (ppm)	^{1}H (ppm)
1	37.34	(1.21-1.24), (3.04-3.08)	16	28.07	(0.91-0.95), (1.68-1.72)
2	23.60	(1.95-1.99), (2.24-2.30)	17	34.20	
3	122.49	5.39	18	59.14	(1.30-1.36)
4	134.05		19	39.60	(0.70-0.77)
5	49.36	(1.68-1.72)	20	39.58	(1.21-1.26)
6	20.26	(1.28-1.32), (1.56-1.59)	21	31.46	(1.30-1.36), 2H
7	32.80	(1.13-1.18), (1.44-1.47)	22	41.44	(1.13-1.18), (1.30-1.36)
8	45.34		23	22.19	1.66
9	58.90	2.45	24	13.21	1.40
10	35.62		25	19.55	1.18
11	198.61		26	20.98	1.13
12	131.37	5.76	27	29.17	0.75
13	163.23		28	17.73	0.73
14	44.15		29	21.53	0.86
15	27.71	(0.76-0.80), (1.86-1.93)			

Fig. 5.129. Numbered structure of **13**.

Five small fragments of the molecule were derived from the couplings in the ^{1}H-^{1}H COSY and HMBC spectra of **13,** which would lead to a subsequent connectivity to form the total structure (**Fig. 5.130**).

First fragment was deduced as a double bond system from the couplings of CH$_3$-23 (δ 1.66, 22.19) to C-4 (δ 134.05), C-3 (δ 122.49) and further to C-5 (δ 49.31).
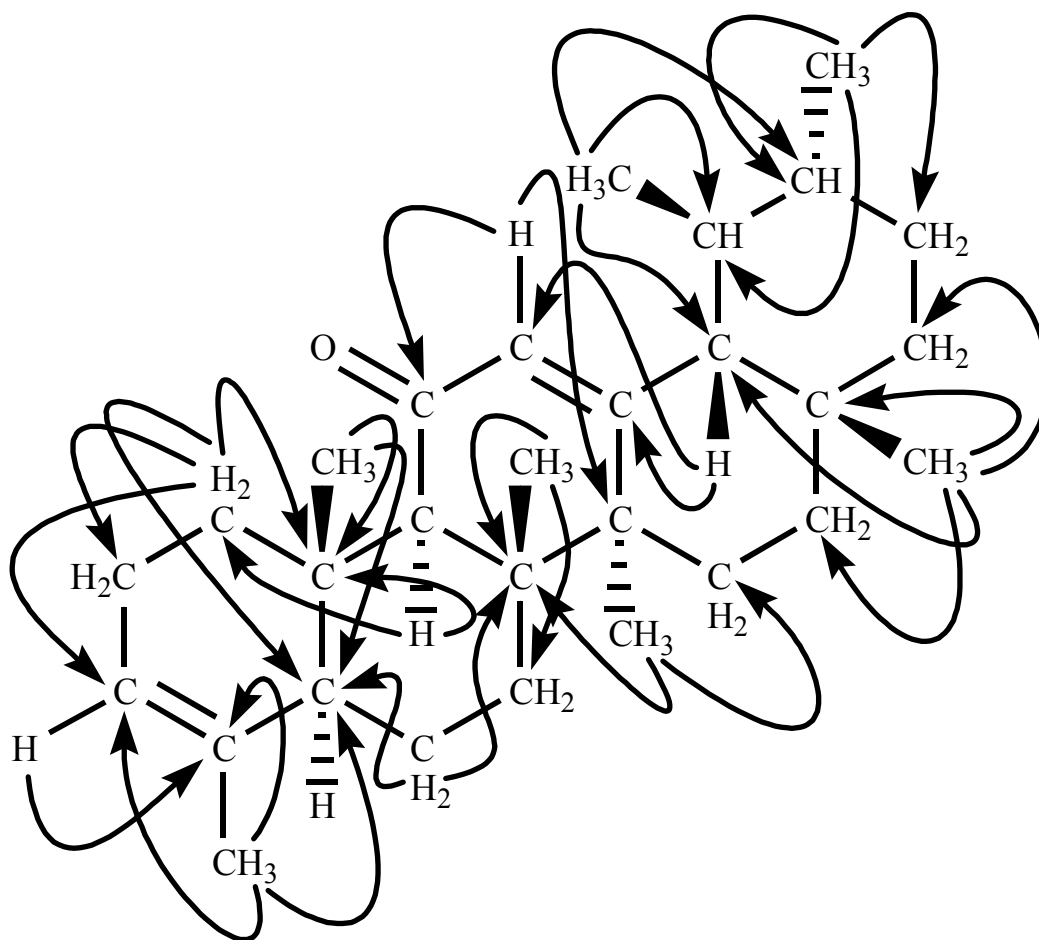
Fig. 5. 130. HMBC couplings of **13**.

The second double bond was derived from the coupling of H-12 (δ 5.76) with C-13 (δ 163.23). H-12 was further related to the carbonyl carbon C-11 (δ 198.61) and to its adjacent carbon C-9 (δ 58.90). On the other side of the double bond H-12 showed couplings with C-14 (δ 44.15) and C-26 (δ 20.98).

A third fragment had established the connection between these two double bond systems. CH_3-24 (δ 1.40, 13.21) was found to couple with C-10 (δ 35.62), C-5 (δ 49.36) and C-9 (δ 58.90).

The fourth fragment was deduced from the couplings of CH_3-25 (δ 1.18, 19.55) to C-8 (δ 45.34), C-7 (δ 32.80), C-9 (δ 58.90) and finally to C-14 (δ 44.15). CH_3-26 (δ 1.13, 20.98) was also found to couple with C-14 (δ 44.15), C-8 (δ 45.34) and further with C-15 (δ 27.71).

The final fragment was derived from the couplings of CH_3-28 (δ 0.73, 17.73) with C-19 (δ 39.60) and C-18 (δ 59.14). CH_3-29 (δ 0.86, 21.53) was coupled with C-19, C-20 (δ 39.58) and C-21 (δ 31.46). CH_3-27 (δ 0.75, 29.17) was found to couple with C-17 (δ 34.20), C-18 (δ 59.14), C-16 (δ 28.07) and with C-22 (δ 41.44). A further connection was provided by the detection of the coupling for the neighbouring H-21 (δ 1.32-1.29, 2H) and H-22 protons (δ 1.33-1.35, 1.16-1.21, 2H) in the ^{1}H-^{1}H COSY spectrum.

In the NOESY spectrum of **13** the couplings between H-1 (δ 3.04-3.08) with CH_3-24 (δ 1.40, 13.21) and with CH_3-25 (δ 1.18, 19.55) indicated that this proton is in β position. The same was observed with the correlation of H-2β (δ 2.24-2.30) to CH_3-24. H-5α (δ 1.68-1.72) was observed to couple with H-1α (δ 1.21-1.24), H-9 (δ 2.45), H-7α (δ 1.44-1.47). These correlations were confirmed by the couplings of H-9 with H-1α, H-7α, H-19α (δ 0.70-0.77) and CH_3-26 (δ 1.13, 20.98). H-9 was further observed to correlate with H-12 (δ 5.76) which was assumed to be a result of the increase in the planarity of ring C because of the keto group at C-11. Moreover, the existence of this keto group reduced the shielding effect of ring E, so that the number of correlations observed between ring E and the rest of the molecule was found to be increased in **13** compared to **8**.

CH_3-26 was found to correlate to H-15α (δ 1.86-1.93), H-19α and H-16α (δ 0.91-0.95) which also correlate to H-7α. CH_3-26 also showed a coupling with CH_3-28 (δ 0.86, 21.53) which further correlated to H-19α. The correlation of CH_3-27 (δ 0.75, 29.17) to CH_3-25 and H-18 (δ 1.30-1.36) indicated that H-18 was β to the ring system. This was also confirmed by the correlations of H-18 to CH_3-28 (δ 0.73, 17.73) and H-15β (δ 0.76-0.78). The final correlations observed in this spectrum were between CH_3-25 and H-16β (δ 1.68-1.72), H-3 (δ 5.39) and CH_3-23 (δ 1.66, 22.19) as well as H-3 and CH_3-24 (**Fig. 5.131**).
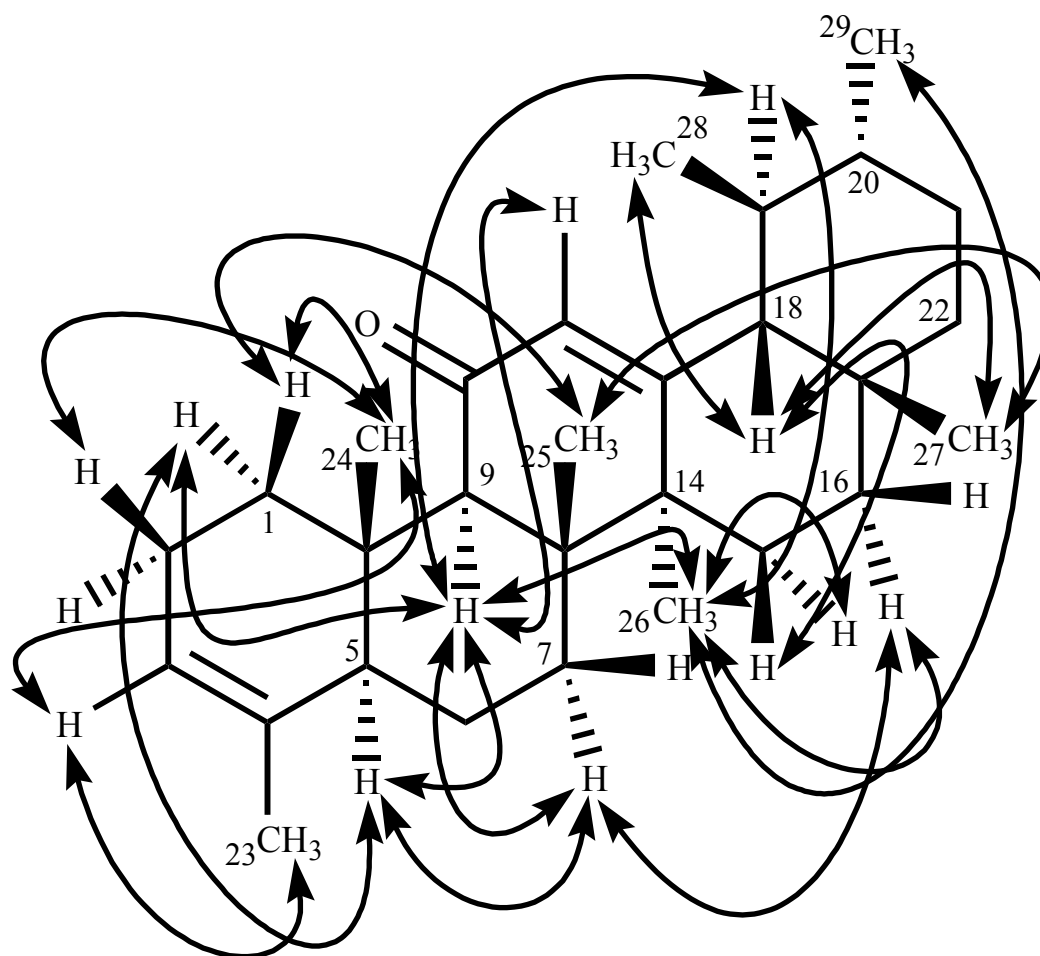
Fig. 5.131. NOESY correlations of **13**.

5.7.3 The Pyrolysate of *Boswellia serrata*

The pyrolysate of *B. serrata* was investigated by GC and GC-MS after it was determined with the specially designed SPA set-up for this purpose. During these investigations the presence of the nortriterpenes, **8** (11.2%), **9** (3.0%), **10** (1.2%), **11** (0.6%), **12** (0.2%) and **13** (3.9%) which were derived from boswellic acids and additionally, the diagnostic markers of *B. serrata*, namely its diterpenoic constituents, m-camphorene (6.4%), p-camphorene (2.9%), cembrene A (2.6%) and cembrenol (22.6%) were detected without any alterations. Different than *B. carterii* resin, the amyrin derivatives, α-amyrin and α-amyrenone (1.8%), β-amyrin and β-amyrenone (0.9%) that were present in *B. serrata* resin were detected in the triterpenoic region of the gas chromatogram of the pyrolysate together with the nortriterpenes. Besides, sabinene (4.0%), limonene (2.0%), α-cubebene (1.7%), β-bourbonene (1.5%), γ-muurolene (0.9%) were observed in this pyrolysate (**Fig. 5.132**).
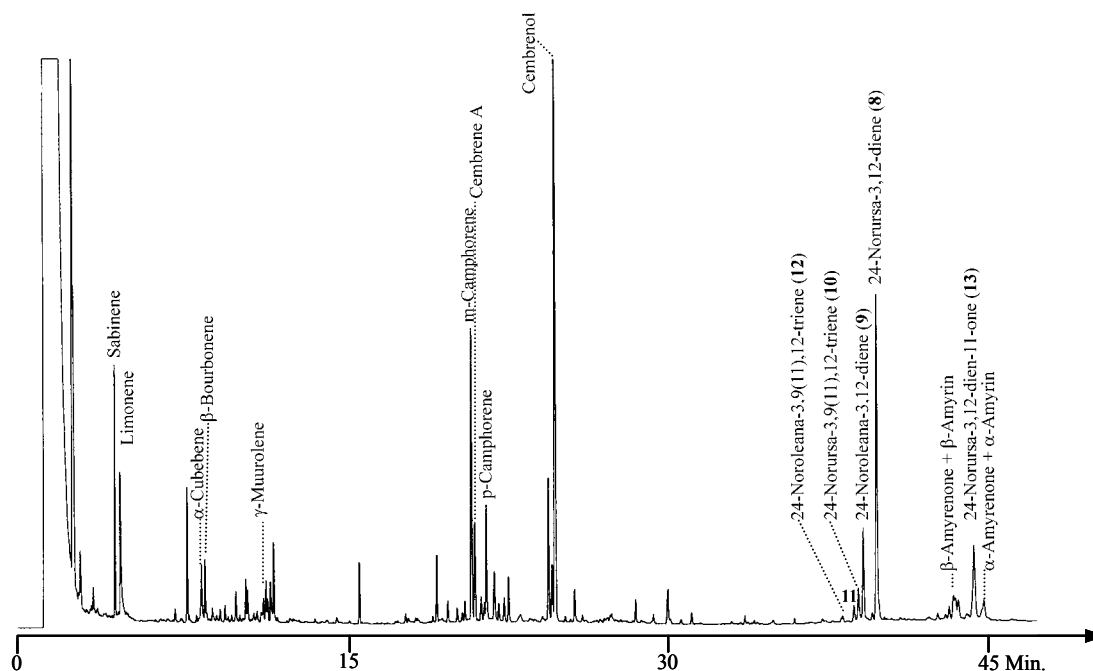
Fig. 5.132. Gas chromatogram of the pyrolysate of *B. serrata*. (25 m fused silica capillary column with CPSil 5 CB, 100 °C, 5 °C/min up to 300 °C, injector at 250 °C, detector at 320 °C, carrier gas 0.5 bars H_2).

The pyrolysate of *B. serrata* was silylated to find out whether the tirucallic acids were detectable in this fraction as in the case of *B. carterii*. The GC, GC-MS investigations of this silylated pyrolysate fraction showed that all three tirucallic acid derivatives, 3-hydroxy-8,9,24,25-tetradehydr-TA, 3-*O*-acetyl-8,9,24,25-tetradehydro-TA and 3-oxo-8,9,24,25-tetradehydro-TA were present (**Fig. 5.133**).
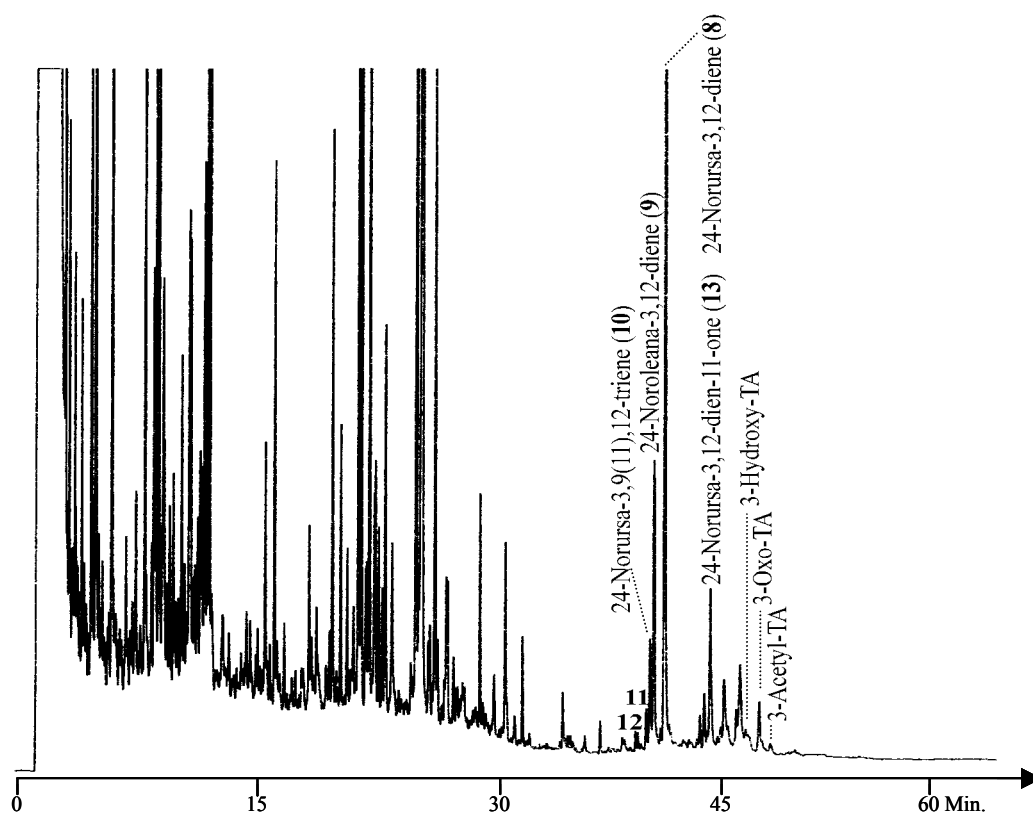
Fig. 5.133. Gas chromatogram of the silylated pyrolysate of *B. serrata* (25 m fused silica capillary column with CPSil 5 CB, 100 °C, 5 °C/min up to 300 °C, injector at 250 °C, detector at 320 °C, carrierr gas 0.5 bars H_2).

5.7.4 The Pyrolysate of *Boswellia frereana* Birdw.

The GC and GC-MS investigations performed on the pyrolysate of *B. frereana* indicated that the diagnostic markers for this *Boswellia* species, dimer of α-phellandrene (5.4%) and lupeol (12.2%) were stable in these experimental conditions (**Fig. 5.134**).
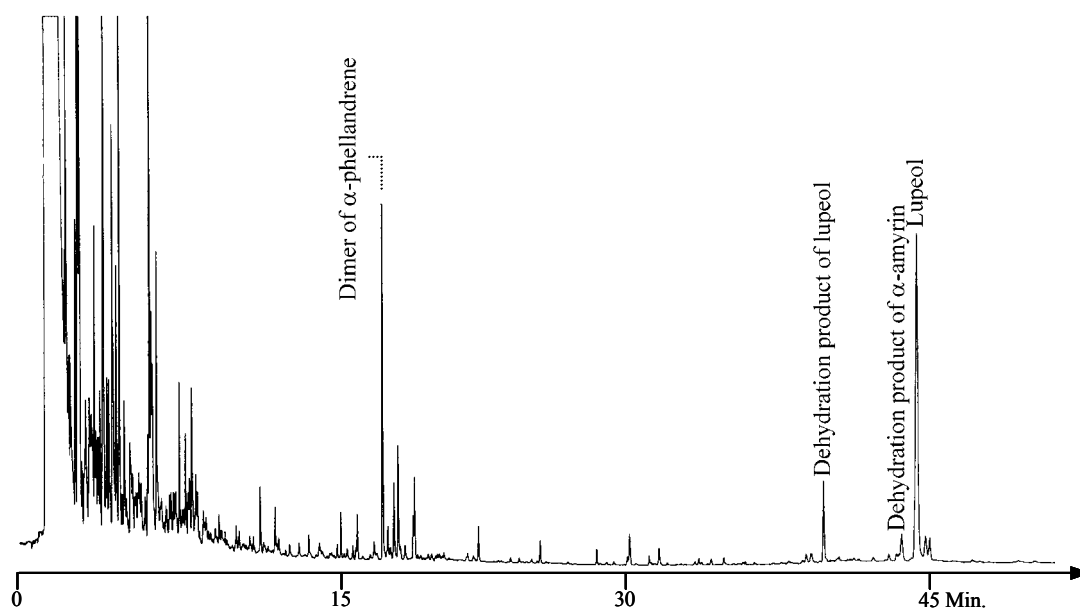
Fig. 5.134. Gas chromatogram of the pyrolysate of *B. frereana* (25 m fused silica capillary column CPSil 5 CB, 100 °C, 5 °C/min up to 300 °C, injector at 250 °C, detector at 320 °C, carrier gas 0.5 bars H_2).

The peak which was assigned as lupeol, was isolated by CC and preparative TLC. It was further identified by 1- and 2-D NMR spectroscopy. The data obtained in these NMR measurements were compared with a reference sample of lupeol (Roth). The NMR data of the reference sample was consistent with the data of the isolated substance.

Another point observed in this analysis was that the dehydration product of lupeol, lupeol-3-ene was found to occur during the injection of the sample but not in the pyrolysation of the resin. This was also detected in the GC analysis of the reference sample of lupeol.

5.7.5 The Pyrolysate of *Boswellia neglecta*

The essential oil of the Ethiopian *Boswellia* species was previously found to be rich in monoterpenoic constituents. The sudies on its triterpenoic constituents indicated that it has also contained several α- and β- amyrin derivatives and their epimers.

In the pyrolysate of this species the composition of these triterpenoic constituents was not altered. α-Amyrin (9.1%), β-amyrin (0.7%), *epi*-α-amyrin (1.6%), β-amyrenone (1.4%), as well as a partial dehydration of α- and β-amyrin (3-,12-dien-α-amyrin (3.4%) and 3,12-dien-β-amyrin (1.1%)) were found in the sample. The formation of the dehydration products was also assumed to occur during the injection of the sample (**Fig. 5.135**).

181
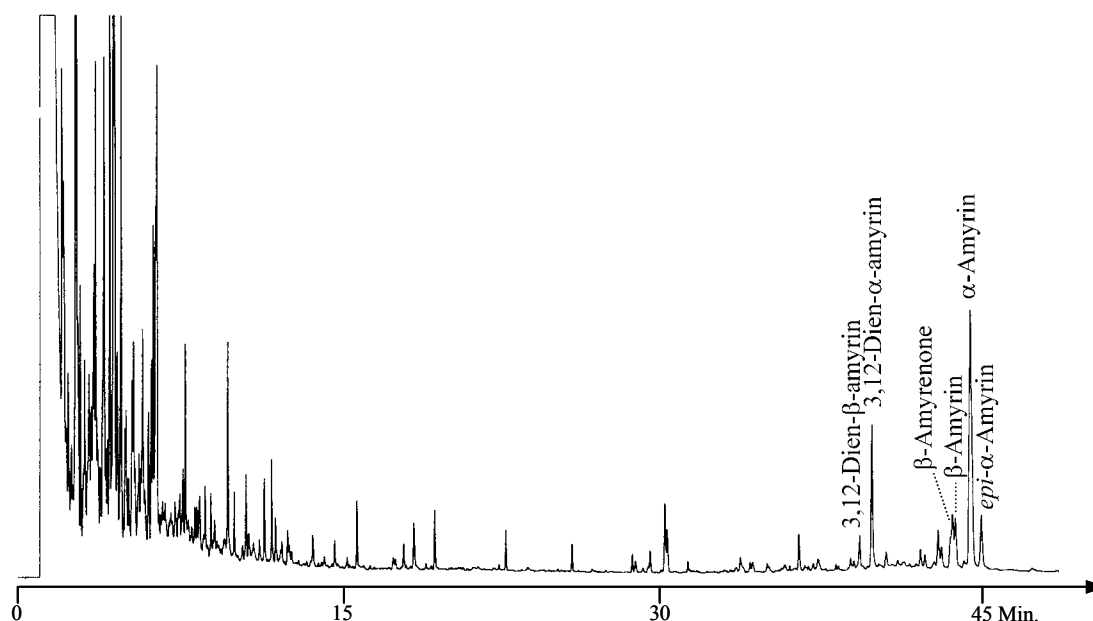
Fig. 5.135. Gas chromatogram of the pyrolysate of *B. neglecta* (25 m fused silica capillary column with CPSil 5 CB, 100 °C, 5 °C/min up to 300 °C, injector at 250 °C, detector at 320 °C, carrier gas 0.5 bars H_2).

5.7.6 The Pyrolysate of *Boswellia rivae*

The second Ethiopian *Boswellia* species was also found to be rich in monoterpenoic constituents in its essential oil but different than *B. neglecta* it was found to contain small amounts of α- and β-boswellic acids besides the amyrin derivatives in its triterpenoic composition.

In the pyrolysate of *B. rivae* 24-norursa-3,12-diene (**8**) (18.7%) was detected in large amounts. The presence of this compound was confirmed after its mass and NMR data were compared with the one obtained from *B. carterii*.

The presence of the other nortriterpenes, **9** (4.0%), **10** (1.2%), **11** (0.7%), **12** (0.5%), that occured from boswellic acids through deacetylation and dehydration which accompanied by decarboxylation reactions, pointed out that *B. rivae* resin contained not only α- and β-BA as detected in the acid fraction but also the other derivatives of boswellic acids in trace amounts.

Nevertheless, the presence of 24-norursa-3,12-dien-11-one (**13**) was not detected in the pyrolysate. Therefore it was concluded, the 11-keto derivatives of β-boswellic acid, KBA and AKBA, were not available in *B. rivae*.

Other than the nortriterpenes (**8-12**), α-amyrin (4.2%), β-amyrin (0.9%), their 3-keto derivatives, α-amyrenone (2.8%), β-amyrenone (2.3%) and *epi*-β-amyrin (0.9%) were also detected in the pyrolysate of *B. rivae* (**Fig. 5.136**).
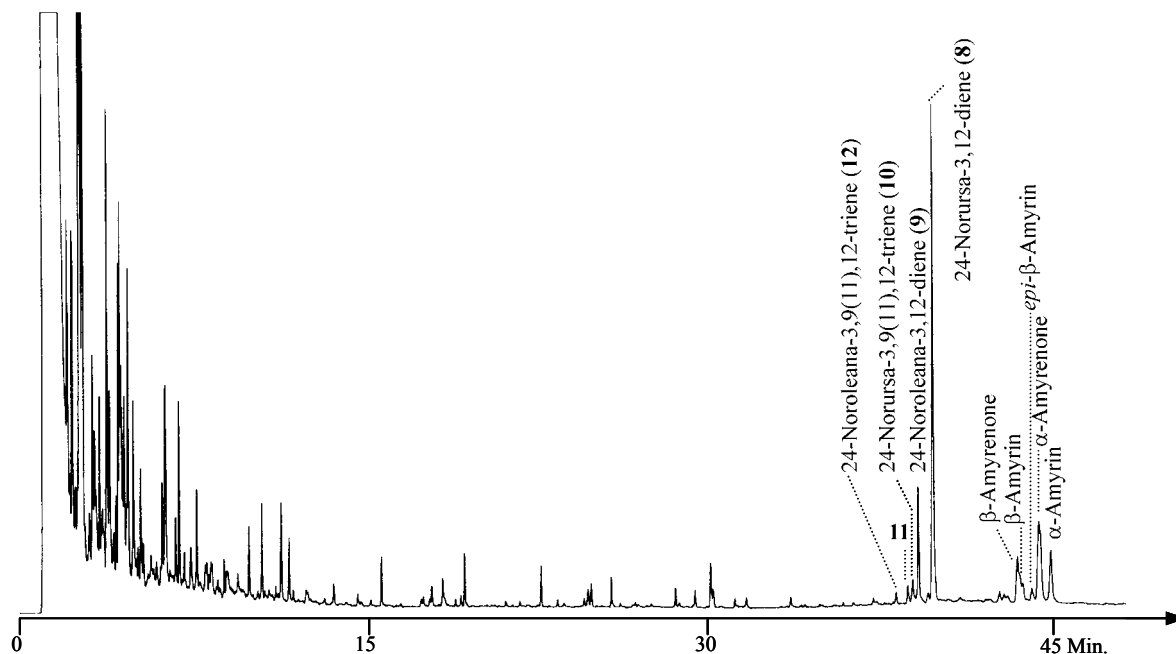
Fig. 5.136. Gas chromatogram of the pyrolysate of *B. rivae* (25 m fused silica capillary column with CPSil 5 CB, 100 °C, 5 °C/min up to 300 °C, injector at 250 °C, detector at 320 °C, carrier gas 0.5 bars H$_2$).

5.7.7 *Curie*-point pyrolysis-GC/MS Experiments

Intriguing results have been determined with the specially designed SPA model during the investigations of the pyrolysates of olibanum species. Particularly the results concerning the stability of the diterpenoic constituents were identified as the diagnostic markers for different olibanum species. They had to be tested with conventional methods to prove their validity with this new experimental set-up. For this reason *B. carterii* and *B. serrata* resins were analysed with *Curie*-point (670 °C) pyrolysis-GC/MS.

In the case of *B. carterii* the presence of octylacetate, cembrene C, verticilla-4(20),7,11-triene, incensole and incensole acetate were clearly observed. Determination of the parallel results with this analysis approved the capability of the newly designed SPA set-up. Moreover, the thermal stability of the diterpenoic compounds of *B. carterii* even at these temperatures was found surprising. Additionally the formation of the nortriterpenes **8-10** and **13** were detected.

Similar results were obtained in the case of *B. serrata*. The diagnostic constituents of this species, m-camphorene, p-camphorene, cembrenol were clearly detected in the pyrolysis-GC/MS investigation. However, instead of cembrene A, cembrene C was observed although this constituent was only found in the essential oil of *B. carterii* before. It was assumed that the isomerisation of cembrene A into cembrene C at these high temperatures had occurred. This was also considered as an explanation for the absence of cembrene A peak in the *B.*

carterii sample. In the analysis of *B. serrata* by pyrolysis-GC/MS the nortriterpenes **8**, **9** and **13** were detected in trace amounts (**Fig. 5.137**).
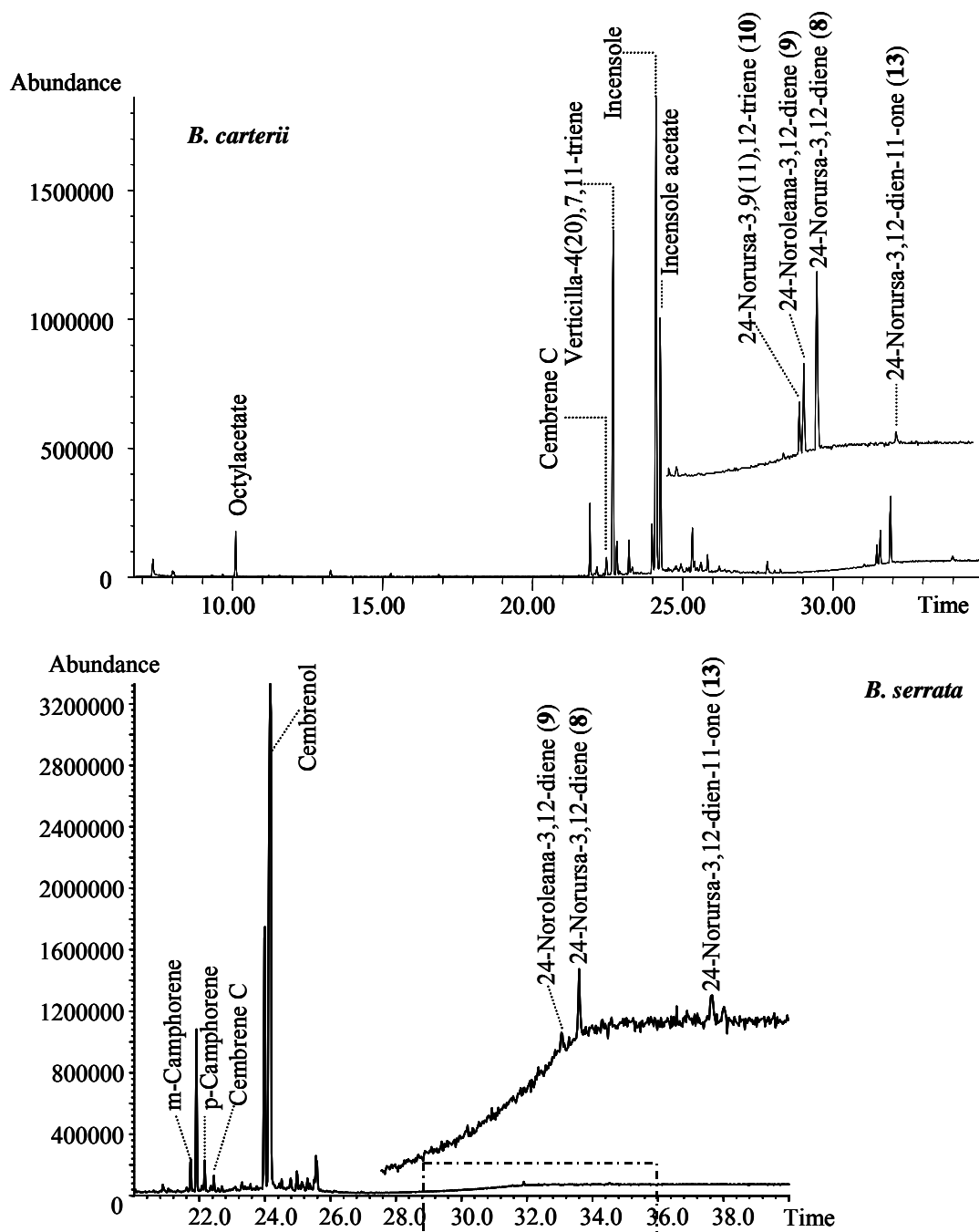
Fig. 5.137. TICs of *Curie*-point (670 °C) pyrolysis-GC/MS measurements of *B. carterii* and *B. serrata* (Pyrolysis at 670 °C for 10 seconds, pyrolysis head was heated to 200 °C and the products were transferred (270 °C) to the injection port at 250 °C. For GC 30 m DB5 MS capillary column, 100 °C, 5 °C/min up to 300 °C was used).

5.8   Pharmaceutical Investigations on Olibanum

The variable uses of olibanum resin and its traditional applications in folk medicine provided a valuable interest to study the pharmacological effects of its constituents. The strong antiinflammatory activity of the boswellic acids has been well known in the last decade. But there has been very little work performed on different kind of pharmaceutical effects of olibanum such as antibacterial, antioxidant, antimicrobial, antiviral, *etc*. activities.

For example, in a study performed on the antibacterial activity of different essential oils against *Candida albicans*, the oil of *B. carterii* showed a moderate activity (MIC 1.0%, between 0.03-2.0%) against this species[173]. On the other hand, in another study testing the antimicrobial effects of essential oils against *Streptococcus pneumoniae*, *B. carterii* was found completely inactive[174]. However, in both cases essential oil was tested directly. It was not possible to detect the activity of single constituents.

In this study, five *Boswellia* species were tested for their antibacterial and antioxidant activity. The different fractions prepared from olibanum (essential oil, pyrolysate, acid fractions) provided an advantage for the screening of the constituents of *Boswellia* species. These fractions supplied an assignment of a single or a group of substances related to the observed activities. The use of TLC plates also increased the possibility to observe the constituents which have such activities easily with a single experiment.

5.8.1   Antibacterial Activity of Olibanum

The antibacterial activity of olibanum was tested with a bioautography test, Chrom Biodip[®] (Merck) against *Bacillus subtilis*. *B. subtilis* served as an indicator since its growth is inhibited by antibiotics with the formation of visible zones on TLC plates.

B. subtilis is a gram-positive bacterium with a fast growth rate. It forms dry colonies and cause hemolysis on bloodagar. Single strains are resistant to antibiotic. It is considered as an opportunistic pathogen[175].

The method involved the separation of substance mixtures using HPTLC plates and subsequent visualisation of the zones formed by the growth-inhibiting substances. This was established by dipping the developed HPTLC plates into the culture medium and incubating it overnight (19 h) in an incubation box at 30 °C. For the detection, MTT-solution (3-(4,5-dimethyl-2-thiazolyl)-2,5-diphenyl-2H-tetrazolium bromide) was sprayed on the plates revealing a slightly yellow surface. After 30 minutes remain the inhibition zones as yellow (or white) as the background turns into blue-violet.

5.8.1.1 Antibacterial Activity of the Essential Oils of Olibanum

The essential oils of five *Boswellia* species, *B. carterii*, *B. serrata*, *B. frereana*, *B. neglecta* and *B. rivae* were tested for their antibacterial activity against *Bacillus subtilis*.

The essential oils were applied in two sets on a full length plate (10 x 20 cm). After the development of the plate in cyclohexane: ethylacetate (8:2), it was cut into two parts. While one set of samples derivatised with anisaldehyde solution, the other set was used for the incubation of the bacteria overnight. In this way, a comparable detection of the essential oils with UV_{254nm} and daylight detection after anisaldehyde derivatisation, together with the zones indicating antibacterial activity was simultaneously possible (**Fig. 5.138**).

As a result of the Biodip test, only two bands of *B. carterii* showed antibacterial activity. These bands corresponded with verticilla-4(20),7,11-triene together with cembrene A and C, and incensyl acetate.
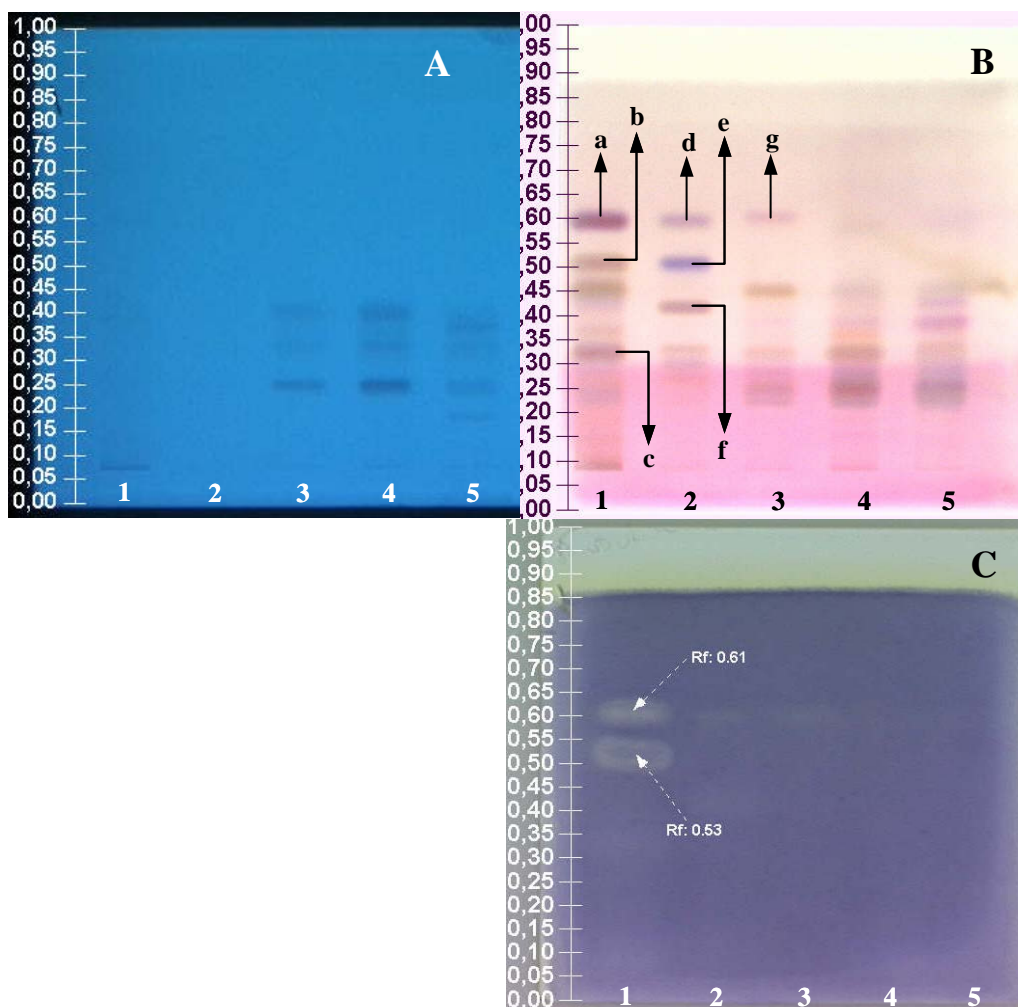
Fig. 5.138. TLC plates prepared for the Biodip test of essential oils of olibanum. Samples **1**: *B. carterii*, **2**: *B. serrata*, **3**: *B. frereana*, **4**: *B. neglecta*, **5**: *B. rivae*. HPTLC LiChrospher® Si 60F$_{254S}$ (Merck) plates, mobile phase: cyclohexane: ethylacetate (8:2), development distance : 7 cm. **A**: UV detection at 254 nm., **B**: Detection at daylight after derivatisation with anisaldehyde spray solution with subsequent heating the plate at 105 °C., **C**: Detection at daylight after BIODIP application. Bands **a**: Verticilla-4(20),7,11-triene, cembrene A, cembrene C, **b**: Incensyl acetate, **c**: Incensole, **d**: m-Camphorene, p-camphorene, cembrene A, **e**: Kessane, **f**: Cembrenol, **g**: Dimers of α-phellandrene.

5.8.1.2   *Antibacterial Activity of the Acid Fractions of Olibanum*

The acid fractions of five *Boswellia* species, prepared by 10% KOH extraction method, were applied on a TLC plate and developed with chloroform: diisopropylether: methanol (7:2.5:0.5) mixture for the antibacterial activity test (**Fig. 5.139**).

187
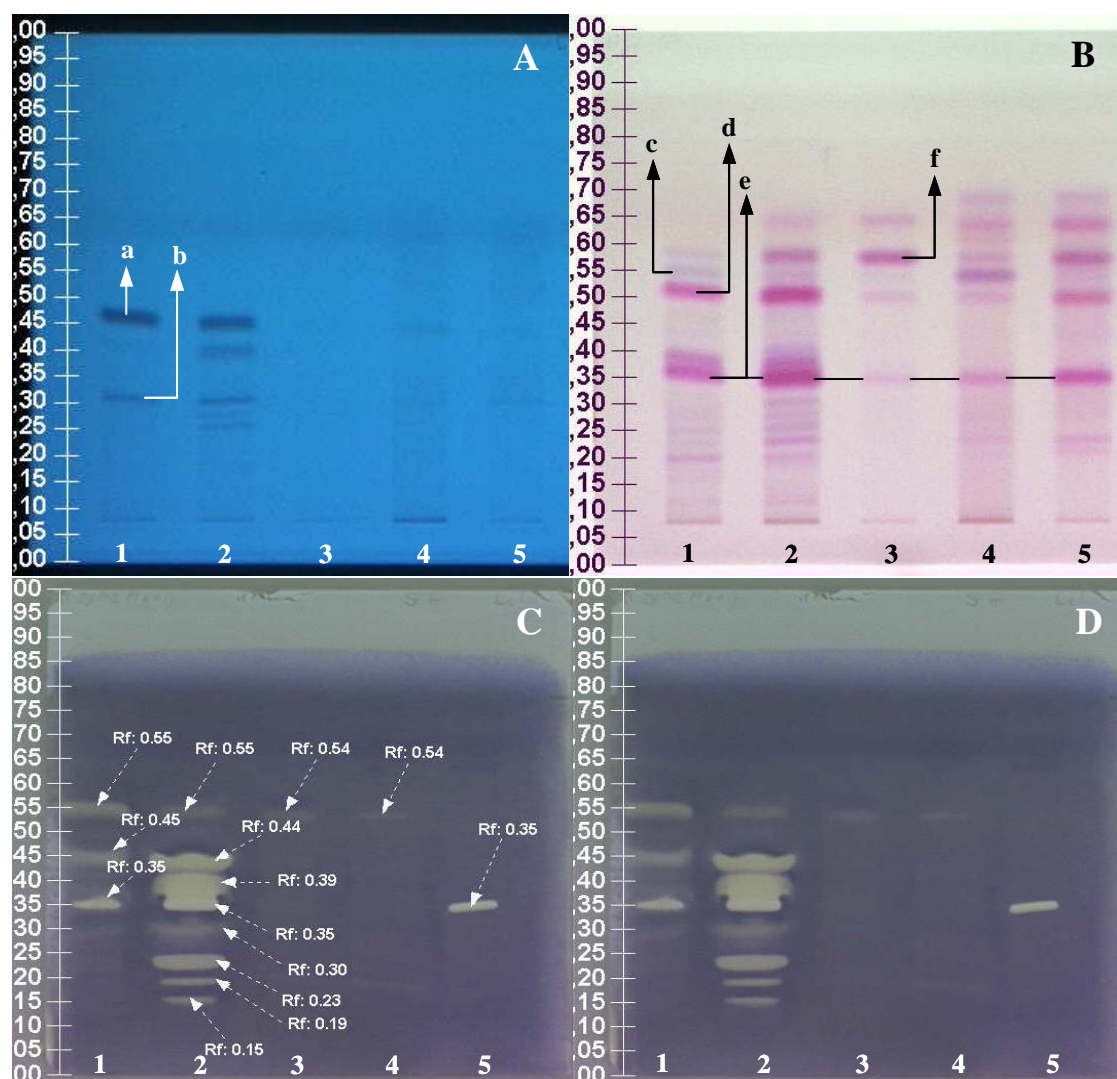
Fig. 5.139. TLC plates prepared for the Biodip test of the acid fractions of olibanum. Samples **1**: *B. carterii*, **2**: *B. serrata*, **3**: *B. frereana*, **4**: *B. neglecta*, **5**: *B. rivae*. HPTLC LiChrospher® Si 60F$_{254S}$ (Merck) plates, mobile phase: chloroform: diisopropylether : methanol (7:2.5:0.5), development distance : 7 cm. **A**: UV detection at 254 nm., **B**: Detection at daylight after derivatisation with anisaldehyde spray solution with subsequent heating the plate at 105°C., **C** and **D**: Detection at daylight after BIODIP application. Bands **a**: AKBA, **b**: KBA, **c**: 3-Oxo-TA, **d**: α- and β-Acetyl-BA, **e**: α- and β-BA, **f**: Lupeol.

The acid fractions of *B. carterii* and *B. serrata* were found to show the highest antibacterial activity. In *B. carterii*, an antibacterial activity of AKBA, α- and β-BA, 3-oxo-TA was observed. In *B. serrata* the activity of these compounds was found to be stronger. Additionally, in *B. serrata* an activity of the artifacts (formed at R$_f$: 0.15, 0.19 and 0.23 due to the acidification with HCl) and an activity for the band at R$_f$: 0.39 were detected. In the acid

fractions of both species the activity of KBA were found to be weak and no antibacterial effect of 3-*O*-acetyl-α- and β-BAs was observed.

Among the other *Boswellia* species, *B. frereana*, *B. neglecta* and *B. rivea*, an antibacterial effect was only observed for the α-and β-BA constituents of *B. rivea*. Although *B. frereana* and *B. neglecta* were known to contain α- and β-BA, it was assumed that the concentration of these compounds was not sufficient for an inhibitory action.

5.8.1.3 Antibacterial Activity of Pyrolysates of Olibanum

The pyrolysates of *Boswellia* species were applied on a HPTLC plate and developed with cyclohexane: ethylacetate (8:2) mixture.

An antibacterial activitiy was detected in all species mostly in those zones where triterpenoic constituents were found. In *B. carterii* the band containing the nortriterpenes (**8-12**), verticilla-4(20),7,11-triene and the cembrene derivatives was found to be active as well as incensyl acetate.

In *B. serrata*, the band of nortriterpenes (**8-12**) including m- and p-camphorene, cembrene A shows an inhibitory effect. A weak zone was detected at R_f: 0.20 which was assumed to be formed by 3-Oxo-8,9,24,25-tetradehydro-TA. 24-Norursa-3,12-dien-11-one (**13**) derived from the pyrolysis of AKBA and KBA in both *B. carterii* and *B. serrata* species showed no inhibitory activity.

B. frereana showed a weak antibacterial effect in the zone where the dimers of α-phellandrene and amyrin derivatives were eluted. Lupeol was found to be inactive against *B. subtilis*. In the case of *B. neglecta*, the activity of the amyrin derivatives as detected again. In *B. rivae*, this activity increased with the additional effect of the nortriterpenoic constituents (**8-12**) (**Fig. 5.140**).
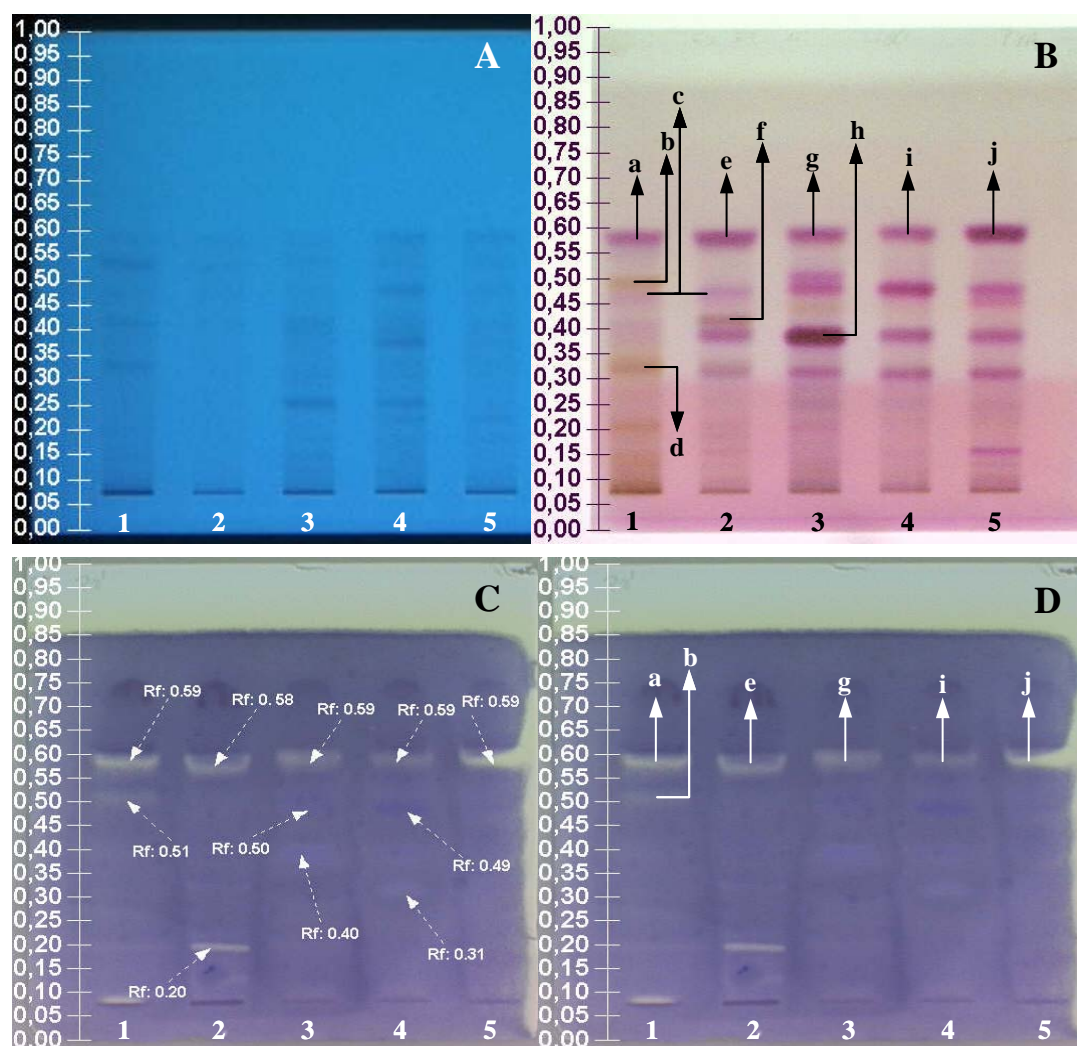
Fig. 5. 140. TLC plates prepared for the Biodip test of the pyrolysates of olibanum. Samples **1**: *B. carterii*, **2**: *B. serrata*, **3**: *B. frereana*, **4**: *B. neglecta*, **5**: *B. rivae*. HPTLC LiChrospher® Si 60F$_{254S}$ (Merck) plates, mobile phase: cyclohexane:ethylacetate (8:2), development distance : 7 cm. **A**: UV detection at 254 nm., **B**: Detection at daylight after derivatisation with anisaldehyde spray solution with subsequent heating at 105°C., **C** and **D**: Detection at daylight after Biodip application. Bands **a**: Nortriterpenes (8-12), verticilla-4(20),7,11-triene, cembrene A, cembrene C, isocembrene, cembrene **b**: Incensyl acetate, **c**: 24-Norursa-3,12-dien-11-one, **d**: Incensole, **e**: Nortriterpenes (8-12), m-camphorene, p-camphorene, cembrene A, α-amyrin, β-amyrin, **f**: Cembrenol, **g**: Dimers of α-phellandrene, α-amyrin, **h**: Lupeol, **i**: α-amyrin, β-amyrin, *epi*-α-amyrin, 3,12-dien-α-amyrin, 3,12-dien-β-amyrin, **j**: Nortriterpenes (8-12), α-amyrin, β-amyrin, *epi*-β-amyrin.

5.8.1.4 Antimicrobial Activity of Single Constituents

Some isolated substances from olibanum essential oil, acid fraction and pyrolysate were subjected to the Biodip test for a more precise identification of their antibacterial activity. A

strong inhibitory effect of incensyl acetate, 3-*O*-acetyl-8,9,24,25-tetradehydro-TA, AKBA, KBA, verticilla-4(20),7,11-triene, α- and β-BA was clearly observed. Cembrene A, and 24-norursa-3,12-diene (**8**) were found to have a weak antibacterial activity which might also depend on the concentration of the applied substances. Lupeol was again found to be completely inactive in this experiment (**Fig. 5.141**).
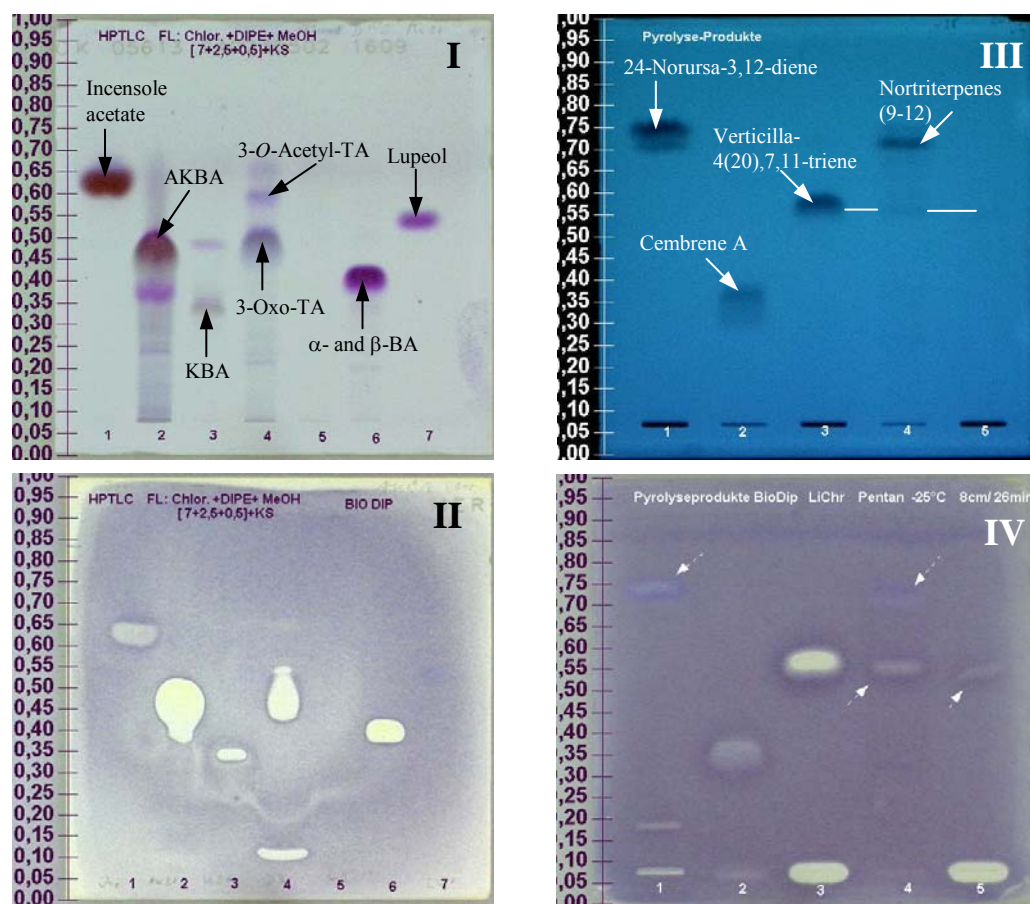
Fig. 5.141. Biodip test results of the single constituents of olibanum. (HPTLC Lichrospher® Si 60F254S (Merck), mobile phase: **I:** chloroform:diisopropylether:methanol (7:2.5:0.5), **II:** *n*-Pentane at –25 °C. development distance: 8 cm., Samples **I: 1:** Incensyl acetate, **2:** AKBA, **3:** KBA, **4:** 3-*O*-Acetyl-TA, **5:** 3-Oxo-TA, **6:** α- and β-BA, **7:** Lupeol, **II: 1:** 24-Norursa-3,12-diene (8), **2:** Cembrene A, **3:** Verticilla-4(20),7,11-triene (5 μl), **4:** Nortriterpenes (9-12), **5:** Verticilla-4(20),7,11-triene (3 μl). Detection **I:** At day light after derivatisation with anisaldehyde, subsequent heating at 105 °C. **II and IV:** Biodip test results at daylight, **III:** UV detection at 254 nm.

5.8.2 Antioxidative Activity of *Boswellia* species

Antioxidative activity of *Boswellia* species were tested on TLC plates by derivatising the plates with a free radical 2,2-dipheyl-1-picrylhydrazil (DPPH) (**Fig. 5.141**). The reagent was dissolved in methanol (app. 0.2% (w/v)) and sprayed over the TLC plate. The substances which have a potential radical scavenging effect showed white inhibition zones over a violet background.

2,2-Diphenyl-1-picrylhydrazil
(DPPH)
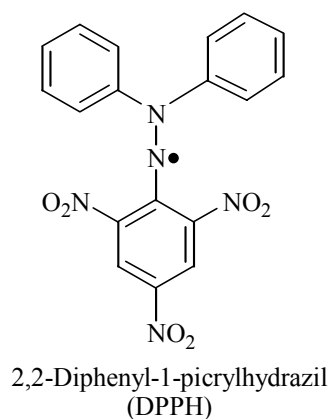
Fig. 5.141. 2,2-Diphenyl-1-picrylhydrazil (DPPH), antioxidative activity test reagent.

The different fractions of the *Boswellia* species were tested again separately. The acid fractions of the species showed no activity against DPPH.

5.8.2.1 *Antioxidative Activity of the Essential Oils of Boswellia Species*

The essential oils of olibanum were applied on TLC plates and developed with cyclohexane: ethylacetate (8:2) (**Fig. 5.142**).

None of the diagnostic markers identified in the essential oils of *Boswellia* species showed a radical scavenging effect. Only the bands in the essential oil of *B. serrata* at R_f:0.29, *B. frereana* at R_f: 0.29 and *B. neglecta* at R_f: 0.29 and 0.25 showed moderate activities. The corresponding compounds could not be identified in this study, as not sufficient material could be provided.
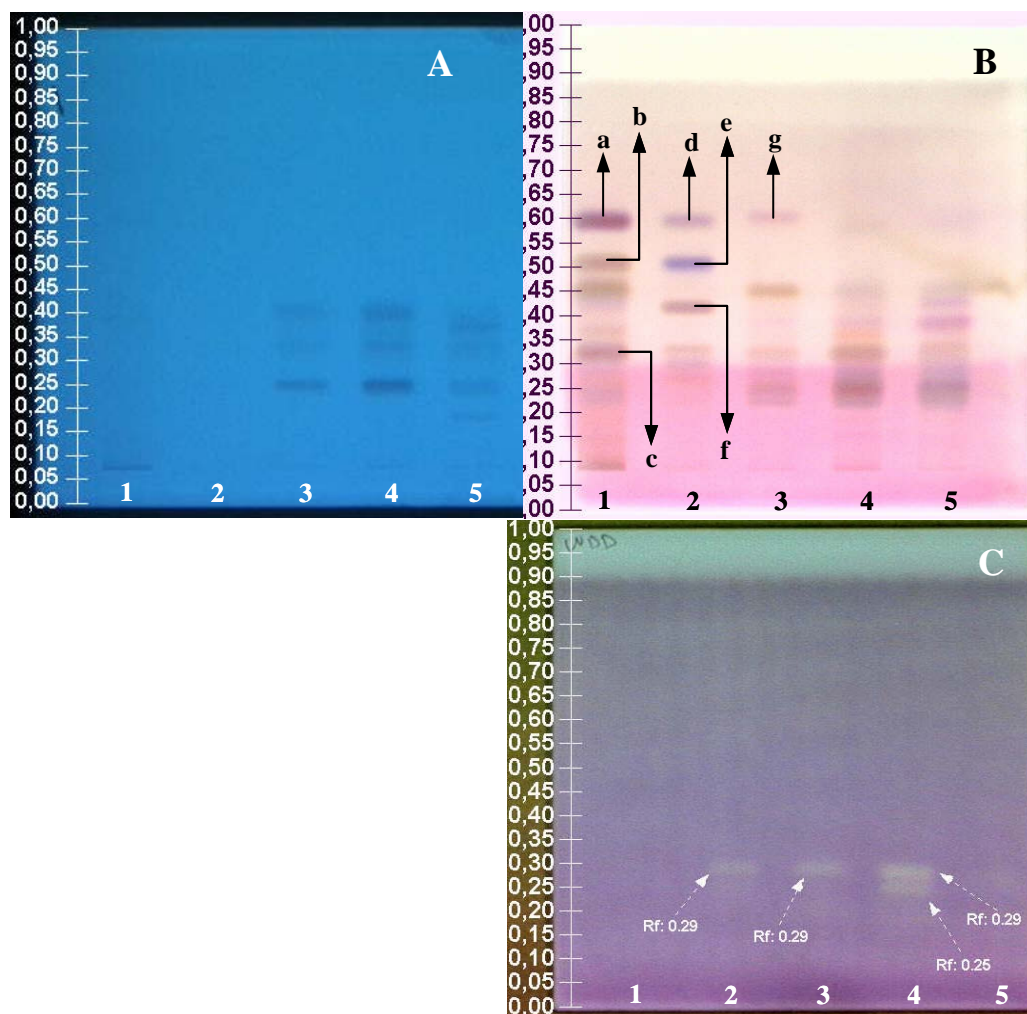
Fig. 5.142. Essential oils of olibanum tested for their antioxidative activity. Samples **1:** *B. carterii*, **2:** *B. serrata*, **3:** *B. frereana*, **4:** *B. neglecta*, **5:** *B. rivae*. HPTLC LiChrospher® Si 60F$_{254S}$ (Merck) plates, mobile phase: cyclohexane: ethylacetate (8:2), development distance : 7 cm. **A:** UV detection at 254 nm., **B:** Detection at daylight after derivatisation with anisaldehyde spray solution with subsequent heating the plate at 105 °C., **C:** Detection at daylight DPPH derivatisation. Bands **a:** Verticilla-4(20),7,11-triene, cembrene A, cembrene C, **b:** Incensyl acetate, **c:** Incensole, **d:** m-Camphorene, p-camphorene, cembrene A, **e:** Kessane, **f:** Cembrenol, **g:** Dimers of α-phellandrene.

5.8.2.2 Antioxidative Activity of the Pyrolysates of Boswellia Species

The pyrolysates of *Boswellia* species were applied on a TLC plate and developed with cyclohexane: ethylacetate (8:2) solvent mixture. Subsequently the plate was derivatised with DPPH solution to find out the antioxidant substances.

The pyrolysis products of boswellic acids, the nortriterpenes (**8-13**) and the diagnostic markers of olibanum showed no activity in this test. However, similar bands were found to

have antioxidative effect in the pyrolysates of *B. serrata*, *B.frereana* and *B. neglecta* compared to their essential oils (**Fig. 5.143**).
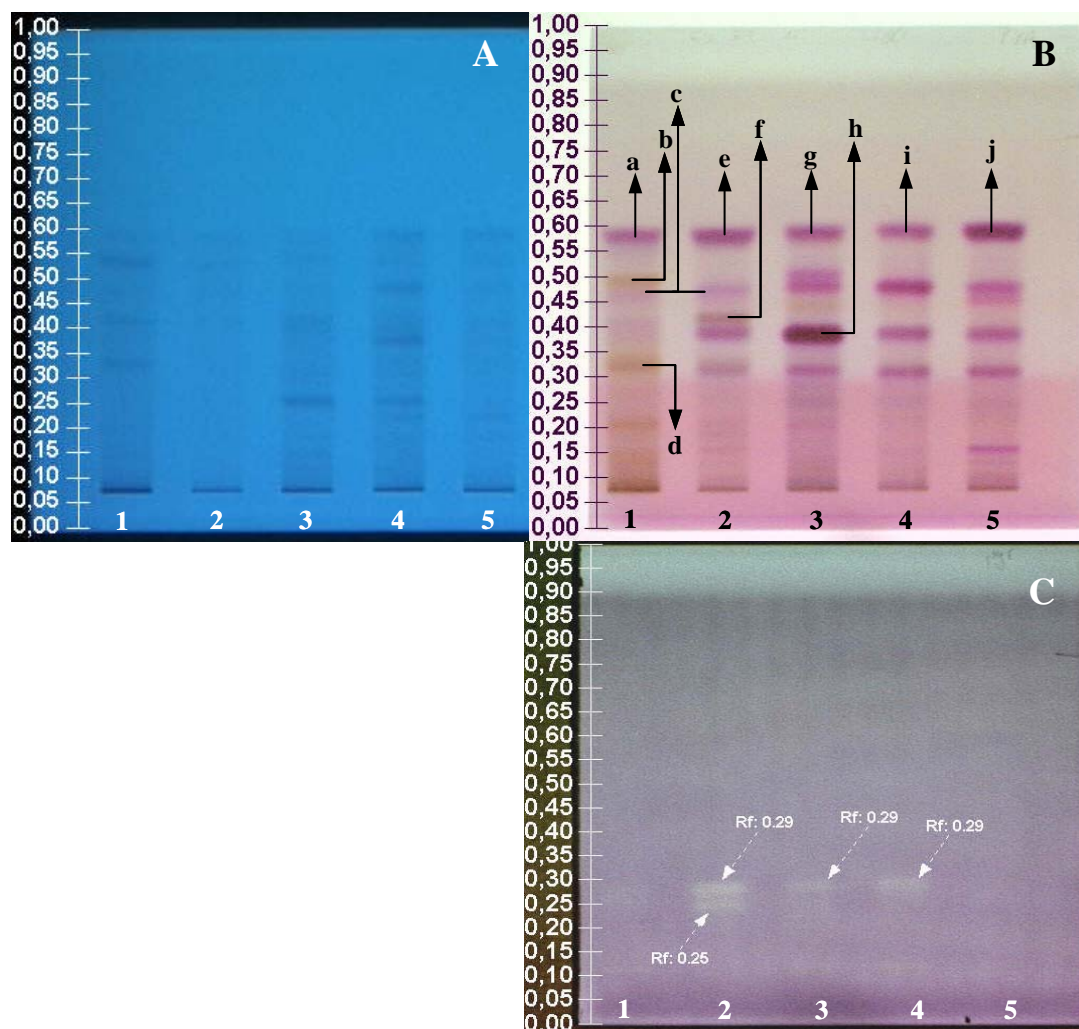
Fig. 5.143. Pyrolysates of olibanum tested for their antioxidative effect. Samples **1:** *B. carterii*, **2:** *B. serrata*, **3:** *B. frereana*, **4:** *B. neglecta*, **5:** *B. rivae*. HPTLC LiChrospher® Si 60F$_{254S}$ (Merck) plates, mobile phase: cyclohexane:ethylacetate (8:2), development distance : 7 cm. **A:** UV detection at 254 nm., **B:** Detection at daylight after derivatisation with anisaldehyde spray solution with subsequent heating at 105°C., **C:** Detection at daylight after DPPH derivatisation. Bands **a:** Nortriterpenes (8-12), verticilla-4(20),7,11-triene, cembrene A, cembrene C, isocembrene, cembrene **b:** Incensyl acetate, **c:** 24-Norursa-3,12-dien-11-one, **d:** Incensole, **e:** Nortriterpenes (8-12), m-camphorene, p-camphorene, cembrene A, α-amyrin, β-amyrin, **f:** Cembrenol, **g:** Dimers of α-phellandrene, α-amyrin, **h:** Lupeol, **i:** α-amyrin, β-amyrin, *epi*-α-amyrin, 3,12-dien-α-amyrin, 3,12-dien-β-amyrin, **j:** Nortriterpenes (8-12), α-amyrin, β-amyrin, *epi*-β-amyrin.

6 Discussion

The concern of this study was the chemical investigations performed on different types of olibanum resins. Olibanum (weihrauch) is an oleo-gum resin that exudes from incisions in *Boswellia* species, a tree endemic to North Africa, the Arabian Peninsula and India.

In this study the essential oils, acid fractions and pyrolysis fractions of *Boswellia carterii*, *B. serrata*, *B. frereana*, *B. neglecta* and *B. rivae* were investigated with various chemical methods including GC, GC-MS, SPME, TLC, pyrolysis-GC-MS and a newly designed SPA method for the analysis of pyrolysates. Additionally, these preparations were subjected to pharmacological tests for their antibacterial and antioxidative effects.

The commercial and pharmacological importance of olibanum demands a rapid identification of the origin of the resin. Therefore the identification of diagnostic markers of authentic samples acquired considerable attention.

The essential oils that were prepared by hydrodistillation of the *Boswellia* species showed typical constituents in their GC and TLC investigations. These diterpenoic constituents were recognized to be diagnostic markers for each species.

The presence of three diterpenoic constituents in *B. carterii* which are verticilla-4(20),7,11-triene (**1**), that was isolated for the first time in this study, cembrene A as well as incensole and incensole acetate (**2**) provided an immediate recognition of this resin from the other species on TLC plates. Earlier reports indicated octylacetate as the major constituent of the resin which was also detected in GC investigations as the most concentrated peak in the oil. But most important of all the acrid odour of this substance provided also a physical differentiation of the resin.

The diagnostic markers for *B. serrata* were detected as cembrene A, m-camphorene (**4**), p-camphorene (**5**) and most importantly cembrenol (**6**), a diterpenoic alcohol that existed only in this India originated olibanum type. Compounds **4** and **5** were known to be the constituents of hop oil but they were identified in *B. serrata* for the first time.

The essential oil analysis of *B. serrata* indicated the presence of a monoterpenoic constituent, 5,5-dimethyl-1-vinylbicyclo-[2.1.1]hexane (**3**) which was detected in the essential oil of *Mentha cardiaca* before. It was isolated and identified from *B. serrata* for the first time. In addition to these, *B. serrata* was recognized to be the only species that contained a number of sesquiterpenoic constituents in its essential oil.

The GC investigations of the essential oils of *B. frereana*, *B. neglecta* and *B. rivae* showed that these oils were composed of a high number of monoterpenoic constituents. Nevertheless, *B. frereana* was recognizable because of its diterpenoic constituent. Isomers of the dimer of α-phellandrene (**7**) were detected both on GC and TLC investigations in the essential oil of *B.*

frereana (**Fig. 6.1**). Additionally, *B. frereana* was found to be the softest resin of these five samples which might be helpful for a physical classification.

Verticilla-4(20),7,11-triene (**1**)   Incensole   Incensole acetate (**2**)

5,5-Dimethyl-1-vinylbicyclo-[2.1.1]hexane (**3**)   m-Camphorene (**4**)   p-Camphorene (**5**)

Cembrene A   Cembrenol (**6**)   α-Phellandrene dimer (**7**)
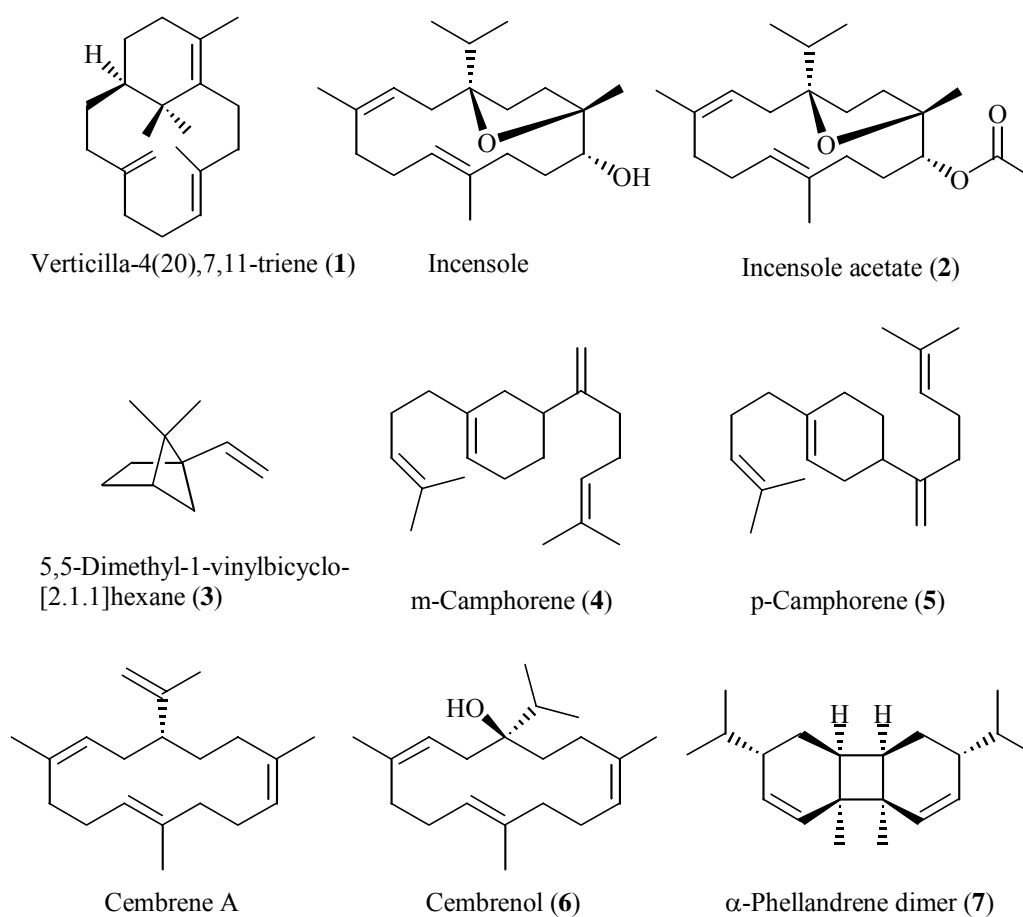
Fig. 6.1. The isolated and identified constituents from the essential oil of *Boswellia* species.

The fragrance of the resin was tried to be identified by SPME experiments. The high concentration of octylacetate in *B. carterii* resulted in the acrid odor of this resin. The resin of *B. serrata* was identified by the mixture of myrcene and methylchavicol where as *B. frereana* by α-pinene, p-cymene and bornylacetate. The experiments performed at high temperatures produced comparable results to the composition of the essential oils.

Not only has the identification of the essential oils but also the acid fractions of the resin samples had considerable importance. The "*boswellic acids*" were identified in olibanum as pentacyclic triterpenoic acids which follow the ursane and oleanane basic skeletons.

Recently, their antiinflammatory activity against 5-lipoxygenase, an enzyme that induces the production of LTA_4-E_4 type leukotrienes, was proved. However, the phytopharmaceuticals prepared from olibanum could not show a reproducible and constant effect in each batch.

During the standardization of these drugs some points concerning the differences caused in the quality of the resin such as the harvesting time, harvesting periods from the same tree, the methods used in the preparation of the acid fraction from olibanum, the identification of the labile constituents, the experimental conditions in which the resin constituents are not stable, should be clarified.

The investigations performed in this study were planned to focus on the changes caused by the different preparation methods of acid fractions and stability of the constituents of these fractions.

In the first step acid fractions of *B. carterii* and *B. serrata* were prepared according to different methods recognized in the earlier studies.

Five of these methods involved primarily the use of different basic solutions, KOH, NaOH, $Mg(OH)_2$ and $Ba(OH)_2$. A final preparation of the acid fractions was the separation of the acidic constituents from the resin material by the use of anion-exchange resin. All these methods were performed to compare the results by GC and TLC investigations in which the alterations on the boswellic acids could be detected.

The basic extraction procedures were mainly composed of three steps. The formation of the salt of the acids is followed by the acidification of these salts and subsequently, the reextraction of the acids by an organic solvent. However, the resulting gas chromatograms showed some alterations in the composition of these constituents and their concentrations. In these investigations it was observed that 10% KOH extraction gave the best acid fraction composition of both *B. carterii* and *B. serrata*.

A better visualisation of these alterations was observed by TLC investigations. In the acid fractions prepared by $Mg(OH)_2$ and $Ba(OH)_2$ new bands were observed at R_f: 0.43. In the other cases the appearance of the bands at R_f: 0.26 (over KBA) as the plate exposed to high temperatures (120 °C) after development. These observations pointed to an artifact formation that was subsequently identified by "*stress tests*".

The stability of the acidic constituents of olibanum was examined by treating a polar extract of the resin with basic solutions and exposing this extract to acid vapour and heat separately. Eventually each step of the basic extraction methods were tested for the artifact formation. All these results were compared with an acid fraction determined by anion-exchange resin elution.

As a result of these "*stress tests*" it was proposed that in the group of boswellic acids the constituents that has a hydroxy or methoxy functionality at C-11 caused the artefact formation. Dehydration caused by HCl was represented with a band on TLC plate at R_f: 0.43 whereas the dehydration caused by heat (120 °C) after the development showed a band at R_f: 0.26. Their detection under UV at 254 nm indicated an increase in the conjugation leading to an increase in the absorption of the molecule. The formation of these bands was also detected

by multiwave scans of the TLC plates. An additional 2-D TLC experiment proved that these two bands could be related to each other.

The effect of HCl vapour was compared with the effect of other acidic reagents used in different steps of these investigations. Acetic acid was used in the regeneration of the triterpenoic acids during anion-exchange extraction whereas formic acid was used in the mobile phase for the development of the plates. The effect of both acids was found negligible compared to HCl.

The investigations on the acid fractions of olibanum showed that *B. carterii* and *B. serrata* are the only species that have boswellic acids in content. Three tirucallic acid derivatives were also observed in both resins (**Fig. 6.2**). However, the presence of α- and β-amyrin derivatives was detected in *B. serrata* in addition.

α-Boswellic acid

R₁ = OH, R₂, R₃ = H $\quad$ β-Boswellic acid
R₁ = OH, R₂ = OH, R₃ = H $\quad$ 11-Hydroxy-β-boswellic acid
R₁ = OAc, R₂ = OH, R₃ = H $\quad$ 3-*O*-Acetyl-11-hydroxy-β-boswellic acid
R₁ = OAc, R₂, R₃ = H $\quad$ 3-*O*-Acetyl-β-boswellic acid
R₁ = OH, R₂, R₃ = O $\quad$ 11-Keto-β-boswellic acid
R₁ = OAc, R₂, R₃ = O $\quad$ 3-*O*-Acetyl-11-keto-β-boswellic acid

R = OH $\quad$ 3-Hydroxy-8,24-dien-tirucallic acid
R = OAc $\quad$ 3-*O*-Acetyl-8,24-dien-tirucallic acid
R = O $\quad$ 3-Oxo-8,24-dien-tirucallic acid
$\quad\quad\quad$ (3-Oxoelema-8,24-dien-21-carbonic acid)

Fig. 6.2. Tetra- and pentacyclic triterpenoic acids in olibanum.

B. frereana, *B. neglecta* and *B. rivae* showed totally different compositions than the former resin samples in their acid fractions prepared by 10% KOH method.

Lupeol and *epi*-lupeol detected in the acid fraction of *B. frereana* where lupeol was recognized as another diagnostic marker for this species. On the other hand, *B. neglecta* and *B. rivae* were found to contain mainly α- and β-amyrin and their derivatives. Surprisingly, in all three species α- and β-boswellic acids were detected at low concentrations. However, *B. rivae* was found to contain the highest amount of these triterpenoic acids.

The identification of the acidic constituents was performed by GC and GC-MS after silylation of the prepared fractions. During these analyses the MS of the single constituents indicated that the RDA reaction occurs in 12-ursene and 12-oleanene type of pentacyclic triterpenes primarily. The RDA fragment including ring D and E of both type of compounds altered only in the position of a single methyl group at C-20. With 12-ursene type of triterpenes C-17, C-19 and C-20 were occupied with methyl groups whereas with 12-oleanene types C-20 was occupied with two methyl groups.

The signal for this RDA fragment was found to be equal in abundance for both types of compounds. However, in this study, the decisive difference was observed as a result of a methyl cleavage from this fragment. The tertiary carbenium ion formed in oleanane type of triterpenes were found to be more stable than the secondary carbenium ion formed in ursane type of triterpenes as a result of this methyl cleavage. This stability difference was reflected to the intensity of the signals representing these ions. Not only with boswellic acids but also the reference substances, α- and β-amyrin, showed the same effect in GC-MS investigations.

The pyrolysis fractions of *Boswellia* species were determined by a new designed solid phase adsorption set-up. The pyrolysates were adsorbed on Super Q® phase by vacuum emission after the resin granules came in contact with red-hot charcoal. The investigation of the pyrolysates was performed by GC and GC-MS.

In the pyrolysate of *B. carterii* and *B. serrata* the stability of the diterpenoic constituents was found intriguing. Dehydration, deacetylation reactions that accompanied by decarboxylation of boswellic acids was found to contribute to the formation of newly identified nor-triterpenoic constituents. The isolations of these constituents were achieved by TLC performed at different temperatures. 24-Norursa-3,12-diene (**8**) was isolated from a natural source for the first time. 24-Norursa-3,12-dien-11-one (**13**) was isolated and identified for the first time in this study (**Fig. 6.3**).

These results were compared with conventional analysis techniques. The *Curie*-point (670 °C) pyrolysis-GC/MS investigations were performed on *B. carterii* and *B. serrata* resins. Even at these high temperatures the thermal stability of the diterpenoic constituents, verticilla-4(20),7,11-triene (**1**), incensole, incensole acetate (**2**), cemberene, cembrene C in *B. carterii* and m-camphorene (**4**), p-camphorene (**5**) as well as cembrenol (**6**) in *B. serrata*, was found surprising.

24-Norursa-3,12-diene   24-Norursa-3,12-dien-11-one
(8)   **(13)**
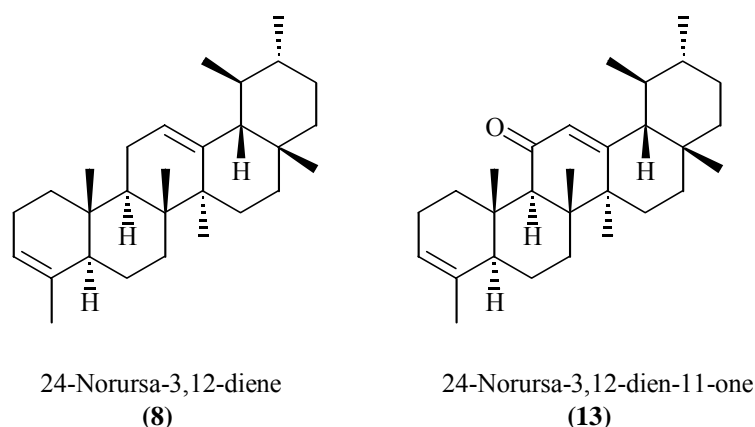
Fig. 6.3. The nortriterpenes isolated and identified from the pyrolysate of *B. carterii*.

The pyrolysates of *B. frereana* and *B. neglecta* were determined with SPA set-up. They showed nearly no changes in their composition, none of the nortriterpenes were observed in the analysis of these species.

Most surprisingly, in the pyrolysate of *B. rivae* the presence of the nortriterpenes (**8-12**) were detected as well as amyrin derivatives. This observation was interesting when the presence of only α- and β-boswellic acids in its acid fraction considered. The formation of the compounds (**10-12**) in the pyrolysate indicated that the other members of the boswellic acids were also present in this resin but most probably in trace amounts. Nevertheless, KBA and AKBA should be excluded since the pyrolysis product of AKBA and KBA, 24-norursa-3,12-dien-11-one (**13**) was not detected in the pyrolysate of *B. rivae*.

The pharmacological tests on olibanum were performed for the detection of antibacterial and antioxidative activity of the different resin fractions prepared in this study.

The antibacterial activity against *Bacillus subtilis* was found to be in essential oils only in *B. carterii*. Verticilla-4(20),7,11-triene (**1**) and incensole acetate (**2**) were detected as active substances.

The acid fractions of *B. carterii* and *B. serrata* showed high antibacterial effects. In *B. carterii* AKBA, α- and β-BA and 3-oxo-TA, in *B. serrata* in addition to these KBA showed a moderate activity. Artifacts formed in *B. serrata* because of the HCl treatment during the determination of the acid fraction surprisingly showed inhibition zones against *B. subtilis*. The presence of α- and β-BA in *B. rivae* was observed once more with this experiment with the formation of inhibitory zone.

During the testing of the pyrolysates of olibanum species, *B. carterii* showed inhibition zones for 24-norursa-3,12-diene (**8**) and incensole acetate (**2**) as well as cembrene A. The active zones in the pyrolysate of *B. serrata* that corresponded to **8** and cembrene A confirmed this activity. *B. frereana* showed no inhibition zone for lupeol but weak activity of amyrin

derivatives which was also detected as in the case of *B. neglecta*. *B. rivae*, however, presented a stronger activity because of the presence of **8** in its pyrolysate.

The radical scavenging effect against DPPH was observed for the antioxidative tests. Both essential oils and pyrolysates showed weak effects in *B. serrata*, *B.frereana* and *B. neglecta*. The acid fractions of olibanum resins were found to be totally inactive in this case.

7 Summary

In this study, essential oils, acid fractions, and pyrolysates of *Boswellia carterii, B. serrata, B. frereana, B. neglecta* and *B. rivae* were investigated. In addition, antibacterial and antioxidative activities of these samples were tested.

Investigations on the essential oils, which were carried out by GC, GC-MS, and TLC, led to the identification of the diagnostic markers for each species. During these investigations, a diterpenoic constituent of *B. carterii*, verticilla-4(20),7,11-triene (**1**), was isolated and identified for the first time from a natural source. In addition, 5,5-dimethyl-1-vinylbicyclo-[2.1.1]hexane (**3**), m-camphorene (**4**), p-camphorene (**5**) from *B. serrata*, and a dimer of α-phellandrene (**7**) from *B. frereana* were isolated and identified in *Boswellia* for the first time (**Fig. 6.1**).

SPME investigations, performed on the essential oils and resin samples, showed that the major constituents are predominantly responsible for the fragrance of olibanum.

The acid fractions of olibanum were investigated by GC or GC-MS after derivatisation. The stability of these fractions was checked by the application of "*stress tests*" by 1- or 2-D TLC. Acid fractions were prepared using various published methods and compared with own investigations. The results allowed the identification of artifacts in these extracts and - moreover- the reaction step in the procedure causing the formation of these artifacts, especially when HCl was used even in small amounts. These results were considered as decisive facts in quality control of the phytopharmaceuticals involving boswellic acids.

The investigations on acid fractions of olibanum by GC and GC-MS also showed that only *B. carterii* and *B. serrata* contain derivatives of pharmacologically active boswellic acids and tirucallic acids, whereas in *B. frereana* lupeol and *epi*-lupeol were detected. Derivatives of α- and β-amyrin were formed in *B. neglecta* and *B. rivae*. Among these three species, *B. rivae* was the only one that also contained small amounts of α- and β-BA.

In order to obtain toxicologically relevant data, pyrolysates of olibanum originating from incensing were collected by a newly designed solid phase adsorption set-up where the pyrolysates were adsorbed on Super Q$^{®}$ phases. The investigations were performed by GC and GC-MS. The formation of nortriterpenoic constituents was observed as a result of dehydration, deacetylation reactions accompanied by decarboxylation of boswellic acids in *B. carterii* and *B. serrata*. The isolation of 24-norursa-3,12-diene (**8**) directly from the pyrolysate was achieved by CC and TLC at different temperatures. In addition, 24-norursa-3,12-dien-11-one (**13**) (**Fig. 6.3**) was isolated and identified for the first time in this study. Moreover, the stability of the diterpenoic constituents of these species even at high temperatures were surprising. The results were compared with *Curie*-point (670 °C) pyrolysis-GC-MS and found consistent.

The antibacterial activity of olibanum was tested for *Bacillus subtilis* by using a Biodip test-kit. Among the essential oils, only that of *B. carterii* showed antibacterial activity for verticilla-4(20),7,11-triene (**1**) and incensyl acetate (**2**).

The acid fractions of *B. carterii* and *B. serrata* showed high antibacterial effects for AKBA, α- and β-BA and 3-oxo-8,9,24,25-tetradehydro-TA whereas KBA exhibited a moderate activity (**Fig. 6.2**).

Both *B. carterii* and *B. serrata* pyrolysates, showed inhibition zones for 24-norursa-3,12-diene (**8**) and cembrene A. In addition, incensyl acetate (**2**), present in the pyrolysate of *B. carterii* had showed an antibacterial activity. In contrast, the pyrolysates of *B. frereana* and *B. neglecta* were found to be inactive. These results could support the successful use of certain *Boswellia* resins as a desinfectant in traditional ceremonies.

Antioxidative activities were tested with DPPH. Both essential oils and pyrolysates of olibanum species showed no relevant effects for *B. serrata*, *B. frereana* and *B. neglecta*. The acid fractions of olibanum resins were found to be inactive under the conditions tested.

8 Zusammenfassung

In Rahmen dieser Arbeit wurden die etherischen Öle, die Säurefraktionen und die Pyrolysate von *Boswellia carterii*, *B. serrata*, *B. frereana*, *B. neglecta* und *B. rivae* untersucht. Zusätzlich wurden die Proben biologischen Tests unterzogen, um eine mögliche antibakterielle und antioxidative Wirkung aufzuzeigen.

Die etherischen Öle zeigten in den DC- und GC -Untersuchungen artspezifische Unterschiede hinsichtlich ihrer Inhaltsstoffe. Als taxonomische Marker konnten für jede *Boswellia*-Art bestimmte Diterpene erkannt werden. Verticilla-4(20),7,11-trien (**1**) wurde zum ersten Mal in dieser Studie aus *B. carterii* isoliert. Zusätzlich wurden 5,5-Dimethyl-1-vinylbicyclo[2.1.1] hexan (**3**), m-Camphoren (**4**), p-Camphoren (**5**) aus *B. serrata* sowie ein Dimer von α-Phellandren (**7**) aus *B. frereana* erstmals aus Boswellia-Arten isoliert (**Fig. 6.1**).

Mit Hilfe von SPME-Headspace Untersuchungen, die mit den etherischen Ölen und Harzproben durchgeführt wurden, konnten die charakteristischen Komponenten identifiziert werden, die für den "Duft" von Olibanum verantwortlich sind.

Anders als üblich wurde das Muster der nichtflüchtigen Boswelliasäuren nach Derivatisierung dieser Fraktionen mittels GC und GC-MS untersucht. Die Stabilität der Säurefraktionen wurde mit Hilfe von "*Stresstests*" dünnschichtchromatographisch bestimmt. Es konnte gezeigt werden, dass unterschiedliche Aufarbeitungsmethoden, besonderes solche, die in früheren Untersuchungen Anwendung fanden, zur Artefaktbildung führen. Diese Artefakte wurden identifiziert und darüber hinaus der Reaktionsschritt, der zu ihrer Bildung führt. Diese Ergebnisse sind wichtig für die Qualitätskontrolle entsprechender Phytotherapeutika.

Die Untersuchung der Säurefraktionen von *B. carterii* und *B. serrata* zeigte, dass nur diese beiden Arten die pharmakologisch aktiven Boswelliasäuren und Tirucalsäuren enthalten. In *B. frereana* konnten Lupeol und *epi*-Lupeol, in *B. neglecta* und *B. rivae* hauptsächlich α- und β-Amyrin-Derivate nachgewiesen werden.

Um toxikologisch relevante Daten über die Pyrolyseprodukte, die während der Inzensierung entstehen, zu erhalten, wurden diese mit einem speziell entwickelten SPA-System an Super Q$^{®}$ Phasen adsorbiert und mit Hilfe von GC und GC-MS analysiert. Bei den Boswelliasäuren von *B. carterii* und *B. serrata* führten Dehydrierungs- und Deacetylierungs-Reaktionen, begleitet von Decarboxylierungen, zur Bildung neuer Nortriterpene. Dabei wurden 24-Norursa-3,12-dien (**8**) und das entsprechende in Position 11-oxygenierte Keton (**13**) (**Fig. 6.3**) erstmals als Komponente des Pyrolysates isoliert. Die Trennung und Isolierung dieser neuen Verbindungen gelang dünnschichtchromatographisch bei tiefen Temperaturen (< -10 °C). Auffällig war die thermische Stabilität der Diterpene. Die Ergebnisse aus den SPA-Studien waren vergleichbar mit *Curie*-Punkt (670 °C) Pyrolyse-GC-MS Untersuchungen.

Mit Hilfe biologischer Tests wurden die unterschiedlichen Harzfraktionen auf ihre antibakterielle und antioxidative Aktivität überprüft.

Eine antibakterielle Wirkung der ätherischen Öle gegenüber *Bacillus subtilis* konnte nur für *B. carterii* festgestellt werden. Verticilla-4(20),7,11-trien (**1**) und Incensylacetat (**2**) wurden als die aktiven Substanzen erkannt.

Die Säurefraktionen von *B. carterii* und *B. serrata* zeigten starke antibakterielle Aktivität. Verantwortlich dafür waren AKBA, α- und β-BA und 3-Oxo-8,9,24,25-tetradehydro-TA (**Fig. 6.2**).

Die Tests der Pyrolysate von *B. carterii* zeigten für 24-Norursa-3,12-dien (**8**) eine antibakterielle Aktivität und ebenfalls für Incensylacetat (**2**) und Cembren A. Die Pyrolysate von *B. serrata* zeigten entsprechende Aktivitätszonen für 24-Norursa-3,12-dien und Cembren A. Die Pyrolysate von *B. frereana* und *B. neglecta* waren inaktiv. Diese Ergebnisse könnten die erfolgreiche Verwendung bestimmter Boswellia-Harze als „Hygiene-Hilfsmittel" während religiöser Zeremonien belegen.

Die antioxidative Aktivität wurde mit Hilfe eines DPPH-Tests untersucht. Die etherischen Öle und Pyrolysate von *B. serrata*, *B. frereana* und *B. neglecta* zeigten keine relevante Aktivität. Auch die Säurefraktionen von Olibanum zeigten in diesem Test keine Aktivität.

9 Experimental Part

9.1 Materials and Methods

9.1.1 Analytical Gas Chromatography

For analytical purposes Orion Micromat 412 gas chromatograph equipped with two 25 m long fused silica capillary columns (i.d.= 0.25 mm) which were packed with CPSil 5CB and CPSil 19CB (Chrompack) phases, respectively, with a film thickness of 0.25 μm was used.

Alternatively, a second analytical gas chromatograph Carlo Erba HRGC 4160 was used in the analysis that was equipped with 23 m fused silica capillary column (i.d.= 0.25 mm) packed with CPSil 5CB (Chrompack).

To monitor enantiomeric separations gas chromatographs from Carlo Erba series 2150 to 4160 were used. The instruments were equipped with 25 m long fused silica capillaries one of which was packed with 80% 6-methyl-2,3-pentyl-γ-CD and the other one with 50% 6-TBDMS-2,3-methyl-β-CD, in polysiloxane OV 1701.

All instruments were equipped with flame ionization detectors (FID) and split injectors with a split ratio of 1:30. Hydrogen (0.5 bars) was used as carrier gas. The injector and detector temperatures were arranged to 200 °C and 250 °C, respectively, for essential oil and SPME analysis. These values were adjusted to 250 °C for injector and 320 °C for detector for the investigation of the pyrolysates and acid fractions.

Merck-Hitachi D-2500 Integrators were used to report the retention times and integrate the peak area.

9.1.2 Preparative Gas Chromatography

Preparative separations were performed using alternatively modified Varian 1400 and Varian 2800 GCs. Both instruments were equipped with stainless steel packed columns (**Table 8.1**). Injector and detector (FID) temperatures were kept at 200 °C and 250 °C, respectively. Helium (purity factor 4.6) was used as carrier gas at a flow rate of 240 ml/min.

The principle of preparative GC can be explained as the fractionation of a sample with a simultaneous detection by means of gas chromatographic separation. The analysed sample was separated into fractions with the help of a split valve (split ratio app. 1:400) placed at the end of the column. The split valve divided the eluted samples into two parts. The small amount was led to the detector through a deactivated capillary (i.d. 0.25 mm) to monitor the gas chromatogram. Simultaneously, the rest of the substances were pointed to an exit through a silylated steel tube which was directly connected to an PTFE tube (Reichelt, 1.5 mm x 30 cm) that was cooled in a liquid nitrogen bath. The original sample was fractioned by changing

these PTFE tubes at different time intervals. Further analysis were performed on these fractions after these PTFE tubes were washed with suitable solvents.

Table 8.1. The available packed columns used in preparative GCs.

6.4% polysiloxane SE-30 on Chromosorb W-HP (4.3 mm x 1.85 m)
6.4% polysiloxane SE-52 on Chromosorb W-HP (4.3 mm x 1.85 m)
6.4% 2,6-methyl-3-pentyl-β-CD mixed with SE-52 (1:1, w/w) on Chromosorb W-HP (5.3 mm x 2.0 m)
2.5% 2,6-methyl-3-pentyl-γ-CD mixed with OV 1701 (1:1, w/w) on Chromosorb G-HP (5.3 mm x 2.0 m)
6.5% 6-TBDMS-2,3-methyl-β-CD mixed with SE-52 (1:1, w/w) on Chromosorb W-HP (5.3 mm x 1.95 m)
6% 6-methyl-2,3-pentyl-γ-CD mixed with PS-086 (1:1, w/w) on Chromosorb W-HP (5.1 mm x 2.05 m)

The gas chromatogram was recorded by a W+W Recorder 312 from W+W Electronics Scientific Instruments (Basel/Switzerland).

A third preparative GC system was composed of a Gerstel PFC preparative fraction collector coupled with an Agilent Technologies 6890N Network GC system with an autosampler Agilent 7683 Series Injector. The gas chromatograph was equipped with either 30 m megabore capillary DB 1 (Hewlett Packard/USA) column with an inner diameter of 0.53 mm and a film thickness of 5 μm or 30 m megabore capillary DB 1701 (Hewlett Packard/USA) column with inner diameter of 0.53 mm and a film thickness of 1.5 μm.

Helium was used as carrier gas in a constant flow mode at a rate of 5 ml/min. The detector (FID) and the inlet were heated to 250 and 200 °C, respectively.

The substances were divided into two deactivated capillaries by a cross split with a ratio of 1:10 at the end of the column. Through the detector control capillary (7.1 cm x 0.05 mm) which was connected to this cross split the gas chromatograms were monitored for each run. The main part of the injected sample was transferred to the fraction collector (Gerstel PFC preparative fraction collector) through the transfer capillary (80 cm x 0.45 mm) which could be heated to 50-300 °C. In the fraction collector the transfer capillary enters another splitting device which has an octagon shape and could also be heated to 50-300 °C. The subtances transferred to this splitting device were divided into six fractions through deactivated capillaries (18 cm x 0.45 mm) which were introduced to glass traps. The working principle of the splitting device was the magnetic diversion of the pressure applied in the system. This was controlled by special software that provided to programme the time intervals to divert the target fractions into different glass traps. The fractions collected in glass traps were kept at –30 °C. The last exit of the splitting device was occupied with another deactivated capillary

(18 cm x 0.45 mm) that was introduced to a glass trap at room temperature which was considered as waste.

A Controller 505 (Gerstel/Germany) had supplied the electronic control for switching the magnetic valves according to the programmed intervals.

A Julabo FP 50 Instrument (Julabo/Germany) cooled the traps down to –30 °C. Ethanol was used in the system.

9.1.3   Mass Spectrometry: GC-MS analysis

Electron impact (70 eV) GC-MS measurements were performed with a Hewlett-Packard HP 5890 gas chromatograph, that was equipped with a 25 m fused silica capillary column with polydimethylsiloxane CPSil 5CB, coupled to a VG Analytical 70-250S mass spectrometer (ion source 250 °C). A temperature program with an initial temperature of 80 °C, increased 10 °C/min up to 270 °C was used for essential oils and SPME analysis with two minutes solvent delay by injection. The injector temperature was adjusted to 200 °C for these analyses. For the analysis of pyrolysis and silylated acid fractions this program was changed to 130 °C initial temperature with an increase of 20 °C/min up to 300 °C with a solvent delay of three minutes. Injection temperature in this case was adjusted to 250 °C.

9.1.4   *Curie*-point" pyrolysis-GC-MS

The pyrolysis GC-MS was conducted with a HP 5890 Series II gas chromatograph coupled to a HP 5989A mass spectrometer. Pyrolysis was performed with a Pyromat instrument (GSG Mess- und Analysengeräte GmbH/Germany) at 670 °C for 10 seconds. The pyrolysis head was heated to 200 °C and the pyrolysis products were transferred to the injection port (270 °C) at 250 °C. The gas chromatograph was equipped with a 30 m DB-5 MS (Varian) capillary column (i.d. 0.25 mm, film thickness 0.25 μm) .

9.1.5   Solid-Phase Micro Extraction

Supelco SPME kit was used. The analysis conditions were summarized in Table 8.2.

Table 8.2.   Headspace-SPME analysis conditions of *Boswellia* species.

Adsroption phase	Analysed sample	Headspace adsorption conditions	Desorption Conditions
7 μm PDMS	1 ml hydrodistillate	1 h at room temperature	At 200 °C 2 min.
100 μm PDMS	1 gr powdered granules	1 h at room temperature	At 200 °C 2 min.
100 μm PDMS	1 gr granules	1 h heated at 150 °C	At 200 °C 2 min.
100 μm PDMS	1 gr granules	3 min 850 °C in muffle oven	At 200 °C 2 min.

The adsorption phases 7 μm PDMS was bonded whereas 100 μm PDMS was non-bonded. The bonded phases were mainly used where organic solvents involved in the experiment as in the case of the analysis of essential oils.

9.1.6 Column Chromatography and Thin Layer Chromatography

The column chromatography (CC) was performed by using Silica gel 60 (60-230 mesh) from Merck.

Thin layer chromatography was performed on glass plates of Lichrosphere® Si 60$_{F254S}$, Lichrosphere RP-18 and HPTLC Si 60$_{F254}$ and aluminium plates of Silica gel 60 F$_{254}$ (0.25 mm thick) from Merck (Darmstadt/Germany) at 20 °C generally.

For the preparative TLC separations at –25 °C the set-up and the solvents were cooled in advance. The samples were developed as usual over aluminium plates of Silica gel 60 F$_{254}$ at –25 °C.

Anisaldehyde spray solution was used for the derivatisation of the plates. This solution was prepared by mixing 0.5 ml anisaldehyde with 10 ml glacial acetic acid, 85 ml methanol and 5 ml concentrated H_2SO_4 in this order. The detection of the plates was performed at daylight after heating the plate to 105 °C until optimal coloration was observed.

The samples were applied on TLC plates by the help of Desaga AS 30 instrument. The derivatisation reagents were sprayed with Desaga DS 20 instrument. The documentation of the TLC plates were performed by video system Desaga CabUVVIS equipped with a Color Camera HV-C20E/K-S4 (Hitachi Denshi Ltd./Japan). The fotos were printed by CP700 Mitsubishi printer.

The multiwavescaning of the plates were completed by Desaga Densitometer CD 60.

9.1.7 NMR-Spectrometry

The measurements of ^{1}H-, ^{13}C- (BB, DEPT, PENDANT), HMQC, HMBC-, NOESY- spectra were performed with instruments Bruker AMX 400 (^{1}H: 400.1 MHz, ^{13}C: 100.6 MHz) and Bruker DRX 500 (^{1}H: 500.1 MHz, ^{13}C: 125.8 MHz).

Tetramethylsilane (TMS-d$_{12}$) was used as an internal standart (δ = 0.00). TMS and the deutoriated solvents (C_6D_6, $CDCl_3$) were obtained from Deutero GmbH (Kastellaun, Germany).

9.1.8 Polarimetry

Polarimetric measurements were performed with a Perkin-Elmer 341 polarimeter at a wavelength of 589 nm at 20 °C. 1 dm long cuvettes were used to measure the samples.

9.1.9 Plant Material

The resin samples which were investigated are listed in Table 8.3.

Table 8.3. The list of olibanum samples investigated in this study. WB: Willy Benecke GmbH (Hamburg/Germany), CER: C.E. Roeper (Hamburg/Germany).

Sample	Identification	Sample	Identification
O1	Olibanum granules from Caelo-*B. Carterii*	O20	WB Olibanum Somalia (7108/lot 3)
O2	Olibanum Ethiopian-*B.carterii* (certificated)	O21	CER (58.508) Olibanum 1st choice
O3	Olibanum Egypt (old product)	O22	CER (58.512) Oli. Somalia 1st choice
O4	Olibanum Egypt (new product)	O23	CER (58.500) Olibanum Sudan peasize
O5	Olibanum Oman	O24	CER (58.510) Oli. Ethiopian peasize faq.
O6	Olibanum India-*B. serrata*	O25	CER (58.446) Oli. India siftings DAB 6
O7	Olibanum from Turkey (wholesaler product)	O26	Oli. SCF ext. from Flavex Naturextrakte
O8	Olibanum India (gift from Uni. Tübingen)	O27	Oli. India from Ayfer Kaur (Turkey)
O9	Olibanum from Biomex	O28	WB Olibanum Somalia (7181/lot 0)
O10	H15 tablets	O29	WB Olibanum Somalia-Maidi (lot 112)
O11	Weihrauch capsuls	O30	WB Olibanum Indian No.1 (lot 15-11-00)
O12	Olibanum from Iraq	O31	WB Oli. Somalia No.1 (lot GT AWEIS)
O13	*B. serrata* in semi-liquid form	O32a	WB Olibanum Somalia (7181/ lot 2 pale)
O14	WB Olibanum Somalia No.1 (7181/lot 5)	O32b	WB Olibanum Somalia (7181/ lot 2 dark)
O15	WB Olibanum Somalia dark (7182/lot 2)	O33	WB Olibanum Sudan (6985/ lot 33-1)
O16	WB Olibanum Somalia No.1 (7181/lot 2)	O34	Olibanum oil-*B. thurifera* (England)
O17	WB Olibanum India lot LE 1487 (*B.serrata*)	O35	*B. neglecta* from Ethiopia
O18	WB olibanum Sudan No.1 (6891/lot 5)	O36	*B. rivae* from Ethiopia
O19	WB Oli. Somalia-Aden-Kenia (7181/ lot 1)		

Five master samples were chosen for further analysis. O2 was found to be a typical sample for *B. carterii* was obtained from Ethiopia (Certificate no. 002424 of the Agricultural and Crop Protection Department of Ethiopia) whereas samples for *B. serrata* (O30) and *B. frereana* (O19 or O29) were determined from Willy Benecke GmbH (WB) in Hamburg/Germany. *B. neglecta* and *B. rivae* were obtained from Ethiopia as authentic samples.

9.2 Experimental Procedures

9.2.1 Determination of Essential oils

The resin material was hydrodistilled continuously for 3 hours and the essential oil was collected in 1 ml n-hexane (p.a.)

9.2.2 Determination of Acid Fractions

The acid fractions of *B. carterii* and *B. serrata* were determined with six different methods.

9.2.2.1 Acid Fraction Determined by Ba(OH)₂ Extraction

10 g olibanum resin was powdered and stirred for 48 hours in 20 ml diethylether (Et₂O). Suspension was filtered and the residue was washed with 5 ml of Et₂O for four times. To the ether extract 20 ml saturated Ba(OH)₂ aqueous solution and 1 g of Ba(OH)₂ powder were added. This mixture was stirred for 100 hours. The formation of a white precipitate was observed during stirring. The precipitate was filtered and subsequently washed with 20 ml Et₂O. The residue was let to suspend in 100 ml of Et₂O and stirred for 24 hours. The precipitate was filtered and washed with 20 ml of Et₂O once more. It was observed that the gummy character was nearly disappeared. To obtain the Ba salt of the acids the original procedure let the precipitate to dry in oven at 80°C and then powder it. However, the acid fraction was determined in this work by dissolving this precipitate in distilled water and acidifying it with aqueous solution of dilute HCl. The pH of the solution was tried to be kept at 6 during the dropwise addition of the acid solution. After pH= 6 was reached the precipitate was filtered and washed with distilled water until the decantate had a pH value of 7. The precipitate was dissolved in Et₂O and before the solvent was evaporated under vacuum the solution was filtered over anhydrous Na₂SO₄ to dry. After the evaporation of Et₂O a white powder was obtained.

9.2.2.2 Acid Fraction Determined by Mg(OH)₂ Extraction

10 g olibanum resin was extracted with 50 ml Et₂O. 200 ml saturated aqueous solution of Mg(OH)₂ and 1 g of powdered Mg(OH)₂ was added to this Et₂O extract and mixed for 24 hours. The white precipitate was filtered and brought to suspension in Et₂O for further mixing. The liquid part of this suspension was assumed to have the gummy part of the resin. The suspension was dried under vacuum to obtain Mg salts of the acids. Another suspension was prepared with the addition of bidistilled water to this salt mixture. At this point in the original procedure concentrated HCl was used for the acidification of the salt mixture to obtain a pH of 2-3. In this work the acidification was performed with diluted HCl and the

solution was controlled periodically to have a pH of 6-5. In the next step the acidified mixture was extracted with Et_2O. Subsequent elution of this Et_2O fraction over anhydrous Na_2SO_4 was followed by the evaporation of Et_2O.

9.2.2.3 Acid Fraction Determined by NaOH Extraction

10 g olibanum was extracted with 100 ml Et_2O. The Et_2O extract was stirred with 30 ml 2M NaOH for three times. The aqueous layer was separated and acidified with HCl. In this method also the use of concentrated acid was avoided as given in the procedure. Instead dilute HCl was used for acidification as mentioned in former procedures. After acidification the solution was extracted with Et_2O. Drying the Et_2O fraction over anhydrous Na_2SO_4 was followed by the evaporation of the solvent and the mixture of acids were obtained as white powder.

9.2.2.4 Acid Fraction Determined by 10% KOH Extraction

10 g olibanum was extracted with 100 ml Et_2O. The extract was mixed with 40 ml 10% KOH aqueous solution for two times. The dark orange suspension was separated from the mixture. The fraction was acidified with 3M HCl to pH 5. The organic acids were extracted with 30 ml CH_2Cl_2 for three times. The CH_2Cl_2 extract was washed with distilled water until the aquous part of this mixture had a neutral pH value. The resulting extract was dried over anhydrous Na_2SO_4 and the solvent was evaporated to obtain a white powder of acid mixture.

9.2.2.5 Acid Fraction Determined by 2% KOH Extraction

10 g olibanum was extracted with 50 ml methanol for three times. After filtration the extract was concentrated to nearly 30 ml until it becomes a thick solution. This concentrated solution was dissolved in 100 ml of 2% KOH aqueous solution and extracted with 30 ml ethylacetate five times. The aqueous phase was separated and neutralized with 2% HCl to pH = 6. The acidic constituents were separated by a 30 ml ethylacetate extraction five times. The organic phase was washed with distilled water, then dried over anhydrous Na_2SO_4 and finally the solvent was evaporated to dryness.

9.2.2.6 Acid Fraction Determined by Using Anion-Exchange Resin

100 ml Amberlite[©] 900 (Supelco) anion-exchange resin was conditioned with 10% NaOH aqueous solution in a 500 ml glass beaker. The resin was washed with ethanol:water gradient to elute the excess base until the decantate was neutralised. A 100 ml ethanol extract was prepared from 10 g olibanum. 1 ml of this extract was applied on already conditioned anion-

exchange resin and stirred for 15 minutes. The decantate was filtered and the resin was washed with fresh ethanol until no spots were observed on control TLCs. The acids were extracted with 10% acetic acid in ethanol. The solvent was evaporated to obtain the acid fraction of olibanum.

9.2.2.7 Silylation of the Acid Fractions

The silylation of the samples was achieved by the addition of 100 µl MSTFA to 100 µg powdered sample. In the case of liquid samples 100 µl MSTFA was added to 100µl sample after the sample was dried. After the addition of the reagent, the sample was kept overnight at room temperature to react. The silylated samples were kept at –25°C to avoid decompositions for further investigations.

9.2.2.8 Pyridinium dichromate (PDC) Oxidation of Secondary Alcohols

α-Amyrin and β-amyrin were oxidized with PDC to obtain α- and β-amyrenone. To 1 mg of α-amyrin in dry CH_2Cl_2 1 mg of PDC was added and the mixture was stirred at room temperature for 3 hours. Molecular sieve can be used in the reaction mixture to avoid moisture. The reaction mixture was diluted with 20 ml Et_2O, filtered through a short column of Florisil (Merck). The eluate was dried over $MgSO_4$, filtered and the solvent was evaporated to give α-amyrenone.

9.2.3   Determination of Pyrolysis Fractions

A SPA set-up was designed for the determination of the pyrolysates. 10 cm glass cartridges were filled with approximately 100 mg Super Q[®] adsorbent (AllTech Chemicals) and the adsorbent was fixed with silylated glasswool from both ends of the cartridges. Three of these cartridges were positioned across the openings of the censer by the help of a metal support similar to "spider legs". The other ends of the cartridges were connected with silicon tubes to a vacuum applier.

As the resin granules were spread over red-hot coal that was placed in the censer, the smoke formation was observed. These pyrolysis products were adsorbed on the Super Q phases by the application of 500 mbars of vacuum until no more smoke formation observed in the censer.

The analyses of the pyrolysates were performed by GC and GC-MS after the glass cartridges were washed with diethylether to prepare an extract of these products.

9.2.4 Pharmacological Tests

9.2.4.1 Antibacterial Activity Tests

These analyses were performed with the Chrom Biodip® Antibiotics test kit from Merck.

9.2.4.2 Antioxidative Activity Tests

The potent radical scavenger compounds of olibanum were determined by spraying methanolic solution of DPPH (2,2-diphenyl-1-picrylhydrazil, 95%) (Fluka) (2 mg/10 ml) over the developed TLC plate, to detect subsequently the formation of white inhibition zones on blue-violet background.

9.3 Characterisation of the Isolated Compounds

Verticilla-4(20),7,11-triene (1):

^{1}H-NMR (500 MHz, C_6D_6): δ 0.95 (3H, s, H-17), 1.02 (3H, s, H-16), 1.54 (3H, s, H-19), 1.60 (3H, s, H-18), 5.18 (1H, dd, J = 5.9, 3.9 Hz, H-7), 4.83 (1H, s, H-20), 4.80 (1H, s, H-20), 2.81 (1H, ddd, J = 15.1, 10.5, 4.1 Hz, H-3b), 2.45 (1H, dt, J = 4.1, 12.6 Hz, H-9b), 2.29-1.96 (11H, m), 1.80-1.68 (2H, m), 1.44-1.40 (2H, m).

^{13}C-NMR (125 MHz, C_6D_6): δ 16.79 (q, C-19), 21.01 (q, C-18), 25.84 (t, C-14), 26.11 (t, C-10), 26.86 (q, C-17), 29.94 (t, C-16), 30.71 (t, C-13), 31.96 (t, C-2), 32.97 (t, C-3), 33.38 (q, C-16), 36.56 (t, C-5), 37.58 (s, C-15), 39.57 (t, C-9), 44.09 (d, C-1), 108.94 (t, C-20), 128.03 (s, C-12), 130.00 (d, C-7), 133.47 (s, C-8) 136.85 (s, C-11), 153.34 (s, C-4).

Mass (EI, 70 eV), m/z (rel.int.): 272 [M]$^+$(20), 257 (75), 243 (2), 229 (16), 216 (5), 201 (15), 189 (35), 173 (19), 161 (36), 147 (38), 133 (100), 121 (73), 107 (61), 93 (64), 79 (56), 67 (54), 55 (60), 41 (89).

Incensole acetate (2):

^{1}H-NMR (500 MHz, C_6D_6): δ 0.88 (3H, d, J = 6.9 Hz), 0.93 (d, J = 6.9 Hz), 1.18 (3H, s), 1.61 (3H, s), 1.66 (3H, s), 1.71 (3H, s), 5.13 (1H, d, J = 10.1 Hz), 5.40 (1H, dd, J = 12, 6.1 Hz), 5.47 (1H, m), 1.46-1.53 (1H, m), 1.53-1.59 (3H, m), 1.83-1.94 (2H, m), 1.96-2.02 (3H, m), 2.01-2.07 (1H, m), 2.14-2.28 (6H, m).

^{13}C-NMR (125 MHz, C_6D_6): δ 16.24 (q, C-18), 17.81(q, C-19) 18.10 (q, C-17), 18.23 (q, C-16), 20.84 (q, C-22), 22.37 (q, C-20), 25.31 (t, C-6), 28.29 (t, C-10), 30.85 (t, C-14), 32.34 (t, C-2), 33.91 (t, C-9), 35.46 (d, C-15), 35.88 (t, C-13), 38.94 (t, C-5), 75.46 (d, C-), 76.45 (d,

C-11), 83.49 (s, C-12), 89.41 (s, C-1), 121.51 (d, C-3), 126.01 (d, C-7), 133.29 (s, C-8), 135.31 (s, C-4), 170.34(s, C-21).

Mass (EI, 70 eV), m/z (rel.int.): 348 $[M]^+$ (10), 305 (2), 288 (8), 245 (6), 150 (24), 135 (16), 121 (22), 107 (19), 93 (32), 81 (42), 71 (80), 55 (36), 43 (100).

5,5-Dimethyl-1-vinylbicyclo-[2.1.1]hexane (3):

^{1}H-NMR (500 MHz, C_6D_6): δ 0.69 (3H, s), 0.89 (1H, d, J = 7.25 Hz), 1.08 (3H, s), 1.94 (1H, s), 5.02 (1H, dd, J_{trans} = 15.7, J_{gem} = 2.2 Hz), 5.08 (1H, dd, J_{cis}= 11.3, J_{gem} = 2.2), 5.88 (1H, dd, J_{trans} = 17, J_{cis} = 10.7 Hz), 1.49-1.54 (2H, m), 1.61-1.68 (2H, m), 1.98-2.02 (1H, m).

^{13}C-NMR (125 MHz, C_6D_6): δ 19.39 (q, C-9), 19.83 (q, C-10), 26.55 (t, C-2), 30.43 (t, C-3), 39.12 (t, C-6), 44.44 (d, C-4), 47.0 (s, C-5), 56.2 (s, C-1), 115.15 (t, C-8), 137.91 (s, C-7).

Mass (EI, 70 eV), m/z (rel.int.): 136 $[M]^+$ (2), 121 (20), 108 (24), 93 (100), 79 (40), 77 (42), 69 (60), 67 (62), 55 (15), 53 (16), 41 (80).

m-Camphorene (4):

^{1}H-NMR (500 MHz, C_6D_6): δ 1.60 (3H, s), 1.61 (3H, s), 1.68 (6H, s), 4.75 (1H, s), 4.76 (1H, s), 5.39 (1H, s), 5.10 (1H, dd, J = 6.9, 6.6 Hz), 5.12 (1H, dd, J = 6.3, 6.3 Hz), 1.33-1.41 (1H, m), 1.75-1.77 (1H, m), 1.85-1.91 (1H, m), 1.94-1.99 (2H, m), 2.02-2.05 (1H, m), 2.06-2.08 (5H, m), 2.11-2.15 (3H, m).

^{13}C-NMR (125 MHz, C_6D_6): δ 17.70 (q, C-20), 17.72 (q, C-12), 25.70 (q, C-11, C-19), 25.87 (t, C-8), 26.54 (t, C-3), 26.87 (t, C-15), 28.01 (t, C-6), 34.62 (t, C-4), 34.87 (t, C-14), 37.87 (t, C-7), 40.41 (d, C-5), 107.16 (t, C-18), 120.29 (d, C-2), 124.34 (d, C-16), 124.43 (d, C-9), 131.35 (s, C-10), 131.51 (s, C-17), 137.51 (s, C-1), 154.45 (s, C-13).

Mass (EI, 70 eV), m/z (rel.int.): 272 $[M]^+$ (8), 257 (4), 229 (10), 203 (8), 187 (6), 161 (10), 147 (10), 133 (10), 119 (24), 105 (22), 91 (37), 79 (20), 69 (100), 55 (15), 41 (77).

p-Camphorene (5):

^{1}H-NMR (500 MHz, C_6D_6): δ 1.60 (3H, s), 1.61 (3H, s), 1.68 (6H, s), 4.74 (1H, s), 4.76 (1H, s), 5.41 (1H, s), 5.10 (1H, m), 5.12 (1H, m), 1.41-1.49 (1H, m), 1.79-1.84 (1H, m), 1.87-1.91 (1H, m), 1.93-1.96 (2H, m), 2.00-2.02 (1H, m), 2.04-2.07 (5H, m), 2.10-2.14 (4H, m).

^{13}C-NMR (125 MHz, C_6D_6): δ 17.70 (q, C-12), 17.72 (q, C-20), 25.69 (q, C-11, C-19), 26.53 (t, C-8), 31.44 (t, C-3), 26.86 (t, C-15), 29.09 (t, C-6), 40.00 (d, C-4), 34.89 (t, C-14), 37.61 (t, C-7), 28.37 (t, C-5), 107.09 (t, C-18), 120.40 (d, C-2), 124.35 (d, C-16), 124.43 (d, C-9), 131.50 (s, C-10), 131.35 (s, C-17), 137.43 (s, C-1), 154.34 (s, C-13).

Mass (EI, 70 eV), m/z (rel.int.): 272 [M]$^+$ (10), 257 (5), 229 (16), 203 (8), 187 (6), 161 (14), 147 (14), 133 (19), 119 (22), 105 (24), 93 (63), 79 (25), 69 (100), 55 (18), 41 (77).

α-Phellandrene Dimer (7):

^{1}H-NMR (500 MHz, C$_6$D$_6$): δ 0.91 (6H, d, J = 6.9 Hz), 0.92 (6H, d, J = 6.6 Hz), 1.03 (6H, s), 5.65 (2H, dd, J = 10.40, 2.3 Hz), 5.73 (2H, J = 10.40 Hz), 1.15 (2H, t, J = 11.7 Hz), 1.49 (2H, dd, J = 5.6, 11.6), 1.56-1.62 (2H, m), 1.99-2.02 (2H, m), 2.03 (2H, s).

^{13}C-NMR (125 MHz, C$_6$D$_6$): δ 19.48 (q, C-15, C-17), 19.69 (q , C-14, C-18), 22.26 (q , C-19, C-20), 22.69 (t, C-1, C-10), 32.17 (d, C-13, C-16), 37.78 (d, C-2, C-9), 37.96 (d, C-12, C-11), 129.92 (d, C-3, C-8), 134.89 (d, C-4, C-7), 43.84 (s, C-5, C-6).

Mass (EI, 70 eV), m/z (rel.int.): 272 [M]$^+$ (1), 136 (46), 105 (3), 93 (100), 77 (16), 55 (2), 43 (8).

24-Norursa-3,12-diene (8):

^{1}H-NMR (500 MHz, C$_6$D$_6$): δ 0.92 (3H, s), 0.96 (3H, s), 1.15 (3H, s), 1.16 (3H, s), 1.68 (3H, s), 0.97 (3H, d, J = 6.6 Hz), 0.98 (3H, d, J = 6.6 Hz), 5.26 (1H, bs), 5.34 (1H, dd, J = 6.8, 2.8 Hz), 0.87-0.89 (2H, m), 0.96-1.00 (1H, m), 1.00-1.02 (1H, m), 1.27-1.38 (5H, m), 1.40-1.44 (3H, m), 1.48-1.52 (2H, m), 1.60-1.66 (2H, m), 1.73-1.76 (1H, m), 1.87-1.90 (1H, m), 1.95-1.97 (3H, m), 2.02-2.06 (2H, m).

^{13}C-NMR (125 MHz, C$_6$D$_6$): δ 13.22 (q, C-24), 17.92 (q, C-29), 18.18 (q, C-26), 20.99 (t, C-6), 21.89 (q, C-28), 22.08 (q, C-23), 23.49 (t, C-2), 23.85 (q, C-25), 24.58 (t, C-11), 27.20 (t, C-15), 28.79 (t, C-16), 29.38 (q, C-27), 31.91 (t, C-21), 33.10 (t, C-7), 34.39 (s, C-17), 35.81 (s, C-10), 36.85 (t, C-1), 40.22 (d, C-20), 40.33 (d, C-19), 40.75 (s, C-8), 42.19 (t, C-22), 42.96 (s, C-14), 44.97 (d, C-9), 49.32 (d, C-5), 59.89 (d, C-18), 121.00 (d, C-3), 125.72 (d, C-12), 135.34 (s, C-4), 140.54 (s, C-13).

Mass (EI, 70 eV), m/z (rel.int.): 394 [M]$^+$ (6), 379 (4), 218 (100), 203 (23), 189 (18), 175 (16), 161 (16), 147 (13), 133 (16), 122 (18), 107 (17), 95 (17), 81 (14), 67 (8), 55 (15), 41 (14).

24-Norursa-3,12-dien-11-one (13):

^{1}H-NMR (500 MHz, C$_6$D$_6$): δ 0.73 (3H, d, J = 6.3 Hz), 0.86 (3H, d, J = 6.6 Hz), 0.75 (3H, s), 1.13 (3H, s), 1.18 (3H, s), 1.40 (3H, s), 1.66 (3H, s), 5.39 (1H, s), 5.75 (1H, s), 2.45 (1H, s), 3.04-3.08 (1H, dd, J = 5.7, 12.6), 0.70-0.80 (2H, m), 0.91-0.95 (1H, m), 1.13-1.18 (2H, m), 1.21-1.26 (2H, m), 1.28-1.36 (5H, m), 1.44-1.47 (1H, m), 1.56-1.59 (1H, m), 1.68-1.72 (2H, m), 1.86-1.93 (1H, m), 1.95-1.99 (1H, m), 2.24-2.30 (1H, m).

¹³C-NMR (125 MHz, C_6D_6): δ 13.21 (q, C-24), 17.73 (q, C-28), 19.55 (q, C-25), 20.26 (t, C-6), 20.98 (q, C-26), 21.53 (q, C-29), 22.19 (q, C-23), 23.60 (t, C-2), 27.71 (t, C-15), 28.07 (t, C-16), 29.17 (q, C-27), 31.46 (t, C-21), 32.80 (t, C-7), 34.20 (s, C-17), 35.62 (s, C-10), 37.34 (t, C-1), 39.58 (d, C-20), 39.60 (d, C-19), 41.44 (t, C-22), 44.15 (s, C-14), 45.34 (s, C-8), 49.36 (d, C-5), 58.90 (d, C-9), 59.14 (d, C-18), 122.49 (d, C-3), 131.37 (d, C-12), 134.05 (s, C-4), 163.23 (s, C-13), 198.61 (s, C-11).

Mass (EI, 70 eV), m/z (rel.int.): 408 [M]⁺ (44), 393 (25), 353 (17), 286 (5), 273 (22), 255 (8), 232 (100), 217 (10), 203 (14), 189 (8), 175 (10), 161 (18), 147 (17), 135 (36), 119 (17), 105 (19), 95 (18), 81 (10), 69 (9), 55 (18), 41 (17).

10 Bibliography

[1] F. J. Lipp, Duncan Baird Publishers Ltd., **2001**.

Kräuter Heilkunde, Heilung und Harmonie, Symbolik, Rituale und Folklore Östliche und Westliche Traditionen

[2] W. Sandermann, Springer Verlag, **1960**.

Naturharze, Terpentinöl . Tallöl

[3] J. G. Mayer, B. Uehleke, K. Saum, Zabert Sandmann Verlag, München, **2003**.

Handbuch der Kloster-Heilkunde

[4] L. Ruzicka, *Proc. Chem. Soc.*, **1959**, 341-360.

History of the Isoprene Rule

[5] H. Hlasiwetz and F. Hinterberger, *Z. Chem.*, **1868**, 380-381.

Über die Zersetzung des Terpentinöls bei der Glühhitze

[6] E. Breitmaier, B.G. Teubner Stuttgart-Leipzig, **1999**.

Terpene. Aromen, Düfte, Pharmaka, Pheromone

[7] A. Tschirch, Verlag von gebrüder Borntraeger, Leipzig, **1906**.

Die Harze und Harzbehälter mit Einschluss der Milchsäfte.

[8] H. Wolff-Berlin, Stuttgart Wissenschaftliche Verlag GmbH, **1923**.

Die Natürlichen Harze

[9] O. Wallach, *Liebig's Ann. Chem.*, 239(**1887**), 1-45.

Zur Kenntnis der Terpene und der Ätherischen Öle

[10] L. Ruzicka, *J. Chem. Soc.*, 1582 (**1932**).

The Life and Work of Otto Wallach

[11] L. Ruzicka, *Experientia*, 9(**1953**), 357-367.

The Isoprene Rule and the Biogenesis of Terpenic Compounds

[12] L. Ruzicka, *Ann. Rev. Biochem.*, 42(**1973**), 1-20.

In the borderland between Bioorganic Chemistry and Biochemistry

[13] E. M. Hairfield, H. H. Hairfield, L. H. Pentz, *Perf. Flav.*, 9(**1984**), 33-36.

A Rapid Test for the Identification of Incense Resins

[14] M.C. Wani, H. L. Taylor, M.E. Wall, P. Coggin, A. T. McPhail, *J. Am. Chem. Soc.* , 93(**1971**), 2325-2327.

Plant antitumor agents: VI. The Isolation and Structure of Taxol, a Novel Antileukemic and Antitumor Agent from Taxus brevifolia.

[15] N. H. Oberlies, J. A. Greer, M. C. Wani, *HerbalGram: J. Am. Bot. Coun.*, 57 (**2003**), 12-13.

Taxol® Discovery Commemorated in Washington State; Plaque Honors Researchers Wall and Wani, and the First Pacific Yew Collection

[16] N. Kuhnert, *Pharm. unserer Zeit*, 1(**2000**), 32-39.

Hundert Jahre Aspirin® Die Geschichte des wohl erfolgreichsten Medikaments des letzten Jahrhunderets

[17] G. Richter, Georg Thieme Verlag, Stuttgart-New York, **1996**.

Biochemie der Pflanzen

[18] K. Bratt, Dissertation for PhD in Organic Chemistry, University of Uppsala, Sweden, **2000**.
      Secondary Plant Metabolites as Defense Against Herbivores and Oxidative Stress- Synthesis, Isolation and Biological Evaluation

[19] D. V. Banthorpe, B. V. Charlwood, M. J. O. Francis, *Chem. Rev.*, 72(2), **1972**, 115-155.
      The Biosynthesis of Monoterpenes

[20] J. D. Conolly, R.A. Hill, Chapmann ND Hall, New York, **1992**.
      Dictionary of Terpenoids

[21] G. Richter, Georg Thieme Verlag, Stuttgart, **1998**.
      Stoffwechselphysiologie der Pflanzen. Physiologie und Biochemie des Primär- und Sekundärstoffwechsels

[22] L. Ruzicka, *Pure Appl. Chem.*, 6(**1963**), 493-523.
      Perspektiven der Biogenese und der Chemie der Terpene

[23] O. W. Thiele, Georg Thieme Verlag, Stuttgart, **1979**.
      Lipide, Isoprenoide mit Steroiden

[24] T. J. Bach, *Lipids*, 30(**1995**), 191-202.
      Some New Aspects of Isoprenoid Biosynthesis in Plants-A Review

[25] P. A. Tavormina, M. H. Gibbs, J. W. Huff, *J. Am. Chem. Soc.*, 78(**1956**), 4498-4499.
      The Utilization of β-Hydroxy-β-methyl-δ-valerolactone in Cholesterol Biosynthesis

[26] J. W. Cornforth, R.H. Cornforth, G. Popjak, L. Yengoyan, *J. Biol. Chem.*, 241(**1966**), 3970-3987.
      Studies on the Biosynthesis of Cholesterol

[27] A. E. Purcell, G. A. Thompson, J. Borner, *J. Biol. Chem.* ,239 (**1959**), 1081-1084.
      The Incorporation of Mevalonic Acid into Tomato Carotenoids

[28] I. F. Durr, H. Rudney, *J. Biol. Chem.*, 235(**1960**), 2572-2578.
      The Reduction of β-Hydroxy-β-methylglutaryl Coenzyme A to Mevalonic Acid

[29] K. Bloch, S. Chaykin, A. H. Phillips, A. de Waard, *J. Biol. Chem.*, 234(**1959**), 2595-2604.
      Mevalonic Acid Pyrophosphate and Isopentenylpyrophosphate

[30] P. M. Dewick, *Nat. Prod. Rep.*, 19 (**2002**), 181-222.
      The Biosynthesis of C_5-C_{25} Terpenoid Compounds

[31] K. J. Treharne, E. I. Mercer, T. W. Goodwin, *Biochem. J.*, 99(**1966**), 239-245.
      Incorparation of [^{14}C]Carbon Dioxide and [2-^{14}C]Mevalonic Acid into Terpenoids of Higher Plants during Chloroplast Development

[32] M. Rohmer, M. Knani, P. Simonin, B. Sutter, H. Sahm, *Biochem. J.*, 295 (**1993**), 517-524.
      Isoprenoid Biosynthesis in Bacteria: A Novel Pathway for the Early Steps Leading to Isopentenyl diphosphate

[33] M. Rohmer, *Nat. Prod. Rep.*, 16 (**1999**), 565-574.
      The Discovery of a Mevalonate-independent Pathway for Isoprenoid Biosynthesis in Bacteria, Algae and Higher Plants

[34] M. Rohmer, M. Seemann, S. Horbach, S. Bringer-Meyer, H. Sahm, *J. Am. Chem. Soc.*, 118(**1996**), 2564-2566.
      Glyceraldehyde 3-Phosphate and Pyruvate as Precursors of Isoprenic Units in an Alternative Non-mevalonate Pathway for Terpenoid Biosynthesis

[35] G. A. Sprenger, U. Schörken, T. Wiegert, S. Grolle, A. A. de Graaf, S. V. Taylor, T. P. Begley, S. Bringer-Meyer, H. Sahm, *Proc. Nat. Acad. Sci.*, 94(**1997**), 12857-12862.

Identification of a thiamin-dependent synthase in Escherichia coli required for the formation of the 1-deoxy-D-xylulose 5-phosphate precursor to isoprenoids, thiamin, and pyridoxol

[36] S. R. Putra, L. M. Lois, N. Campos, A. Boronat, M. Rohmer, *Tetrahedron Lett.*, 39(**1998**), 23-26.

Incorporation of [2,3-$^{13}C_2$]- and [2,4-$^{13}C_2$]-D-1-Deoxyxylulose into Ubiquinone of Escherichia coli via the Mevalonate-Independent Pathway for Isoprenoid Biosynthesis

[37] L. Charon, J.-F. Hoeffler, C. Pale-Grosdemange, L.-M. Lois, N. Campos, A. Borona, M. Rohmer, *Biochem. J.*, 346(**2000**), 737-742.

Deuterium-labelled isotopomers of 2-C-methyl-erythritol as tools for the elucidation of the 2-C-methyl-erythritol 4-phosphate pathway for isoprenoid biosynthesis

[38] J.-F. Hoeffler, A. Hemmerlin, C. Grosdemange-Billiard, T. J. Bach, M. Rohmer, *Biochem. J.*, 366(**2002**), 573-583.

Isoprenoid biosynthesis in higher plants and in E. coli; on the branching in the methylerythritol phosphate pathway and the independent biosynthesis of isopentenyl diphosphate and dimethylallyl diphosphate

[39] M. Rodriguez-Concepcion, N. Campos, L.M. Lois, C. Maldonado, J.-F. Hoeffler, C. Grosdemange-Billiard, M. Rohmer, A. Boronat, *FEBS Lett.*, 473(**2000**), 328-332.

Genetic evidence of branching in the isoprenoid pathway for the production of isopentenyl diphosphate and dimethylallyl diphosphate in Escherichia coli

[40] F. Rohdich, S. Hecht, K. Gärtner, P. Adam. C. Krieger, S. Amslinger, D. Arigoni, A. Bacher, W. Eisenreich, *Proc. Nat. Acad. Sci.*, 99(**2002**), 1158-1163.

Studies on the nonmevalonate terpene biosynthetic pathway: Metabolic role of IspH (LytB) protein

[41] T. Kuzuyama, H. Seto, *Nat. Prod. Rep.*, 20(**2003**), 171-183.

Diversity of the biosynthesis of the isoprene units

[42] M. Rohmer, B. Sutter, H. Sahm, *J. Chem. Soc. Chem. Commun.*, **1989**, 1471-1472.

Bacterial Sterol Surrogates. Biosynthesis of the Side-chain of Bacteriohopanetetrol and of a Carbocyclic Pseudopentose from ^{13}C-Labelled Glucose in Zymomonas mobilis

[43] H. K. Lichtenthaler, J. Schwender, A. Disch, M. Rohmer, *FEBS Lett.*, 400(**1997**), 271-274.

Biosynthesis of isoprenoids in higher plant chloroplasts proceeds via a mevalonate-independent pathway

[44] D. Arigoni, S. Sagner, C. Latzel, W. Eisenreich, A. Bacher, M. H. Zenk, *Proc. Nat. Acad. Sci.*, 94(**1997**), 10600-10605.

Terpenoid biosynthesis from 1-deoxy-d-xylulose in higher plants by intramolecular skeletal rearrangement

[45] H. K. Lichtenthaler, M. Rohmer, J. Schwender, *Physiol. Plant.*, 101(**1997**), 643-646.

Two independent biochemical pathways for isopentenyl diphosphate and isoprenoid biosynthesis in higher plants

[46] W. Knöss, B. Reuter, J. Zapp, *Biochem. J.*, 326(**1997**), 449-454.

Biosynthesis of the labdane diterpene marrubiin in Marrubium vulgare via a non-mevalonate pathway

[47] A. Disch, A. Hemmerlin, T. J. Bach, M. Rohmer, *Biochem. J.*, 331(**1998**), 615-621.

Mevalonate-derived isopentenyl diphosphate is the biosynthetic precursor of ubiquinone prenyl side chain in tobacco BY-2 cells

[48] S. Steinbacher, J. Kaiser, W. Eisenreich, R. Huber, A. Bacher, F. Rohdich, *J. Biol. Chem.*, 278(**2003**), 18401-18407.

Structural basis of fosmidomycin action revealed by the complex with 2-C-methyl-D-erythritol 4-phospahte synthase (IspC). Implications for the catalytic mechanism and anti-malaria drug development.

[49] O. Laule, A. Fürholz, H.-S. Chang, T. Zhu, X. Wang, P. B. Heifetz, W. Gruissem, B. M. Lange, *Proc. Nat. Acad. Sci.*, 100(**2003**), 6866-6871.

Crosstalk between cytosolic and plastidial pathways of isoprenoid biosynthesis in Arabidopsis thaliana

[50] J. B. Harborne, *Nat. Prod. Rep.*, 18(**2001**), 361-379.

Twenty-five years of chemical ecology

[51] H. Grisebach, J. Ebel, *Angew. Chem.*, 90(**1978**), 668-681.

Phytoalexine, chemische Abwehrstoffe höherer Pflanzen?

[52] A. J. Hick, M. C. Luszniak, J. A. Pickett, *Nat. Prod. Rep.*, 16(**1999**), 39-54.

Volatile isoprenoids that control insect behaviour and development

[53] G. Rücker, *Angew. Chem.*, 85(**1973**), 895-920.

Sesquiterpene

[54] G. Buchbauer, H. Spreitzer, G. Keiner, *Pharm. unserer Zeit*, 19(**1990**), 28-37.

Biologische Wirkungen von Diterpenen

[55] C. H. Brieskorn, *Pharm. unserer Zeit*, 16(**1987**), 161-179.

Triterpenoide, physiologische Funktionen und therapeutische Eigenschaften

[56] R. Hegnauer, in *Vorkommen und Analytik Ätherischer Öle* by K-H. Kubeczka, Georg Thieme Verlag, Stuttgart, **1979**.

Verbreitung ätherischer Öle im Pflanzenreich

[57] F.-C. Czygan, *Pharm. unserer Zeit*, 10(**1981**), 109-121.

Ätherische Öle und Duft kulturhistorisch betrachtet

[58] A. Koedam, in *Vorkommen und Analytik Ätherischer Öle* by K-H. Kubeczka, Georg Thieme Verlag, Stuttgart, **1979**.

Antimikrobielle Wirksamkeit ätherischer öle

[59] H. Schilcher, *Dtsch. Apoth. Ztg.*, 124(**1984**), 1433-1442.

Ätherischer Öle-Wirkungen und Nebenwirkungen

[60] H. Wagner, Gustav-.Fischer Verlag, Stuttgart-New York, **1993**.

Pharmazeutische Biologie, Drogen und Ihre Inhalts Stoffe

[61] G. Ohloff, Springer Verlag, 1990.

Riechstoffe und Geruchssinn- Die Molekülare Welt der Düfte

[62] M. Hesse, H. Meier, B. Zeeh, Thieme Verlag, Stuttgart, **1997**.

Spectroscopic Methods in Organic Chemistry

[63] H. Friebolin, VCH Verlagsgesellschaft GmbH, Weinheim, **1991**.

Basic One- and Two-Dimensional NMR Spectroscopy

[64] E. Breitmaier, John Wiley & Sons, West Sussex, **1995**.

Structure Elucidation by NMR in Organic Chemistry

[65] J. Hormer, M.C. Perry, *J. Chem. Soc. Chem. Commun.*, **1994**, 373-374.
      New Method for NMR Signal Enhancement by Polarization transfer and Attached Nucleus Testing

[66] E.L. Eliel, S.H. Wilen, L.N. Mander, John Wiley and Sons, USA, **1994**.
      Stereochemistry of Organic Compounds

[67] K. Mislow, J. Siegel, *J. Am. Chem. Soc.*, 106(**1984**), 3319-3328.
      Stereoisomerism and Local Chirality

[68] V.R.A. Hegstrom, D.K. Kondepudi, *Spektrum der Wissenschaft*, 3(**1990**), 56-67.
      Händigkeit im Universum

[69] I. Agranat, H. Caner, J. Caldwell, *Nat. Rev.*, 1(**2002**), 753-768.
      Putting Chirality to Work: The Strategy of Chiral Switches

[70] W.A. König, *Hüthig Buch Verlag*, Heidelberg, **1992**.
      Gas Chromatographic Enantiomer Separation with Modified Cyclodextrins

[71] W.A. König, B. Gehrcke, D. Icheln, P. Evers, J. Dönnecke, W. Wang, *J. High Res. Chrom.*, 15(**1992**), 367-372.
      New, Selectively Substituted Cyclodextrins as Stationary Phases fo the Analysis of Chiral Constituents of Essential Oils

[72] M. Junge, W.A. König, *J. Sep. Sci.*, 26(**2003**), 1607-1614.
      Selectivity tuning of cyclodextrin derivatives by specific substitution

[73] I. Hardt, W.A. König, *J. Chrom. A*, 666(**1994**), 611-615.
      Preparative enantiomer separation with modified cyclodextrins as chiral stationary phases

[74] W.A. König, *Chirality*, 10(**1998**), 499-504.
      Enantioselective Capillary Gas Chromatography in the Investigation of Stereochemical Correlations of Terpenoids

[75] A.M. Adio, C. Paul, W.A. König, H. Muhle, *Phytochem.*, 61(**2002**), 79-91.
      Volatile components from European liverworts Marsupella emarginata, M. aquatica and M. alpina

[76] R. Lu, C. Paul, S. Basar, W.A. König, T. Hashimoto, Y. Asakawa, *Phytochem.*, 63(**2003**), 581-587.
      Sesquiterpene constituents from the liverwort Bazzania japonica

[77] W.A. König, C. Fricke, Y. Saritas, B. Momeni, G. Hohenfeld, *J. High Res. Chrom.*, 20(**1997**), 55-61.
      Adulteration or Natural Variability? Enantioselective Gas Chromatography in Purity Control of Essential oils

[78] D. Frohne, U. Jensen, Wissenschaftliche Verlagsgesellschaft Stuttgart, **1998**.
      Systematik des Pflanzenreichs

[79] K. Vollesen, *The Flora of Ethiopia*, Vol. 3, I. Hedberg, S. Edward (editors), Addis Ababa University: Addis Ababa, **1989**, 442-478.
      Burseraceae

[80] M. Thulin, A. M. Warfa, *Kew Bull.*, Vol 42(3), **1986**, 487-500.
      The Frankincense Trees (Boswellia spp., Burseraceae) of Northern Somalia and Southern Arabia

[81] W. Blaschek, R. Hänsel, K. Keller, J. Reichling, H. Rimpler, G. Schneider (Hrsg.), 5. Auflage, *Springer Verlag*, Berlin-Heidelberg, **1998**.
      Hagers Handbuch der Pharmazeutischen Praxis

[82] D. Martinetz, K. Lohs, J. Janzen, Wissenschaftliche Verlagsgesellschaft Stuttgart, **1989**.
      Weihrauch und Myrrhe, Kulturgeschichte und wirtschaftliche Bedeutung, Botanik-Chemie-Medizin

[83] J. Verghese, *Perfumer and Flavorist*, Vol. 13(1), **1988**, 1-12.
      Olibanum in Focus

[84] J. Stenhouse, *Lieb. Ann. Chem.* , 35(**1840**), 304-306.
      Zusammensetzung des Elemi- und Olibanumöls

[85] A. Tschirch, O. Halbey, *Arch. Pharm.*, 236(**1898**), 487-502.
      Untersuchungen über die Sekrete. 28: Über das Olibanum

[86] A. Winterstein, G. Stein, *Hoppe-Syler's Z. Physiol. Chem*, 208(**1932**), 9-25.
      Untersuchungen in der Saponinreihe. X. Mitteilung, Zur Kenntnis der Mono-oxy-triterpensäuren

[87] L. Ruzicka, W. Wirz, *Helv. Chim. Acta*, 22(**1939**), 132-135.
      Zur Kenntnis der Triterpene. Umwandlung der α-Boswellinsäure in β-Amyrin

[88] L. Ruzicka, W. Wirz, *Helv. Chim. Acta*, 24(**1941**), 248-252.
      ZurKenntnis der Triterpene. Bereitung des epi-β-Amyrins aus α-Boswellinsäure und aus β- Amyron

[89] G. Snatzke, L. Vértesy, *Monatsh. Chem.*, 98(**1967**), 121-132.
      Über die Neutralen Sesqui- und Triterpene des Weihrauchs

[90] R. S. Pardhy, S. C. Bhattacharyya, *Ind. J. Chem.*, 16B, **1978**, 174-175.
      Tetracyclic Triterpene Acids from the Resin of Boswellia serrata Roxb.

[91] R. S. Pardhy, S. C. Bhattacharyya, *Ind. J. Chem.*, 16B, **1978**, 176-178.
      β-Boswellic acid, Acetyl-β-boswellic acid, Acetyl-11-keto-β-boswellic acid and 11-Keto-β-boswellic acid, Four Pentacyclic Triterpene Acids from the Resin of Boswellia serrata Roxb.

[92] R. S. Pardhy, S. C. Bhattacharyya, *Ind. J. Chem.*, 16B, **1978**, 171-173.
      Structure of Serratol, a New Diterpene Cebranoid Alcohol from Boswellia serrata Roxb.

[93] H. Obermann, *Dragoco Reports*, 24(**1977**), 260-265.
      Die chemischen und geruchlichen Unterschiede von Weihrauchharzen

[94] P. Maupetit, *Perfumer and Flavorist*, 9(**1984**), 19-37.
      New Constituents in Olibanum Resinoid and Essential Oil

[95] A. M. Humphrey, J. R. Harris, C.A. Mansfield, D. M. Michalkiewicz, M. Milchrad, D. A. Moyler, A. Osbiston, S. Smith, B. Starr, T. M. Stevens, J. J. Wilson, *Analyst*, 118(**1993**), 1089-1098.
      Application of Gas-Liquid Chromatography to the Analysis of Essential oils. Part XVI. Monographs for Five Essential Oils

[96] D. Hochmuth, D. Joulain, W. A. König, **2001**. University of Hamburg, Germany.
      MassFinder Software and Databank

[97] D. Joulain, W.A. König, E. B.-Verlag, Hamburg, Germany, **1998**.
      The Atlas of Spectral Data of Sesquiterpene Hydrocarbons

[98] S. M. A. Wahab, E. A. Aboutabl, S. M. El-Zalabani, H. A. Fouad, H. L. De pooter, B. El-Fallaha, *Planta Med.*, 53(**1987**), 382-384.
      The Essential Oil of Olibanum

[99]   G. Vernin, C. Boniface, J. Metzger, Y. Maire, A. Rakotorijaona, D. Fraisse, C. Parkanyi, *Proceedings of the 6th International Flavor Conference, Flavors and Off-Flavors*, **1989**.
        GC-MS Data Bank Analysis of the Essential Oils from Boswellia frereana Bidw. And Boswellia carterii Birdw.

[100]   B. M. Lawrence, *Perfumer and Flavorist*, 17(**1992**), 61-66.
        Progress in Essential Oils

[101]   P. Kreis, U. Hener, A. Moslandl, *Dtsch. Apoth. Ztg.*, 130(**1990**), 985-988.
        Chirale Inhaltsstoffe ätherisher Öle

[102]   S. Basar, A. Koch, W. A. König, *Flav. Frag. J.*, 16(**2001**), 315-318.
        A verticillane-type diterpene from Boswellia carterii essential oil

[103]   R. Nicoletti, M. L. Forcellese, *Tetrahedron.*, 24(**1968**), 6519-6525.
        The Structure of Incensole-oxide

[104]   M. L. Forcellese, R. Nicoletti, U. Petrossi, *Tetrahedron*, 28(**1972**), 325-331.
        The Structure of Isoincensole-oxide

[105]   M. L. Forcellese, R. Nicoletti, C. Santarelli, *Tetrahedron Lett.*, 39(**1973**), 3783-3786.
        The Revised Structure of Isoincensole-oxide

[106]   T. Kato, C. C. Yen, T. Uyehara, Y. Kitahara, *Chem. Lett.*, **1977**, 565-568.
        Cyclization of Polyenes XXIII, Synthesis and Stereochemistry of Isoincensole-oxide

[107]   A.O. Barakat, J. Rullkötter, *Org. Mass. Spec.*, 28(**1993**), 157-162.
        Gas Chromatographic/Mass Spectrometric Analysis of Cembrenoid Diterpenes in Kerogen from a Lacustrine Sediment

[108]   I) D.F. Wiemar, J. Meinwald, G.D. Prestwich, I. Miura, *J. Org. Chem.*, 44(**1979**), 3950-3952.
        Cembrene A and (3Z)-Cembrene A: Diterpenes from a Termite Soldier (Isoptera Termitidae Termitinae)
        II) D.L. Mattern, W.D. Scott, C.A. McDaniel, P.J. Weldon, D.E. Garves, *J. Nat. Pro.*, 60(**1997**), 828-831.
        Cembrene A and a Congeneric Ketone Isolated from the Paracloacal Glands of the Chinese Alligator (Alligator sinensis)

[109]   S. Corsano, R. Nicoletti, *Tetrahedron*, 23(**1967**), 1977-1984.
        The Structure of Incensole

[110]   H. Erdtman, T. Norin, M. Sumimoto, A. Morrisson, *Tetrahedron Lett.*, 51(**1964**), 3879-3886.
        Verticillol, A Novel Type of Conifer Diterpene

[111]   Y. Asakawa, Springer-Verlag, Vienna, **1995**.
        Progress in the Chemistry of Organic Natural Products

[112]   B. Karlsson, A.-M. Pilotti, A.-C. Söderholm, T. Norin, S. Sundin, M. Sumimoto, *Tetrahedron*, 34(**1978**), 2349-2354.
        The Structure and Absolute Configuration of Verticillol, A Macrocyclic Diterpene Alcohol from the Wood of Sciadopitys verticillata Sieb. Et Zucc. (Taxodiaceae)

[113]   C. B. Jackson, G. Pattenden, *Tetrahedron Lett.*, 26(**1985**), 3393-3396.
        Total Synthesis of Verticillene, The Putative Biogenetic precursor of the Taxane Alkaloids

[114]   M. J. Begley, C. B. Jackson, G. Pattenden, *Tetrahedron Lett.*, 26(**1985**), 3397-3400.
        Investigation of Transannular Cyclisations of Verticillanes to the Taxane Ring System

[115] M. J. Begley, C. B. Jackson, G. Pattenden, *Tetrahedron,* 46(**1990**), 4907-4924.

Total Synthesis of Verticillene. A Biomimetic Approach to the Taxane Family of Alkaloids

[116] T. Kato, T. Hirano, M. Hoshikawa, T. Uyehara, *Bull. Chem. Soc. Jap.*, 69(**1996**), 221-228.

Synthesis of 10-Cyanoverticillene and Its Reactions Directed Toward the Verticillol Synthesis

[117] T. Kumagai, F. Ise, T. Uyehara, T. Kato, *Chem. Lett.*, **1981**, 25-28.

Synthesis of trans-4,8,12,15,15-Pentamethylbicyclo[9,3,1]pentadeca-3E,7Z,12Z-triene, A Geometrical Isomer of Anhydroverticillol

[118] J. W. Hogg, B. M. Lawrence, *Can. Flav. Ind.*, 3(**1972**), 321-323.

Essential oils and their constituents. VIII. New bicyclic monoterpene from Mentha cardiaca.

[119] H. Lammens, M. Verzele, *Bull. Soc. Chim. Belg.*, 77(**1968**), 497-503.

The Aroma of Hops. III. The Occurrence of Diterpenes in Hop Oil

[120] W. Eisfelder, P. Weyerstahl, *Liebigs Ann. Chem.*, **1977**, 988-998.

Diels-Alder-Reaktion von Myrcen mit Isopren

[121] E. Klein, H. Obermann, *Tetrahedron Lett.*, 4(**1978**), 349-352.

(S)-1-Isopropyl-4,8,12-trimethyl-cyclotetradeca-3E,7E,11E-trien-1-ol, Ein Neues Cembrenol aus dem Öl von Olibanum

[122] G. Strappaghetti, S. Corsano, A. Craveiro, G. Proietti, *Phytochem.*, 21(**1982**), 2114-2115.

Constituents of Essential oil of Boswellia frereana

[123] J. E. Baldwin, J. P. Nelson, *J. Am. Chem. Soc.*, 31(**1965**), 336-338.

Cycloadditions. VI. Photosensitized Dimerization of α-Phellandrene

[124] K. H. C. Baser, B. Demirci, A. Dekebo, E. Dagne, *Flav. Frag. J.*, 18(**2003**), 153-156.

Essential oils of some Boswellia spp., Myrrh and Opopanax

[125] H. Lord, J. Pawliszyn, *J. Chrom. A*, 885(**2000**), 153-193.

Evolution of solid-phase microextraction technology

[126] M. E. Miller, J. D. Stuart, *Anal. Chem.*, 71(**1999**), 23-27.

Comparison of Gas-Sampled and SPME-Sampled Static Headspace for the Determination of Volatile Flavor Components

[127] H.W. Chin, R.A. Benhard, M. Rosenberg, *J. Food. Sci.*, 61(**1996**), 1118-1122.

Solid Phase Microextraction for Cheese Volatile Compound Analysis

[128] Z. Zhang, J. Pawliszyn, *Anal. Chem.*, 65(**1993**), 1843-1852.

Headspace Solid-Phase Microextraction

[129] U. Sellerberg, *PTA-Forum*, 22(**2003**), 16-17.

Weihrauch Zur Ehre Gottes und zum Nutzen Kranker

[130] H. Safayhi, H.P.T. Ammon, *Pharm. Z.*, 142(**1997**), No. 39, 11-20.

Pharmakologische Aspekte von Weihrauch und Boswelliasäuren

[131] H.P.T. Ammon, T. Mack, G.B. Singh, H. Safayhi, *Planta Med.*, 57(**1991**), 203-207.

Inhibition of Leukotriene B$_4$ Formation in Rat Peritoneal Neutrophils by an Ethanolic Extract of the Gum Resin Exudate of Boswellia serrata

[132] I) J.C.E. Simpson, N.E. Williams, *J. Chem. Soc.*, 140(**1938**), 686-688.

The Triterpene Group. Part I. β-Boswellic acid

II) J.C.E. Simpson, N.E. Williams, *J. Chem. Soc.*, 140(**1938**), 1712-1721.

The Triterpene Group. Part III. The Double Bond of β-Boswellic acid

III) L. Ruzicka, W. Wirz, *Helv. Chim. Acta*, 22(**1939**), 132-135.

Zur Kenntnis der Triterpene. Umwandlung der α-Boswellinsäure in β-Amyrin

IV) L. Ruzicka, W. Wirz, *Helv. Chim. Acta*, 24(**1941**), 248-252.

Zur Kenntnis der Triterpene. Bereitung des epi-β-Amyrins aus α-Boswellinsäure und aus β-Amyron

V) L. Ruzicka, W. Wirz, *Helv. Chim. Acta*, 22(**1939**), 948-951.

Zur Kenntnis der Triterpene. Umwandlung der β-Boswellinsäure in α-Amyrin

VI) W. Klyne, W.M. Stokes, *J. Chem. Soc.*, **1954**, 1979-1988.

The Molecular Rotations of Polycyclic Compounds. Part III. Polycyclic Alcohols and their Derivatives.

VII) A. Bowers, T.G. Halsall, G.C. Sayer, *J. Chem. Soc.*, **1954**, 3070-3084.

The Chemistry of the Triterpenes and Related Compounds. Part XXV. Some Stereochemical Problems concerning Polyporenic Acid C.

VIII) J.L. Beton, T.G. Halsall, E.R.H. Jones, *J. Chem. Soc.*, **1956**, 2904-2909.

The Chemistry of Triterpenes and Related Compounds. Part XXVIII. β-Boswellic acid

[133] G.G. Allan, *Phytochem.*, 7(**1968**), 963-973.

The Stereochemistry of The Boswellic Acids

[134] M.d.C. Recio, R.M. Giner, S. Manez, J.L. Rios, *Planta Med.*, 61(**1995**), 182-185.

Structural Requirements for the Anti-inflammatory Activity of Natural Triterpenoids

[135] M. J. Müller, *Pharm. unserer Zeit*, 24(**1995**), 264-272.

Der Leukotriensignalweg- ein vielversprechender Ansatzpunkt für Inhibitoren in der Therapie entzündlicher Erkrankungen

[136] E. Mayatepek, G.F. Hoffmann, *Ped. Res.*, 37(**1995**), 1-9.

Leukotrienes: Biosynthesis, Metabolism, and Pathophysiologic Significance

[137] H. Safayhi, E.-R. Sailer, H.P.T. Ammon, *Mol. Pharm.*, 47(**1995**), 1212-1216.

Mechanism of 5-Lipoxygenase Inhibition by Acetyl-11-keto-β-boswellic Acid

[138] E.-R. Sailer, L.R. Subramanian, B. Rall, R.F. Hoernlein, H.P.T. Ammon, H. Safayhi, *Bri. J. Pharm*, 117(**1996**), 615-618.

Acetyl-11-keto-β-boswellic acid (AKBA): structure requirements for binding and 5-lipoxygenase inhibitory activity

[139] E.-R. Sailer, S. Schweizer, S.E. Boden, H.P.T. Ammon, H. Safayhi, *Eur. J. Biochem.*, 256(**1998**), 364-368.

Characterisation of an acetyl-11-keto-β-boswellic acid and arachidonate-binding regulatory site of 5-lipoxygenase using photoaffinity labeling

[140] A. Altmann, L. Fischer, M. Schubert-Zsilavecz, D. Steinhilber, O. Werz, *Biochem. Biophys. Res. Commun.*, 290(**2002**), 185-190.

Boswellic Acids Activate p42^{MAPK} and p38 MAPK and Stimulate Ca^{+2} Mobilization

[141] O. Sander, G. Herborn, R. Rau, *Z. Rheum.*, 57(**1998**), 11-16.

Ist H15(Harzextrakt von Boswellia serrata, „Weihrauch") eine sinnvolle Ergänzung zur etabilierten medikamentösen Therapie der chronischen Polyarthritis? – Ergebnisse einer doppelblinden Pilotstudie

[142] I.Gupta, A. Parihar, P. Malhotra, S. Gupta, R. Lüdtke, H. Safayhi, H.P.T. Ammon, *Planta Med.*, 67(**2001**), 391-395.

Effects of Gum Resin of Boswellia serrata in Patients with Chronic Colitis

[143] H. Gerhardt, *Med. Welt*, 52(**2001**), 37-39.

Therapeutischer Nutzen des Boswellia serrata-Extrakts H15

[144] H.Gerhardt, F. Seifert, P. Buvari, H. Vogelsand, R. Repges, *Z. Phytother.*, 22(**2001**), 69-75.

Therapie des aktiven Morbus Crohn mit dem Boswellia serrata-Extrakt H15

[145] C.F. Krieglstein, C. Antoni, E.J.M. Rijcken, M. Laukötter, H.-U. Spiegel, S.E. Boden, S. Schweizer, H. Safayhi, N. Senninger, G. Schürmann, *Int. J. Col. Dis.*, 16(**2001**), 88-95.

Acetyl-11-keto-β-boswellic Acid, a constituent of a herbal medicine from Boswellia serrata resin, attenuates experimental ileitis

[146] H.P.T. Ammon, *Wien. Med. Wschr.*, 152(**2002**), 373-378.

Boswelliasäuren (Inhaltsstoffe des Weihrauchs) als wirksame Prinzipien zur Behandlung chronischer entzündlicher Erkrankungen

[147] H. Safayhi, S. E. Boden, S.Schweizer, H.P.T. Ammon, *Planta Med.*, 66(**2000**), 110-113.

Concentration-Dependent Potentiating and Inhibitory Effects of Boswellia Extracts on 5-Lipoxygenase Product Formation in Stimulated PMNL

[148] S. Schweizer, A.F.W. von Brocke, S.E. Boden, E. Bayer, H.P.T. Ammon, H. Safayhi, *J. Nat. Pro.*, 63(**2000**), 1058-1061.

Workup-Dependent Formation of 5-Lipoxygenase Inhibitory Boswellic Acid Analogues

[149] S.E. Boden, S. Schweizer, T. Bertsche, M. Düfer, G. Drews, H. Safayhi, *Mol. Pharm.*, 60(**2001**), 267-273.

Stimulation of Leukotriene Synthesis in Intact Polymorhonuclear Cells by the 5-Lipoxygenase Inhibitor 3-oxo-Tirucallic Acid

[150] H. Safayhi, B. Rall, E.-R. Sailer, H.P.T. Ammon, *J. Pharm. Exp. Ther.*, 281(**1997**), 460-463.

Inhibition by Boswellic Acids of Human Leukocyte Elastase

[151] Y. Shao, C.-T. Ho, C.-K. Chin, V. Badmaev, W. Ma, M.-T. Huang, *Planta Med.*, 64(**1998**), 328-331.

Inhibitory Activity of Boswellic Acids from Boswellia serrata against Human Leukemia HL-60 Cells in Culture

[152] R.F. Hoernlein, Th. Orlikowsky, C. Zehrer, D. Niethammer, E.R. Sailer, Th. Simmet, G.E. Dannecker, H.P.T. Ammon, *J. Pharm. Exp. Ther.*, 288(**1999**), 613-619.

Acetyl-11-keto-β-boswellic Acid Induces Apoptosis in HL-60 and CCRF-CEM Cells and Inhibits Topoisomerase I

[153] T. Syrovets, B. Büchele, E. Gedig, J. R. Slupsky, T. Simmet, *Mol. Pharm.*, 58(**2000**), 71-81.

Acetyl-Boswellic Acids are Novel Catalytic Inhibitors of Human Topoisomerases I and IIα

[154] Y.S. Park, J.H. Lee, J. Bondar, J.A. Harwalakr, H. Safayhi, M. Golubic, *Planta Med.*, 68(**2000**), 397-401.

Cytotoxic Action of Acetyl-11-keto-β-Boswellic Acid (AKBA) on Meningioma Cells

[155] J.-J. Liu, A. Nilsson, S. Oredsson, V. Badmaev, W.-Z. Zhao, R.-D. Duan, *Carcinogen.*, 23(**2002**), 2087-2093.

Boswellic acids trigger apoptosis via a pathway dependent on caspase-8 activation but independent on Fas/Fas ligand interaction in colon cancer HT-29 cells.

[156] E. Fattorusso, C. Santacroce, C. F. Xaasan, *Phytochem.*, 22(**1983**), 2868-2869.

4(23)-Dihydroroburic Acid From The Resin (Incense) Of Boswellia carterii

[157] E.M. Hairfield, H.H. Hairfield, *J. Chrom. Sci.*, 27(**1989**), 127-133.

GC, GC/MS, and TLC of β-Boswellic acid and O-Acetyl-β-boswellic acid from B. serrata, B. carterii and B. papyrifera

[158] S. Schweizer, Dissertation für der Fakültät für Chemie und Pharmazie, Eberhard-Karls-Universität Tübingen, **2000**.

Isolierung und Charakterisierung genuiner und nich-genuiner Triterpene aus dem Weihrauchharz und deren Wirkung auf die Leukotrienbiosynthese in vitro

[159] Fluka, Chemika, Silylating Agents, Silicon Compounds Edition, **1988**, 31-32.

N-Methyl-N-trimethylsilyl-trifluoroacetamide, MSTFA

[160] H. Budzikiewicz, J.M. Wilson, C. Djerassi, *J. Am. Chem. Soc.*, 85(**1963**),3688-3699.

Mass Spectrometry in Stuructural and Stereochemical Problems. XXXII. Pentacyclic Triterpenes

[161] M. Burnouf-Radosevich, N.E. Delfel, R. England, *Phytochem.*, 24(**1985**), 2063-2066.

Gas Chromatography-Mass Spectrometry of Oleanane- and Ursane-type Triterpenes- Application to Chenopodium quinoa Triterpenes

[162] E.J. Corey, G. Schmidt, *Tetrahedron Lett.*, 5(**1979**), 399-402.

Useful Procedures for the Oxidation of Alcohols Involving Pyridinium Dichromate in Aprotic Media

[163] Kondo K., Toyota, M., Asakawa Y., *Phytochem.*, 29(**1990**), 2197-2199.

ent-Eudesmane type sesquiterpenoids from Bazzania species

[164] *Biochemical Applications of Mass Spectrometry*, 1st suppl. vol., ed. G.R. Waller, O.C. Dermer, John Wiley & Sons, New York, **1980**.

[165] A.J. Koch, Short Lecture at the *50th Annual Congress of the Society for Medicinal Plant Research*, Barcelona, Spain, **2002**.

Stability Testing of Boswellia Species and Its Preparations by HPLC

[166] J. Jauch, *PCT Int. App.*, Patent No. WO 2002085921, **2002**.

Simple method for the synthesis of boswellic acids and derivatives thereof.

[167] J. von Melding, *PTA Heute*, 3(**2003**), 82.

Lagerung und Haltbarkeit von Arzneimitteln

[168] C. O'Brien, *New Scientist*, 171(**2001**), 5-7.

Holly Smoke

[169] I) M. Pailer, O. Scheidl, H. Gutwillinger, E. Klein, H. Obermann, *Monatsh. Chem.*, 112 (**1981**), 341-358.

Über die Zusammensetzung des Pyrolysates von Weihrauch „Aden", dem Gummiharz von Boswellia carteri Birdw.,1. Mitt.

II) M. Pailer, O. Scheidl, H. Gutwillinger, E. Klein, H. Obermann, *Monatsh. Chem.*, 112(**1981**), 595-603.

Über die Zusammensetzung des Pyrolysates von Weihrauch „Aden", dem Gummiharz von Boswellia carteri Birdw.,2. Mitt.

III) M. Pailer, O. Scheidl, H. Gutwillinger, E. Klein, H. Obermann, *Monatsh. Chem.*, 112(**1981**), 987-1006.

Über die Zusammensetzung des Pyrolysates von Weihrauch „Aden", dem Gummiharz von Boswellia carteri Birdw.,3. Mitt.

[170]   I) P.F. van Bergen, T.M. Peakman, E.C. Leigh-Firbank, R.P. Evershed, *Tetrahedron Lett.*, 38(**1997**), 8409-8412.

Chemical Evidence for Archaeological frankincense: Boswellic Acids and their Derivatives in Solvent Soluble and Insoluble Fractions of Resin-Like Materials

II) R.P. Evershed, P.F. van Bergen, T.M. Peakman, E.C. Leigh-Firbank, *Nature*, 390(**1997**), 667-668.

Archaeological frankincense

[171]   W.S. Powell, *Anal. Biochem.*, 115(**1981**), 267-277.

Separation of Icosenoic Acids, Monohydroxyicosenoic Acids, and Prostaglandins by High-Pressure - Liquid Chromatography on a Silver Ion-Loaded Cation-Exchange Column

[172]   W.W. Christie, G.H. McG. Breckenridge, *J. Chromatog.*, 469(**1989**), 261-269.

Separation of cis and trans Isomers of Unsaturated Fatty Acids by High-Performance Liquid Chromatography in the Silver Ion Mode

[173]   K.A. Hammer, C.F. Carson, T.V. Riley, *J. Antimic. Chemo.*, 42(**1998**), 591-595.

In-vitro activity testing of essential oils, in particular Melaleuca alternifolia (tea tree) oil and tea tree oil products, against Candida spp.

[174]   D. Horne, M. Holm, C. Oberg, S. Chao, D.G. Young, *J. Ess. Oil Res.*, 13(**2001**), 387-392.

Antimicrobial Effects of Essential Oils on Streptococcus pneumoniae

[175]   *Pschyrembel Klinisches Wörterbuch*, 257th edition, ed. H. Hildebrandt, Wörterbuch-Redaktion des Verlages, de Gruyter, **1994**, New York.

List of Abbreviations

1-D	One dimensional
2-D	Two dimensional
ABA	3-*O*-Acetyl-β-boswellic acid
AKBA	3-*O*-Acetyl-11-keto-β-boswellic acid
ATP	Adenosine triphosphate
BA	β-boswellic acid
CC	Column Chromatography
CD	Cyclodextrine
DEPT	Distorsionless enhancement by polarisation transfer
DMAPP	Dimethylallyl pyrophosphate
DXP	1-Deoxy-*D*-xylulose 5-phosphate
FID	Flame ionization detector
Fig.	Figure
GAP	Glyceraldehyde 3-phosphate
GC	Gas Chromatography
GC-MS	Gas Chromatography-Mass Spectrometry
HLE	Human leukocyte elastase
HMBC	Heteronuclear multiple bond correlation
HMBDP	1-Hydroxy-2-methyl-2-*E*-butenyl 4-diphosphate
HMG-CoA	*S*-3-Hydroxy-3-methyl-glutaryl coenzyme A
HMQC	Heteronuclear multiple quantum correlation
HPLC	High pressure liquid chromatography
HPTLC	High performance thin layer chromatography
IDP	Isopentenyl diphosphate
IR	Infrared and Raman Spectroscopy

KBA	11-Keto-β-boswellic acid
LC-MS	Liquid Chromatography-Mass Spectrometry
MEP	2-C-Methyl-*D*-erythritol 4-phosphate
MS	Mass Spectrometry
MSTFA	N-Methyl-N-trimethylsilyl trifluoroacetamide
MVA	Mevalonic acid
NMR	Nuclear Magnetic Resonance
NOE	Nuclear Overhauser Effect
PAH	Polyaromatic Haydrocarbons
PDMS	Polydimethyl siloxane
PENDANT	Polarization enhancement nurtured during attached nucleus testing
PMNL	Polymorpho human leukocytes
RDA	Retro Diels Alder
SPA	Solid phase adsorption
SPME	Solid phase microextraction
TA	Tirucallic acid
TLC	Thin layer chromatography
TMS	Trimethylsilyl
UV	Ultraviolet and Visible Spectroscopy

List of Chemicals

Name of the Chemical	R	S	Symbol of Danger
Acetone	11-36-66-67	(2-)9-16-26	Xi F
Benzene-d6	45-11-46-48/23/24/25	53-45	F T
Chloroform-d1	22-38-40-48/20/22	(2-)36/37	Xn
Dichloromethane	40	(2-)23/24/25-36/37	Xn
Ethylacetate	11	?	F
Diethylether	12-19-22-66-67	(2-)9-16-29-33	F+ Xn
Hexane	11-38-48/20-51/53-62-65-67	(2-)9-16-29-33-36/37-61-62	F N Xn
Pentane	12-51/53-65-66-67	(2-)9-16-29-33-61-62	F+ Xn N
Toluol	11-20	(2-)9-16-29-33	F Xn
Formic acid	61	53-45	T
Heptane	11-38-50/53-65-67	(2-)9-16-29-33-60-61-62	F N Xn
Barium hydroxide	20/22	(2-)28	Xn
Hydrochloric acid	34-37	(1/2-)26-45	C
Sodium sulfate	-----	?	-----
Magnesium hydroxide	36/37/38	?	Xi
Potassium hydroxide	22-35	(1/2-)26-36/37/39-45	C
Magnesiumsulfate	-----	?	-----
Pyridinium dichromate	49-43-50/53	53-45-60-61	T N
MSTFA	10-36/37/38	?	Xi
Amberlite	?	?	A
Florisil	?	?	A
Silica gel	40-37	?	Xi
Ethanol	11	(2-)7-16	F
Sodium hydroxide	35	(1/2-)26-37/39-45	C
Acetic acid	10-35	(1/2-)23-26-45	C
Super Q	?	?	-----
DPPH	?	?	A

Curriculum Vitae

Personal Information

Name	Simla Basar
Date of Birth and Place	29 Juli 1972, Istanbul (Turkey)

Educational Information

1983-1990	Kadiköy Anatolian High School, Istanbul, Turkey
1991-1997	"Bachelor of Science" in Chemie, Bogazici University, Istanbul, Turkey
	"Teaching Certificate" in Chemistry Education, Bogazici University, Istanbul, Turkey
1997-1999	"Master of Science" in Chemie, Bogazici University, Istanbul, Turkey
Since February 2000	PhD in Chemie, University of Hamburg

Academical Activities

March-Mai 1997	Effective Teaching Certificate, BÜREM, Bogazici University, Istanbul, Turkey
26 February 2003	Boswellia Symposium 2003
17-18 Juli 2003	MedChem Workshop

Professional Experiences

1997-1999	"Teaching Assistant" for the instrumental analysis and qualitative organic analysis for senior students.